The role of the Fanconi anemia pathway in sporadic head and neck cancer

Chantal Stoepker

Reading committee: prof.dr. P.J.F. Snijders
prof.dr. M. van den Brekel
dr. R.M. Wolthuis
dr. P. Knipscheer

Layout and cover design: Chantal Stoepker
Printing: Gildeprint BV, Enschede, The Netherlands

The research described in this thesis was performed at the Department of Clinical Genetics of the VU University Medical Center, Amsterdam, The Netherlands, and financially supported by CCA/V-ICI Amsterdam and the Fanconi Anemia Research Fund, Portland, OR, U.S.A.

ISBN: 978-94-6233-146-4

VRIJE UNIVERSITEIT

The role of the Fanconi anemia pathway in sporadic head and neck cancer

ACADEMISCH PROEFSCHRIFT

ter verkrijging van de graad Doctor aan
de Vrije Universiteit Amsterdam,
op gezag van de rector magnificus
prof.dr. V. Subramaniam,
in het openbaar te verdedigen
ten overstaan van de promotiecommissie
van de Faculteit der Geneeskunde
op vrijdag 11 december 2015 om 9.45 uur
in de aula van de universiteit,
De Boelelaan 1105

door

Chantal Stoepker

geboren te Den Helder

promotoren: prof.dr. H.P.J. te Riele
prof.dr. R.H. Brakenhoff

Voor Johan

Contents

Chapter 1 *9*
General introduction

Chapter 2 *49*
SLX4, a coordinator of structure-specific endonucleases, is mutated in a new Fanconi anemia subtype

Chapter 3 *73*
Whole exome sequencing reveals uncommon mutations in the recently identified Fanconi anemia gene *SLX4/FANCP*

Chapter 4 *85*
Mutations in *ERCC4*, encoding the DNA-repair endonuclease XPF, cause Fanconi anemia

Chapter 5 *105*
Defects in the Fanconi anemia pathway and chromatid cohesion in head and neck cancer

Chapter 6 *133*
DNA helicases FANCM and DDX11 are determinants of PARP inhibitor sensitivity

Chapter 7 *159*
Synthetic lethal interactions with FA deficiency identified by genetic screens in head and neck cancer cell lines

Chapter 8 *187*
Discussion

Summary *195*

Nederlandse samenvatting *201*

Addendum *207*
Curriculum Vitae
Dankwoord/Acknowledgements

CHAPTER 1

General introduction

Many thousands of toxic DNA lesions, such as mutations or breaks arise in each human cell every day[1–3]. While the majority of these lesions are induced by mutagenic by-products of normal cell metabolism or during DNA replication, they also occur due to exogenous sources (*e.g.* sunlight, radiation or cigarette smoke). Since DNA damage can have deleterious effects as it interferes with DNA replication and gene transcription, and can lead to permanent changes which might drive carcinogenesis, the cell is equipped with a variety of lesion-specific DNA repair mechanisms (*e.g.* base excision repair, nucleotide excision repair, mismatch repair, non-homologous end joining, homologous recombination and crosslink repair)[3]. The importance of DNA damage repair is further demonstrated by the finding that inherited mutations in DNA repair genes often predispose to cancer[2,3]. For example, individuals with mutations in any of the seventeen known genes involved in the rare genomic instability syndrome Fanconi anemia (FA) have a defect in DNA crosslink repair and are prone to develop acute myeloid leukemia (AML) and malignancies of the head and neck region[4–7]. Interestingly, patients with other diseases, such as the telomere maintenance disease Dyskeratosis congenita, have also an extremely high risk to specifically develop AML and head and neck tumors[4,8].

The study of cancer predisposition diseases has helped to reveal and understand biological mechanisms that secure genomic stability and prevent carcinogenesis. This is highlighted by studies of FA, which have elucidated important insights into cancer pathogenesis and chemotherapy resistance. In this chapter, general introductions on FA as well as the defective DNA repair mechanism in this syndrome are described. The aim of the research described in this thesis is to better understand the role of an FA-defect in the etiology of sporadic head and neck cancer and to which extent this defect can be exploited in anti-cancer therapy. Insights in the molecular pathogenesis of head and neck squamous cell carcinoma (HNSCC) are therefore also discussed.

1. Hallmarks and diagnosis of Fanconi anemia

Fanconi anemia was first described by and named after the Swiss pediatrician Guido Fanconi in the early 1900s[9]. In a case report published in 1927, he described a family in which three brothers had a blood picture which was typical of pernicious anemia and died[10]. They also suffered from several physical abnormalities, such as microcephaly, intensive brown skin pigmentation and hypoplasia of the testes. Later on it became clear that the disease is heterogeneous and characterized by a broad variety of congenital malformations, progressing bone marrow failure and increased cancer risk[11].

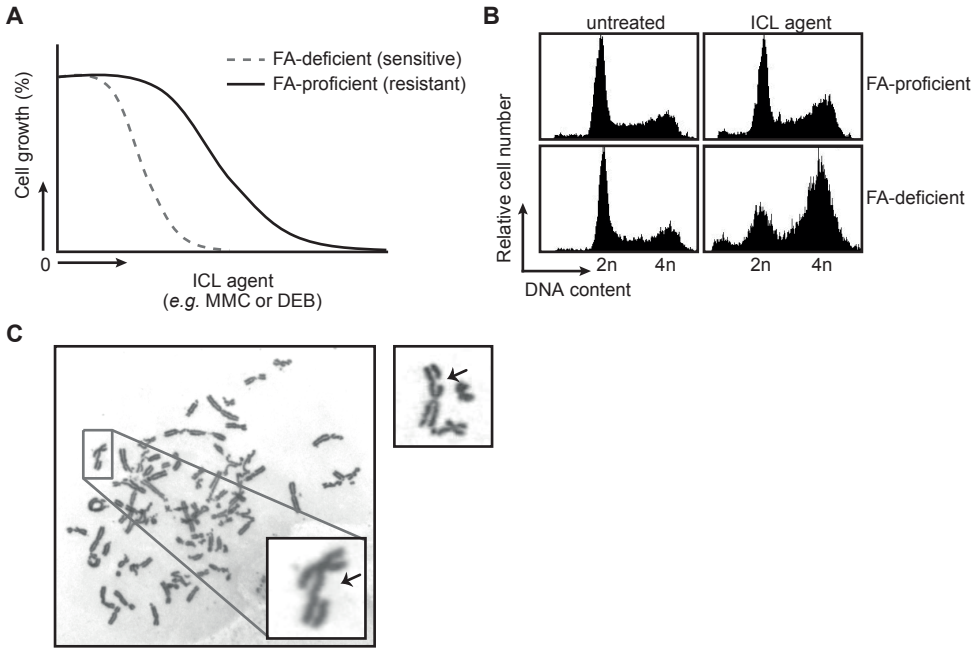

Figure 1 Hypersensitivity of FA-deficient cells to DNA interstrand cross-linking agents. Cells derived of FA patients are sensitive to DNA interstrand cross-linking (ICL) agents (*e.g.* mitomycin C (MMC) or diepoxybutane (DEB) in terms of growth inhibition (**A**), G2/M arrest (**B**) and chromosomal breakage (**C**). After treatment with an ICL agent, FA-deficient cells accumulate in the G2/M phase of the cell cycle and exhibit chromosomal aberrations, such as breaks and gaps.

1.1. The chromosomal breakage assay as the gold standard in diagnosing Fanconi anemia

The clinical manifestations of FA are highly variable[11]. Patients may present with an overall short stature, low birth weight, congenital abnormalities of the head (*e.g.* microcephaly), eyes (*e.g.* microphtalmia), skin (*e.g.* hyperpigmentation or café-au-lait spots) or abnormalities involving central nervous, gastrointestinal and skeletal system (*e.g.* absent or extra thumbs). The majority (75%-90%) of FA patients develops bone marrow failure during the first decade of life[12,13]. However, since physical abnormalities can be subtle or absent, hematological problems are often the first indication for FA and were the main cause of mortality. Several patients lack both the clinical manifestations of bone marrow failure and congenital abnormalities, and in these cases AML or head and neck squamous cell carcinoma (HNSCC) at a young age may be the first sign of FA. The variability of clinical symptoms and the low prevalence of the disease can make accurate diagnosis of FA difficult. However, at the cellular level FA patients have a single unifying feature; FA-deficient cells are hypersensitive to DNA interstrand cross-linking (ICL) agents (*e.g.* mitomycin C (MMC), diepoxybutane (DEB) and cisplatin (CDDP)) and to endogenous

aldehydes[14–16]. Upon treatment with these compounds, FA-deficient cells arrest in the G2 phase of the cell cycle and cells that managed to enter M phase exhibit many chromosomal aberrations, such as chromosome breaks, radials and gaps (**Fig. 1**). Therefore, this hallmark is used in the diagnosis of FA by performing a chromosomal breakage assay on T lymphocytes of suspected FA individuals[17]. Those individuals with a significant increase in the number of ICL-induced breaks are further screened for mutations in any of the 17 FA genes (further discussed in section 2). Conventional Sanger sequencing of all FA genes without first performing a chromosomal breakage test can also immediately be used in diagnosing FA. The high number of FA and FA-associated genes, some of which have many exons, makes Sanger sequencing time-consuming and costly, but it is beneficial if the specific mutation is known within an FA family. Although sequencing of all FA genes is not yet routinely used to test for FA, it is likely that next generation sequencing may become a valuable tool for FA genotyping in the future[18,19]. Nevertheless, to determine the pathogenicity of unclassified sequence variants in FA genes, the chromosomal breakage assay will still be relevant.

1.2. Complications of the chromosomal breakage test: diagnostic overlap and somatic mosaicism

Although the chromosomal breakage assay has been considered as the gold standard to test for FA, there are two complications. First, the chromosomal breakage assay is not entirely specific for FA and therefore, misdiagnosis may occur. MMC-induced chromosomal breakage has been observed in lymphocytes of individuals suffering from Nijmegen breakage syndrome, Roberts syndrome or Warsaw breakage syndrome[20–23]. Nijmegen breakage syndrome is caused by mutations in a DNA repair gene (*NBS1*), while the last two syndromes are caused by defective sister chromatid cohesion (see **box 1**).

Second, the presence of somatic mosaicism (reversion of a pathogenic allele to wild type) in hematopoietic progenitor cells from FA patients may hamper the interpretation of the chromosomal breakage data[24–26]. Somatic mosaicism results in two subpopulations of lymphocytes, one of which is hypersensitive to DNA interstrand cross-linking agents, while the reverted cells are not sensitive anymore. Somatic mosaicism is relatively common in FA patients (estimated at 10-30%) and can be caused by new compensatory DNA mutations in the affected genes (*e.g.* additional insertions/deletions that restore the reading frame), spontaneous genetic reversion of FA mutations (back mutations) or in case of compound heterozygous FA patients by intragenic mitotic recombination[24–27]. Occasionally, the number of reverted cells can reach such a high level in mosaic FA patients that a false negative result may occur. To avoid this complication, skin fibroblasts of FA patients can be

Box 1: Sister chromatid cohesion

During S phase identical DNA molecules (sister chromatids) are generated and hold together by a multiprotein complex, called cohesin. Sister chromatid cohesion is essential for the correct segregation of chromosomes during mitosis, but it also plays a role in DNA repair and transcription regulation[28]. Cohesin is a ring-shaped complex that consists of SMC1, SMC3, RAD21 and STAG1 or STAG2. In G1 phase, cohesin is loaded onto the DNA by the NIPBL-MAU2 heterodimer, while PDS5 and WAPL promote its unloading. Subsequently, in S phase, ESCO1/2 acetylate SMC3 and sororin is recruited, leading to establishment of cohesion (cohesin complexes are stably bound to chromatin and encircle the two sister chromatids). Finally, during mitosis cohesin is dissociated from the chromatin, which is mediated by phosphorylation events. These events can be counteracted by shugoshin 1 (SGO1) and its partner protein phosphatase 2A (PP2A) to fine tune the timely and correct release of cohesin during mitosis[28–30].

Sister chromatid cohesion defects can result in premature sister chromatid separation, causing aneuploidy. Germline mutations in genes involved in sister chromatid cohesion have been linked to several syndromes, collectively known as cohesinopathies. Roberts syndrome is caused by bi-allelic mutations in *ESCO2* (ref 31), while bi-allelic mutations in *DDX11* cause Warsaw Breakage syndrome[32]. Moreover, mutations in *SMC1A* (ref 33), *SMC3* (ref 34), *RAD21* (ref 35), *NIPBL*[36,37] and *HDAC8* (ref 38) are associated with a third cohesinopathy: Cornelia de Lange syndrome. Finally, mutations in genes involved in sister chromatid cohesion were detected in several tumor types. In particular, mutations in *STAG2* are frequently found in bladder cancer, but also in glioblastoma, Ewing's sarcoma and melanoma[30].

tested for ICL sensitivity, since mosaicism has not been observed in tissues other than blood[17].

2. Genetic basis of Fanconi anemia: 17 FA genes

Fanconi anemia is not only a heterogeneous disease with respect to the clinical features but also at the genetic level; mutations in several genes can cause FA[39–62]. This genetic heterogeneity among FA patients was revealed by cell fusion experiments between different FA cell lines (also known as complementation analysis). These cell lines were able to complement each other's ICL sensitivity, indicating the involvement of multiple genes[63]. Currently, seventeen complementation groups (FA-A, -B, -C, -D1, -D2, -E, -F, -G, -I, -J, -L, -M, -N, -O, -P, -Q and -S) representing seventeen separate FA genes are known (**Table 1**)[39–62]. Fanconi anemia is primarily inherited in an autosomal recessive pattern, except for complementation group B, in which *FANCB* mutations are inherited in an X-linked recessive manner[48]. Similar to other X-linked recessive syndromes in which males are much more frequently affected, no female FANCB patients have yet been reported.

2.1. Identification of presently known FA genes and their contribution to FA

Several approaches have been used to identify the presently known FA genes: complementation cloning (*FANCA*, *FANCC*, *FANCE*, *FANCF* and *FANCG*)[39,40,42–44], protein interaction studies by using co-immunoprecipitation followed by mass spectrometry (*FANCB*, *FANCL* and *FANCM*)[47,48,51], positional cloning (*FANCA*, *FANCD2*, *FANCI*, *FANCJ* and *FANCO*)[41,45,49,52,56], candidate-gene approaches (*FANCD1*, *FANCI*, *FANCN* and *FANCP* (see **Chapter 2** of this thesis))[46,53–55,57,58] and next generation sequencing (*FANCQ* (see **Chapter 4** of this thesis) and *FANCS*)[59,62]. *FANCC* was the first FA gene identified in 1992 (ref. 39), followed by *FANCA* in 1996 (refs. 40 and 41). Pathogenic mutations in these two genes together with mutations in *FANCG* are found in the majority of FA individuals (**Table 1**). It has been suggested that the *FANCA* gene might be hypermutable, whereas founder effects may explain the high numbers of FA-C and FA-G patients[11]. In contrast, for some complementation groups only a few patients have been described in literature. Remarkably, the first patient described belonging to complementation group FA-M has in addition to bi-allelic *FANCM* mutations, also bi-allelic mutations in *FANCA*[64]. Although this raised the question whether *FANCM* is an FA gene, correction of the FANCA-defect in lymphoblasts of this patient did not restore ICL sensitivity, indicating that the ICL-sensitivity did not depend on the *FANCA* mutation. Moreover, FANCM can interact with other FA proteins and is part of the FA core complex, consisting of eight FA proteins which are involved in mono-ubiquitination of FANCD2 and FANCI (further discussed in section 5.5). Taken together, this indicates that FANCM is important for ICL repair and plays a role in the FA pathway.

Besides FA patients with *FANCM* mutations, the occurrence of individuals with bi-allelic mutations in *FANCO*, *FANCQ* or *FANCS* is also rare (**Table 1**). Only one consanguineous family (2 affected individuals) with mutations in *FANCO* have been reported[56]. Of note, FANCO is a provisional term as individuals with mutations in *FANCO* (*RAD51C*) present with an FA-like syndrome: they have a milder ICL-induced chromosomal breakage phenotype and thus far they do not display bone marrow failure or cancer. Likewise, hematological problems were also absent in two patients with bi-allelic mutations in *FANCS*/*BRCA1* and, therefore, are also associated with an FA-like disorder[61,62]. Finally, in a small percentage of patients with FA-like symptoms no mutations were found in any of the 17 known FA genes, suggesting the involvement of more, yet to be identified, FA genes.

2.2. Different mutations in one gene can cause distinct clinical outcomes

One of the newest members of the FA protein family is FANCQ (also known as ERCC4/XPF)[59] (see **Chapter 4** of this thesis). Remarkably, mutations in the *FANCQ*/*ERCC4*/*XPF* gene have been associated with four different syndromes: Xeroderma pigmentosum (XP), XFE progeroid syndrome, Fanconi anemia and a syndrome with

combined features of XP and Cockayne syndrome (CS), termed XPCS[65].

The product of the *FANCQ/ERCC4/XPF* gene forms a complex with the DNA binding protein ERCC1 to function as a structure-specific DNA endonuclease[65]. This nuclease is involved in both ICL-repair as well as in the removal of sunlight-induced UV photolesions and bulky DNA adducts by nucleotide excision repair (NER)[65–67]. NER can be divided into two subpathways (global genome NER and transcription-coupled NER), and although these subpathways differ in their initial DNA damage recognition process, XPF acts in both pathways in the incision step near the adduct[68]. XPF is also responsible for the incisions that unhook the cross-linked nucleotide during ICL repair[69]. Since XPF is involved in both NER as well as ICL repair, the type of mutation in *XPF* and the balance between NER and ICL-repair activities dictates outcome[59]. *XPF* mutations that primarily affect NER will cause XP, while an FA manifestation is caused by mutations in *XPF* that disturb ICL-repair. Moreover, when both repair pathways are compromised, individuals will present with XFE or XPCS.

Table 1 Fanconi anemia genes

Gene	also known as	Chromosome location	First reported in	Percentage of patients
FANCA		16q24.3	1996	64.5
FANCB*	*FAAP95*	Xp22.2	2004	2.0
FANCC		9q22.32	1992	10.6
FANCD1	*BRCA2*	13q13.1	2002	2.5
FANCD2		3p25.3	2001	2.9
FANCE		6p21.31	2000	1.3
FANCF		11p14.3	2000	1.7
FANCG		9p13.3	1998	9.0
FANCI	*KIAA1794*	15q26.1	2007	1.5
FANCJ	*BRIP1/ BACH1*	17q23.2	2005	2.0
FANCL	*PHF9/ FAAP43*	2p16.1	2003	0.4
FANCM	*KIAA1596/ FAAP250*	14q21.2	2005	0.1
FANCN	*PALB2*	16p12.2	2007	0.6
FANCO[§]	*RAD51C/ RAD51L2*	17q22	2010	0.1
FANCP	*SLX4/ BTBD12*	16p13.3	2011	0.5
FANCQ	*XPF/ ERCC4*	16p13.12	2013	0.1
FANCS[#]	*BRCA1*	17q21.31	2013/ 2014	0.1

* X-linked recessive inheritance, § Individuals with mutations in RAD51C are associated with an FA-like syndrome as these patients did not yet develop bone marrow failure or cancer and their chromosomal breakage test showed less chromosomal aberrations compared to other FA patients. Therefore, *FANCO* is a provisional term. #Likewise, the two reported FA-S patients did not develop bone marrow failure yet and therefore bi-allelic mutations in *BRCA1* are also associated with an FA-like disorder. Data obtained from the Rockefeller University Fanconi Anemia database (www.rockefeller.edu/fanconi/).

3. Fanconi anemia and increased cancer risk

Approximately 75%-90% of FA individuals develop bone marrow failure during their first decades of life[12,13]. In addition, the incidence of other life-threatening hematological abnormalities, such as myelodysplastic syndrome and acute myeloid leukemia (AML), is also high in FA patients. Specifically, the risk to develop AML is 800-fold higher than in the general population, with a median onset age of 14 years[5,7]. Unless treated, the progressive depletion of normal bone marrow or the development of leukemia represents the primary cause of morbidity in FA patients. The treatment of choice for FA patients with severe bone marrow failure is hematopoietic stem cell transplantation. Since outcomes of bone marrow transplantations have improved tremendously, the next challenge that FA patients face is the high predisposition to develop solid tumors, in particular squamous cell carcinomas of the head and neck region, esophagus and anogenital area[5,12]. The risk for all solid tumors combined is approximately 50-fold higher than in the general population, whereas the susceptibility to develop HNSCC is even 500- to 700-fold higher[5–7]. Remarkably, the occurrence and the type of cancer can differ between the various FA complementation groups (**Table 2**). Patients with bi-allelic mutations in *FANCD1* (*BRCA2*) or *FANCN* (*PALB2*) have the most severe phenotype as they have a higher probability, different spectrum and earlier onset of malignancy. Unlike individuals of other FA complementation groups, these patients have a severe predisposition to develop childhood solid cancers, such as Wilms tumor (kidney cancer), neuroblastoma and medulloblastoma[46,54,55,70–74].

Inactivating mutations in some FA genes confer already susceptibility to cancer in monoallelic carriers (**Table 2**). Individuals with heterozygous germline mutations in *FANCD1* (*BRCA2*), *FANCJ*, *FANCN* (*PALB2*), *FANCO* (*RAD51C*) or *FANCS* (*BRCA1*) are prone to develop breast and ovarian cancer[75–81]. *FANCD1* (*BRCA2*) mutation carriers have also an increased risk of developing melanoma, prostate or pancreas cancer[82,83]. Pancreas cancer susceptibility is also seen in *FANCN* (*PALB2*) mutation carriers[84], and two recent articles showed a potential increased risk of breast and colorectal cancer for *FANCM* germline mutation carriers[85,86]. In conclusion, FA patients as well as some FA mutation carriers are prone to develop a tumor, demonstrating the important role of FA proteins in suppressing tumorigenesis.

4. DNA interstrand cross-linking agents in the treatment of cancer

ICL-inducing drugs, such as mitomycin C and cisplatin have remarkable anti-cancer properties and are widely used in the treatment of cancer. The ICL-inducing agent nitrogen mustard, which is also a well-known chemical warfare agent, was actually the first chemotherapeutic drug used in the treatment of cancer[87]. The idea to use this ICL agent for cancer treatment arose more than 60 years ago and originated from observations during the First World War. Autopsy findings from soldiers dying

of mustard gas showed severe suppression of hematopoiesis[88,89]. During World War II in 1943, these observations were extended after a German air raid bombed the US Merchant Ship S.S. *John Harvey*, which was anchored in the Italian harbor Bari and contained a secret cargo of sulphur mustard bombs. The attack caused the detonation of the bombs and no one aboard survived. Consequently, the inhabitants of Bari were not warned or aware that they were under attack by mustard gas. The survivors of the disaster became leukopenic, confirming the remarkable sensitivity of normal lymphoid tissue to the cytotoxic action of mustard gas[88]. One year before this disaster, Louis Goodman and Alfred Gilman were already assigned to investigate the potential therapeutic value of nitrogen mustard. They reasoned that nitrogen mustard might also have therapeutic possibilities for treating lymphomas, which they first validated

Table 2 Cancer types in FA patients and mutation carriers

Gene	Cancer type in FA individuals	Cancer type in mutation carriers
FANCA	AML, HNSCC, esophageal cancer, gynecological cancers and liver cancers	No cancers
FANCB	See FANCA	No cancers
FANCC	See FANCA	No cancers
FANCD1 (BRCA2)	AML, ALL, medulloblastoma, neuroblastoma and Wilms tumor	Melanoma, breast, ovarian, pancreatic and prostate cancer
FANCD2	See FANCA	No cancers
FANCE	See FANCA	No cancers
FANCF	See FANCA	No cancers
FANCG	See FANCA	No cancers
FANCI	See FANCA	No cancers
FANCJ	AML, HNSCC	Breast and ovarian cancer
FANCL	No cancer reported yet	No cancers
FANCM	No cancer reported yet	Breast and colorectal cancer
FANCN (PALB2)	AML, medulloblastoma, neuroblastoma, Wilms tumor and haemangioendothelioma	Breast, ovarian and pancreatic cancer
FANCO (RAD51C)	No cancer reported yet	Breast and ovarian cancer
FANCP (SLX4)	HNSCC (1 patient)	No cancers
FANCQ (XPF)*	Mutations that cause an FA phenotype are not yet associated with cancer, while XP causing mutations confer susceptibility to basal and squamous cell carcinoma of the skin	No cancers
FANCS (BRCA1)	Breast and ovarian cancer (both 1 patient)	Breast and ovarian cancer

*Depending on the type of mutation, individuals present with one of 4 syndromes: XP, FA, XFE progeroid syndrome or XPCS. Table adjusted from Kottemann and Smogorzewska[81].

with animal studies and later by treating a patient with lymphoma. Their findings were published in 1946 and opened new avenues in the treatment of cancer[87,90,91].

4.1. Different DNA interstrand cross-linking agents and sources

Nitrogen mustards (*e.g.* chlorambucil or melphalan) are still used in the treatment of cancer, in particular lymphoid tumors. In addition to nitrogen mustards, other classes of cross-linking agents, such as platinum compounds (*e.g.* cisplatin), mitomycin C and psoralens, have been identified[92,93]. Mitomycin C is an anti-cancer antibiotic isolated from *Streptomyces* and needs to be metabolized by the cell to become an active ICL-inducing agent, whereas psoralens form ICLs upon activation by UV irradiation. Cisplatin, discovered by Dr. Rosenberg in 1965 and the most widely used cross-linking drug today, does not require activation[94]. Rosenberg found that cisplatin inhibits bacterial cell division, which led to the hypothesis that cisplatin may also inhibit the proliferation of rapidly dividing cancer cells. The anti-cancer activity of cisplatin was indeed confirmed in a mouse model and it is now used either alone or in combination with radiotherapy or other anti-cancer agents in the treatment of a wide spectrum of solid tumors, including testicular, ovarian, head and neck as well as small-cell lung cancers[95,96]. Although cisplatin is one of the most effective anti-cancer drugs, major problems are the toxicity profile and the intrinsic resistance or the development of resistance in patients who initially responded to this therapy. The clinically acquired resistance can be caused by metabolic inactivation, increased DNA damage repair or decreased drug accumulation due to reduced uptake or increased efflux of cisplatin[97]. Of note, the various classes of cross-linking agents induce other damaging DNA lesions besides interstrand crosslinks, such as mono-adducts and intrastrand cross-links. Moreover, these chemotherapeutic drugs cause different numbers of ICLs: psoralens form the highest fraction of ICLs (up to 40%), whereas mitomycin C causes 5-10% ICLs and CDDP even less than 5%[92,98–100]. Although a small fraction of the DNA lesions induced by mitomycin C and cisplatin are ICLs, these lesions are believed to be the main determinant of toxicity as ICLs interfere with important cellular processes, such as DNA replication and transcription.

Undoubtedly, we did not evolve mechanisms of ICL repair to defend ourselves only against the toxic effects of chemotherapeutic agents. Moreover, FA patients have not necessarily been exposed to these drugs but nonetheless frequently develop congenital abnormalities and cancer, raising the question about the identity of the endogenous agent that generates FA-associated DNA damage. A potential source of endogenous cross-linking agents are by-products of normal cellular metabolism. For example, lipid peroxidation (oxidative degradation of lipids) causes the production of aldehydes, which are able to damage DNA. Aldehyde concentrations are also influenced by a high fat diet and alcohol use[101–104]. As expected, FA cells are indeed

sensitive to aldehydes (*e.g.* acetaldehyde and formaldehyde)[14,105–107], suggesting that the endogenous DNA damage caused by aldehydes is counteracted by the FA repair pathway. Another endogenous source that could be responsible for the generation of ICLs include abasic sites (site on DNA without a purine/ pyrimidine base), which can arise spontaneously (~10,000 sites per cell per day) or as an intermediate of base excision repair[108]. Spontaneous hydrolysis of the glycosidic bond in DNA causes abasic sites, which exist in equilibrium between a ring-open aldehyde and ring closed hemiacetal. The ring-open aldehyde can form ICLs by reacting with the exocyclic amino group of adenine or guanine residues on the opposite strand[108,109].

5. The FA pathway

The FA pathway (**Fig. 2 and Table 3**) is involved in the repair of replication blocking lesions (in particular ICLs) and can be divided into two components: an upstream part, which is required for mono-ubiquitination of FANCD2 and FANCI, and a downstream part that is not necessary for this posttranslational modification. Eight upstream FA proteins (FANCA, -B,-C, -E, -F, -G, -L and -M) together with several FA-associated proteins form the FA core complex, which functions as an E3 ubiquitin ligase to mono-ubiquitinate FANCD2 and FANCI. Mono-ubiquitination of these two FA proteins is believed to be a key event in the pathway and results in their localization to damaged chromatin, where they coordinate downstream repair events. Although repair of ICLs can occur in a replication independent way, the FA pathway is coupled to DNA replication[110,111]. Subsequent sections discuss the FA pathway and the different steps in ICL repair in more detail.

5.1. Step 1: Sensing of DNA interstrand cross-link damage by Fanconi anemia proteins

ICLs that covalently join both strands of a DNA double helix have always intuitively been regarded as absolute blocks for the replicative machinery, necessitating repair prior to resumption of DNA replication. Longstanding models of ICL repair indicated that the encounter of an ICL by a single replication fork initiates repair[112]. However, work based on replication of a crosslinked plasmid in *Xenopus laevis* egg extracts resulted in a new model in which collisions on both sides of an ICL are envisioned as the trigger for repair[110,113]. The stalled replication forks, either from one or both sides of an ICL, are recognized by the DNA translocase FANCM and its binding partners FAAP24, MHF1 (FAAP16) and MHF2 (FAAP10)[114–116]. Deletion of these proteins results in a cellular FA phenotype with reduced FANCD2 mono-ubiquitination, increased chromosomal breakage and ICL sensitivity. They can form three distinct complexes: one containing all 4 proteins (FANCM-FAAP24-MHF1/2), a heterodimer of FANCM-FAAP24 and a complex consisting of FANCM-MHF1/2, in

which multiple MHF1 and MHF2 proteins form a heterotetrameric structure[115,117,118]. The conserved HhH_2 domain at the C-terminus of FANCM enables FANCM to form a heterodimer with FAAP24, whereas the interaction with the MHF1/2 protein complex is mediated via the region following the helicase domain of FANCM[114–116]. Many studies have been performed to elucidate the binding preference of FANCM, FAAP24 and MHF1/2 to various DNA substrates. FANCM binds specifically to Holliday junctions and replication forks[119,120], whereas FAAP24 and MHF prefer to bind to single-stranded and double-stranded DNA, respectively[114–116,121]. Moreover, FAAP24 also displays affinity to splayed arm DNA and 3'-flap DNA, while the MHF complex, like FANCM, can bind to branched DNA structures (*e.g.* Holliday junctions and replication forks). This resulted in an initial model in which FANCM, FAAP24 and MHF simultaneously bind different parts of a stalled replication fork: FANCM at the branch point and FAAP24 and MHF at the surrounding ssDNA and dsDNA, respectively[115]. Two alternative models were suggested when, in addition to the DNA binding preferences of FANCM and its partners alone, the impact of the interaction between FANCM, FAAP24 and MHF1/2 on DNA binding activity was investigated. The DNA binding preference of FANCM was not affected by the presence of FAAP24 or vice versa[119], while the binding affinity of the MHF-FANCM complex changed. Although there is some discrepancy regarding the preference of MHF alone to bind to dsDNA over branched DNA (most likely depending on salt concentrations), the FANCM-MHF complex prefers and has an increased affinity to bind to branched DNA[122,123]. This resulted in two models: 1) both FANCM and MHF bind to the branch point of a stalled replication fork due to the remodeling activity of FANCM on MHF, thereby changing the DNA binding preference of MHF from dsDNA by MHF alone to branched DNA by the FANCM-MHF complex[122]. 2) MHF functions as a heterotetramer[117,118] and binds concurrently to the two DNA arms of a replication fork, followed by the recruitment and increased binding affinity of FANCM to the DNA junction[123]. Regardless of which model is true, both FAAP24 as well as the MHF heterotetramer are required for the localization of FANCM to the stalled replication fork to trigger repair or stimulate replication fork restart[116,124].

5.2. Step 2: Remodeling of the stalled replication fork and replication traverse by FANCM

Besides a role in sensing ICL-induced stalled replication forks, FANCM exerts multiple roles downstream this step in maintaining genome stability. First, biochemical studies have shown that FANCM contains an ATP-dependent branch point translocase activity, which promotes migration of Holliday junctions, replication fork reversal and D-loop dissociation[51,119,120,125]. The branch migration activity of FANCM is independent of FAAP24, while MHF exerts a stimulatory effect on FANCM's ability to process branched DNA structures[115,116,119]. As the result of the

combined branch migration and fork reversal activities of FANCM, replication fork regression occurs, providing an important mechanism to stabilize stalled replication forks or to allow repair factors to gain access to the replication-blocking lesion[125–127]. Thereby, FANCM is essential for constant progression of replication forks as well as for resumption of DNA replication after DNA damage[128]. Since accumulating evidence showed that replication fork collisions on both sides of an ICL are the trigger for repair[110,113,129], the remodeling activity of FANCM-MHF might aid in stabilizing the first stalled replication fork or promoting dormant origin firing until a second replication fork approaching from the opposite direction encounters the ICL.

As an alternative to an approaching replication fork from the opposite direction, replication traverse has been suggested[130]. This is a translocase-based mechanism in which DNA replication forks bypass ICLs without unhooking them (leaving the unrepaired ICL behind and allowing fork progression). Similar to the dual fork collision model, replication traverse will also result in an X-shaped DNA molecule that triggers repair[113,129,130]. Although it requires the translocase activity of FANCM-MHF1/2 complex and only takes a few minutes, it is unclear how DNA replication forks bypass or "traverse" ICLs. Possible scenarios could be the translocation of the MCM replicative helicase complex by FANCM (MCM complex jumps over the ICL) or a new MCM or a different replicative DNA helicase is recruited on the other side of the ICL[129,130]. However, the recruitment of a new MCM or other replicative DNA helicase is unlikely given the absence of known MCM loading mechanisms during S-phase. Of note, it has been demonstrated by using *Xenopus* egg extract that BRCA1 promotes unloading of the replicative helicase complex, which is an essential and early event in the repair of cross-links [131]. Finally, it is remarkable that FANCM and the MHF proteins are the only FA core complex proteins with orthologs in yeast[51,115], implying that the traverse activity as well as the branch migration activity of these proteins occurred before the emergence of the complete FA pathway.

5.3. Step 3: Checkpoint activation mediated by FAAP24

The third important step in repairing DNA ICLs is to allow enough time to repair the lesion before going to the next phase of the cell cycle. Several studies demonstrated a role of FANCM and FAAP24 in promoting intra-S-phase and G2-phase cell cycle arrest by checkpoint activation when a replication fork encounters an ICL (**Fig. 2**)[127,132,133]. However, comprehensive research of one research group showed that FAAP24 plays the primary role in checkpoint activation thereby stopping the cell cycle[133]. Activation of the checkpoint, which is mediated by the serine/threonine-specific protein kinases ATR and CHEK1, begins when a stretch of single-stranded DNA coated by RPA is generated as consequence of an ICL-induced stalled replication fork. ATRIP, a binding partner of ATR, binds to the RPA-coated ssDNA and recruits ATR[134]. Activation of these two proteins (ATR-ATRIP) requires

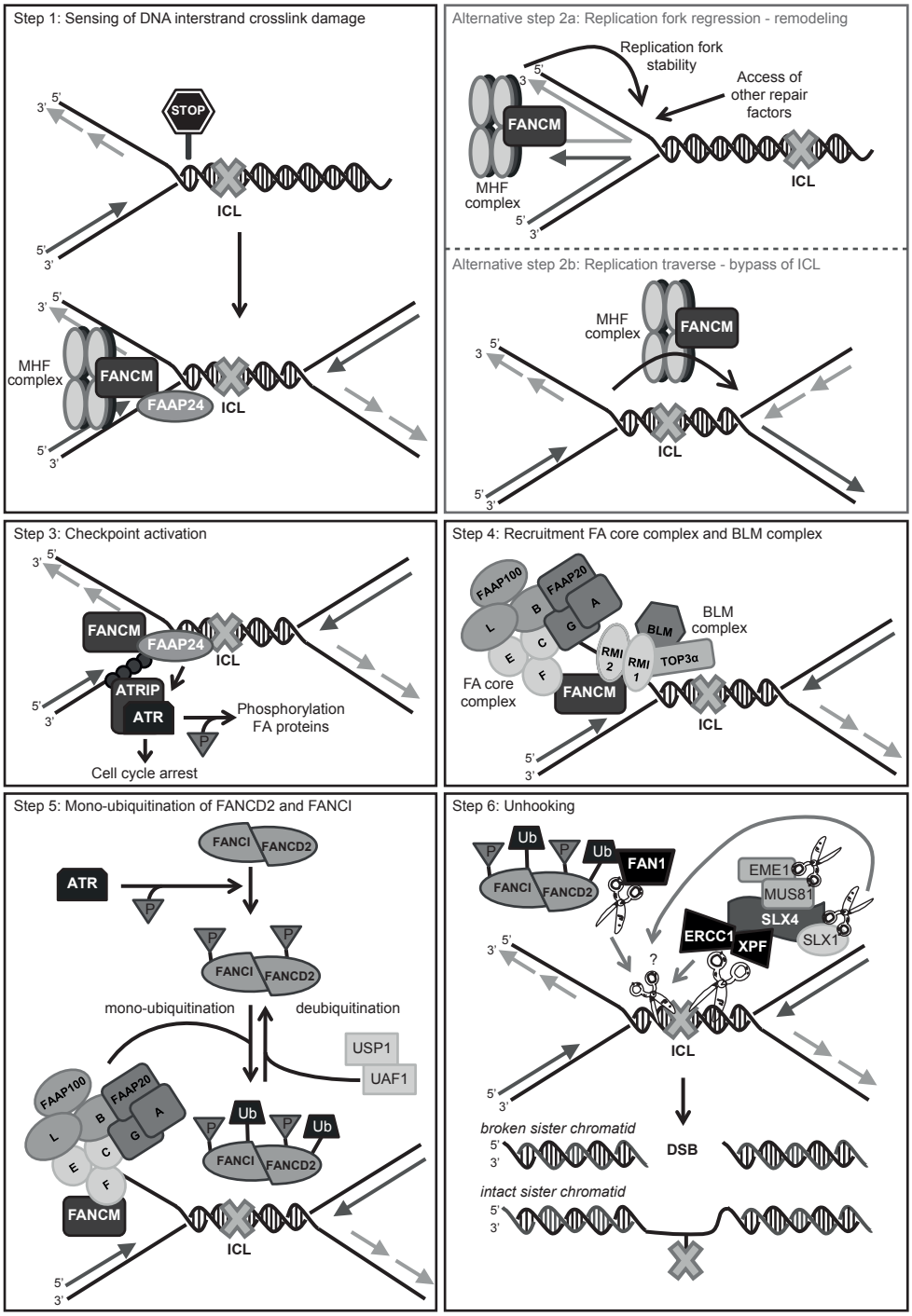
Step 1: Sensing of DNA interstrand crosslink damage
STOP
ICL
MHF complex
FANCM
FAAP24
Alternative step 2a: Replication fork regression - remodeling
Replication fork stability
Access of other repair factors
Alternative step 2b: Replication traverse - bypass of ICL
Step 3: Checkpoint activation
ATRIP
ATR
Phosphorylation FA proteins
Cell cycle arrest
Step 4: Recruitment FA core complex and BLM complex
FAAP100
FAAP20
BLM
BLM complex
RMI 2
RMI 1
TOP3α
FA core complex
Step 5: Mono-ubiquitination of FANCD2 and FANCI
FANCI
FANCD2
mono-ubiquitination
deubiquitination
USP1
UAF1
Ub
Step 6: Unhooking
FAN1
EME1
MUS81
SLX4
SLX1
ERCC1
XPF
broken sister chromatid
DSB
intact sister chromatid

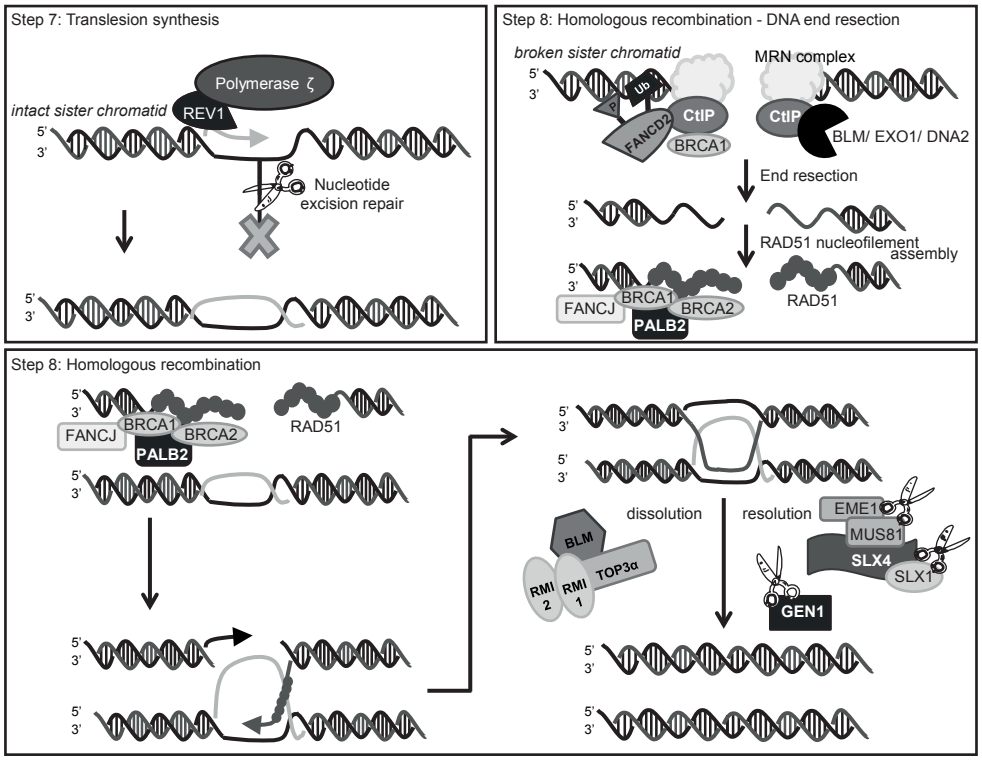

Figure 2 The Fanconi anemia (FA) pathway.
A stalled replication fork due to encountering of an interstrand crosslinks (ICL) will be detected by FANCM, FAAP24 and MHF1 and 2 (**step 1**). Given that an X shaped DNA molecule is the trigger for repair, FANCM-MHF1/2 complex may remodel the replication fork to stabilize the fork until a second replication fork approaching from the opposite direction encounters the ICL (**alternative step 2a**) or FANCM-MHF promotes replication traverse, in which the ICL is bypassed or "traversed" by the replicative MCM DNA helicase leading to replication fork progression. The precise mechanism is unclear and it could also be that a different DNA helicase is loaded onto the distal site of the ICL (**alternative step 2b**). FAAP24 activates ATR, which leads to activation of the intra-S-phase and G2/M checkpoints, allowing enough time to repair the DNA damage. In addition, ATR phosphorylates several FA proteins, such as FANCD2 and FANCI (**step 3 and 5**). FANCM recruits two protein complexes to the site of DNA damage: the FA core complex and the BLM complex (**step 4**). The FA core complex mono-ubiquitinates FANCD2 and FANCI, which is a central event in the FA pathway and is required for downstream repair events (**step 5**). Mono-ubiquitinated FANCD2 promotes incisions near the ICL. The different structure-specific endonucleases can interact with the scaffold protein SLX4 (FANCP). XPF (FANCQ) is the primary enzyme that makes the 3' incision to the ICL. The 5' side of the ICL may be incised by SLX1, FAN1 or even also XPF (**step 6**). As a consequence of unhooking, an intact but crosslinker damaged and a broken sister chromatid are generated. The intact sister chromatid is repaired by translesion synthesis, in which REV1 and Polymerase ζ (zeta) play an important role (**step 7**) combined with nucleotide excision repair, whereas the broken sister chromatid is repaired by homologous recombination (**step 8**). Homologous recombination is initiated by DNA end resection (facilitated by the MRN (MRE11, RAD50, NBS1) complex, CtIP, BLM EXO1 and DNA2), followed by RAD51 nucleofilament formation (mediated by BRCA1, BRCA2 and PALB2) and strand invasion. Finally, the Holliday junction that is generated during homologous recombination is dissolved by the BLM complex or resolved by SLX4-SLX1, MUS81-EME1 or GEN1.

additional regulators, such as the RAD17-RFC complex, the Rad9-Hus1-Rad1 (9-1-1) complex and TOPBP1 (refs. 135 and 136). The 9-1-1 complex is loaded onto DNA by the RAD17-RFC complex at the junction of ssDNA and dsDNA[137,138]. This is eventually followed by the recruitment of TOPBP1, which can interact with RAD17, the 9-1-1 complex and autophosphorylated ATR to increase the kinase activity of ATR and facilitate ATR to recognize its substrates[136,139–144]. Finally, the phosphorylation of ATR substrates (*e.g.* CHEK1) leads to intra-S-phase and G2/M checkpoint activation. The process of ATR activation by FANCM-FAAP24 is still not fully understood, but may occur: 1) via interaction with the checkpoint protein HCLK2, which facilitates ATR activation and CHEK1 stabilization[127,145,146], 2) through regulating RPA recruitment at ICL-induced stalled replication forks[132] 3) or by FANCM mediated TOPBP1 retention[147].

Interestingly, ATR or its downstream phosphorylation target CHEK1 appears to directly regulate the FA pathway by the phosphorylation of multiple FA proteins (FANCA, FANCD2, FANCE, FANCG, FANCI and FANCM)[148–158]. ATR-mediated phosphorylation of FANCM (S1045) is required to localize FANCM to ICLs and to mediate FANCM-FAAP24-dependent ATR/CHEK1 signaling[156]. Phosphorylation of FANCA (S1449 by ATR[154]), FANCD2 (T691, S717 by ATR/ATM[152] and S331 by CHEK1 (ref. 155), FANCE (T346 and S374 by CHEK1 (ref. 153), FANCG (S7 by CHEK1 (ref. 150) and FANCM (S1045 by ATR[156]) are required for resistance to ICL-inducing agents and facilitates the mono-ubiquitination of FANCD2 and FANCI, whereas phosphorylation of FANCI is even an absolute prerequisite for the mono-ubiquitination of FANCD2 (ref. 158). Thereby, this posttranslational modification step functions as a switch to stimulate FANCD2 mono-ubiquitination in order to activate the FA pathway.

5.4. Step 4: Recruitment of the FA core and Bloom's protein complexes by FANCM

Besides 1) sensing ICL damage, 2) remodeling ICL-stalled replication forks and 3) checkpoint activation, the fourth role of FANCM is the recruitment of two distinct protein complexes: the FA core complex and the Bloom's complex (**Fig. 2**)[51,124,159]. The FA core complex is responsible for mono-ubiquitination of FANCD2 and FANCI. Although FANCM and MHF are part of this large complex, the majority of FANCM-MHF does not associate with the FA core complex[115]. This further suggests that besides the recruitment of other FA proteins and stimulating FANCD2 mono-ubiquitination, FANCM and MHF1/2 have additional roles. Indeed, as mentioned before, FANCM and MHF1/2 are involved in both remodeling of stalled replication forks as well as replication traverse, which is independent of the FA core complex. Besides the FA core complex, FANCM can also interact with RMI1 and Topoisomerase IIIα to recruit the Bloom's complex (RMI1, RMI2, BLM and TopoIII) to the site of DNA damage[159]. This complex is also known as the dissolvasome as it is involved in the separation

of Holliday junctions that can arise as DNA intermediates during DNA repair[160]. BLM is a multifunctional protein involved in 1) DSB repair (*e.g.* via 5' end resection and resolving double Holliday junction (dHJ) structures)[161], 2) the suppression of sister chromatid exchanges[162] and 3) stimulating replication restart by promoting fork regression[163]. Interestingly, FANCM and BLM share similar functions as both, BLM deficiency and FANCM deficiency caused an increased frequency of sister chromatid exchanges[159,164,165] and both proteins have been implicated in replication fork progression. Therefore, the Bloom's protein complex might be recruited to ICL-induced stalled replication forks by FANCM to stimulate fork regression, followed by replication fork stabilization, or to mediate downstream steps of ICL repair (*e.g.* repair of DSBs or dHJ resolution)[159].

In summary, ICLs are recognized by the FA and FA-associated proteins FANCM, MHF1/2 and FAAP24, which have cooperative as well as unique functions[133]. All four proteins play an important role in the resistance to DNA crosslinking agents and the recruitment of the FA core complex. In addition, FANCM, MHF1 and MHF2 are also involved in replication fork remodeling and replication traverse, while FANCM-FAAP24 act in DNA damage-induced checkpoint activation.

5.5. Step 5: Mono-ubiquitination of FANCD2 and FANCI by the FA core complex

Mono-ubiquitination of the FANCD2-FANCI heterodimer is believed to be the central event in the FA pathway and is essential for downstream repair steps[81]. ATR-mediated phosphorylation of FANCI initiates mono-ubiquitination of FANCI and FANCD2 (ref 158). The post-translational modification of these two proteins is executed by a multisubunit E3 ubiquitin ligase complex, also known as the FA core complex, and the E2 ubiquitin conjugating enzyme UBE2T[166,167]. The FA core complex can be further divided into three subcomplexes: 1) the FANCA, FANCG and FAAP20 (A-G-20) subcomplex, 2) the FANCC, FANCE and FANCF (C-E-F) subcomplex and 3) the FANCB-FANCL-FAAP100 (B-L-100) subcomplex, which forms the catalytic module of which the RING domain protein FANCL bears the E3 ligase activity[47,167–169]. Although all three proteins of the B-L-100 complex are absolutely essential for mono-ubiquitination of FANCD2, it is unclear how FANCB and FAAP100 contribute to this post-translational modification[167,169]. Since the B-L-100 subcomplex is more active in FANCD2 mono-ubiquitination than FANCL alone, a conceivable role could be that FANCB and FAAP100 stimulate the E3 ligase activity of FANCL by stabilizing the protein or by supporting a conformation that enhances substrate recognition and positioning[167,169]. Moreover, the interaction of the FA core complex with chromatin probably enhances the activity of the complex further as mono-ubiquitination of FANCD2 is augmented by the presence of DNA[167].

The work of Huang *et al.*[169] and Rajendra *et al.*[167] showed unexpectedly that not all FA core complex members contribute equally to mono-ubiquitination of

FANCD2, of which the amount correlated with ICL sensitivity. Residual FANCD2 mono-ubiquitination was observed in DT40 cells or gene-targeted mammalian cells depleted of members of the A-G-20 or C-E-F subunits. This is in contrast to FA patient-derived cell lines, in which FANCD2 mono-ubiquitination is absent in all FA core complex complementation groups except for complementation group FA-M[64]. Despite these differences, the A-G-20 and C-E-F subunits are important and most likely contribute to activity, substrate recognition, specificity and localization of the complex to damaged chromatin[167,169]. Indeed, FANCF has been shown to interact with FANCM[159], thereby facilitating the localization of the FA core complex to ICL-induced stalled replication forks, whereas the A-G-20 subcomplex might be recruited via RNF8-mediated ubiquitination of histone H2A[170]. Besides stabilizing FANCA, FAAP20 contains an UBZ (ubiquitin binding zinc finger) domain capable of interacting with K63-linked ubiquitin chains on histone H2A, which are catalyzed by RNF8 and UBC13[170–173]. Thus, the A-G-20 and C-E-F subcomplexes might be independently recruited to ICLs via RNF8 or FANCM, respectively. However, the recruitment of the FA core complex could also be cell cycle dependent in which the RNF8-FAAP20 cascade plays a role in the recruitment of the FA core complex in a replication-independent manner, while FANCM, MHF and FAAP24 operate during S phase (replication-dependent recruitment)[170].

Finally, not only mono-ubiquitination of FANCD2 and FANCI is an essential step in the FA pathway, but also the deubiquitination of these proteins is important as disruption of either ubiquitination or deubiquitination results in abnormal DNA ICL repair[53,174–179]. The deubiquitination enzyme (DUB) USP1 (ubiquitin-specific protease 1) together with its binding partner UAF1 are responsible for deubiquitinating FANCD2 and FANCI[53,174,175]. Depletion of these proteins causes elevated levels of FANCD2 and FANCI mono-ubiquitination as well as cellular sensitivity to ICL agents[53,174,175,177]. Moreover, Usp1 knockout mice (of which a large percentage die soon after birth) recapitulate many phenotypical aspects of FA, including growth retardation, gonadal dysfunction, haematopoietic defects and ICL sensitivity[176,179]. An FA-like phenotype in terms of growth retardation, reduced fertility and ICL induced chromosomal instability was also observed in *Uaf1*$^{+/-}$ mice, whereas *Uaf1*$^{-/-}$ mice die during embryogenesis[178]. Taken together, protein ubiquitination as well as deubiquitination are important regulatory mechanisms for the repair of ICLs.

5.6. Step 6: Unhooking of the crosslink by structure-specific endonucleases

Mono-ubiquitination of the FANCD2-FANCI heterodimer is followed by incisions at both sides of the ICL in one of the cross-linked strands, which is also known as unhooking (**Fig. 2**). In the dual convergence and replication traverse models (see section 5.2.), the DNA structure around the ICL would be an X-shaped form. In the dual fork convergence model, the 3' ends of both converged leading strands initially

stall 20-40 nucleotides from the ICL, followed by the release of the MCM DNA replicative helicase mediated by BRCA1 (refs. 131 and 180). Subsequently, one leading strand advances to within 1 nucleotide of the ICL and the opposite parental strand is incised on either side of the ICL by structure-specific endonucleases[180]. Depletion of FANCD2 in *Xenopus* egg extract or failure to mono-ubiquitinate FANCD2 prevents unhooking of the crosslink, demonstrating the importance of mono-ubiquitinated FANCD2 to promote incisions near the ICL[181]. Six nucleases (XPF-ERCC1, MUS81-EME1, SLX1, FAN1, SNM1A and SNM1B) have been implicated in ICL repair as deficiency in any of these six nucleases leads to cellular hypersensitivity to ICL-inducing agents[129,182–192]. XPF-ERCC1, MUS81-EME1, SLX1 and FAN1 have structure-specific endonuclease activity and might be responsible for the incisions near the crosslink, while SNM1A and SNM1B possess exonuclease activity, which might be required after the primary incisions at the crosslink are made[192]. Besides endonuclease activity, FAN1 also exhibits 5'- 3'exonuclease activity[112].

Through direct interaction, the scaffold protein SLX4/FANCP acts as a docking platform for the recruitment of three endonucleases (XPF-ERCC1, MUS81-EME1 and SLX1) to the site of DNA damage[185,189,191]. Since SLX4 contains two tandem ubiquitin-binding zinc finger (UBZ) domains, which can bind to ubiquitin, it is tempting to speculate that SLX4 binds to mono-ubiquitinated FANCD2 and thereby, regulates the unhooking step by the recruitment of structure-specific endonucleases. This has indeed been shown in chicken DT40 cells, in which the UBZ domain of SLX4 is responsible for the interaction with ubiquitinated FANCD2[193], but could not be recapitulated in human cells[194]. Nevertheless, one of the UBZ domains of SLX4 is important to localize SLX4 to the site of damage, but the ubiquitinated ligand in question seems not to be FANCD2 in human cells[194].

Based on DNA substrate preferences, XPF-ERCC1 and MUS81-EME1 are likely candidates to cut on the 3' side of an ICL-associated X-shaped DNA structure, while SLX1 and FAN1 might prefer the 5' side[112]. Accumulating evidence suggests that XPF-ERCC1 is the most likely nuclease to unhook a DNA crosslink in the context of the FA pathway, while MUS81-EME1 probably cleaves ICL-induced stalled replication forks when normal fork processing is disrupted, resulting in an accumulation of double strand breaks[192,195,196]. First, the interaction of SLX4 with XPF-ERCC1 is important for ICL repair, whereas the interaction of SLX4 with MUS81-EME1 is dispensable for repairing crosslinks[197]. Moreover, the interaction of XPF-ERCC1 with recombinant mini-SLX4 (encompassing the N terminal domain, only capable of binding to XPF-ERCC1), enhances the nuclease activity of XPF-ERCC1 towards splayed arm and ICL-containing structures[198]. Secondly, MUS81 depleted cells are less sensitive to ICL-inducing agents compared to XPF-depleted cells[112]. Thirdly, work based on replication of a crosslinked plasmid in *Xenopus* egg extract indeed showed that depletion of XPF, but not of MUS81 prevented the incisions near the crosslink[69].

Since neither of the two incisions (3' or 5' incision) occur in XPF-depleted *Xenopus* egg extracts, XPF might be responsible for both incisions. Alternatively, the 5' incision cannot take place without the 3' incision and is actually made by a different endonuclease (*e.g.* SLX1 or FAN1), which requires prior incision by XPF-ERCC1 on the 3' side of the ICL-associated X-shaped structure before it can cut the 5' side[129]. Of note, FAN1 contains an UBZ4-type ubiquitin binding domain which can interact with mono-ubiquitinated FANCD2 (refs. 186–188 and 190). Although FAN1 deficiency results in ICL sensitivity, FAN1 inactivation does not lead to FA but to chronic kidney disease[199,200]. Collectively, these data suggest that FAN1 might function in ICL repair, but the precise role of FAN1 as well as of SLX1 is unclear.

5.7. Step 7: translesion synthesis

An intact as well as a broken sister chromatid are generated as a consequence of flanking incisions near an ICL. The intact sister chromatid is repaired by DNA translesion synthesis (TLS) (**Fig. 2**). This is a mechanism in which specialized low fidelity polymerases bypass bulky damaged lesions that block the processivity of normal replicative polymerases[201–203]. By using the *Xenopus* replication system, it was shown that in addition to the nucleolytic incisions, FANCD2 mono-ubiquitination is required for facilitating the TLS step in ICL repair[181]. Several TLS polymerases, including polymerase eta (Pol η/ POLH), polymerase iota (Pol ι/ POLI), polymerase kappa (Pol κ/ POLK), REV1, polymerase zeta (Pol ζ/ POLZ) and polymerase nu (Pol ν/ POLN), have been implicated in ICL repair[202]. Based on biochemical studies, these polymerases are capable of inserting a base opposite the unhooked ICL and/ or are responsible for extension of the nascent DNA beyond the crosslinked base pair, though the efficiency is dependent on the structure and the extent of endo- or exonucleolytic processing of the ICL[202,204,205]. REV1 and polymerase ζ, which consists of the catalytic subunit REV3L and accessory subunit REV7, are key players in ICL repair as cells deficient in either one of these proteins are hypersensitive to ICL-inducing agents[180,206–214]. REV1 is a deoxycytosine monophosphate (dCMP) transferase that can insert a cytosine opposite an unhooked ICL, which is then extended by polymerase zeta[215–217]. The bypassed crosslink is subsequently removed by nucleotide excision repair (**Fig. 2**)[109]. Of note, similar to Rev1-deficient cells, FA patient cells are hypomutagenic in response to UV[218] and a lower frequency of spontaneous point mutations was observed in FANCC-depleted chicken DT40 cells[211]. These results further suggest that the FA pathway is important for mediating error prone TLS. The role of Polymerase zeta in replication-dependent ICL repair was supported by studying ICL repair in Rev7-depleted *Xenopus* egg extract[180]. In the absence of Rev7, ICL repair was defective due to absence of the TLS extension step, while the nucleotide opposite the ICL was still inserted, most likely by Rev1 (ref. 180). By using a non-replicating plasmid-based reporter assay, it was also demonstrated

that REV1 and Pol ζ are involved in bypass of psoralen, MMC or cisplatin site-specific ICLs in a replication-independent manner[213,219]. In the G0/G1 phase of the cell cycle, TLS polymerases are recruited to ICLs by ubiquitinated proliferating nuclear antigen (PCNA)[202,220–222], whereas the coordination of TLS polymerases to the site of damage in S phase is less clear-cut, though a role of FAAP20 in recruiting REV1 has been suggested[173]. Of note, Pol η, Pol κ or Pol ν have also been implicated in ICL repair and cells deficient in one of these polymerases display an FA phenotype in terms of sensitivity to ICL-inducing agents[204,223–232]. However, the precise role of these polymerases in ICL repair is unclear, but these polymerases might play a minor role in the repair of crosslinked DNA depending on the structure of the ICL or in specific pathways or situations[109].

5.8. Step 8: homologous recombination

The intact sister chromatid, which is generated by the incision events, is repaired by translesion synthesis, whereas the broken sister chromatid is repaired by homologous recombination (HR) using the sister that has been repaired by TLS as a template[81,109]. Several FA proteins that operate downstream of FANCD2 mono-ubiquitination are implicated in HR, including FANCD1 (BRCA2), FANCJ, FANCN (PALB2), FANCO (RAD51C) and FANCS (BRCA1). Homologous recombination repair (HRR) is initiated by end resection of the double strand break by nucleolytic degradation of the 5' strand[233,234]. This is performed by the combined action of CtIP and the MRN (MRE11-RAD50-NBS1) complex, together with BLM, EXO1 and DNA2 refs. 235 and 236). Remarkably, CtIP can interact with two FA proteins: mono-ubiquitinated FANCD2 (refs. 237–239) and when phosphorylated with BRCA1 (ref. 240). These interactions aid in the recruitment of CtIP to DSBs generated during ICL processing[237–239], accelerates CtIP-mediated end resection[241] and in turn favor repair of these breaks by HR[234,242]. As a consequence of end resection, the 3' single-stranded stretch of DNA is initially coated by replication protein A (RPA), and subsequently displaced by the key facilitator of HR, RAD51, to form long helical polymers wrapped around the ssDNA tail[243,244]. The assembly of RAD51 nucleofilaments specifically onto ssDNA protected by RPA requires the help of a variety of mediator proteins, including several FA proteins, such as BRCA1 (FANCS), BRCA2 (FANCD1), PALB2 (FANCN) and RAD51C (FANCO)[245–247]. Besides the interaction with CtIP, BRCA1 can also directly interact with PALB2 (refs. 248 and 249) and FANCJ[77]. Since PALB2 binds in addition directly to BRCA2 and RAD51 (refs. 247, 250 and 251), PALB2 not only mediates the localization of BRCA2 and RAD51 to the site of damage, but it also bridges BRCA1-BRCA2 interactions[248,249]. Evidence also supports a role for FANCJ in homologous recombination, but it is still unclear at what step and how FANCJ precisely participates in HRR. BRCA2 and PALB2 are both essential for the specific assembly and stability of RAD51 nucleofilaments, thereby stimulating RAD51-

mediated strand exchange[250–260]. This strand invasion into an intact homologous DNA molecule (in case of ICL repair: the sister chromatid that has been repaired by TLS) results in the formation of a displacement D-loop, followed by DNA synthesis of the ssDNA ends to generate a double Holliday junction (HJ) intermediate[244]. Finally, this double HJ intermediate is dissolved by the BLM-RPM-TOP3α complex, which is plausibly recruited to the site of damage by FANCM, or resolved by structure-specific endonucleases (*e.g.* SLX4-SLX1, MUS81-EME1 or GEN) that cleave symmetrically HJs[261].

Table 3 Function of FA proteins

Protein	Function
FANCA	Part of FA core complex; mono-ubiquitinates FANCD2-FANCI
FANCB	Part of the catalytic module of the FA core complex, mono-ubiquitinates FANCD2-FANCI
FANCC	Part of FA core complex; mono-ubiquitinates FANCD2-FANCI
FANCD1 (BRCA2)	Homologous recombination; loads RAD51 onto DNA
FANCD2	Coordinates downstream repair events
FANCE	Part of FA core complex; mono-ubiquitinates FANCD2-FANCI
FANCF	Part of FA core complex; mono-ubiquitinates FANCD2-FANCI
FANCG	Part of FA core complex; mono-ubiquitinates FANCD2-FANCI
FANCI	Coordinates downstream repair events
FANCJ	Homologous recombination, 3'-5' helicase; unwinds G-quadruplex structures
FANCL	Part of the catalytic module of the FA core complex (FANCL bears E3 ligase activity) , mono-ubiquitinates FANCD2-FANCI
FANCM	Part of FA core complex, recruits FA core and BLM complex to site of damage; 5'-3' translocase and checkpoint activation
FANCN (PALB2)	Homologous recombination; localizes and promotes BRCA2 function
FANCO (RAD51C)	Homologous recombination
FANCP (SLX4)	Scaffold protein for several endonucleases: XPF-ERCC1, MUS81-EME1 and SLX1
FANCQ (XPF)	Structure-specific endonuclease involved in unhooking ICL, role in nucleotide excision repair
FANCS (BRCA1)	Homologous recombination, DNA repair pathway choice, unloading replicative helicase complex
FAAP10-FAAP16 (MHF1-MHF2) complex	Stimulates branch migration and replication fork reversal activities of FANCM Recruitment of FANCM to chromatin Stabilizes FANCM and FAAP24 Required for optimal FANCD2 mono-ubiquitination
FAAP20	Part of FA core complex; mono-ubiquitinates FANCD2-FANCI, stabilizes FANCA
FAAP24	ATR-dependent checkpoint activation upon ICL damage
FAAP100	Part of the catalytic module of the FA core complex, mono-ubiquitinates FANCD2-FANCI

6. HNSCC

Bi-allelic germline mutations in FA genes predispose to head and neck cancer: FA patients have a more than 500 to 700 times higher risk to develop HNSCC than an unaffected individual. These tumors are often located within the oral cavity, *e.g.* at the edge of the tongue and the gingival areas[6]. Other etiological factors in the development of head and neck cancer and the molecular carcinogenesis of HNSCC are described in this section.

6.1. Smoking, alcohol consumption and HPV infection as underlying cause of HNSCC

Despite familial predisposition to HNSCC, most head and neck tumors seem to occur sporadically. These tumors account for more than a half million new cases a year, making HNSCC the sixth common cancer by incidence worldwide[262]. The two most important risk factors for the development of head and neck cancer are tobacco use and excessive alcohol consumption, which have a synergistic effect. In addition to these exogenous risk factors, infection with high-risk types of human papilloma virus (HPV) is causative for a subset of head and neck cancers[263,264]. The presence of HPV is particularly common in tumors that arise in the oropharynx, which are associated with a favorable outcome[265–268]. The incidence of these tumors is increasing in most European countries including the Netherlands, as well as the United States[269–272]. Given that infection with high-risk HPV is also a well-known etiologic factor in cervical carcinogenesis[273], a change in sexual behavior (*e.g.* increase in practice of oral sex) might explain the observed increase[274]. Of note, an early study showed that many head and neck tumors in FA patients were HPV-positive[275]. However, the assay that was used to detect HPV was likely too sensitive, which may have resulted in many false positive cases. The association between HPV and HNSCC in individuals affected with FA could not be confirmed in other studies, suggesting that HPV might not be the main cause of head and neck cancer in FA patients[276,277]. Notwithstanding, the data on the role of HPV in anogenital tumors in FA patients are concordant, and the large majority of these tumors are HPV-positive. Hence, preventive vaccination is still encouraged. FA patients are advised not to smoke or use alcohol, but it is often difficult for young adults to follow this. The danger of alcohol consumption for FA patients is now better understood by recent evidence showing that FA-deficient cells are hypersensitivity to acetaldehyde, which is a byproduct of alcohol metabolism. Thus, alcohol consumption may increase genomic instability in these cells, and thereby might promote carcinogenesis in FA patients[14,107].

6.2. Genetic predisposition to head and neck cancer

Besides FA, there are several other syndromes associated with an increased risk of

head and neck cancer. Patients with Dyskeratosis congenita (DC), an inherited bone marrow failure syndrome clinically similar to FA, have a relative risk of more than 1100-fold for HNSCC[4]. Currently, mutations in nine genes (*DKC1*, *TINF2*, *TERC*, *TERT*, *WRAP53* (*TCAB1*), *CTC1*, *RTEL1*, *NHP2* and *NOP10*) leading to aberrant telomere biology have been reported to be causative of DC[278]. A second syndrome associated with an increased risk of HNSCC, but also of melanoma and pancreatic cancer, is familial atypical multiple mole melanoma (FAMMM), which is caused by an inactivating germline mutation in *CDKN2A*, encoding the p16 protein involved in cell cycle regulation[279,280]. The *CDKN2A* gene is often mutated or deleted in a wide variety of malignancies, emphasizing its important role as a tumor suppressor gene. The third gene in which a mutation leads to an unusually high risk of head and neck cancer is *ATR*[281]. In this gene, a specific heterozygous missense mutation was found in individuals affected with familial cutaneous telangiectasia and increased cancer risk. This mutation predominantly predisposes to oropharyngeal cancer as 10 out of 24 affected individuals (all part of one family) developed this tumor. Rare germline mutations in *ATR* have also been reported in Seckel syndrome-1 (SCKL1), which is an autosomal recessive disorder characterized by growth retardation, dwarfism, microcephaly, mental retardation and the characteristic "bird-headed" facial appearance, but not by an increased cancer risk[282]. However, one specific mutation and only five individuals with SCKL1 belonging to two related families have been described, making it uncertain whether the clinical phenotype of ATR deficiency has been fully identified. Furthermore, germline mutations in *TP53* or *BLM* are associated with Li-Fraumeni syndrome or Bloom syndrome, respectively, and predispose to a variety of cancers, including HNSCC. Finally, a role for hereditary susceptibility factors in the development of HNSCC is suggested by the observation that first-degree relatives of patients with HNSCC have an increased incidence to develop head and neck cancer as well[283–285]. This might be explained by the inheritance of genetic polymorphisms in genes affecting the function of carcinogen activating or detoxifying enzymes (*e.g.* cytochrome P450 group, *GSTM1*, *ALDH2*), or functioning in the apoptotic pathway (*e.g. BIRC5*) or DNA repair pathways (*e.g. XRCC1* and *XPD*)[285–287].

6.3. Treatment of patients with head and neck cancer

HNSCCs are staged according to the tumor dimensions and growth patterns as well as the dimension and number of lymph node metastasis in the neck and at distant sites. Depending on the stage and site of the disease, patients with sporadic HNSCC are treated with surgery, radiotherapy, chemotherapy or a combination of these modalities. About one third of HNSCC patients presents with early stage disease and is treated either by surgery or radiotherapy alone[288]. Patients with advanced disease stages, representing two third of HNSCC patients, require a

multi-modality treatment approach, in which surgery is frequently combined with postoperative radiotherapy and/or chemoradiation. The latter consists of systemic cisplatin administration combined with locoregional radiotherapy and is, combined with surgery for salvage, increasingly performed to achieve organ-preservation. Cisplatin is very toxic and causes nausea and vomiting, myelosuppression, renal failure and deafness. Particularly when combined with concomitant radiotherapy also severe mucositis and tissue damage may occur leading to long term sequelae such as feeding tube dependence. For patients who are unfit to receive cisplatin, bioradiation can be applied, which consists of the concomitant application of cetuximab (anti-EGFR antibody) and radiotherapy[289]. In contrast to patients with early-stage tumors, those with advanced malignancies have a poor prognosis and only 40-50% will survive for 5 years after treatment[288]. These survival rates are poor because patients often develop locoregional recurrences, distant metastases and second primary tumors. The latter relates to the phenomenon of "field cancerization" and incomplete resection of genetically altered mucosal changes. HPV-induced head and neck cancers have a very favorable prognosis, and several clinical trials to de-intensify therapy have been initiated.

The survival outcomes for FA patients with HNSCC are relatively poor due to limited treatment options. Chemoradiation is excluded for the treatment of HNSCC in FA patients as all cells of these patients are very sensitive to cisplatin. Even reduced cisplatin dosing results in very high toxicities and organ failure followed by a fatal outcome. Severe complications are also observed after radiotherapy. Therefore, the mainstay of treatment for FA HSNCC patients is surgery, preferably at an early stage, eventually combined with postoperative radiotherapy[290]. FA patients seem not to have additional toxicity profiles for cetuximab, indicating that bioradiation or adjuvant cetuximab treatments are reasonable alternatives[291]. The lack of peer reviewed meta-analyses on the treatment results of HNSCC in FA patients hampers the development of international guidelines for this specific patient group.

6.4. Molecular carcinogenesis of HNSCC

A better understanding of the molecular pathogenesis of sporadic as well as FA head and neck cancer may lead to novel strategies for early diagnosis and anti-cancer therapies as well as improved tailoring of existing treatment options for the individual patient. Because bone marrow transplantation outcomes have substantially improved over the past decades, more FA patients survive long-term and face the very high risk of developing head and neck cancer[290].

A plethora of studies, including genome-wide exome sequencing projects and a comprehensive multi-platform characterization of hundreds of head and neck tumors performed by The Cancer Genome Atlas, has appeared on the identification of genetic and epigenetic changes causing HNSCC[288,292–295]. These changes lead to

cancer-related phenotypes, the so called hallmarks of cancer, which encompass limitless replicative potential, self-sufficiency in growth signals, insensitivity to anti-growth signals, ability to evade apoptosis, invasion and metastasis, angiogenesis, deregulation of cellular energy metabolism and evasion of immune destruction[296,297]. Most genomes of head and neck tumors are highly unstable with many copy number alterations (CNA) (deletions or amplifications) and structural aberrations (chromosomal fusions). Chromosome regions 3p, 8p and 18q are frequently lost in HNSCC, whereas 3q, 5p and 8q are often gained[288,292,294,295]. In contrast to CNAs of whole chromosome arms, changes in copy number of small regions were also observed: co-amplifications of 11q13 and 11q22 (harboring genes implicated in cell cycle regulation (*CCND1*), cell death (*BIRC2*) and Hippo pathway signaling (*YAP1*)), focal amplifications of 3q26/28 (involving *TP63*, *SOX2*, two squamous lineage transcription factors and the oncogene *PIK3CA*, which plays a role in cell growth, survival, proliferation and differentiation in response to various growth factors), focal amplifications of 7p11.2 and 17q12 (containing growth factor receptors *EGFR* and *ERBB2*) and focal deletions of 9p21.3 (which is the location of the cell cycle regulator *CDKN2A*)[288,292,294,295]. In addition, numerous genes were significantly found mutated in head and neck cancer, such as *TP53*, *CDKN2A*, *HRAS*, *PTEN*, *PIK3CA*, *SMAD4*, *NOTCH1*, *CASP8*, *FAT1*, *FBXW7*, *AJUBA* and *NSD1* (for an overview of gains and losses and mutations, see **Table 4**)[288,292,294,295]. Of note, many mutated genes were located in regions of CNAs, often leading to loss of heterozygosity[292,295].

Although more than 95% of sporadic head and neck cancers are squamous cell carcinomas, the disease is heterogeneous and several subclasses of HNSCC exist at the histological and genetic level[288]. Different genetic changes as well as distinctive prognostic implications were observed between HPV-infected and non-infected tumors, whereas a second divergence is based on karyotyping and ploidy analysis. This results in three subgroups of HNSCC: 1) HPV positive tumors; 2) HPV negative tumors, which are aneuploid and have many CNAs; and 3) a small group of (near)-diploid tumors without CNAs[288,292,298–300]. The last subgroup is likely driven by mutation rather than CNAs and contain a three-gene pattern: activating mutations in *HRAS* (role in cell division in response to growth factor stimulation), inactivating mutations in *CASP8* (role in apoptosis) and wild type *TP53*[292,300,301]. Although *TP53* is the most commonly mutated gene in HNSCC, mutations in *TP53* are rare in HPV-positive tumors[288]. This is not surprising as inactivation of the tumor suppressor protein p53 in HPV-infected HNSCC is achieved by the expression of viral oncoprotein E6, which binds p53 and targets the protein for degradation[302,303]. Likewise, inactivation of *CDKN2A* by mutations, methylation or loss of 9p21 and/or amplification of *CCND1*, leading to deregulation of the RB pathway and driving the G1-S phase transition of the cell cycle, is also rare in HPV-positive tumors, because the viral oncogene E7 destabilizes the retinoblastoma protein (pRb)[288].

Table 4 Common genetic changes in HNSCC

Gene	Affected pathway	Chromosome location	Predominant in tumor type	Genetic change
CASP8	Apoptosis	2q33.1	(Near)-diploid	Mutations
TP63	Squamous lineage transcription factor	(3q26/28) 3q		(Focal) amplification
SOX2	Squamous lineage transcription factor	(3q26/28) 3q		(Focal) amplification
PIK3CA	PI3K/AKT signaling pathway	3q		Amplification Activating mutations
FBXW7	E3 ubiquitin protein ligase, involved in the degradation of MYC and NOTCH1	4q31.3		Mutations
FAT1	WNT/β-catenin signaling; role in cell migration and invasion	4q35.2	HPV-	Mutations
NSD1	Histone 3 lys 36 (H3K36) methyltransferase	5q35.2		Mutations
EGFR	Growth factor receptor	7p11.2		Focal amplification
MYC	Transcription factor, role in cell cycle progression	8q	HPV-	Amplification
CDKN2A	Cell cycle inhibitor/ regulator	9p21.3	HPV-	Focal deletion Mutations Methylation
NOTCH1	Squamous cell diferentiation	9q34.3		Mutations
PTEN	PI3K/AKT signaling pathway	10q23.31		Mutations
HRAS	MAPK/ERK pathway	11p15.5	(Near)-diploid	Activating mutations
CCND1	Cell cycle regulation	11q13 and 11q22	HPV-	Co-amplification
BIRC2	Cell death	11q13 and 11q22	HPV-	Co-amplification
YAP1	Hippo pathway signaling	11q13 and 11q22		Co-amplification
AJUBA	WNT/β-catenin signaling, role in cell division and implicated in Hippo pathway signaling	14q11.2	HPV-	Mutations
TRAF3	Role in innate and acquired anti-viral responses, involved in NF-κβ activation	14q32.32	HPV+	Mutations
TP53	Role in genome maintenance	17p13.1	HPV-	Mutations
ERBB2	Growth factor receptor	17q12		Focal amplification
SMAD4	TGF-beta signaling	18q 18q21.2		Loss Mutations
E2F1	Cell cycle regulation (HPV associated)	20q11.21	HPV+	Focal amplification

Moreover, HPV-positive tumors were distinguished by focal amplifications of *E2F1* (also involved in the G1-S phase transition) and deletions and truncating mutations in *TRAF3*, which plays a role in innate and acquired anti-viral responses[304] and of which loss deregulates NF-κB signaling[292].

Taken together, by (epi)genetic changes many pathways are affected resulting in deregulated cell cycle progression (HPV infection, inactivation of *TP53* and *CDKN2A*, overexpression of CCND1 and E2F1), evasion of apoptosis (deregulated NF-κB signaling, inactivation of *BIRC2*, *CASP8* or *TRAF3*), aberrant cell polarity and differentiation (inactivation of *NOTCH1*, *AJUBA* and *FAT1* causing aberrant Wnt/β-catenin signaling), and increased cell growth and proliferation in the absence of growth signals (activating mutations in *PIK3CA* and *HRAS* and amplifications of *EGFR*)[292].

7. Aim and outline of this thesis

Fanconi anemia patients are strongly predisposed to develop head and neck squamous cell carcinomas. Although our knowledge of FA is increasing, it is still not clear whether inactivation of the FA-BRCA pathway also contributes to the pathogenesis of head and neck tumors in non-FA patients. The aim of this study is to examine the role of the FA-BRCA pathway in sporadic HNSCC and whether a defect in this pathway can be exploited as a target in cancer therapy.

To explore the occurrence of FA-BRCA pathway inactivation in sporadic HNSCC, it is important to know all proteins involved in this DNA repair pathway. Therefore, part of the work in this thesis has focused on a better understanding of the FA-BRCA pathway by discovering mutations in genes that cause Fanconi anemia. In **Chapters 2-4**, we describe two newly identified FA genes: *SLX4* (*FANCP*) and *XPF* (*FANCQ*). Bi-allelic germline mutations in these genes were found in individuals diagnosed with Fanconi anemia. In total, 17 FA and several FA-associated genes are known now. In **Chapter 5**, we examined whether inactivation of any of these 17 genes occur in sporadic head and neck tumor cell lines. Only a minority of cell lines had a defective FA-BRCA pathway: one cell line contained a homozygous nonsense mutation in *FANCM*, and in another cell line *FANCF* methylation was observed.

The last part of this thesis concerns the therapeutic exploitation of the FA-BRCA pathway. Bi-allelic mutations in the well-known breast cancer susceptibility gene *BRCA2* cause Fanconi anemia. Since BRCA2-deficient cancer cells are hypersensitive to PARP inhibition, we investigated whether defects in other FA genes also sensitize cells to PARP inhibition (**Chapter 6**). The data suggest that PARP inhibitors might be beneficial in the treatment of tumors with *FANCM* mutations. To find additional drugable gene targets in FA-HNSCC cells, we generated cell models and performed genome wide siRNA screens in FA-deficient and corrected cells (**Chapter 7**).

Finally, the results described in this thesis are discussed in **Chapter 8**.

References

1. Lindahl, T. & Barnes, D. E. Repair of endogenous DNA damage. Cold Spring Harb. Symp. Quant. Biol. 65, 127–33 (2000).
2. Hoeijmakers, J. DNA Damage, Aging, and Cancer. The new England journal of medicine 361(15): 1475–85 (2009).
3. Ciccia, A. & Elledge, S. J. The DNA damage response: making it safe to play with knives. Mol. Cell 40, 179–204 (2010).
4. Alter, B. P. *et al.* Malignancies and survival patterns in the National Cancer Institute inherited bone marrow failure syndromes cohort study. Br. J. Haematol. 150, 179–88 (2010).
5. Alter, B. P., Greene, M. H., Velazquez, I. & Rosenberg, P. S. Cancer in Fanconi anemia. Blood 101, 2072 (2003).
6. Kutler, D. I. *et al.* High incidence of head and neck squamous cell carcinoma in patients with Fanconi anemia. Arch. Otolaryngol. Head. Neck Surg. 129, 106–12 (2003).
7. Rosenberg, P. S., Greene, M. H. & Alter, B. P. Cancer incidence in persons with Fanconi anemia. Blood 101, 822–6 (2003).
8. Alter, B. P., Giri, N., Savage, S. A. & Rosenberg, P. S. Cancer in dyskeratosis congenita. Blood 113, 6549–57 (2009).
9. Lobitz, S. & Velleuer, E. Guido Fanconi (1892-1979): a jack of all trades. Nat. Rev. Cancer 6, 893–8 (2006).
10. Fanconi, G. Familiäre infantile perniziosaartige Anämie (perniziöses Blutbild und Konstitution). Jahrb. für Kinderheilkd. und Phys. Erziehung 117, 257–280 (1927).
11. Auerbach, A. D. Fanconi anemia and its diagnosis. Mutat. Res. 668, 4–10 (2009).
12. Kutler, D. I. *et al.* A 20-year perspective on the International Fanconi Anemia Registry (IFAR). Blood 101, 1249–56 (2003).
13. Butturini, A. *et al.* Hematologic abnormalities in Fanconi anemia: an International Fanconi Anemia Registry study. Blood 84, 1650–5 (1994).
14. Langevin, F., Crossan, G. P., Rosado, I. V, Arends, M. J. & Patel, K. J. Fancd2 counteracts the toxic effects of naturally produced aldehydes in mice. Nature 475, 53–8 (2011).
15. Sasaki, M. S. & Tonomura, A. A high susceptibility of Fanconi's anemia to chromosome breakage by DNA cross-linking agents. Cancer Res. 33, 1829–36 (1973).
16. Auerbach, A. D. & Wolman, S. R. Susceptibility of Fanconi's anaemia fibroblasts to chromosome damage by carcinogens. Nature 261, 494–6 (1976).
17. Oostra, A. B., Nieuwint, A. W. M., Joenje, H. & de Winter, J. P. Diagnosis of fanconi anemia: chromosomal breakage analysis. Anemia 2012, 238731 (2012).
18. Knies, K. *et al.* Genotyping of fanconi anemia patients by whole exome sequencing: advantages and challenges. PLoS One 7, e52648 (2012).
19. Ameziane, N. *et al.* Diagnosis of fanconi anemia: mutation analysis by next-generation sequencing. Anemia 2012, 132856 (2012).
20. Gennery, A. R. *et al.* The clinical and biological overlap between Nijmegen Breakage Syndrome and Fanconi anemia. Clin. Immunol. 113, 214–9 (2004).
21. Nakanishi, K. *et al.* Interaction of FANCD2 and NBS1 in the DNA damage response. Nat. Cell Biol. 4, 913–20 (2002).
22. New, H. V *et al.* Nijmegen breakage syndrome diagnosed as Fanconi anaemia. Pediatr. Blood Cancer 44, 494–9 (2005).
23. Van der Lelij, P., Oostra, A. B., Rooimans, M. A., Joenje, H. & de Winter, J. P. Diagnostic Overlap between Fanconi Anemia and the Cohesinopathies: Roberts Syndrome and Warsaw Breakage Syndrome. Anemia 2010, 565268 (2010).
24. Lo Ten Foe, J. R. *et al.* Somatic mosaicism in Fanconi anemia: molecular basis and clinical significance. Eur. J. Hum. Genet. 5, 137–48
25. Waisfisz, Q. *et al.* Spontaneous functional correction of homozygous fanconi anaemia alleles reveals novel mechanistic basis for reverse mosaicism. Nat. Genet. 22, 379–83 (1999).
26. Gregory, J. J. *et al.* Somatic mosaicism in Fanconi anemia: evidence of genotypic reversion in lymphohematopoietic stem cells. Proc. Natl. Acad. Sci. U. S. A. 98, 2532–7 (2001).
27. Youssoufian, H. & Pyeritz, R. E. Mechanisms and consequences of somatic mosaicism in humans. Nat. Rev. Genet. 3, 748–58 (2002).
28. Peters, J.-M. & Nishiyama, T. Sister chromatid cohesion. Cold Spring Harb. Perspect. Biol. 4, (2012).
29. Remeseiro, S. & Losada, A. Cohesin, a chromatin engagement ring. Curr. Opin. Cell Biol. 25, 63–71 (2013).
30. Losada, A. Cohesin in cancer: chromosome segregation and beyond. Nat. Rev. Cancer 14, 389–93 (2014).
31. Vega, H. *et al.* Roberts syndrome is caused by mutations in ESCO2, a human homolog of yeast ECO1 that is essential for the establishment of sister chromatid cohesion. Nat. Genet. 37, 468–70

(2005).
32. Van der Lelij, P. *et al.* Warsaw breakage syndrome, a cohesinopathy associated with mutations in the XPD helicase family member DDX11/ChlR1. Am. J. Hum. Genet. 86, 262–6 (2010).
33. Musio, A. *et al.* X-linked Cornelia de Lange syndrome owing to SMC1L1 mutations. Nat. Genet. 38, 528–30 (2006).
34. Deardorff, M. A. *et al.* Mutations in Cohesin Complex Members SMC3 and SMC1A Cause a Mild Variant of Cornelia de Lange Syndrome with Predominant Mental Retardation. Am. J. Hum. Genet. 80, 485–494 (2007).
35. Deardorff, M. A. *et al.* RAD21 mutations cause a human cohesinopathy. Am. J. Hum. Genet. 90, 1014–27 (2012).
36. Tonkin, E. T., Wang, T.-J., Lisgo, S., Bamshad, M. J. & Strachan, T. NIPBL, encoding a homolog of fungal Scc2-type sister chromatid cohesion proteins and fly Nipped-B, is mutated in Cornelia de Lange syndrome. Nat. Genet. 36, 636–41 (2004).
37. Krantz, I. D. *et al.* Cornelia de Lange syndrome is caused by mutations in NIPBL, the human homolog of Drosophila melanogaster Nipped-B. Nat. Genet. 36, 631–5 (2004).
38. Deardorff, M. A. *et al.* HDAC8 mutations in Cornelia de Lange syndrome affect the cohesin acetylation cycle. Nature 489, 313–7 (2012).
39. Strathdee, C. A., Gavish, H., Shannon, W. R. & Buchwald, M. Cloning of cDNAs for Fanconi's anaemia by functional complementation. Nature 356, 763–767 (1992).
40. Lo Ten Foe, J. R. *et al.* Expression cloning of a cDNA for the major Fanconi anaemia gene, FAA. Nat. Genet. 14, 320–3 (1996).
41. Apostolou S, Whitmore SA, Crawford J, Lennon G, Sutherland GR, Callen DF, Ianzano L, Savino M, D'Apolito M, Notarangelo A, Memeo E, Piemontese MR, Zelante L, Savino A, Gibson RA, Tipping AJ, Morgan NV, Hassock S, Jansen S, de Ravel TJ, Van Berkel C, Pronk, M. R. Positional cloning of the Fanconi anaemia group A gene. Nat. Genet. 14, 324–8 (1996).
42. De Winter, J. P. *et al.* The Fanconi anaemia group G gene FANCG is identical with XRCC9. Nat. Genet. 20, 281–3 (1998).
43. De Winter, J. P. *et al.* Isolation of a cDNA representing the Fanconi anemia complementation group E gene. Am. J. Hum. Genet. 67, 1306–8 (2000).
44. De Winter, J. P. *et al.* The Fanconi anaemia gene FANCF encodes a novel protein with homology to ROM. Nat. Genet. 24, 15–6 (2000).
45. Timmers, C. *et al.* Positional cloning of a novel Fanconi anemia gene, FANCD2. Mol. Cell 7, 241–8 (2001).
46. Howlett, N. G. *et al.* Biallelic inactivation of BRCA2 in Fanconi anemia. Science 297, 606–9 (2002).
47. Meetei, A. R. *et al.* A novel ubiquitin ligase is deficient in Fanconi anemia. Nat. Genet. 35, 165–70 (2003).
48. Meetei, A. R. *et al.* X-linked inheritance of Fanconi anemia complementation group B. Nat. Genet. 36, 1219–24 (2004).
49. Levitus, M. *et al.* The DNA helicase BRIP1 is defective in Fanconi anemia complementation group J. Nat. Genet. 37, 934–5 (2005).
50. Litman, R. *et al.* BACH1 is critical for homologous recombination and appears to be the Fanconi anemia gene product FANCJ. Cancer Cell 8, 255–65 (2005).
51. Meetei, A. R. *et al.* A human ortholog of archaeal DNA repair protein Hef is defective in Fanconi anemia complementation group M. Nat. Genet. 37, 958–963 (2005).
52. Dorsman, J. C. *et al.* Identification of the Fanconi anemia complementation group I gene, FANCI. Cell. Oncol. 29, 211–8 (2007).
53. Smogorzewska, A. *et al.* Identification of the FANCI protein, a monoubiquitinated FANCD2 paralog required for DNA repair. Cell 129, 289–301 (2007).
54. Xia, B. *et al.* Fanconi anemia is associated with a defect in the BRCA2 partner PALB2. Nat. Genet. 39, 159–61 (2007).
55. Reid, S. *et al.* Biallelic mutations in PALB2 cause Fanconi anemia subtype FA-N and predispose to childhood cancer. Nat. Genet. 39, 162–4 (2007).
56. Vaz, F. *et al.* Mutation of the RAD51C gene in a Fanconi anemia-like disorder. Nat. Genet. 42, 406–9 (2010).
57. Stoepker, C. *et al.* SLX4, a coordinator of structure-specific endonucleases, is mutated in a new Fanconi anemia subtype. Nat. Genet. 43, 138–41 (2011).
58. Kim, Y. *et al.* Mutations of the SLX4 gene in Fanconi anemia. Nat. Genet. 43, 142–6 (2011).
59. Bogliolo, M. *et al.* Mutations in ERCC4, encoding the DNA-repair endonuclease XPF, cause Fanconi anemia. Am. J. Hum. Genet. 92, 800–6 (2013).
60. Kashiyama, K. *et al.* Malfunction of nuclease ERCC1-XPF results in diverse clinical manifestations and causes Cockayne syndrome, xeroderma pigmentosum, and Fanconi anemia. Am. J. Hum. Genet. 92, 807–19 (2013).

61. Domchek, S. M. *et al.* Biallelic deleterious BRCA1 mutations in a woman with early-onset ovarian cancer. Cancer Discov. 3, 399–405 (2013).
62. Sawyer, S. L. *et al.* Biallelic Mutations in BRCA1 Cause a New Fanconi Anemia Subtype. Cancer Discov. 5, 135–42 (2014).
63. De Winter, J. P. & Joenje, H. The genetic and molecular basis of Fanconi anemia. Mutat. Res. 668, 11–9 (2009).
64. Singh, T. R. *et al.* Impaired FANCD2 monoubiquitination and hypersensitivity to camptothecin uniquely characterize Fanconi anemia complementation group M. Blood 114, 174–80 (2009).
65. Sijbers, A. M. *et al.* Xeroderma pigmentosum group F caused by a defect in a structure-specific DNA repair endonuclease. Cell 86, 811–22 (1996).
66. Gregg, S. Q., Robinson, A. R. & Niedernhofer, L. J. Physiological consequences of defects in ERCC1-XPF DNA repair endonuclease. DNA Repair (Amst). 10, 781–91 (2011).
67. Ahmad, A. *et al.* Mislocalization of XPF-ERCC1 nuclease contributes to reduced DNA repair in XP-F patients. PLoS Genet. 6, e1000871 (2010).
68. Marteijn, J. A., Lans, H., Vermeulen, W. & Hoeijmakers, J. H. J. Understanding nucleotide excision repair and its roles in cancer and ageing. Nat. Rev. Mol. Cell Biol. 15, 465–81 (2014).
69. Klein Douwel, D. *et al.* XPF-ERCC1 acts in Unhooking DNA interstrand crosslinks in cooperation with FANCD2 and FANCP/SLX4. Mol. Cell 54, 460–71 (2014).
70. Alter, B. P., Rosenberg, P. S. & Brody, L. C. Clinical and molecular features associated with biallelic mutations in FANCD1/BRCA2. J. Med. Genet. 44, 1–9 (2007).
71. Hirsch, B. *et al.* Association of biallelic BRCA2/FANCD1 mutations with spontaneous chromosomal instability and solid tumors of childhood. Blood 103, 2554–9 (2004).
72. Reid, S. *et al.* Biallelic BRCA2 mutations are associated with multiple malignancies in childhood including familial Wilms tumour. J. Med. Genet. 42, 147–51 (2005).
73. Wagner, J. E. *et al.* Germline mutations in BRCA2: shared genetic susceptibility to breast cancer, early onset leukemia, and Fanconi anemia. Blood 103, 3226–9 (2004).
74. Offit, K. *et al.* Shared genetic susceptibility to breast cancer, brain tumors, and Fanconi anemia. J. Natl. Cancer Inst. 95, 1548–51 (2003).
75. Narod, S. *et al.* Increasing incidence of breast cancer in family with BRCA1 mutation. Lancet 341, 1101–2 (1993).
76. Wooster, R. *et al.* Localization of a breast cancer susceptibility gene, BRCA2, to chromosome 13q12-13. Science 265, 2088–90 (1994).
77. Cantor, S. B. *et al.* BACH1, a novel helicase-like protein, interacts directly with BRCA1 and contributes to its DNA repair function. Cell 105, 149–60 (2001).
78. Cantor, S. *et al.* The BRCA1-associated protein BACH1 is a DNA helicase targeted by clinically relevant inactivating mutations. Proc. Natl. Acad. Sci. U. S. A. 101, 2357–62 (2004).
79. Rahman, N. *et al.* PALB2, which encodes a BRCA2-interacting protein, is a breast cancer susceptibility gene. Nat. Genet. 39, 165–7 (2007).
80. Meindl, A. *et al.* Germline mutations in breast and ovarian cancer pedigrees establish RAD51C as a human cancer susceptibility gene. Nat. Genet. 42, 410–4 (2010).
81. Kottemann, M. C. & Smogorzewska, A. Fanconi anaemia and the repair of Watson and Crick DNA crosslinks. Nature 493, 356–63 (2013).
82. Easton, D. F. *et al.* Cancer risks in two large breast cancer families linked to BRCA2 on chromosome 13q12-13. Am. J. Hum. Genet. 61, 120–8 (1997).
83. Cancer risks in BRCA2 mutation carriers. J. Natl. Cancer Inst. 91, 1310–6 (1999).
84. Jones, S. *et al.* Exomic sequencing identifies PALB2 as a pancreatic cancer susceptibility gene. Science 324, 217 (2009).
85. Kiiski, J. I. *et al.* Exome sequencing identifies FANCM as a susceptibility gene for triple-negative breast cancer. Proc. Natl. Acad. Sci. U. S. A. 111, 15172–7 (2014).
86. Smith, C. G. *et al.* Exome resequencing identifies potential tumor-suppressor genes that predispose to colorectal cancer. Hum. Mutat. 34, 1026–34 (2013).
87. Goodman, L. S. *et al.* Landmark article Sept. 21, 1946: Nitrogen mustard therapy. Use of methyl-bis(beta-chloroethyl)amine hydrochloride and tris(beta-chloroethyl)amine hydrochloride for Hodgkin's disease, lymphosarcoma, leukemia and certain allied and miscellaneous disorders. . JAMA 251, 2255–61 (1984).
88. Hirsch, J. An anniversary for cancer chemotherapy. JAMA 296, 1518–20 (2006).
89. Krumbhaar, E. B. & Krumbhaar, H. D. The Blood and Bone Marrow in Yelloe Cross Gas (Mustard Gas) Poisoning: Changes produced in the Bone Marrow of Fatal Cases. J. Med. Res. 40, 497–508.3 (1919).
90. GILMAN, A. & PHILIPS, F. S. The biological actions and therapeutic applications of the B-chloroethyl amines and sulfides. Science 103, 409–15 (1946).
91. GOODMAN, L. S. & WINTROBE, M. M. Nitrogen mustard therapy; use of methyl-bis (beta-chloroethyl) amine hydrochloride and tris (beta-chloroethyl) amine hydrochloride for Hodgkin's

disease, lymphosarcoma, leukemia and certain allied and miscellaneous disorders. J. Am. Med. Assoc. 132, 126–32 (1946).
92. Dronkert, M. L. & Kanaar, R. Repair of DNA interstrand cross-links. Mutat. Res. 486, 217–47 (2001).
93. Wang, L. C. & Gautier, J. The Fanconi anemia pathway and ICL repair: implications for cancer therapy. Crit. Rev. Biochem. Mol. Biol. 45, 424–39 (2010).
94. ROSENBERG, B., VANCAMP, L. & KRIGAS, T. INHIBITION OF CELL DIVISION IN ESCHERICHIA COLI BY ELECTROLYSIS PRODUCTS FROM A PLATINUM ELECTRODE. Nature 205, 698–9 (1965).
95. Basu, A. & Krishnamurthy, S. Cellular responses to Cisplatin-induced DNA damage. J. Nucleic Acids 2010, (2010).
96. Rosenberg, B., VanCamp, L., Trosko, J. E. & Mansour, V. H. Platinum compounds: a new class of potent antitumour agents. Nature 222, 385–6 (1969).
97. Kelland, L. The resurgence of platinum-based cancer chemotherapy. Nat. Rev. Cancer 7, 573–84 (2007).
98. Averbeck, D., Papadopoulo, D. & Moustacchi, E. Repair of 4,5',8-trimethylpsoralen plus light-induced DNA damage in normal and Fanconi's anemia cell lines. Cancer Res. 48, 2015–20 (1988).
99. Tomasz, M. Mitomycin C: small, fast and deadly (but very selective). Chem. Biol. 2, 575–9 (1995).
100. Eastman, A. Reevaluation of interaction of cis-dichloro(ethylenediamine)platinum(II) with DNA. Biochemistry 25, 3912–5 (1986).
101. Kozekov, I. D. *et al.* DNA interchain cross-links formed by acrolein and crotonaldehyde. J. Am. Chem. Soc. 125, 50–61 (2003).
102. Folmer, V., Soares, J. C. M., Gabriel, D. & Rocha, J. B. T. A high fat diet inhibits delta-aminolevulinate dehydratase and increases lipid peroxidation in mice (Mus musculus). J. Nutr. 133, 2165–70 (2003).
103. Brooks, P. J. & Theruvathu, J. A. DNA adducts from acetaldehyde: implications for alcohol-related carcinogenesis. Alcohol 35, 187–93 (2005).
104. Stone, M. P. *et al.* Interstrand DNA cross-links induced by alpha,beta-unsaturated aldehydes derived from lipid peroxidation and environmental sources. Acc. Chem. Res. 41, 793–804 (2008).
105. Ridpath, J. R. *et al.* Cells deficient in the FANC/BRCA pathway are hypersensitive to plasma levels of formaldehyde. Cancer Res. 67, 11117–22 (2007).
106. Rosado, I. V, Langevin, F., Crossan, G. P., Takata, M. & Patel, K. J. Formaldehyde catabolism is essential in cells deficient for the Fanconi anemia DNA-repair pathway. Nat. Struct. Mol. Biol. 18, 1432–4 (2011).
107. Garaycoechea, J. I. *et al.* Genotoxic consequences of endogenous aldehydes on mouse haematopoietic stem cell function. Nature 489, 571–5 (2012).
108. Dutta, S., Chowdhury, G. & Gates, K. S. Interstrand cross-links generated by abasic sites in duplex DNA. J. Am. Chem. Soc. 129, 1852–3 (2007).
109. Clauson, C., Schärer, O. D. & Niedernhofer, L. Advances in understanding the complex mechanisms of DNA interstrand cross-link repair. Cold Spring Harb. Perspect. Med. 3, a012732 (2013).
110. Räschle, M. *et al.* Mechanism of replication-coupled DNA interstrand crosslink repair. Cell 134, 969–80 (2008).
111. Akkari, Y. M., Bateman, R. L., Reifsteck, C. A., Olson, S. B. & Grompe, M. DNA replication is required To elicit cellular responses to psoralen-induced DNA interstrand cross-links. Mol. Cell. Biol. 20, 8283–9 (2000).
112. Zhang, J. & Walter, J. C. Mechanism and regulation of incisions during DNA interstrand cross-link repair. DNA Repair (Amst). 19, 135–42 (2014).
113. Zhang, J. *et al.* DNA interstrand cross-link repair requires replication-fork convergence. Nat. Struct. Mol. Biol. 22, 242–7 (2015).
114. Ciccia, A. *et al.* Identification of FAAP24, a Fanconi anemia core complex protein that interacts with FANCM. Mol. Cell 25, 331–43 (2007).
115. Yan, Z. *et al.* A histone-fold complex and FANCM form a conserved DNA-remodeling complex to maintain genome stability. Mol. Cell 37, 865–78 (2010).
116. Singh, T. R. *et al.* MHF1-MHF2, a histone-fold-containing protein complex, participates in the Fanconi anemia pathway via FANCM. Mol. Cell 37, 879–86 (2010).
117. Tao, Y. *et al.* The structure of the FANCM-MHF complex reveals physical features for functional assembly. Nat. Commun. 3, 782 (2012).
118. Yang, H. *et al.* Saccharomyces cerevisiae MHF complex structurally resembles the histones (H3-H4)2 heterotetramer and functions as a heterotetramer. Structure 20, 364–70 (2012).
119. Gari, K., Décaillet, C., Stasiak, A. Z., Stasiak, A. & Constantinou, A. The Fanconi anemia protein FANCM can promote branch migration of Holliday junctions and replication forks. Mol. Cell 29, 141–8 (2008).

120. Xue, Y., Li, Y., Guo, R., Ling, C. & Wang, W. FANCM of the Fanconi anemia core complex is required for both monoubiquitination and DNA repair. Hum. Mol. Genet. 17, 1641–52 (2008).
121. Wang, Y. *et al.* Structure analysis of FAAP24 reveals single-stranded DNA-binding activity and domain functions in DNA damage response. Cell Res. 23, 1215–28 (2013).
122. Fox, D. *et al.* The histone-fold complex MHF is remodeled by FANCM to recognize branched DNA and protect genome stability. Cell Res. 24, 560–75 (2014).
123. Zhao, Q. *et al.* The MHF complex senses branched DNA by binding a pair of crossover DNA duplexes. Nat. Commun. 5, 2987 (2014).
124. Kim, J. M., Kee, Y., Gurtan, A. & D'Andrea, A. D. Cell cycle-dependent chromatin loading of the Fanconi anemia core complex by FANCM/FAAP24. Blood 111, 5215–22 (2008).
125. Gari, K., Décaillet, C., Delannoy, M., Wu, L. & Constantinou, A. Remodeling of DNA replication structures by the branch point translocase FANCM. Proc. Natl. Acad. Sci. U. S. A. 105, 16107–12 (2008).
126. Bernstein, K. A. & Rothstein, R. At loose ends: resecting a double-strand break. Cell 137, 807–10 (2009).
127. Collis, S. J. *et al.* FANCM and FAAP24 function in ATR-mediated checkpoint signaling independently of the Fanconi anemia core complex. Mol. Cell 32, 313–24 (2008).
128. Luke-Glaser, S., Luke, B., Grossi, S. & Constantinou, A. FANCM regulates DNA chain elongation and is stabilized by S-phase checkpoint signalling. EMBO J. 29, 795–805 (2010).
129. Zhang, J. & Walter, J. C. Mechanism and regulation of incisions during DNA interstrand cross-link repair. DNA Repair (Amst). 19, 135–42 (2014).
130. Huang, J. *et al.* The DNA translocase FANCM/MHF promotes replication traverse of DNA interstrand crosslinks. Mol. Cell 52, 434–46 (2013).
131. Long, D. T., Joukov, V., Budzowska, M. & Walter, J. C. BRCA1 promotes unloading of the CMG helicase from a stalled DNA replication fork. Mol. Cell 56, 174–85 (2014).
132. Huang, M. *et al.* The FANCM/FAAP24 complex is required for the DNA interstrand crosslink-induced checkpoint response. Mol. Cell 39, 259–68 (2010).
133. Wang, Y. *et al.* FANCM and FAAP24 maintain genome stability via cooperative as well as unique functions. Mol. Cell 49, 997–1009 (2013).
134. Zou, L. & Elledge, S. J. Sensing DNA damage through ATRIP recognition of RPA-ssDNA complexes. Science 300, 1542–8 (2003).
135. Zou, L., Cortez, D. & Elledge, S. J. Regulation of ATR substrate selection by Rad17-dependent loading of Rad9 complexes onto chromatin. Genes Dev. 16, 198–208 (2002).
136. Kumagai, A., Lee, J., Yoo, H. Y. & Dunphy, W. G. TopBP1 activates the ATR-ATRIP complex. Cell 124, 943–55 (2006).
137. Ellison, V. & Stillman, B. Biochemical characterization of DNA damage checkpoint complexes: clamp loader and clamp complexes with specificity for 5' recessed DNA. PLoS Biol. 1, E33 (2003).
138. Zou, L., Liu, D. & Elledge, S. J. Replication protein A-mediated recruitment and activation of Rad17 complexes. Proc. Natl. Acad. Sci. U. S. A. 100, 13827–32 (2003).
139. Delacroix, S., Wagner, J. M., Kobayashi, M., Yamamoto, K. & Karnitz, L. M. The Rad9-Hus1-Rad1 (9-1-1) clamp activates checkpoint signaling via TopBP1. Genes Dev. 21, 1472–7 (2007).
140. Lee, J. & Dunphy, W. G. Rad17 plays a central role in establishment of the interaction between TopBP1 and the Rad9-Hus1-Rad1 complex at stalled replication forks. Mol. Biol. Cell 21, 926–35 (2010).
141. Lee, J., Kumagai, A. & Dunphy, W. G. The Rad9-Hus1-Rad1 checkpoint clamp regulates interaction of TopBP1 with ATR. J. Biol. Chem. 282, 28036–44 (2007).
142. Liu, E. *et al.* The ATR-mediated S phase checkpoint prevents rereplication in mammalian cells when licensing control is disrupted. J. Cell Biol. 179, 643–57 (2007).
143. Mordes, D. A., Glick, G. G., Zhao, R. & Cortez, D. TopBP1 activates ATR through ATRIP and a PIKK regulatory domain. Genes Dev. 22, 1478–89 (2008).
144. Liu, S. *et al.* ATR autophosphorylation as a molecular switch for checkpoint activation. Mol. Cell 43, 192–202 (2011).
145. Rendtlew Danielsen, J. M. *et al.* HCLK2 is required for activity of the DNA damage response kinase ATR. J. Biol. Chem. 284, 4140–7 (2009).
146. Collis, S. J. *et al.* HCLK2 is essential for the mammalian S-phase checkpoint and impacts on Chk1 stability. Nat. Cell Biol. 9, 391–401 (2007).
147. Schwab, R. A., Blackford, A. N. & Niedzwiedz, W. ATR activation and replication fork restart are defective in FANCM-deficient cells. EMBO J. 29, 806–18 (2010).
148. Andreassen, P. R., D'Andrea, A. D. & Taniguchi, T. ATR couples FANCD2 monoubiquitination to the DNA-damage response. Genes Dev. 18, 1958–63 (2004).
149. Pichierri, P. & Rosselli, F. The DNA crosslink-induced S-phase checkpoint depends on ATR-CHK1 and ATR-NBS1-FANCD2 pathways. EMBO J. 23, 1178–87 (2004).
150. Qiao, F. *et al.* Phosphorylation of fanconi anemia (FA) complementation group G protein, FANCG,

at serine 7 is important for function of the FA pathway. J. Biol. Chem. 279, 46035–45 (2004).
151. Sobeck, A. *et al.* Fanconi anemia proteins are required to prevent accumulation of replication-associated DNA double-strand breaks. Mol. Cell. Biol. 26, 425–37 (2006).
152. Ho, G. P. H., Margossian, S., Taniguchi, T. & D'Andrea, A. D. Phosphorylation of FANCD2 on two novel sites is required for mitomycin C resistance. Mol. Cell. Biol. 26, 7005–15 (2006).
153. Wang, X. *et al.* Chk1-mediated phosphorylation of FANCE is required for the Fanconi anemia/BRCA pathway. Mol. Cell. Biol. 27, 3098–108 (2007).
154. Collins, N. B. *et al.* ATR-dependent phosphorylation of FANCA on serine 1449 after DNA damage is important for FA pathway function. Blood 113, 2181–90 (2009).
155. Zhi, G. *et al.* Fanconi anemia complementation group FANCD2 protein serine 331 phosphorylation is important for fanconi anemia pathway function and BRCA2 interaction. Cancer Res. 69, 8775–83 (2009).
156. Singh, T. R. *et al.* ATR-dependent phosphorylation of FANCM at serine 1045 is essential for FANCM functions. Cancer Res. 73, 4300–10 (2013).
157. Shigechi, T. *et al.* ATR-ATRIP kinase complex triggers activation of the Fanconi anemia DNA repair pathway. Cancer Res. 72, 1149–56 (2012).
158. Ishiai, M. *et al.* FANCI phosphorylation functions as a molecular switch to turn on the Fanconi anemia pathway. Nat. Struct. Mol. Biol. 15, 1138–46 (2008).
159. Deans, A. J. & West, S. C. FANCM connects the genome instability disorders Bloom's Syndrome and Fanconi Anemia. Mol. Cell 36, 943–53 (2009).
160. Wu, L. & Hickson, I. D. The Bloom's syndrome helicase suppresses crossing over during homologous recombination. Nature 426, 870–4 (2003).
161. Manthei, K. A. & Keck, J. L. The BLM dissolvasome in DNA replication and repair. Cell. Mol. Life Sci. 70, 4067–84 (2013).
162. Chaganti, R. S., Schonberg, S. & German, J. A manyfold increase in sister chromatid exchanges in Bloom's syndrome lymphocytes. Proc. Natl. Acad. Sci. U. S. A. 71, 4508–12 (1974).
163. Ralf, C., Hickson, I. D. & Wu, L. The Bloom's syndrome helicase can promote the regression of a model replication fork. J. Biol. Chem. 281, 22839–46 (2006).
164. Mosedale, G. *et al.* The vertebrate Hef ortholog is a component of the Fanconi anemia tumor-suppressor pathway. Nat. Struct. Mol. Biol. 12, 763–71 (2005).
165. Bakker, S. T. *et al.* Fancm-deficient mice reveal unique features of Fanconi anemia complementation group M. Hum. Mol. Genet. 18, 3484–95 (2009).
166. Machida, Y. J. *et al.* UBE2T is the E2 in the Fanconi anemia pathway and undergoes negative autoregulation. Mol. Cell 23, 589–96 (2006).
167. Rajendra, E. *et al.* The genetic and biochemical basis of FANCD2 monoubiquitination. Mol. Cell 54, 858–69 (2014).
168. Alpi, A. F., Pace, P. E., Babu, M. M. & Patel, K. J. Mechanistic insight into site-restricted monoubiquitination of FANCD2 by Ube2t, FANCL, and FANCI. Mol. Cell 32, 767–77 (2008).
169. Huang, Y. *et al.* Modularized functions of the Fanconi anemia core complex. Cell Rep. 7, 1849–57 (2014).
170. Yan, Z. *et al.* A ubiquitin-binding protein, FAAP20, links RNF8-mediated ubiquitination to the Fanconi anemia DNA repair network. Mol. Cell 47, 61–75 (2012).
171. Leung, J. W. C. *et al.* Fanconi anemia (FA) binding protein FAAP20 stabilizes FA complementation group A (FANCA) and participates in interstrand cross-link repair. Proc. Natl. Acad. Sci. U. S. A. 109, 4491–6 (2012).
172. Ali, A. M. *et al.* FAAP20: a novel ubiquitin-binding FA nuclear core-complex protein required for functional integrity of the FA-BRCA DNA repair pathway. Blood 119, 3285–94 (2012).
173. Kim, H., Yang, K., Dejsuphong, D. & D'Andrea, A. D. Regulation of Rev1 by the Fanconi anemia core complex. Nat. Struct. Mol. Biol. 19, 164–70 (2012).
174. Nijman, S. M. B. *et al.* The deubiquitinating enzyme USP1 regulates the Fanconi anemia pathway. Mol. Cell 17, 331–9 (2005).
175. Cohn, M. A. *et al.* A UAF1-containing multisubunit protein complex regulates the Fanconi anemia pathway. Mol. Cell 28, 786–97 (2007).
176. Kim, J. M. *et al.* Inactivation of murine Usp1 results in genomic instability and a Fanconi anemia phenotype. Dev. Cell 16, 314–20 (2009).
177. Murai, J. *et al.* The USP1/UAF1 complex promotes double-strand break repair through homologous recombination. Mol. Cell. Biol. 31, 2462–9 (2011).
178. Park, E. *et al.* Inactivation of Uaf1 causes defective homologous recombination and early embryonic lethality in mice. Mol. Cell. Biol. 33, 4360–70 (2013).
179. Parmar, K. *et al.* Hematopoietic stem cell defects in mice with deficiency of Fancd2 or Usp1. Stem Cells 28, 1186–95 (2010).
180. Räschle, M. *et al.* Mechanism of replication-coupled DNA interstrand crosslink repair. Cell 134, 969–80 (2008).

181. Knipscheer, P. *et al.* The Fanconi anemia pathway promotes replication-dependent DNA interstrand cross-link repair. Science 326, 1698–701 (2009).
182. Demuth, I., Digweed, M. & Concannon, P. Human SNM1B is required for normal cellular response to both DNA interstrand crosslink-inducing agents and ionizing radiation. Oncogene 23, 8611–8 (2004).
183. Andersen, S. L. *et al.* Drosophila MUS312 and the vertebrate ortholog BTBD12 interact with DNA structure-specific endonucleases in DNA repair and recombination. Mol. Cell 35, 128–35 (2009).
184. Castor, D. *et al.* Cooperative control of holliday junction resolution and DNA repair by the SLX1 and MUS81-EME1 nucleases. Mol. Cell 52, 221–33 (2013).
185. Fekairi, S. *et al.* Human SLX4 is a Holliday junction resolvase subunit that binds multiple DNA repair/recombination endonucleases. Cell 138, 78–89 (2009).
186. Kratz, K. *et al.* Deficiency of FANCD2-associated nuclease KIAA1018/FAN1 sensitizes cells to interstrand crosslinking agents. Cell 142, 77–88 (2010).
187. Liu, T., Ghosal, G., Yuan, J., Chen, J. & Huang, J. FAN1 acts with FANCI-FANCD2 to promote DNA interstrand cross-link repair. Science 329, 693–6 (2010).
188. MacKay, C. *et al.* Identification of KIAA1018/FAN1, a DNA Repair Nuclease Recruited to DNA Damage by Monoubiquitinated FANCD2. Cell 142, 65–76 (2010).
189. Muñoz, I. M. *et al.* Coordination of structure-specific nucleases by human SLX4/BTBD12 is required for DNA repair. Mol. Cell 35, 116–27 (2009).
190. Smogorzewska, A. *et al.* A Genetic Screen Identifies FAN1, a Fanconi Anemia-Associated Nuclease Necessary for DNA Interstrand Crosslink Repair. Mol. Cell 39, 36–47 (2010).
191. Svendsen, J. M. *et al.* Mammalian BTBD12/SLX4 assembles a Holliday junction resolvase and is required for DNA repair. Cell 138, 63–77 (2009).
192. Wang, A. T. *et al.* Human SNM1A and XPF-ERCC1 collaborate to initiate DNA interstrand cross-link repair. Genes Dev. 25, 1859–70 (2011).
193. Yamamoto, K. N. *et al.* Involvement of SLX4 in interstrand cross-link repair is regulated by the Fanconi anemia pathway. Proc. Natl. Acad. Sci. U. S. A. 108, 6492–6 (2011).
194. Lachaud, C. *et al.* Distinct functional roles for the two SLX4 ubiquitin-binding UBZ domains mutated in Fanconi anemia. J. Cell Sci. 127, 2811–7 (2014).
195. Hanada, K. *et al.* The structure-specific endonuclease Mus81-Eme1 promotes conversion of interstrand DNA crosslinks into double-strands breaks. EMBO J. 25, 4921–32 (2006).
196. Niedernhofer, L. J. *et al.* The Structure-Specific Endonuclease Ercc1-Xpf Is Required To Resolve DNA Interstrand Cross-Link-Induced Double-Strand Breaks. Mol. Cell. Biol. 24, 5776–5787 (2004).
197. Kim, Y. *et al.* Regulation of multiple DNA repair pathways by the Fanconi anemia protein SLX4. Blood 121, 54–63 (2013).
198. Hodskinson, M. R. G. *et al.* Mouse SLX4 is a tumor suppressor that stimulates the activity of the nuclease XPF-ERCC1 in DNA crosslink repair. Mol. Cell 54, 472–84 (2014).
199. Zhou, W. *et al.* FAN1 mutations cause karyomegalic interstitial nephritis, linking chronic kidney failure to defective DNA damage repair. Nat. Genet. 44, 910–5 (2012).
200. Trujillo, J. P. *et al.* On the role of FAN1 in Fanconi anemia. Blood 120, 86–9 (2012).
201. Harder, H. C., Smith, R. G. & Leroy, A. F. Template primer inactivation by cis- and trans-dichlorodiammine platinum for human DNA polymerase alpha, beta, and Rauscher murine leukemia virus reverse transcriptase, as a mechanism of cytotoxicity. Cancer Res. 36, 3821–9 (1976).
202. Ho, T. V. & Schärer, O. D. Translesion DNA synthesis polymerases in DNA interstrand crosslink repair. Environ. Mol. Mutagen. 51, 552–66 (2010).
203. Lange, S. S., Takata, K. & Wood, R. D. DNA polymerases and cancer. Nat. Rev. Cancer 11, 96–110 (2011).
204. Ho, T. V., Guainazzi, A., Derkunt, S. B., Enoiu, M. & Schärer, O. D. Structure-dependent bypass of DNA interstrand crosslinks by translesion synthesis polymerases. Nucleic Acids Res. 39, 7455–64 (2011).
205. Prakash, S., Johnson, R. E. & Prakash, L. Eukaryotic translesion synthesis DNA polymerases: specificity of structure and function. Annu. Rev. Biochem. 74, 317–53 (2005).
206. Sonoda, E. *et al.* Multiple roles of Rev3, the catalytic subunit of polzeta in maintaining genome stability in vertebrates. EMBO J. 22, 3188–97 (2003).
207. Wu, F., Lin, X., Okuda, T. & Howell, S. B. DNA polymerase zeta regulates cisplatin cytotoxicity, mutagenicity, and the rate of development of cisplatin resistance. Cancer Res. 64, 8029–35 (2004).
208. Nojima, K. *et al.* Multiple repair pathways mediate tolerance to chemotherapeutic cross-linking agents in vertebrate cells. Cancer Res. 65, 11704–11 (2005).
209. Gan, G. N., Wittschieben, J. P., Wittschieben, B. Ø. & Wood, R. D. DNA polymerase zeta (pol zeta) in higher eukaryotes. Cell Res. 18, 174–83 (2008).

210. Simpson, L. J. & Sale, J. E. Rev1 is essential for DNA damage tolerance and non-templated immunoglobulin gene mutation in a vertebrate cell line. EMBO J. 22, 1654–64 (2003).
211. Niedzwiedz, W. *et al.* The Fanconi anaemia gene FANCC promotes homologous recombination and error-prone DNA repair. Mol. Cell 15, 607–20 (2004).
212. Sarkar, S., Davies, A. A., Ulrich, H. D. & McHugh, P. J. DNA interstrand crosslink repair during G1 involves nucleotide excision repair and DNA polymerase zeta. EMBO J. 25, 1285–94 (2006).
213. Enoiu, M., Jiricny, J. & Schärer, O. D. Repair of cisplatin-induced DNA interstrand crosslinks by a replication-independent pathway involving transcription-coupled repair and translesion synthesis. Nucleic Acids Res. 40, 8953–64 (2012).
214. Sharma, S., Helchowski, C. M. & Canman, C. E. The roles of DNA polymerase ζ and the Y family DNA polymerases in promoting or preventing genome instability. Mutat. Res. 743-744, 97–110 (2013).
215. Lehmann, A. R. *et al.* Translesion synthesis: Y-family polymerases and the polymerase switch. DNA Repair (Amst). 6, 891–9 (2007).
216. Lin, W. *et al.* The human REV1 gene codes for a DNA template-dependent dCMP transferase. Nucleic Acids Res. 27, 4468–75 (1999).
217. Nelson, J. R., Lawrence, C. W. & Hinkle, D. C. Deoxycytidyl transferase activity of yeast REV1 protein. Nature 382, 729–31 (1996).
218. Papadopoulo, D., Guillouf, C., Mohrenweiser, H. & Moustacchi, E. Hypomutability in Fanconi anemia cells is associated with increased deletion frequency at the HPRT locus. Proc. Natl. Acad. Sci. U. S. A. 87, 8383–7 (1990).
219. Shen, X. *et al.* REV3 and REV1 play major roles in recombination-independent repair of DNA interstrand cross-links mediated by monoubiquitinated proliferating cell nuclear antigen (PCNA). J. Biol. Chem. 281, 13869–72 (2006).
220. Kannouche, P. L., Wing, J. & Lehmann, A. R. Interaction of human DNA polymerase eta with monoubiquitinated PCNA: a possible mechanism for the polymerase switch in response to DNA damage. Mol. Cell 14, 491–500 (2004).
221. Watanabe, K. *et al.* Rad18 guides poleta to replication stalling sites through physical interaction and PCNA monoubiquitination. EMBO J. 23, 3886–96 (2004).
222. Bienko, M. *et al.* Ubiquitin-binding domains in Y-family polymerases regulate translesion synthesis. Science 310, 1821–4 (2005).
223. Misra, R. R. & Vos, J. M. Defective replication of psoralen adducts detected at the gene-specific level in xeroderma pigmentosum variant cells. Mol. Cell. Biol. 13, 1002–12 (1993).
224. Raha, M., Wang, G., Seidman, M. M. & Glazer, P. M. Mutagenesis by third-strand-directed psoralen adducts in repair-deficient human cells: high frequency and altered spectrum in a xeroderma pigmentosum variant. Proc. Natl. Acad. Sci. U. S. A. 93, 2941–6 (1996).
225. Albertella, M. R., Green, C. M., Lehmann, A. R. & O'Connor, M. J. A role for polymerase eta in the cellular tolerance to cisplatin-induced damage. Cancer Res. 65, 9799–806 (2005).
226. Chen, Y., Cleaver, J. E., Hanaoka, F., Chang, C. & Chou, K. A novel role of DNA polymerase eta in modulating cellular sensitivity to chemotherapeutic agents. Mol. Cancer Res. 4, 257–65 (2006).
227. Mogi, S., Butcher, C. E. & Oh, D. H. DNA polymerase eta reduces the gamma-H2AX response to psoralen interstrand crosslinks in human cells. Exp. Cell Res. 314, 887–95 (2008).
228. Minko, I. G. *et al.* Role for DNA polymerase kappa in the processing of N2-N2-guanine interstrand cross-links. J. Biol. Chem. 283, 17075–82 (2008).
229. Minko, I. G. *et al.* Replication bypass of the acrolein-mediated deoxyguanine DNA-peptide cross-links by DNA polymerases of the DinB family. Chem. Res. Toxicol. 21, 1983–90 (2008).
230. Williams, H. L., Gottesman, M. E. & Gautier, J. Replication-independent repair of DNA interstrand crosslinks. Mol. Cell 47, 140–7 (2012).
231. Moldovan, G.-L. *et al.* DNA polymerase POLN participates in cross-link repair and homologous recombination. Mol. Cell. Biol. 30, 1088–96 (2010).
232. Zietlow, L., Smith, L. A., Bessho, M. & Bessho, T. Evidence for the Involvement of Human DNA Polymerase N in the Repair of DNA Interstrand Cross-Links. Biochemistry 48, 11817–11824 (2009).
233. Symington, L. S. & Gautier, J. Double-strand break end resection and repair pathway choice. Annu. Rev. Genet. 45, 247–71 (2011).
234. Chapman, J. R., Taylor, M. R. G. & Boulton, S. J. Playing the end game: DNA double-strand break repair pathway choice. Mol. Cell 47, 497–510 (2012).
235. Sartori, A. A. *et al.* Human CtIP promotes DNA end resection. Nature 450, 509–14 (2007).
236. Nimonkar, A. V *et al.* BLM-DNA2-RPA-MRN and EXO1-BLM-RPA-MRN constitute two DNA end resection machineries for human DNA break repair. Genes Dev. 25, 350–62 (2011).
237. Unno, J. *et al.* FANCD2 binds CtIP and regulates DNA-end resection during DNA interstrand crosslink repair. Cell Rep. 7, 1039–47 (2014).
238. Murina, O. *et al.* FANCD2 and CtIP cooperate to repair DNA interstrand crosslinks. Cell Rep. 7,

1030–8 (2014).
239. Yeo, J. E., Lee, E. H., Hendrickson, E. A. & Sobeck, A. CtIP mediates replication fork recovery in a FANCD2-regulated manner. Hum. Mol. Genet. 23, 3695–705 (2014).
240. Yu, X., Wu, L. C., Bowcock, A. M., Aronheim, A. & Baer, R. The C-terminal (BRCT) domains of BRCA1 interact in vivo with CtIP, a protein implicated in the CtBP pathway of transcriptional repression. J. Biol. Chem. 273, 25388–92 (1998).
241. Cruz-García, A., López-Saavedra, A. & Huertas, P. BRCA1 accelerates CtIP-mediated DNA-end resection. Cell Rep. 9, 451–9 (2014).
242. Escribano-Díaz, C. *et al.* A cell cycle-dependent regulatory circuit composed of 53BP1-RIF1 and BRCA1-CtIP controls DNA repair pathway choice. Mol. Cell 49, 872–83 (2013).
243. West, S. C. Molecular views of recombination proteins and their control. Nat. Rev. Mol. Cell Biol. 4, 435–45 (2003).
244. Suwaki, N., Klare, K. & Tarsounas, M. RAD51 paralogs: roles in DNA damage signalling, recombinational repair and tumorigenesis. Semin. Cell Dev. Biol. 22, 898–905 (2011).
245. Pellegrini, L. *et al.* Insights into DNA recombination from the structure of a RAD51-BRCA2 complex. Nature 420, 287–93 (2002).
246. Thacker, J. The RAD51 gene family, genetic instability and cancer. Cancer Lett. 219, 125–35 (2005).
247. Xia, B. *et al.* Control of BRCA2 cellular and clinical functions by a nuclear partner, PALB2. Mol. Cell 22, 719–29 (2006).
248. Sy, S. M. H., Huen, M. S. Y. & Chen, J. PALB2 is an integral component of the BRCA complex required for homologous recombination repair. Proc. Natl. Acad. Sci. U. S. A. 106, 7155–60 (2009).
249. Zhang, F. *et al.* PALB2 links BRCA1 and BRCA2 in the DNA-damage response. Curr. Biol. 19, 524–9 (2009).
250. Buisson, R. *et al.* Cooperation of breast cancer proteins PALB2 and piccolo BRCA2 in stimulating homologous recombination. Nat. Struct. Mol. Biol. 17, 1247–54 (2010).
251. Dray, E. *et al.* Enhancement of RAD51 recombinase activity by the tumor suppressor PALB2. Nat. Struct. Mol. Biol. 17, 1255–9 (2010).
252. Sharan, S. K. *et al.* Embryonic lethality and radiation hypersensitivity mediated by Rad51 in mice lacking Brca2. Nature 386, 804–10 (1997).
253. Chen, J. *et al.* Stable interaction between the products of the BRCA1 and BRCA2 tumor suppressor genes in mitotic and meiotic cells. Mol. Cell 2, 317–28 (1998).
254. Marmorstein, L. Y., Ouchi, T. & Aaronson, S. A. The BRCA2 gene product functionally interacts with p53 and RAD51. Proc. Natl. Acad. Sci. U. S. A. 95, 13869–74 (1998).
255. Davies, A. A. *et al.* Role of BRCA2 in control of the RAD51 recombination and DNA repair protein. Mol. Cell 7, 273–82 (2001).
256. Moynahan, M. E., Pierce, A. J. & Jasin, M. BRCA2 is required for homology-directed repair of chromosomal breaks. Mol. Cell 7, 263–72 (2001).
257. Moynahan, M. E. & Jasin, M. Mitotic homologous recombination maintains genomic stability and suppresses tumorigenesis. Nat. Rev. Mol. Cell Biol. 11, 196–207 (2010).
258. Jensen, R. B., Carreira, A. & Kowalczykowski, S. C. Purified human BRCA2 stimulates RAD51-mediated recombination. Nature 467, 678–83 (2010).
259. Liu, J., Doty, T., Gibson, B. & Heyer, W.-D. Human BRCA2 protein promotes RAD51 filament formation on RPA-covered single-stranded DNA. Nat. Struct. Mol. Biol. 17, 1260–2 (2010).
260. Thorslund, T. *et al.* The breast cancer tumor suppressor BRCA2 promotes the specific targeting of RAD51 to single-stranded DNA. Nat. Struct. Mol. Biol. 17, 1263–5 (2010).
261. Sarbajna, S. & West, S. C. Holliday junction processing enzymes as guardians of genome stability. Trends Biochem. Sci. 39, 409–19 (2014).
262. Kamangar, F., Dores, G. M. & Anderson, W. F. Patterns of cancer incidence, mortality, and prevalence across five continents: defining priorities to reduce cancer disparities in different geographic regions of the world. J. Clin. Oncol. 24, 2137–50 (2006).
263. Snijders, P. J. *et al.* Prevalence and expression of human papillomavirus in tonsillar carcinomas, indicating a possible viral etiology. Int. J. Cancer 51, 845–50 (1992).
264. Syrjänen, S. Human papillomavirus (HPV) in head and neck cancer. J. Clin. Virol. 32 Suppl 1, S59–66 (2005).
265. Ang, K. K. *et al.* Human papillomavirus and survival of patients with oropharyngeal cancer. N. Engl. J. Med. 363, 24–35 (2010).
266. Gillison, M. L. *et al.* Evidence for a causal association between human papillomavirus and a subset of head and neck cancers. J. Natl. Cancer Inst. 92, 709–20 (2000).
267. Ragin, C. C. R. & Taioli, E. Survival of squamous cell carcinoma of the head and neck in relation to human papillomavirus infection: review and meta-analysis. Int. J. Cancer 121, 1813–20 (2007).
268. Rietbergen, M. M. *et al.* Human papillomavirus detection and comorbidity: critical issues in

selection of patients with oropharyngeal cancer for treatment De-escalation trials. Ann. Oncol. 24, 2740–5 (2013).
269. Chaturvedi, A. K. *et al.* Human papillomavirus and rising oropharyngeal cancer incidence in the United States. J. Clin. Oncol. 29, 4294–301 (2011).
270. Näsman, A. *et al.* Incidence of human papillomavirus (HPV) positive tonsillar carcinoma in Stockholm, Sweden: an epidemic of viral-induced carcinoma? Int. J. Cancer 125, 362–6 (2009).
271. Rietbergen, M. M. *et al.* Increasing prevalence rates of HPV attributable oropharyngeal squamous cell carcinomas in the Netherlands as assessed by a validated test algorithm. Int. J. Cancer 132, 1565–71 (2013).
272. Schache, A. G. *et al.* Evaluation of human papilloma virus diagnostic testing in oropharyngeal squamous cell carcinoma: sensitivity, specificity, and prognostic discrimination. Clin. Cancer Res. 17, 6262–71 (2011).
273. Schiffman, M., Castle, P. E., Jeronimo, J., Rodriguez, A. C. & Wacholder, S. Human papillomavirus and cervical cancer. Lancet 370, 890–907 (2007).
274. D'Souza, G. *et al.* Case-control study of human papillomavirus and oropharyngeal cancer. N. Engl. J. Med. 356, 1944–56 (2007).
275. Kutler, D. I. *et al.* Human papillomavirus DNA and p53 polymorphisms in squamous cell carcinomas from Fanconi anemia patients. J. Natl. Cancer Inst. 95, 1718–21 (2003).
276. Alter, B. P. *et al.* Squamous cell carcinomas in patients with Fanconi anemia and dyskeratosis congenita: a search for human papillomavirus. Int. J. Cancer 133, 1513–5 (2013).
277. Van Zeeburg, H. J. T. *et al.* Clinical and Molecular Characteristics of Squamous Cell Carcinomas From Fanconi Anemia Patients. JNCI J. Natl. Cancer Inst. 100, 1649–1653 (2008).
278. Savage, S. A. Human telomeres and telomere biology disorders. Prog. Mol. Biol. Transl. Sci. 125, 41–66 (2014).
279. Cabanillas, R. *et al.* Novel germline CDKN2A mutation associated with head and neck squamous cell carcinomas and melanomas. Head Neck 35, E80–4 (2013).
280. Vinarsky, V. *et al.* Head and neck squamous cell carcinoma in FAMMM syndrome. Head Neck 31, 1524–7 (2009).
281. Tanaka, A. *et al.* Germline mutation in ATR in autosomal- dominant oropharyngeal cancer syndrome. Am. J. Hum. Genet. 90, 511–7 (2012).
282. O'Driscoll, M., Ruiz-Perez, V. L., Woods, C. G., Jeggo, P. A. & Goodship, J. A. A splicing mutation affecting expression of ataxia-telangiectasia and Rad3-related protein (ATR) results in Seckel syndrome. Nat. Genet. 33, 497–501 (2003).
283. Foulkes, W. D. *et al.* Familial risks of squamous cell carcinoma of the head and neck: retrospective case-control study. BMJ 313, 716–21 (1996).
284. Mork, J., Møller, B. & Glattre, E. Familial risk in head and neck squamous cell carcinoma diagnosed before the age of 45: a population-based study. Oral Oncol. 35, 360–7 (1999).
285. Negri, E. *et al.* Family history of cancer: pooled analysis in the International Head and Neck Cancer Epidemiology Consortium. Int. J. Cancer 124, 394–401 (2009).
286. Flores-Obando, R. E., Gollin, S. M. & Ragin, C. C. Polymorphisms in DNA damage response genes and head and neck cancer risk. Biomarkers 15, 379–99 (2010).
287. Lacko, M., Oude Ophuis, M. B., Peters, W. H. M. & Manni, J. J. Genetic polymorphisms of smoking-related carcinogen detoxifying enzymes and head and neck cancer susceptibility. Anticancer Res. 29, 753–61 (2009).
288. Leemans, C. R., Braakhuis, B. J. M. & Brakenhoff, R. H. The molecular biology of head and neck cancer. Nat. Rev. Cancer 11, 9–22 (2011).
289. Bonner, J. A. *et al.* Radiotherapy plus cetuximab for squamous-cell carcinoma of the head and neck. N. Engl. J. Med. 354, 567–78 (2006).
290. Scheckenbach, K., Wagenmann, M., Freund, M., Schipper, J. & Hanenberg, H. Squamous cell carcinomas of the head and neck in Fanconi anemia: risk, prevention, therapy, and the need for guidelines. Klin. Pädiatrie 224, 132–8 (2012).
291. Wong, W. M. *et al.* Squamous cell carcinoma of the oral tongue in a patient with Fanconi anemia treated with radiotherapy and concurrent cetuximab: a case report and review of the literature. Head Neck 35, E292–8 (2013).
292. Lawrence, M. S. *et al.* Comprehensive genomic characterization of head and neck squamous cell carcinomas. Nature 517, 576–582 (2015).
293. Lui, V. W. Y. *et al.* Frequent mutation of the PI3K pathway in head and neck cancer defines predictive biomarkers. Cancer Discov. 3, 761–9 (2013).
294. Stransky, N. *et al.* The mutational landscape of head and neck squamous cell carcinoma. Science 333, 1157–60 (2011).
295. Agrawal, N. *et al.* Exome sequencing of head and neck squamous cell carcinoma reveals inactivating mutations in NOTCH1. Science 333, 1154–7 (2011).
296. Hanahan, D. & Weinberg, R. A. The hallmarks of cancer. Cell 100, 57–70 (2000).

297. Hanahan, D. & Weinberg, R. A. Hallmarks of cancer: the next generation. Cell 144, 646–74 (2011).
298. Hermsen, M. *et al.* New chromosomal regions with high-level amplifications in squamous cell carcinomas of the larynx and pharynx, identified by comparative genomic hybridization. J. Pathol. 194, 177–82 (2001).
299. Jin, C. *et al.* Cytogenetic abnormalities in 106 oral squamous cell carcinomas. Cancer Genet. Cytogenet. 164, 44–53 (2006).
300. Smeets, S. J. *et al.* Genetic classification of oral and oropharyngeal carcinomas identifies subgroups with a different prognosis. Cell. Oncol. 31, 291–300 (2009).
301. Ciriello, G. *et al.* Emerging landscape of oncogenic signatures across human cancers. Nat. Genet. 45, 1127–1133 (2013).
302. Scheffner, M., Werness, B. A., Huibregtse, J. M., Levine, A. J. & Howley, P. M. The E6 oncoprotein encoded by human papillomavirus types 16 and 18 promotes the degradation of p53. Cell 63, 1129–36 (1990).
303. Werness, B. A., Levine, A. J. & Howley, P. M. Association of human papillomavirus types 16 and 18 E6 proteins with p53. Science 248, 76–9 (1990).
304. Oganesyan, G. *et al.* Critical role of TRAF3 in the Toll-like receptor-dependent and -independent antiviral response. Nature 439, 208–11 (2006).

CHAPTER 2

SLX4, a coordinator of structure-specific endonucleases, is mutated in a new Fanconi anemia subtype

Chantal Stoepker, Karolina Hain, Beatrice Schuster, Yvonne Hilhorst-Hofstee, Martin A. Rooimans, Jûrgen Steltenpool, Anneke B. Oostra, Katharina Eirich, Elisabeth T. Korthof, Aggie W.M. Nieuwint, Nicolaas G.J. Jaspers, Thomas Bettecken, Hans Joenje, Detlev Schindler, John Rouse & Johan P. de Winter

Published in Nature Genetics, 2011. 43(2): 138-141.

DNA interstrand crosslink repair requires several classes of proteins, including structure-specific endonucleases and Fanconi anemia proteins. SLX4, which coordinates three separate endonucleases, was recently recognized as an important regulator of DNA repair. Here we report the first human individuals found to have biallelic mutations in *SLX4*. These individuals, who were previously diagnosed as having Fanconi anemia, add SLX4 as an essential component to the FA-BRCA genome maintenance pathway.

Fanconi anemia is a rare, heterogeneous chromosomal instability syndrome characterized by bone marrow failure, congenital abnormalities, hypersensitivity to DNA crosslinking agents and an increased susceptibility to cancer. Studies to unravel the genetic basis of Fanconi anemia have led to the identification of a previously unidentified genome maintenance pathway which evolved relatively late during evolution and exists — in its fully developed form — only in vertebrates. Fourteen Fanconi anemia genes have been identified[1,2], but a small percentage of individuals diagnosed with Fanconi anemia have remained unclassified, as no pathogenic mutations could be detected in the currently known Fanconi anemia genes.

One of these individuals (EUFA1354), a Dutch male with growth retardation, microcephaly, small eyes, hypopigmentation, thumb abnormalities and hearing loss, was diagnosed with pancytopenia at the age of 9 and Fanconi anemia was suspected (**Table 1**). We confirmed the Fanconi anemia diagnosis by a chromosomal breakage assay on T lymphocyte cultures, which showed increased spontaneous and excessive mitomycin C (MMC)-induced chromosomal aberrations that were well within the range established for Fanconi anemia (**Supplementary Fig. 1**). An EBV-immortalized lymphoblastoid cell line from this individual was also hypersensitive to MMC in terms of chromosomal breakage (**Fig. 1A**) and growth inhibition (**Fig. 1B and Supplementary Fig. 2A**). Notably, these lymphoblasts were also hypersensitive to the topoisomerase I inhibitor camptothecin (**Fig. 1C and Supplementary Fig. 2B**), a feature that until now was considered specific for the Fanconi anemia subgroups D1, M, N and O and which is possibly associated with defects in homologous recombination repair[2,3]. In further support of the Fanconi anemia diagnosis, we observed an elevated MMC-induced accumulation in the G2/M phase of the cell cycle, both in primary and in SV40-immortalized fibroblasts from this individual (**Supplementary Fig. 2C,D**). Somewhat surprisingly, fibroblasts were not very sensitive to the crosslinking drug when using growth inhibition or chromosomal breakage as a readout (**Supplementary Fig. 2E–G**).

Sequence analysis, MMC-induced FANCD2 monoubiquitination and normal formation of nuclear FANCD2 foci (**Supplementary Fig. 3A,B**) excluded a defect in the upstream part of the FA-BRCA pathway in this individual[4]. The induction

Table 1 Clinical phenotypes of individuals with *SLX4* mutations

	EUFA1354	457-1	457-2	457-3
Age at diagnosis[a]	9	9	7 (via 457-1)	7 (via 457-1)
Growth retardation	Short stature (-2.5 s.d. at age 9; -4.5 s.d. at age 18)	Prenatal	Prenatal	Pre- and post-natal
Thumb abnormalities	Hypoplastic right thumb	No	No	No
Facial features	Almond-shaped and short palpebral fissures, bulbous nasal tip, micrognathia, microcephaly (-2.5 s.d.)	No	No	No
Skin abnormalities	Hypopigmented spot on back	No	No	Café-au-lait spots
Ear abnormalities	Bilateral hearing loss, hypoplastic malleus, narrow external ear canals	No	No	No
Kidney abnormalities	No	Horseshoe kidney	No	No
Hematology[b]	Pancytopenia, Hb 2.3 mM/l, leucocytes 3.4 x 10^9/l, neutrophils 0.7 x 10^9/l, thrombocytes 18 x 10^9/l. Individual transplanted at age ten with bone marrow from the mother and is currently (age 18) doing well.	Pancytopenia, Hb 6.1 mM/l, erythrocytes 3.0 x 10^{12}/l, leucocytes 2.7 x 10^9/l, neutrophils 0.42 x 10^9/l, thrombocytes 20 x 10^9/l. Individual received HSCT with BM from an unrelated donor at age 9.5 and is currently (age 11.5) doing well.	Beginning bone marrow failure, erythrocytes 3.7 x 10^{12}/l, leucocytes 3.7 x 10^9/l, neutrophils 0.93 x 10^9/l, thrombocytes 107 x 10^9/l. Current age is 8.5.	Pancytopenia, Hb 5.7 mM/l, erythrocytes 2.8 x 10^{12}/l, leucocytes 2.5 x 10^9/l, neutrophils 0.27 x 10^9/l, thrombocytes 20 x 10^9/l. Individual received HSCT with BM from unrelated donor at the current age of 8.5.
Paternal *SLX4* mutation	c.286delA p.Thr96Leu*fs*X30	c.1093delC p.Gln365Ser*fs*X31	c.1093delC p.Gln365Ser*fs*X31	c.1093delC p.Gln365Ser*fs*X31
Maternal *SLX4* mutation	c.286delA p.Thr96Leu*fs*X30	c.1163+3dupT p.Arg317_Phe387del	c.1163+3dupT p.Arg317_Phe387del	c.1163+3dupT p.Arg317_Phe387del

s.d., standard deviation; HSCT, hematopoietic stem cell transplantation; BM, bone marrow.
[a]Age at diagnosis in years. [b]Normal values: Hb 7.4-9.0 mM/l, erythrocytes (male) 4.7-6.1 x 10^{12}/l, leucocytes 4.5-13.5 x 10^9/l, neutrophils 1.8-8.0 x 10^9/l, thrombocytes 150-450 x 10^9/l.

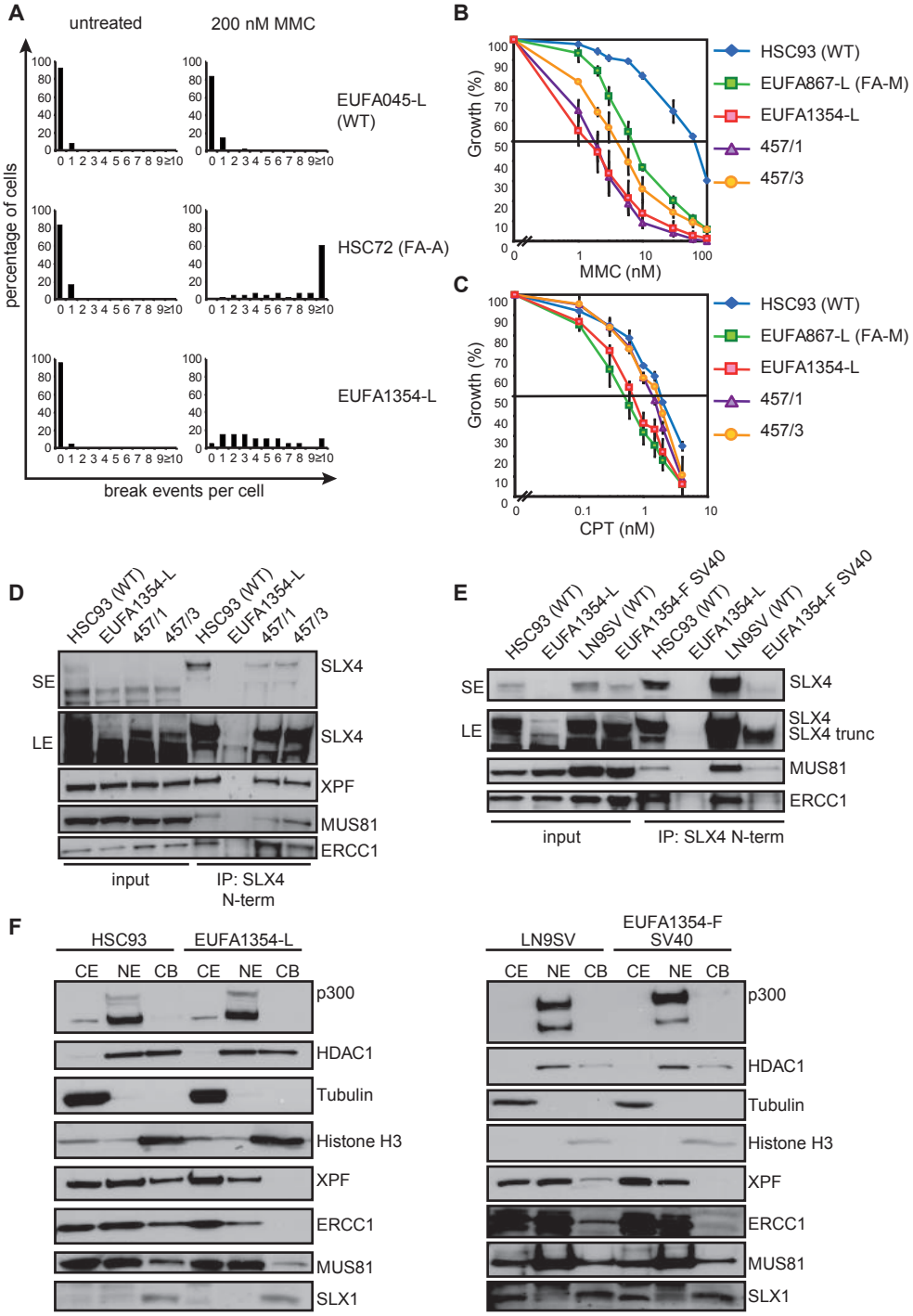
A
untreated
200 nM MMC
EUFA045-L (WT)
HSC72 (FA-A)
EUFA1354-L
percentage of cells
break events per cell
B
Growth (%)
MMC (nM)
HSC93 (WT)
EUFA867-L (FA-M)
EUFA1354-L
457/1
457/3
C
Growth (%)
CPT (nM)
HSC93 (WT)
EUFA867-L (FA-M)
EUFA1354-L
457/1
457/3
D
HSC93 (WT)
EUFA1354-L
457/1
457/3
SE
LE
SLX4
SLX4
XPF
MUS81
ERCC1
input
IP: SLX4 N-term
E
HSC93 (WT)
EUFA1354-L
LN9SV (WT)
EUFA1354-F SV40
SE
LE
SLX4
SLX4
SLX4 trunc
MUS81
ERCC1
input
IP: SLX4 N-term
F
HSC93
EUFA1354-L
LN9SV
EUFA1354-F SV40
CE NE CB CE NE CB
p300
HDAC1
Tubulin
Histone H3
XPF
ERCC1
MUS81
SLX1

Figure 1. Cellular characteristics of individuals with Fanconi anemia with a defect in SLX4.
(**A**) Spontaneous and mitomycin C (MMC)-induced chromosomal breakage in EBV-immortalized lymphoblasts from a healthy individual (EUFA045-L), a FANCA-deficient individual (HSC72) and individual EUFA1354. Percentages of cells with up to ten or more break events per metaphase are shown. (**B**) Growth inhibition of EUFA1354, 457/1 and 457/3 lymphoblasts upon exposure to MMC or (**C**) camptothecin (CPT). Lymphoblasts from a healthy individual (HSC93) and a FANCM-deficient individual (EUFA867-L) were analyzed as controls. Data represent means and s.e.m. from at least two independent experiments. (**D**) Immunoprecipitation and protein blot analysis showing reduced SLX4 expression in lymphoblasts from the affected siblings 457/1 and 457/3 and the absence of full-length SLX4 in lymphoblasts from EUFA1354. The mutant protein in 457/1 and 457/3 interacts with ERCC1, XPF and MUS81, whereas these proteins are not co-precipitated in EUFA1354-L. We performed immunoprecipitation with antibodies against the SLX4 N terminus (1–300) and protein blotting with an antibody against the SLX4 C terminus (1,534–1,834). SE and LE indicate short and long exposures of the blot, respectively. (**E**) Immunoprecipitation and protein blot analysis demonstrating the absence of full-length SLX4 and impaired interactions with MUS81 and ERCC1 in SV40- immortalized EUFA1354 fibroblasts. We used wildtype fibroblasts (LN9SV) as a control. (**F**) Subcellular fractionation of EUFA1354 lymphoblasts and fibroblasts showing reduced chromatin binding of ERCC1 and XPF. We analyzed the cytoplasmic fraction (CE), nuclear extract (NE) and chromatin fraction (CB) and used tubulin, p300 and histone H3 as controls for these fractions. WT, wildtype; FA-A, Fanconi anemia type A; FA-M, Fanconi anemia type M.

of RAD51 and H2AX foci in this individual's fibroblasts suggested a normal DNA damage response (**Supplementary Fig. 3C–F**). We ruled out an abnormality in the downstream Fanconi anemia proteins BRCA2, PALB2 and FANCJ by cell fusion experiments and sequence analysis of the corresponding genes (data not shown), indicating that this individual represented a new Fanconi anemia subtype with a defect in a new player of the FA-BRCA pathway.

Recently, four research groups identified the human SLX4 scaffold protein, which was proposed to function in the processing of DNA repair intermediates and crosslink repair through interaction with the structure-specific endonucleases SLX1, XPF-ERCC1 and MUS81-EME1 (refs. 5-8). SLX4-depleted cells are hypersensitive to crosslinking agents and camptothecin, similar to lymphoblasts from the affected individual EUFA1354. Therefore, we hypothesized that SLX4 might be defective in this individual. Sequence analysis of genomic DNA and complementary DNA (cDNA) from EUFA1354 indeed revealed biallelic mutations in the reading frame of *SLX4* (**Supplementary Fig. 4**). We detected a homozygous, 1-bp deletion (c.286delA) in the first exon of *SLX4* that results in a frameshift at codon 96 and a premature stop at codon 126 (p.Thr96LeufsX30). The consanguineous parents and healthy sister of the affected individual were all heterozygous for this sequence variant.

We obtained additional evidence for SLX4 deficiency in individuals with Fanconi anemia by the identification of a second Fanconi anemia family with pathogenic *SLX4* mutations. Linkage analysis with a genome-wide SNP array showed a common 13.5 Mbp region around the *SLX4* locus in three unclassified German siblings with mild manifestations of Fanconi anemia and bone marrow failure (**Table 1 and Supplementary Fig. 5**). The siblings all inherited a 1-bp deletion in *SLX4* (c.1093delC, p.Gln365SerfsX31) from their father and a splice

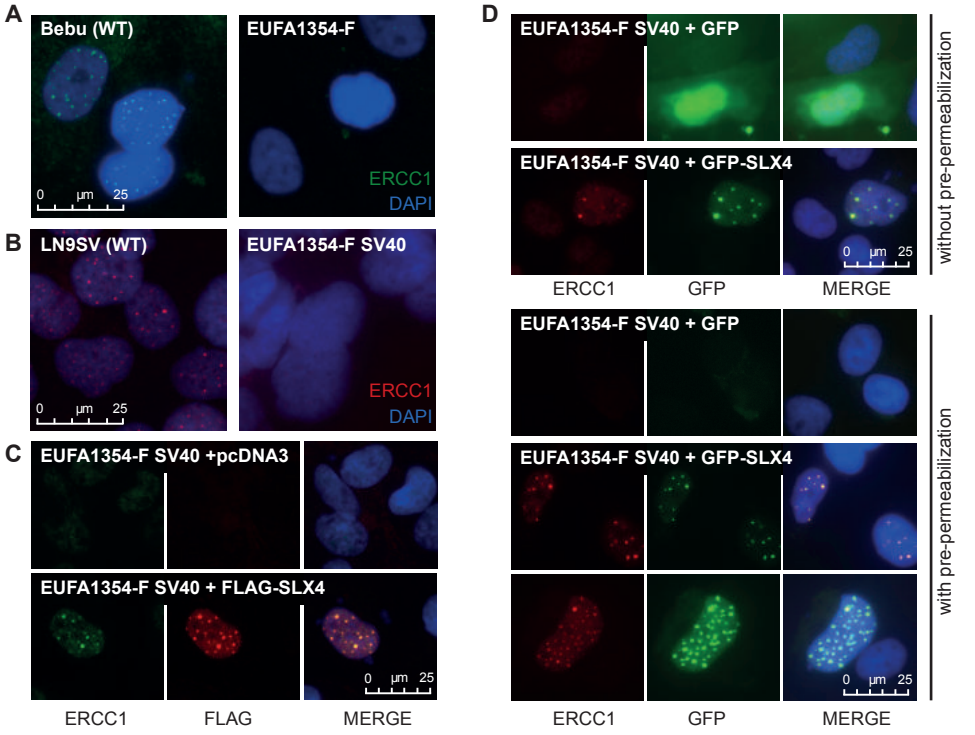
A
Bebu (WT)
EUFA1354-F
ERCC1
DAPI
0 µm 25
B
LN9SV (WT)
EUFA1354-F SV40
ERCC1
DAPI
C
EUFA1354-F SV40 +pcDNA3
EUFA1354-F SV40 + FLAG-SLX4
ERCC1
FLAG
MERGE
D
EUFA1354-F SV40 + GFP
EUFA1354-F SV40 + GFP-SLX4
without pre-permeabilization
with pre-permeabilization
ERCC1
GFP
MERGE

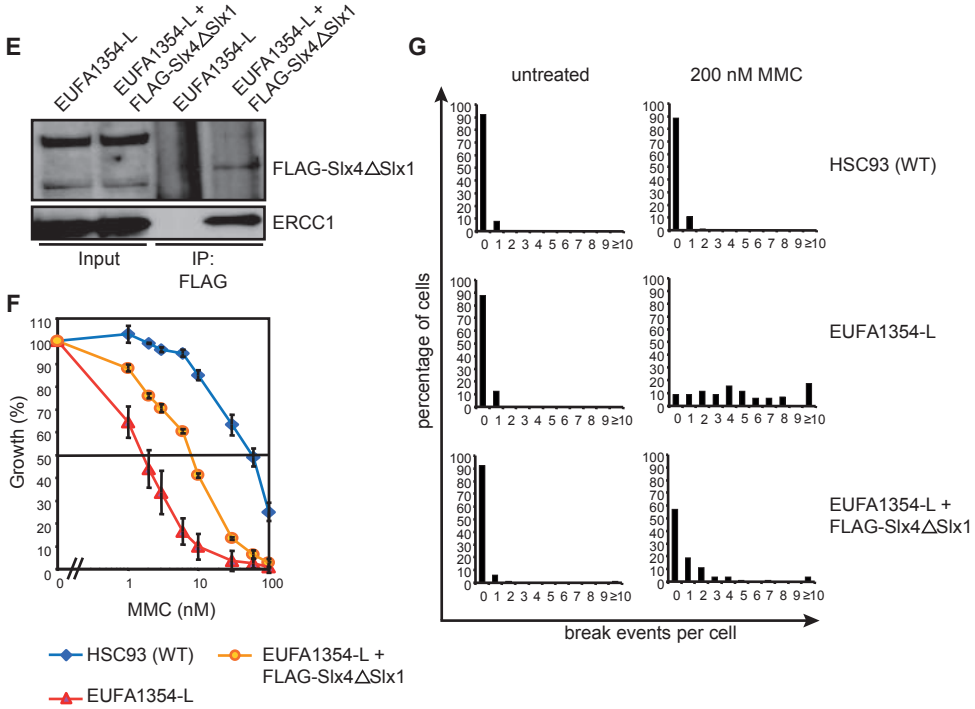
E
EUFA1354-L
EUFA1354-L + FLAG-Slx4ΔSlx1
FLAG-Slx4ΔSlx1
ERCC1
Input
IP: FLAG
F
Growth (%)
MMC (nM)
HSC93 (WT)
EUFA1354-L + FLAG-Slx4ΔSlx1
EUFA1354-L
G
untreated
200 nM MMC
HSC93 (WT)
EUFA1354-L
EUFA1354-L + FLAG-Slx4ΔSlx1
percentage of cells
break events per cell

Figure 2. Functional correction of EUFA1354 fibroblasts and lymphoblasts by exogenous SLX4.
ERCC1 foci are absent in (**A**) primary and (**B**) SV40-immortalized EUFA1354 fibroblasts. Bebu and LN9SV were used as wildtype controls. (**C**) Transient transfection of FLAG-SLX4 in SV40-immortalized EUFA1354 fibroblasts restored their ability to form nuclear ERCC1 foci. An empty vector (pcDNA3) was used as a control. (**D**) Transient transfection of GFP-SLX4 in SV40-immortalized EUFA1354 fibroblasts restored their ability to form nuclear ERCC1 foci. Transient transfection of GFP was used as a control. ERCC1 foci are more pronounced after brief pre-permeabilization with Triton-X100 before fixation, but this removed exogenous GFP. ERCC1 antibody FL297 was used for immunofluoresence, and DAPI (blue) was used as a nuclear counterstaining. (**E**) A mouse Slx4 protein that lacks the Slx1 binding site (FLAG-Slx4ΔSlx1) is stably expressed in EUFA1354 lymphoblasts and interacts with ERCC1. (**F**) FLAG-Slx4ΔSlx1 partially corrects MMC-induced growth inhibition in EUFA1354 lymphoblasts. Data represent means and s.e.m. from two independent experiments. (**G**) FLAG-Slx4ΔSlx1 partially corrects MMC-induced chromosomal breakage in EUFA1354 lymphoblasts. WT, wildtype.

site mutation (c.1163+3dupT) from their mother (**Supplementary Fig. 6A**). The maternal mutation lead to exon 5 skipping, an in-frame deletion that disrupts the UBZ4 domain in SLX4, which may be involved in targeting SLX4 to sites of DNA damage by binding to ubiquitinated proteins (**Supplementary Fig. 6B,C**). We detected the residual mutant SLX4 protein in cell lysates, and this protein was able to interact with XPF, ERCC1 and MUS81 (**Fig. 1D**). Notably, lymphoblasts from these individuals were sensitive to MMC (**Fig. 1B**) but not to camptothecin (**Fig. 1C**), indicating that the mutant protein is partially functional.

We also examined SLX4 protein expression in lymphoblast lysates from EUFA1354. Full-length SLX4 was undetectable by immunoprecipitation with antibodies against the N or C terminus of SLX4, but we detected very low levels of a truncated SLX4 protein with antibodies against the C terminus of SLX4 (**Fig. 1D and Supplementary Fig. 7A**). Consequently, the amounts of XPF-ERCC1 and MUS81 in SLX4 immunoprecipitates were reduced compared to wildtype cells (**Fig. 1D and Supplementary Fig. 7A**). The truncated SLX4 protein was more pronounced in SV40-immortalized fibroblasts from EUFA1354 (**Fig. 1E and Supplementary Fig. 7B**) and may be derived from an alternative translation initiation site present at codon 213. Reciprocal immunoprecipitations with antibodies against ERCC1, XPF or MUS81 readily co-precipitated full-length SLX4 from wildtype cells, but only some truncated SLX4 protein was co-precipitated from EUFA1354 cells (**Supplementary Fig. 7C,D**). When transiently expressed in human HEK293 cells, a truncated SLX4 protein starting from Met213 is able to interact with XPF-ERCC1, MUS81-EME1 and SLX1, similar to full-length SLX4 (**Supplementary Fig. 7E**). These data indicate that the defects seen in the EUFA1354 cells are due to very low concentrations of the truncated SLX4 protein and not because truncated SLX4 is defective in interacting with a specific nuclease.

Gel filtration experiments showed that XPF-ERCC1 and SLX1, which normally exist in two subcomplexes[8], eluted only in the low molecular weight fractions from EUFA1354 fibroblast lysates, whereas the elution of MUS81 was not affected

(**Supplementary Fig. 8**). Subcellular fractionation studies revealed a reduced chromatin association of XPF-ERCC1 in EUFA1354, whereas MUS81 and SLX1 were hardly affected (**Fig. 1F**). These data strongly suggest that the SLX4 defect in EUFA1354 interferes with the function of the XPF-ERCC1 endonuclease, an important player in crosslink repair.

According to a recent study[6], SLX4 accumulates in nuclear foci, where it co-localizes with XPF. We investigated the nuclear localization of ERCC1 in primary and immortalized EUFA1354 fibroblasts. We detected nuclear ERCC1 foci in wildtype cells; however, EUFA1354 fibroblasts lacked these structures (**Fig. 2A,B**). We confirmed this striking result with another ERCC1 antibody[9] (**Supplementary Fig. 9**). EUFA1354 fibroblasts, transiently transfected with SLX4 cDNA, regained their capacity to form ERCC1 foci, which co-localize with both FLAG-SLX4 and GFP-SLX4 (**Fig. 2C,D**). This confirms that the SLX4 defect in EUFA1354 affects the XPF-ERCC1 endonuclease.

To further strengthen the evidence that SLX4 deficiency causes the cellular phenotype in EUFA1354, we tried to correct the MMC hypersensitivity through SLX4 cDNA transfection in EUFA1354 lymphoblasts. Although we were unable to stably express full-length human SLX4, a truncated mouse Slx4 protein that corrects Slx4-deficient mouse embryonic fibroblasts[10] partially restored MMC resistance in terms of cell growth (**Fig. 2E,F**). Chromosomal breakage analysis on individual metaphases showed that only part of the lymphoblasts (57%) had been fully complemented (**Fig. 2G**).

In conclusion, defective SLX4 is associated with a previously unknown subtype of Fanconi anemia, Fanconi anemia-P. The presence of a truncated SLX4-FANCP protein in the individuals reported here indicates that the mutations may be hypomorphic, as has been found for individuals with an alteration in ERCC1 or XPF[11,12]. Because germline mutations in all the other downstream players of the FA-BRCA pathway predispose to breast and/or ovarian cancer, *SLX4* could also be a cancer predisposition gene.

Methods

Ethics statement

The research was carried out after approval by the Institutional Review Board of the Vrije Universiteit Medical Center that adhered to local ethical standards and was initiated only after the relevant informed consents had been obtained. Information and consent of the German family used in this study was in agreement with national legal regulations and the Declaration of Helsinki.

Cell culture and transfection

HEK293 cells were cultured in Dulbecco's Modified Eagle's Medium (DMEM, GIBCO) with 10% FBS (Hyclone), 100 international units ml^{-1} penicillin and 0.1 mg ml^{-1} streptomycin and 1% L-glutamine (Invitrogen). Cells were transiently transfected by calcium phosphate precipitation and incubated for 24–30 h at 37 °C before lysis.

Skin fibroblasts, either primary or immortalized with SV40 large T antigen, were cultured in DMEM or Ham's F-10 with 10% FBS. Fibroblasts were transiently transfected with Amaxa Nucleofector using a

human dermal fibroblasts nucleofector kit.
EBV-transformed lymphoblasts were cultured in RPMI1640 medium containing 10% FBS. Stably expressing lymphoblasts were generated by electroporation of pMEP4 constructs (Invitrogen) and selection on 100 µg/ml hygromycin.

cDNA constructs
The cDNA encoding full-length human SLX4 was generated by PCR on IMAGE clones 6527830 and 4340346 and was cloned into pcDNA5 FRT/TO-FLAG and pcDNA5 FRT/TO-GFP (Invitrogen, Flp-In T-Rex system). For GFP-SLX4 213-end, the pcDNA5 FRT/TO-GFP with full-length SLX4 was used to PCR amplify a fragment encoding SLX4 residues 213–1,834, which was shuttled into pcDNA5 FRT/TO-GFP. Constructs were verified by sequencing. A cDNA construct encoding mouse SLX4 that lacks the SLX1 binding site (amino acids 1,417–1,565 in mouse Slx4 corresponding to amino acids 1,685–1,834 in human SLX4) was a gift of K.J. Patel.

Chromosomal breakage analysis.
Heparinized blood (2 ml) was diluted with 18 ml blood culture medium (Ham's F-10 + 15% FBS + phytohemagglutinin). Subsequently, 5 ml of this suspension was cultured in the presence of 0, 15 or 300 nM MMC. After 72 h, 100 µl demecolcin (10 µg/ml in Hank's Balanced Salt Solution (HBSS)) was added, and cells were incubated for 20 min at 37 °C. Cells were centrifuged, resuspended in 0.075 M KCl and incubated for 20 min at 18–22 °C. The cells were spun down, resuspended in 10 ml fixative (75% methanol and 25% acetic acid), incubated for 30 min at room temperature and centrifuged. The pellet was resuspended in 10 ml fixative and incubated for 5 min at room temperature. This step was repeated and finally the pellet was resuspended in 0.5–1.0 ml fixative. The cell suspension was dropped on a slide and allowed to dry. Slides were incubated for 15 min in 0.1 M HNO_3 and rinsed in tap water and 70% ethanol, respectively. Next, slides were stained for 5 min in a 4% Giemsa solution, rinsed in tap water, allowed to dry and coded. From each coded culture, at least 50 metaphases were examined for chromosomal damage. The presence of chromatid breaks and interchanges was expressed as break events per cell, counting chromatid interchange figures as the minimum number of break events required for their reconstruction. After scoring, the slides were decoded and the results were analyzed.
Lymphoblasts were seeded in 25 cm^2 tissue culture flasks at a density of $2–3 \times 10^6$ per 10 ml fresh Roswell Park Memorial Institute (RPMI) medium containing 10% FBS and cultured at 37 °C for 48 h in the presence of 0 nM or 200 nM MMC. Next, 200 µl of demecolcin (10 µg/ml in HBSS) was added to each culture flask, and the cells were incubated for an additional 20 min at 37 °C. Metaphase spreads were prepared and analyzed as described above.
Fibroblasts (1×10^6 cells in 15 ml Ham's F-10 + 10% FBS) were seeded in an 80 cm^2 tissue culture flask and cultured at 37 °C in the presence or absence of 50 nM mitomycin C. After 48 h, 300 µl of demecolcin (10 µg/ml in HBSS) was added to each culture flask, and cells were incubated for an additional 30 min at 37 °C. Cells were then trypsinized, and metaphase spreads were prepared and analyzed as described above.

Cell cycle analysis
Fibroblasts were cultured for 72 h either without or with MMC (50 nM or 100 nM) in Ham's F-10 medium supplemented with 10% FBS. Cells were harvested by trypsinization and permeabilized in buffer containing 100 mM Tris-HCL (pH 7.5), 150 mM NaCl, 0.5 mM $MgCl_2$, 1 mM $CaCl_2$, 0.2% BSA and 0.1% NP-40 followed by staining of DNA with PI/RNase staining buffer (BD Pharmingen, BD Biosciences). Cell suspensions were analyzed by flow cytometry on a BD FACSCalibur (BD Biosciences) to determine G2/M accumulation as the percentage of cells present in the G2/M phase of the cell cycle.
Lymphoblasts were stained with 4′-6-diamidino-2-phenylindole (DAPI) at a final concentration of 1 µg/ml. Flow histograms were made on an analytical, triple-laser–equipped flow cytometer (LSRII, BD Biosciences). Results were quantified with MPLUS AV software (Phoenix Flow Systems).

Growth inhibition assays
The MMC- and camptothecin-induced growth inhibition assays on lymphoblasts and fibroblasts were performed as previously described[13].

Cell fractionation
Cytoplasmic, nuclear and chromatin fractions were isolated using a Subcellular Protein Fractionation Kit (Thermo Scientific) according to the manufacturer's instructions. Controls used for the fractionation

were tubulin (cytoplasmic fraction), p300 (nuclear fraction), histone H3 (chromatin fraction) and HDAC1 (nuclear and chromatin fraction).

Cell lysis, immunoprecipitation and protein blotting
Cells were lysed on ice with ice-cold lysis buffer containing 50 mM Tris-HCl (pH 7.4), 1% Triton X-100, 0.1% (v/v) 2-mercaptoethanol, 0.27 M sucrose and protease inhibitors for immunoprecipitation. For pull-downs with GFP-Trap beads (ChromoTek), cells were lysed on ice with ice-cold lysis buffer consisting of 10 mM Tris-HCl, (pH 7.5), 150 mM NaCl, 0.5 mM EDTA, 0.5% NP40 and protease inhibitors. Lysates were precleared with 50 µl protein G-Sepharose (50% slurry) for 30 min. Immunoprecipitations and pull-downs were performed for 2 h at 4 °C.
The primary antibodies used for immunoprecipitation and protein blotting were as follows: anti-XPF (Thermo MS-1381), anti-ERCC1 (Thermo MS-671 or Santa Cruz FL297), anti-MUS81 (ImmuQuest IQ285 or Abcam ab14387), anti-EME1 (ImmuQuest IQ284), anti-GFP (Roche 11814460001), anti-GAPDH (Abcam ab8245), anti-p300 (Santa Cruz SC-585), anti-HDAC1 (Santa Cruz SC7872), anti-tubulin (Abcam ab7291), anti-histone H3 (Cell Signaling Technology 9715), anti-FANCD2 (Santa Cruz sc20022) and anti-RAD50 (GeneTex 13B3). Sheep polyclonal antibodies were raised against the first 300 amino acids (SLX4-N) or the last 300 amino acids (SLX4-C) of SLX4 fused to GST. Antibodies were also raised against full-length SLX1-GST expressed in bacteria. SLX4 and SLX1 antibodies were affinity purified before use.

Immunofluorescence
Fibroblasts (100,000 cells per well) were seeded in four-well chamber slides (Nunc). After overnight culture, cells were washed with PBS and pre-permeabilized with 0.25% Triton X-100 in PBS (1 min on ice). Cells were fixed with 4% paraformaldehyde (15 min at room temperature) and permeabilized with 0.5% Triton X-100 in PBS (10–20 min at room temperature). Unspecific binding sites were blocked with PBS + 10% FBS (or PBS + 10% BSA for γH2AX staining) for 1 h at room temperature. Slides were incubated with specific antibodies in blocking buffer (2 h at room temperature). Excess antibody was removed by four washing steps with PBS + 0.2% Triton X-100. Slides were then incubated with secondary antibody labeled with Alexa 594 or Alexa 488 (Invitrogen, 1:1,000) and DAPI (1:1,000) for 1 h at room temperature. Finally, slides were washed four times with PBS + 0.2% Triton X-100 and embedded. Slides were analyzed with a fluorescent microscope (DM5000, Leica). ERCC1 foci were also analyzed 72 h after cDNA transfection.
Lymphoblasts were attached to glass slides by cytocentrifugation. The percentage of foci-positive cells (>10 foci per nucleus) was determined on a Zeiss Axio Imager A1 fluorescence microscope. For each experiment, 200–400 nuclei were analyzed.
The following antibodies were used: anti-FANCD2 (Novus NB100-182, 1:200), anti-RAD51 (gift of R. Kanaar, 1:2,500, or Abcam ab63801), anti-phospho-H2AX (Ser139) (Millipore clone JBW301, 1:400) and anti-ERCC1 (Santa Cruz FL297, 1:200).

Size exclusion chromatography
For gel filtration experiments, cell extracts (3 mg of protein) were loaded on a Superose 6 column (GE Healthcare) in buffer containing 50 mM Tris/HCl (pH 7.4), 1 mM EDTA, 0.2 M sodium chloride and 0.1% (v/v) 2-mercaptoethanol. Molecular weight markers (Bio-Rad) were as follows: thyroglobulin (670 kDa) and bovine gamma globulin (158 kDa). Fraction was denatured and subjected to protein blot analysis.

Sequence analysis
For direct sequencing, PCR products were generated by SLX4-specific primers (**Supplementary Table 1**) PCR fragments were treated with shrimp alkaline phosphatase (30 min at 37 °C) and Exonuclease I (15 min at 80 °C). Sequencing reactions were carried out using 10 pM of primer and the Big Dye Terminator cycle sequencing kit (Applied Biosystems). Samples were analyzed in an ABI 3730 DNA analyzer (Applied Biosystems).

Genome wide SNP array
Genome wide SNP genotypes for the German family members were determined on a HumanHap300v2 Genotyping BeadChip (Illumina Inc.). After scanning the microarrays on a BeadStation 500G with the software BeadScan Ver. 3.7.5.23284, SNP genotypes were called using the software BeadStudio Ver. 3.1.3.0 with the Genotyping Module Ver. 3.2.32 (all from Illumina Inc.).

Acknowledgements
We thank the affected individuals and their families for contributing to this study. We also thank A. Raams, R. Friedl, B. Gottwald and S. Darchinger for expert technical assistance. We acknowledge I. Carr for Phaser software, R. Kanaar for RAD51 antiserum and K.J. Patel for mouse Slx4 cDNA. Financial support was from the Cancer Center Amsterdam-VU Medisch Centrum Institute for Cancer and Immunology (CCA/V-ICI) Amsterdam (to C.S.), the Dutch Cancer Society (to H.J.), Schroeder-Kurth-Fund (to D.S.) and the Medical Research Council UK (to J.R.).

Author contributions
The study was designed by J.P.d.W., J.R., D.S. and H.J. Clinical information of affected individuals and referral for Fanconi anemia diagnosis was coordinated by E.T.K. and Y.H.-H. Fanconi anemia diagnosis was confirmed by A.W.M.N. SNP array studies were coordinated by T.B. Mutational analysis and functional studies were carried out by C.S., K.H., B.S., M.A.R., J.S., A.B.O. and K.E. The ERCC1 focus formation assay was coordinated by N.G.J.J. The manuscript was written by C.S., J.P.d.W., J.R. and D.S., with help from the other authors.

Competing financial interests
The authors declare no competing financial interests.

Supplementary data

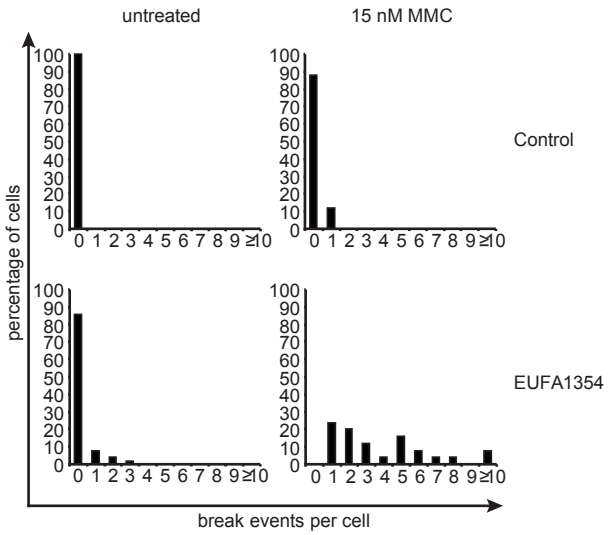

Supplementary Figure 1. Spontaneous and MMC-induced chromosomal breakage in PHA-stimulated lymphocyte cultures from a healthy control and the affected individual (EUFA1354).
Percentages of cells with up to ≥ 10 break events per cell are shown. In EUFA1354 lymphocytes treated with 15 nM MMC, all metaphases were aberrant and exhibited 1 to ≥ 10 break events per cell; at 300 nM MMC 100% of the metaphases had ≥ 10 break events per cell (results not shown).

Right: Supplementary Figure 2. DNA cross-linker and camptothecin sensitivity in EUFA1354 lymphoblasts and fibroblasts.
(**A**) Growth inhibition of EUFA1354 lymphoblasts upon exposure to mitomycin C (MMC) or (**B**) camptothecin (CPT). Lymphoblasts from a healthy individual (HSC93) and a FANCM-deficient individual (EUFA867-L) were analyzed as controls. Data represent means and standard errors of the mean from at least three independent experiments. (**C**) Cell cycle analysis of primary EUFA1354 fibroblasts reveals G2/M arrest after treatment with mitomycin C (MMC). Wild type fibroblasts (Bebu) and FANCJ-deficient fibroblasts (EUFA1333-F) were used as controls. (**D**) MMC-induced G2/M arrest in primary and SV40-immortalized EUFA1354 fibroblasts. Percentages of cells in G2/M arrest are shown. The results are the mean of two independent experiments, with standard errors of the mean. Wild type fibroblasts (Bebu and LN9SV) and FA deficient fibroblasts (EUFA1333-F (FA-J) and GM6914 (FA-A)) were used as controls. (**E**) MMC-induced growth inhibition in primary fibroblasts. Data represent means and standard errors of the mean for three experiments. (**F**) MMC-induced growth inhibition in SV40-immortalized fibroblasts. A representative result of 3 independent experiments is shown. (**G**) Spontaneous and MMC-induced chromosomal breakage in SV40- immortalized fibroblasts. Percentages of cells with up to ≥ 10 break events per cell are shown. The number of EUFA1354 fibroblasts with zero MMC-induced break events per cell is significantly different from wild type cells (p=0.05, two-sample Chi2 test).

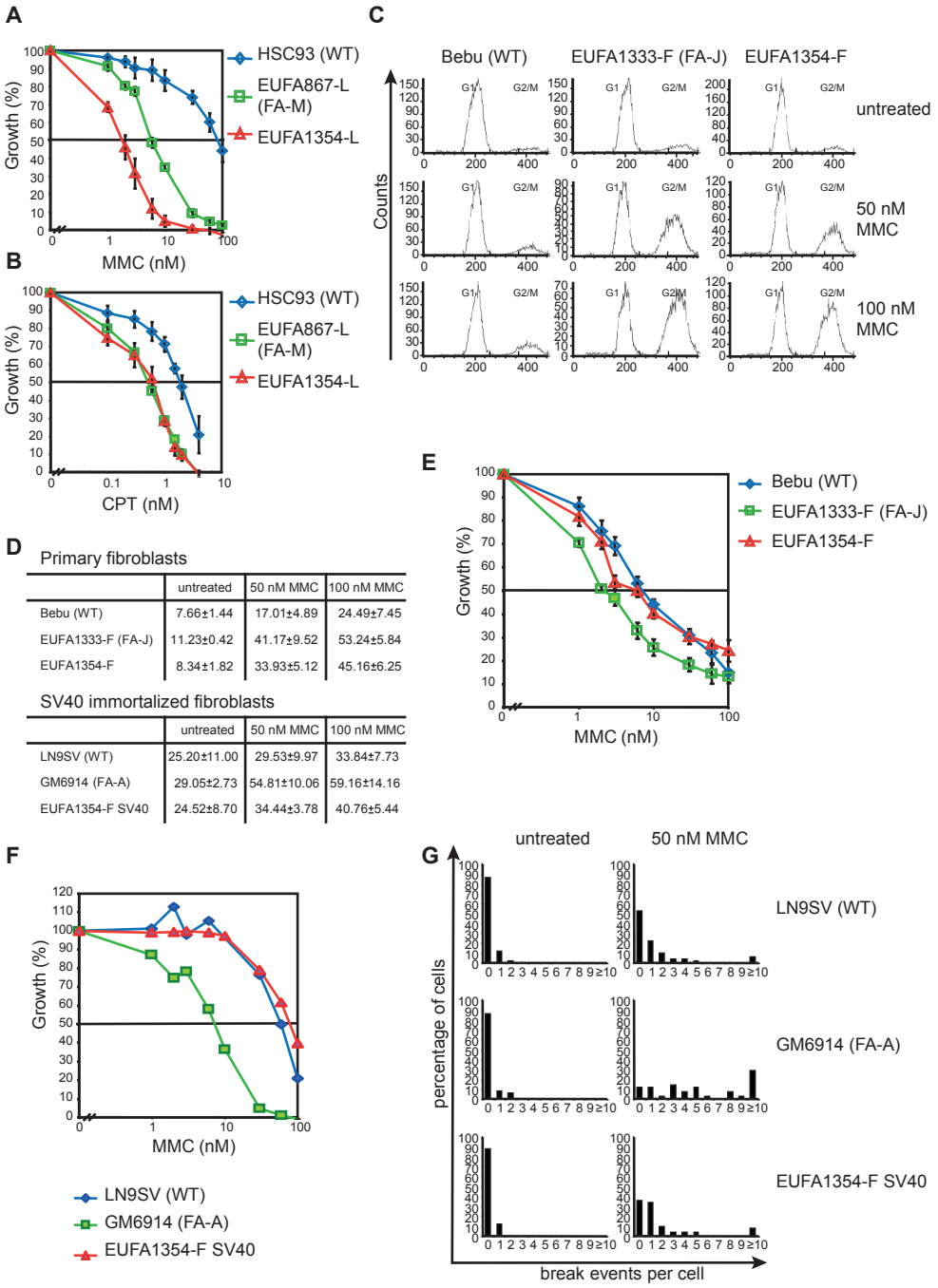

Primary fibroblasts	untreated	50 nM MMC	100 nM MMC
Bebu (WT)	7.66±1.44	17.01±4.89	24.49±7.45
EUFA1333-F (FA-J)	11.23±0.42	41.17±9.52	53.24±5.84
EUFA1354-F	8.34±1.82	33.93±5.12	45.16±6.25

SV40 immortalized fibroblasts	untreated	50 nM MMC	100 nM MMC
LN9SV (WT)	25.20±11.00	29.53±9.97	33.84±7.73
GM6914 (FA-A)	29.05±2.73	54.81±10.06	59.16±14.16
EUFA1354-F SV40	24.52±8.70	34.44±3.78	40.76±5.44

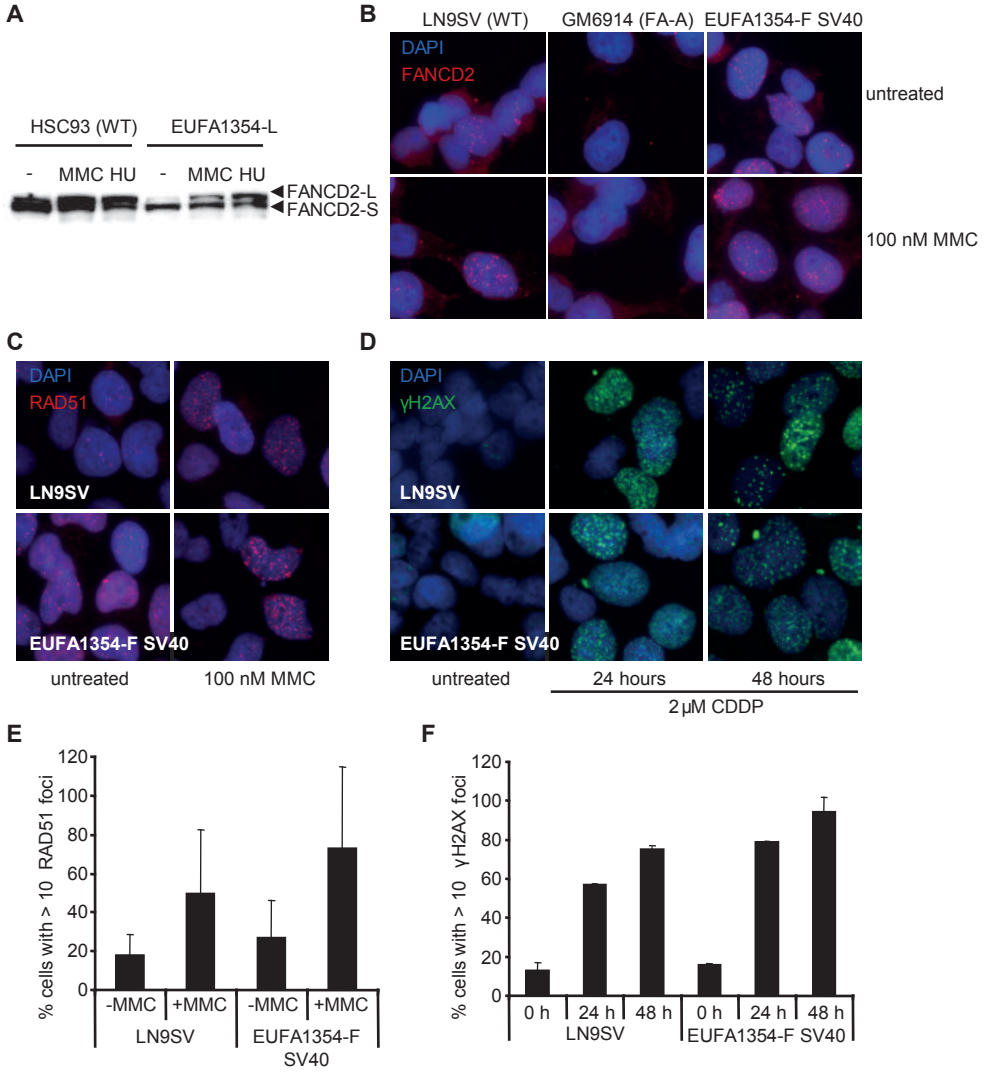

Supplementary Figure 3. Normal FANCD2 monoubiquitination and FANCD2, RAD51 and γ-H2AX focus formation in EUFA1354.
(**A**) Immunoblotting revealed induction of FANCD2 monoubiquitination after treatment with mitomycin C (MMC) or hydroxyurea (HU) in EUFA1354-L lymphoblasts. (**B**) Immunofluorescence demonstrated normal induction of FANCD2 foci (red) in SV40-immortalized EUFA1354 fibroblasts. Wild type (LN9SV) and FANCA-deficient (GM6914) fibroblasts were included as a positive and negative control, respectively. DAPI (blue) was used as a nuclear counterstaining. (**C**) MMC-induced RAD51 foci (red) in SV40- immortalized EUFA1354 fibroblasts and LN9SV wild type fibroblasts. (**D**) Cisplatin-induced γ-H2AX foci (green) in SV40-immortalized EUFA1354 fibroblasts and LN9SV wild type fibroblasts. (**E+F**) Quantification of the results in C and D. Data represent means and standard errors of the mean for two experiments.

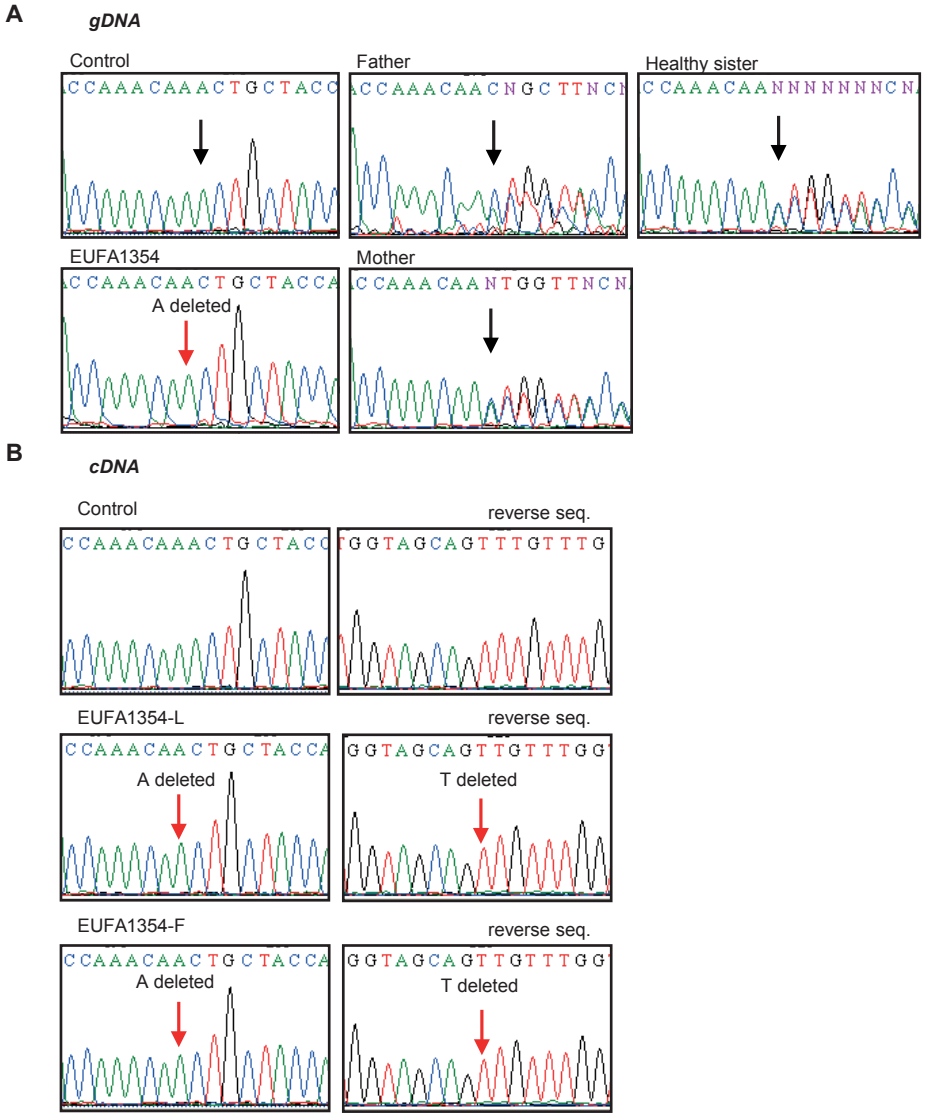

Supplementary Figure 4. *SLX4* mutations in EUFA1354.
(**A**) Sequence analysis of genomic blood DNA of EUFA1354 revealed a homozygous 1-bp deletion in exon 1 of *SLX4* (c.286delA), resulting in a frameshift at codon 96 and premature stop at codon 126 (p.T96LfsX30). The parents (second cousins) and a healthy sister are all heterozygous for the mutation. (**B**) Sequence analysis on cDNA from EUFA1354 lymphoblasts and fibroblasts detected the homozygous 1-bp deletion in *SLX4* (c.286delA).

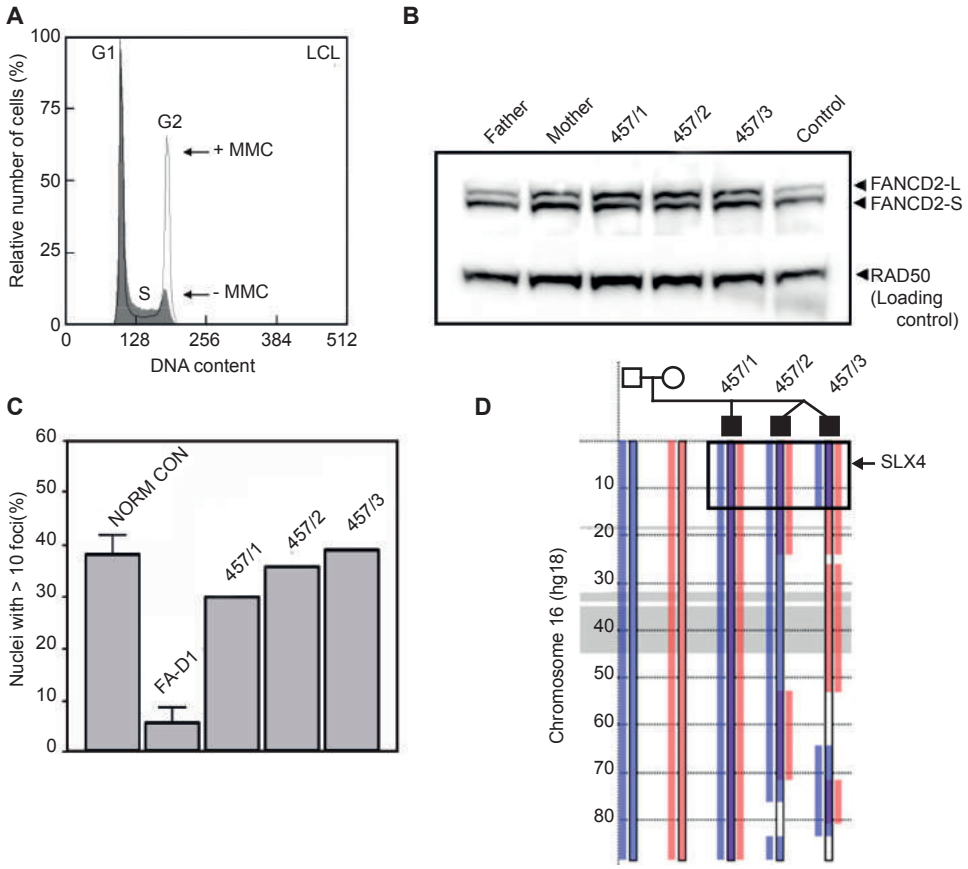

Supplementary Figure 5. Characteristics of the German SLX4 deficient family.
(**A**) G2 phase arrest in the oldest affected German sibling (457/1). Lymphoblast cultures were left untreated (grey) or exposed to 45 nM mitomycin C (MMC) for 48 h (transparent overlay). As a manifestation of FA, cells show exaggerated G2 phase blockage (arrow) in response to MMC. Quantitative analysis of the cell cycle distributions reveals 60.1% G1, 30.2% S and 9.7% G2 phase without MMC and 42.2% G1, 18.3% S and 39.5% G2 phase with MMC. (**B**) Normal FANCD2 monoubiquitination in lymphoblasts from the German FA siblings (457/1-3) suggests a downstream defect in the FA/BRCA pathway. RAD50 served as loading control. (**C**) Normal formation of RAD51 foci in lymphoblasts of the German FA siblings (457/1-3) suggests properly functioning BRCA2, PALB2 and RAD51C. This was confirmed by Western blotting (BRCA2 and PALB2) or sequencing (RAD51C). FANCJ protein levels were also normal. (**D**) Graphic presentation of linkage analysis in the German family by the program Phaser. The disease genotype of chromosome 16 in this family is defined by the first affected sibling (457/1, violet central bar) between the corresponding parental alleles (left paternal blue bar, right maternal red bar). Regions of common linkage (violet) are shown for the second affected sibling (457/2) compared to the first, and for the third affected sibling (457/3) compared to the first. A region common to all three of them extends from 0 to 13.5 K (box). SLX4 lies therein at 3.5-3.6 K (arrow). Regions where only one parental mutation allele has been inherited are shown in that colour. Gaps between the bars characterize regions where the non-mutated alleles have been transmitted. Gray is the centromeric region. This analysis also reveals that the twin siblings are dizygotic.

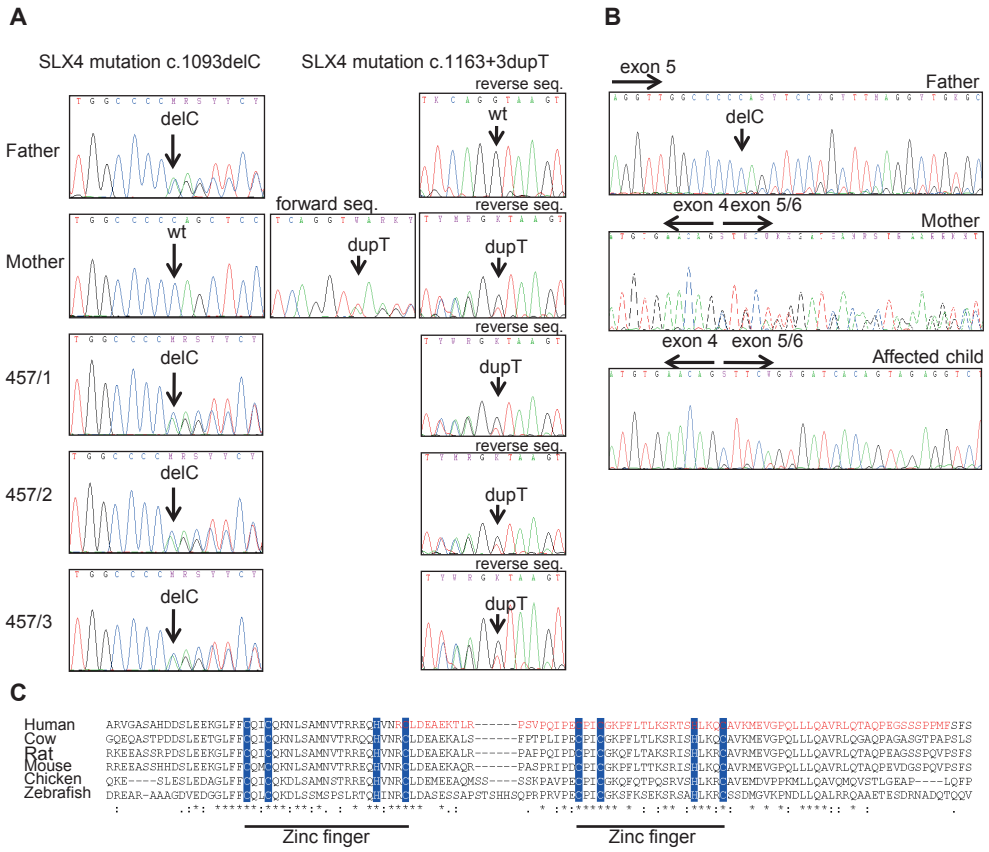

Supplementary Figure 6. *SLX4* mutations in the unclassified German family.
(**A**) Sequence analysis of genomic DNA revealed a 1-bp deletion (c.1093delC) and a splice site mutation (c.1163+3dupT) in the three affected siblings. The deletion was detected in genomic DNA from the father; the splice site mutation was present in genomic DNA from the mother. Only reverse sequences identify the duplication unequivocally in the affected siblings as forward sequences have superimposed sequence resulting from the paternal deletion. "Splicefinder" software (http://www.splicefinder.net/form.php) predicts a decrease of the splice donor score from 20.8 (wild type) to 11.9 (c.1163+3dupT). (**B**) Sequence analysis on cDNA of affected sibling 3 (457/3) shows that c.1163+3dupT causes exon 5 skipping. Underlying sequence without exon 5 skipping from the other mutant allele is minor, suggesting instability of the transcript containing c.1093delC by nonsense-mediated mRNA decay. This finding is confirmed by cDNA sequencing in the father. The transcript that lacks exon 5 sequence due to c.1163+3dupT is stable as indicated by cDNA sequencing in the mother. (**C**) The exon 5 deletion removes amino acids 317-387 (indicated in red) from the SLX4 protein, which disrupts the conserved UBZ4 domain.

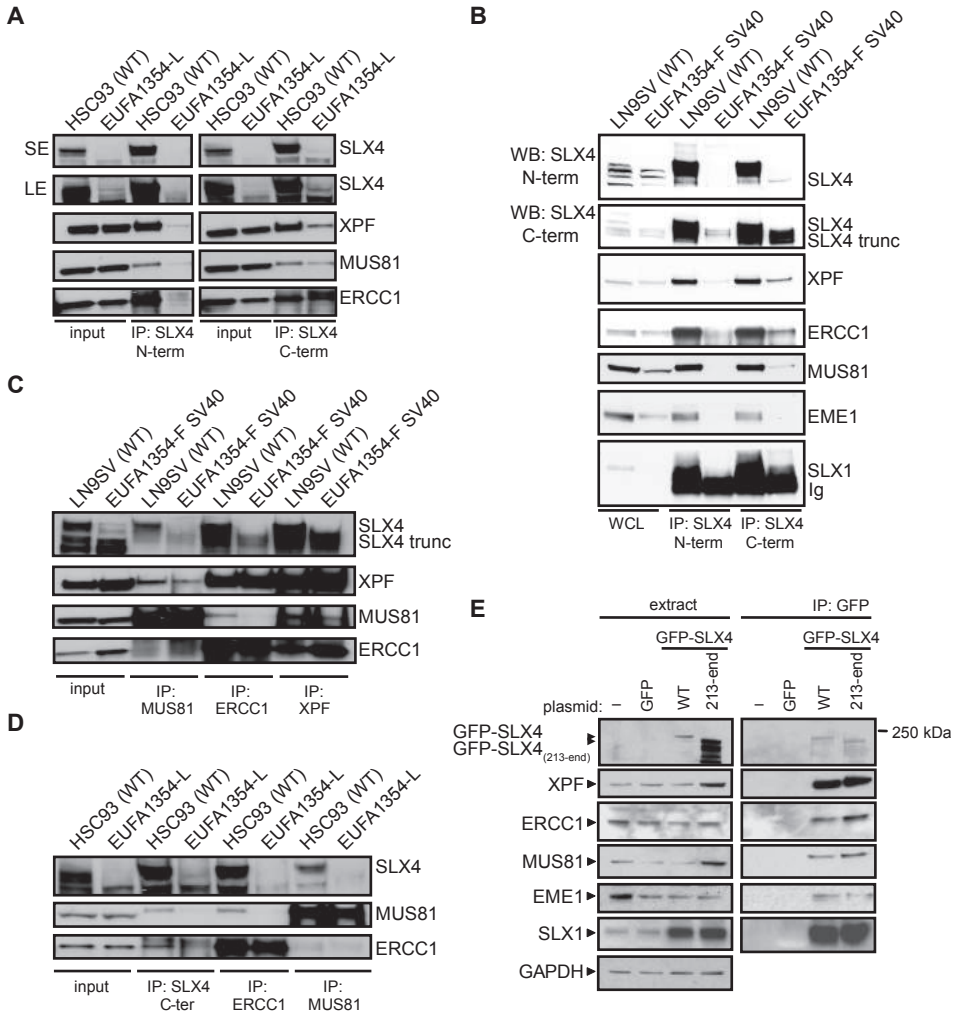

Supplementary Figure 7. SLX4 expression and interaction with structure-specific endonucleases in EUFA1354.

(**A**) Immunoprecipitation (IP) and Western blot analysis showing the absence of full-length SLX4 protein and reduced levels of ERCC1, XPF and MUS81 in SLX4 precipitates from lymphoblasts of the affected individual (EUFA1354-L). Immunoprecipitation was performed with antibodies against the SLX4 N-terminus (1-300) or C-terminus (1534-1834) and Western blotting with the antibody against the SLX4 C-terminus. SE and LE are short and long exposures of the blot. (**B**) Immunoprecipitation (IP) and Western blot analysis revealing absence of full-length SLX4 protein and reduced levels of XPF, ERCC1, MUS81, EME1 and SLX1 in SLX4 precipitates of SV40-immortalized EUFA1354-F fibroblasts. A truncated SLX4 protein is detected. Immunoprecipitation and Western blotting were performed with antibodies against the N-terminus (1-300) or C-terminus (1534-1834) of SLX4. Ig indicates the immunoglobulin light chain. (**C**) Reciprocal immunoprecipitations showing the absence of full-length SLX4 in MUS81, ERCC1 or XPF precipitates from SV40-immortalized EUFA1354 fibroblasts. The truncated SLX4 protein does coprecipitate. SV40-immortalized fibroblasts from a healthy individual (LN9SV) were analyzed as a control. (**D**) Reciprocal immunoprecipitations showing undetectable SLX4 protein in ERCC1 and MUS81 precipitates from EUFA1354-L lymphoblasts. (**E**) A truncated SLX4 protein starting at methionine 213 is able to interact with structure specific endonucleases. HEK293 cells were transiently transfected with

pcDNA5.1 encoding GFP, GFP–SLX4 full–length or GFP– SLX4 (213–end) or with empty vector (–). After 48 hr, cells were lysed and extracts were subjected to immunoprecipitation with anti–GFP antibodies. Precipitates were analysed by Western blotting with the antibodies indicated. "Input" represents cell extracts.

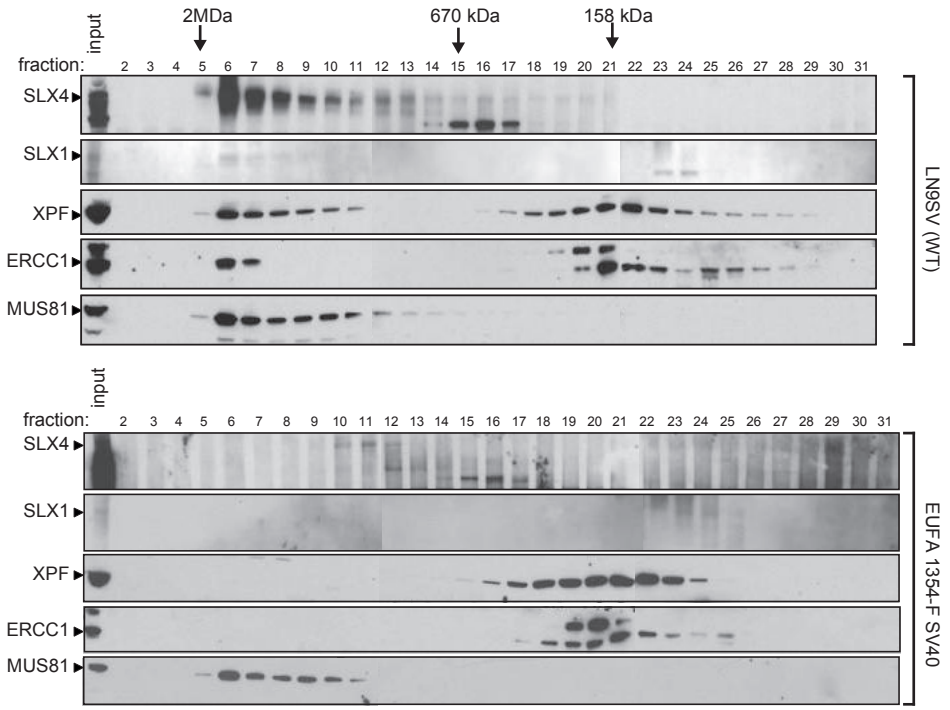

Supplementary Figure 8. XPF/ERCC1 and SLX1 elute only in the low molecular weight fractions from EUFA1354 fibroblast lysates.
Extracts of wild type fibroblasts (LN9SV) or fibroblasts from individual EUFA1354 were analyzed by size exclusion chromatography on a Superose 6 10/300 GL column in buffer containing 0.2 M NaCl. The elution positions of Dextran blue (2 MDa), thyroglobulin (670 kDa) and bovine γ– globulin (158 kDa) are shown.

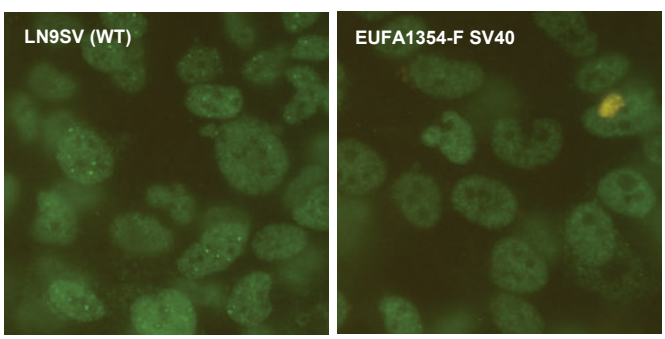

Supplementary Figure 9. Nuclear ERCC1 foci in SV40-immortalized wild type fibroblasts, but not in SV40- immortalized EUFA1354 fibroblasts.
These analyses were carried out with highly specific affinity-purified ERCC1 polyclonal antibody[7].

Supplementary Table 1A. SLX4 specific primers used for sequencing genomic DNA

SLX4ex1F	TGTTTAACCACAGGCCCAAT
SLX4ex1R	GCCCTTTCCAGGAAGTTTTC
SLX4ex2F	ACCAACAAGCAACCAGTCCT
SLX4ex2R	ATCCAGTGAAGTGGCAAAGG
SLX4ex3F	TTCCCGGAGTGCTGATTAGT
SLX4ex3R	ACAACAAAGCTGAGGTGCTG
SLX4ex4AF	GACCCACATTTGCTCCAATC
SLX4ex4AR	AGGGCTCTTTTTCCCTCCA
SLX4ex4BF	TTCAGGCTGTGCGGCTGCAG
SLX4ex4BR	TGCTGCGATTACAGGTGTGAACTAC
SLX4ex5F	AACTTCTGGCCTGGAATTGA
SLX4ex5R	ATACCGGGGGTTTCTTCTTG
SLX4ex6F	CCAGAAGCAGGTTTGTGTGA
SLX4ex6R	CCTTCCTGGACTTTCCATCA
SLX4ex7F	ATGTGATGGCTTCTGCAGTG
SLX4ex7R	AGAGGATTCACTCGCTGTGG
SLX4ex8F	TCTCTTACCTCCCTGGTGGA
SLX4ex8R	CTCACGGATGTCAGGATGTG
SLX4ex9F	GGGTCACTCAGAGGTTGAGG
SLX4ex9R	GCAGGAAGTGAGGGAGAGTG
SLX4ex10F	AGGCTGCAGTAAGCCATGAT
SLX4ex10R	CTGGTCATGGACTTGGGATT
SLX4ex11AF	TGTTTCTGGCAAGGAGTGTG
SLX4ex11AR	CTCCACCTTGTCCCACTGTT
SLX4ex11BF	TTTGCAGCTACTCAGCGAAA
SLX4ex11BR	TTTCTGCTTTGATGGCACAG
SLX4ex11CF	CATCACACAAGTGGGTCGTC
SLX4ex11CR	CTGATTTGGGTCTGGGAAGA
SLX4ex11DF	GCTGTTCTGTGACCGTGAGA
SLX4ex11DR	TCCAGGTTCCAGTGGTCAAT
SLX4ex11EF	GGAGACAGTGACGATGAGCA
SLX4ex11ER	CCCTGGGTCTCATGACTGAT
SLX4ex12F	GTGGCCCATTGTCTCAAGTT
SLX4ex12R	ACCAGACCCAGAGACCACAC
SLX4ex13F	ATAGGGAACGTGGAGTGTGG
SLX4ex13R	GACGGGGGTTTTTGAAGATT
SLX4ex14F	GGACCCGTAGACACCTTCCT
SLX4ex14R	CTCCAAATGCCACCCTAGAA

Supplementary Table 1B. SLX4 specific primers used for sequencing cDNA

1Afor	CAGTACTTTTTGTTCAATTGTGCAAACTC
1Arevseq	TTATCTGAGTGCCGTTTGAGGCAG
1Arev	TCACGTTCATGGCTGAGAGGTTC
1Bfor	TCATCTGTCTGCCTGTCCTG
1Brev	GCATTCGCTGTAGGACCAAT
2for	CCAAAGGATCCTCAAGAGGAGATG
2rev	CACAGAAAGCTCTGCTTGCGTTC
3for	AAGTGGAATTGTCTAGCACGCCAC
3rev	CATCTGCCCACATTGACCTCAAG
4for	GTGCCTATTGCCACTGACTCAG
4rev	GATTTCTGAGATCTGGAGCTCGAAT
5for	GCATCCTCACGCTGTCTAAAGAG
5rev	CAGCAGTCGTCAATTGGAATTGGG
6for	TTCAGCAGGCGGTTCCTGAAAC
6rev	GTGTGATGCTTTCATGATGCTTCC
7for	TAGCAGGCCGAGCTTTCTGAATTC
7forseq	GAAGCATCATGAAAGCATCACACC
7rev	AAATGCCTGTGGAGGCCTGAC

References

1. de Winter, J.P. & Joenje, H. The genetic and molecular basis of Fanconi anemia. Mutat. Res. 668, 11–19 (2009).
2. Vaz, F. *et al.* Mutation of the RAD51C gene in a Fanconi anemia-like disorder. Nat. Genet. 42, 406–409 (2010).
3. Singh, T.R. *et al.* Impaired FANCD2 monoubiquitination and hypersensitivity to camptothecin uniquely characterize Fanconi anemia complementation group M. Blood 114, 174–180 (2009).
4. Shimamura, A. *et al.* A novel diagnostic screen for defects in the Fanconi anemia pathway. Blood 100, 4649–4654 (2002).
5. Fekairi, S. *et al.* Human SLX4 is a Holliday junction resolvase subunit that binds multiple DNA repair/recombination endonucleases. Cell 138, 78–89 (2009).
6. Svendsen, J.M. *et al.* Mammalian BTBD12/SLX4 assembles a Holliday junction resolvase and is required for DNA repair. Cell 138, 63–77 (2009).
7. Andersen, S.L. *et al.* Drosophila MUS312 and the vertebrate ortholog BTBD12 interact with DNA structures-specific endonucleases in DNA repair and recombination. Mol. Cell 35, 128–135 (2009).
8. Muñoz, I.M. *et al.* Coordination of structure-specific nucleases by human SLX4/ BTBD12 is required for DNA repair. Mol. Cell 35, 116–127 (2009).
9. van Vuren, A.J. *et al.* Evidence for a repair enzyme complex involving ERCC1 and complementing activities of ERCC4, ERCC11 and xeroderma pigmentosum group F. EMBO J. 12, 3693–3701 (1993).
10. Crossan, G.P. *et al.* Disruption of mouse Slx4, a regulator of structure-specific nucleases, phenocopies Fanconi anemia. Nat. Genet. advance online publication, doi:10.1038/ng.752 (16 January 2011).
11. Jaspers, N.G.J. *et al.* First reported patient with human ERCC1 deficiency has cerebro-oculo-facio-skeletal syndrome with a mild defect in nucleotide excision repair and severe developmental failure. Am. J. Hum. Genet. 80, 457–466 (2007).
12. Ahmad, A. *et al.* Mislocalization of XPF-ERCC1 nuclease contributes to reduced DNA repair in XP-F patients. PLoS Genet. 6, e1000871 (2010).
13. Joenje, H. *et al.* Classification of Fanconi anemia patients by complementation analysis: evidence for a fifth genetic subtype. Blood 86, 2156–2160 (1995).

CHAPTER 3

Whole exome sequencing reveals uncommon mutations in the recently identified Fanconi anemia gene *SLX4/FANCP*

Beatrice Schuster*, Kerstin Knies*,**Chantal Stoepker**, Eunike Velleuer, Richard Friedl, Birgit Gottwald-Mühlhauser, Johan P. de Winter & Detlev Schindler

* These authors contributed equally to this work.

Published in Human Mutation, 2013. 34(1):93-96.

Fanconi anemia (FA) is a rare genetic disorder characterized by congenital malformations, progressive bone marrow failure (BMF), and susceptibility to malignancies. FA is caused by biallelic or hemizygous mutations in one of 15 known FA genes, whose products are involved in the FA/BRCA DNA damage response pathway. Here, we report on a patient with previously unknown mutations of the most recently identified FA gene, *SLX4*/*FANCP*. Whole exome sequencing (WES) revealed a nonsense mutation and an unusual splice site mutation resulting in the partial replacement of exonic with intronic bases, thereby removing a nuclear localization signal. Immunoblotting detected no residual SLX4 protein, which was consistent with abrogated interactions with XPF/ERCC1 and MUS81/EME1. This cellular finding did not result in a more severe clinical phenotype than that of previously reported FA-P patients. Our study additionally exemplifies the versatility of WES for the detection of mutations in heterogenic disorders such as FA.

Fanconi anemia (FA; MIM# 227650) is an autosomal or X-chromosomal recessive disorder first described in 1927 by the Swiss pediatrician Guido Fanconi[1]. Recently, the carrier frequency in the United States was estimated to be 1:181, corresponding to an incidence of FA of less than 1:100,000 (ref 2). Higher rates have been reported for certain ethnicities or due to isolation or founder effects[3]. The clinical manifestations of FA are variable yet characteristic. Typical congenital malformations include short stature, skin hyper- or hypopigmentations, radial ray defects, and malformations of ears, eyes, and inner organs. Most FA patients develop progressive bone marrow failure in childhood. Furthermore, they have an increased risk of myelodysplastic syndrome (MDS) and hematological malignancies, in particular acute myelogenous leukemia[4-6]. In addition, they are predisposed for solid tumors occurring in young adulthood. FA patients have an up to 700-fold increased risk for squamous cell carcinomas, which arise most frequently in the mucosa of the head and neck or genital regions[2,7]. The reasons for the increased susceptibility of FA patients to neoplasms are not fully understood. Most likely, this is due to a DNA repair defect and genomic instability that characterize the cellular phenotype[8]. FA cells show highly increased rates of chromosomal breakage especially after exposure to DNA-crosslinking agents, accumulate in the G2 phase of the cell cycle, and encounter diminished survival[9-11]. Like the clinical phenotype, the genetic background of FA is very heterogeneous. To date, 15 complementation groups (FA-A, -B, -C, -D1, -D2, -E, -F, -G, -I, -J, -L, -M, -N, -O, and -P) have been delineated. The first identified FA gene, *FANCC* (MIM# 613899), was reported in 1992 (ref 12). Since 2000, nearly every year a new FA gene has been added, most recently *FANCP* (MIM# 613951), encoded by the gene *SLX4*/*BTBD12* (approved symbol *SLX4*; MIM# 613278)[13,14].

Its product interacts with different structure-specific endonucleases such as XPF/ERCC1 (MIM#s 133520, 126380), MUS81/EME1 (MIM#s 606591, 610885) and the Holliday junction resolvase SLX1, by coordinating their activity in DNA repair and recombination[15]. FANCP is involved in the FA/BRCA pathway and the network of DNA interstrand crosslink (ICL) repair. A key step in this pathway is FANCD2 (MIM# 613984) and FANCI (MIM# 611360) monoubiquitination through the FA core complex following DNA damage and replication fork stalling. FANCP acts downstream of these protein modifications, similar to FANCD1 (MIM# 600185), FANCJ (MIM# 605882), FANCN (MIM# 610355), and FANCO (MIM# 602774). FANCP-mutated cells are proficient of RAD51 foci formation, unlike FA-D1- or FA-O cells. Given these facts, a role in the coordination of DNA incision for ICL unhooking seems more likely than one in Holliday junction resolution, even though the precise function of FANCP in the FA/BRCA pathway remains elusive[14,16]. Four families with a total of six affected children have been assigned to complementation group FA-P. Their underlying *SLX4* mutations result in protein truncation and degradation. The presence of residual protein, retained function, and other factors may explain the variable severity of clinical FA manifestations[13-15].

In this study, we report on an additional FA-P patient who was assigned to that complementation group due to *SLX4* mutations identified by whole exome sequencing (WES). *SLX4* proved to be the only FA gene carrying compound heterozygous pathogenic sequence changes that were confirmed by Sanger sequencing. A nonsense and a splice site mutation followed Mendelian segregation in the family of the patient.

The 21-year-old girl of German descent was diagnosed with FA at the age of 5 years, showing FA-typical features including prenatal dystrophy, short stature, hypoplasia of the right thumb, microcephaly, speckles of skin hyperpigmentation at the arms and legs, minor café-au-lait and vitiligo spots, trivial mitral valve prolapse, and hypothyroidism. Apart from the platelets (reduced since age 5, lowest number about 20,000/µl) her blood counts were relatively stable until she developed MDS at 19 years of age. She was successfully transplanted with hematopoietic stem cells from a 10/10 matched unrelated donor. The patient has not developed malignancies up to her current age of 21; nor does she have a strong family history of cancer.

Initially, the clinical suspicion of FA was confirmed by elevated spontaneous and mitomycin C-induced chromosome breakage rates (data not shown) and G2-phase accumulation in lymphocyte, lymphoblastoid (**Fig. 1A**), and fibroblast cultures, which was shown by flow cytometric cell cycle analysis as described in Vaz *et al.* (ref 17).

We isolated genomic DNA from fibroblasts using the GeneJet™ Genomic DNA Purification Kit (Fermentas, St. Leon-Rot, Germany). For isolation of RNA, we employed the Quick-RNA™ MiniPrep Kit (Zymo Research, Freiburg, Germany).

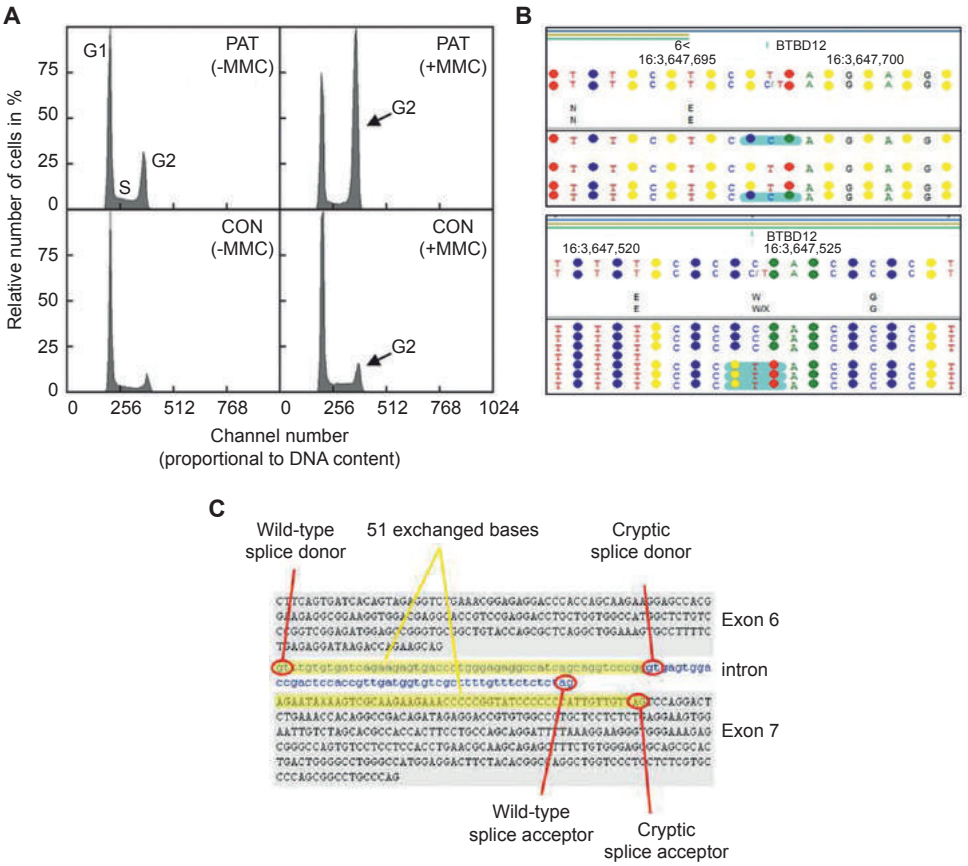

Figure 1. G2-phase arrest and *SLX4/FANCP* mutation.
(**A**) Cell cycle distribution of patient-derived lymphoblastoid cells shows increased G2 arrest without (21.4% of cells in G2) and especially after exposure of cultures to 15 ng/µl MMC (55.4% of cells in G2) compared to a control cell line (0 MMC: 9.1% of cells in G2, 15 ng/µl MMC: 10.9% of cells in G2). (**B**) The graphic chart shows the splice site mutation c.1367-2A>G (upper panel) and the nonsense mutation c.1538G>A (lower panel) by color-space WES data according to NextGENe™ software presentation. The cutout displays from top to bottom the number of the coding exon and the gene name, the chromosomal position, followed by the reference and the patient consensus nucleotide sequences, the corresponding amino acids and, below the horizontal line, the original WES reads. Since *FANCP* (*BTBD12*) is encoded on the minus-strand of gDNA, the sequences and base changes are displayed in reverse complementary manner. (**C**) Depicted is an excerpt from exon 6 to 7 of the Ensembl gDNA sequence of *SLX4/FANCP* (ENSG00000188827). Red circles indicate the wild-type and cryptic splice sites. The 51 bases of exon 7 which are interchanged with the same number of bases of intron 6 are highlighted in yellow.

Translation into cDNA was performed by SuperScript® II Reverse Transcriptase (Invitrogen, Darmstadt, Germany).

Because the patient was among those who remained without detected mutation or assignment to a distinct subtype, we got interested in the significance of WES for molecular diagnostics of FA. We commissioned enrichment and sequencing of the patient's exome to a service provider. Target enrichment was achieved by means

of the SureSelect Human All Exon 50 Mb Kit (Agilent, Boeblingen, Germany) and was followed by next-generation sequencing on a *SOLiD5500xl* instrument (Applied Biosystems, Darmstadt, Germany). Afterward we performed in house analysis of the WES data using NextGENe™ v2.18 software (Softgenetics, State College, PA, USA). The data revealed a total of 103,222,641 reads (**Supplementary Table 1**). Sixty-one percent of these mapped on target and resulted in an 87-fold average coverage of the exome. Altogether we detected 32,013 variants, including novel mutations as well as listed SNPs. Because of the patient's nonconsanguineous descent, we restricted our search to compound heterozygous changes and detected 14,715 unknown (excluding reported polymorphisms) heterozygous variants in coding sequences and adjacent intron portions. In particular, 15 base substitutions were detected in 21 FA and FA-associated genes (91% of exons covered by ≥5 reads). *SLX4* (NM_032444.2) carried two bona fide pathogenic variants. Even though WES could have missed pathogenic mutations in other FA genes, the compound heterozygous finding in SLX4 makes this most unlikely. The mutated positions were covered by 6 and 15 reads, respectively. We observed the nonsense mutation c.1538G>A in exon 7 resulting in a premature stop codon with the predicted effect of protein truncation, p.W513X, and the splice acceptor mutation c.1367-2A>G in intron 6 (**Fig. 1B**). Mutation nomenclature is based on cDNA sequence of *SLX4* transcript ENST00000294008 and nucleotide numbering reflects cDNA numbering with +1 corresponding to the A of ATG initiation codon.

Mutation validation was performed by Sanger technique on a 3130xl instrument (Applied Biosystems, Darmstadt, Germany). The primers for gDNA sequencing included *FANCP*_exon7_for 5'-CAGAAGCAGGTTTGTGTGA-'3 and *FANCP*_exon7_rev 5'-CCTTCCTGGACTTTCCATCA-'3. We resequenced the corresponding regions of *SLX4* in the patient and additionally confirmed the biallelic mutation status and Mendelian segregation of the mutations by sequencing genomic DNA from both parents. The results showed that the splice site mutation was paternally inherited, whereas the nonsense mutation was transmitted maternally (**Supplementary Fig. 1A**).

We analyzed the consequences of c.1367-2A>G by Sanger sequencing of patient's cDNA using the primers *FANCP*_c.1-65_for 5'-CAGTACTTTTTGTTCAATTGTGCAAACTC-'3 and *FANCP*_c. 1570_rev 5'-CACAGAAAGCTCTGCTTGCGTTC-'3. This analysis demonstrated that a cryptic splice acceptor in exon 7 at position c.1417_1418 is used instead of the mutated in intron 6, as it was predicted by in silico analysis. Splice site score calculation using the Web tool *http://rulai.cshl.edu/new_alt_exon_db2/HTML/score.html* revealed a score of 1.2 of the cryptic splice acceptor at positions c.1417_1418 and a score of −1.7 of the mutated one. Of note, this change of the splice acceptor altered the usage of the unaffected wild-type splice donor of intron 6 (score 5.4) to that of a cryptic

splice donor at position c.1366+52_1366+53 (score 10). This fact is indicated by the substitution of the 5'-terminal 51 bases of exon 7 with the 5'-terminal 51 bases of intron 6. The electropherogram of cDNA sequencing demonstrates this finding by the superposition of exactly 51 bases starting at cDNA position 1,367 and ending at 1,417 (**Fig. 1C and Supplementary Fig. 1B**), designated as r.1367_1417delins gtttgtgtgatcagaagagtgaccctgggagaggccatcagcaggtcccgg. The length of the open reading frame does not differ as a result of this aberrant splicing pattern. Other in silico analyses revealed that the deduced wild-type amino acids at positions p.456_472, ENKSRKKKPPVSPPLLL, are predicted to include at positions p.460_464 one of five potential SLX4/FANCP nuclear localization signals (NLS) (http://psort.hgc.jp/form2.html) (**Fig. 2A**). The mutation, denoted p.E456_L4772delinsGLCDQKSDPGRGHQQVP, results in the loss of that potential NLS.

Further experiments similar to those described by Stoepker *et al.* (ref 14) showed that no residual protein is present. Neither by immunoprecipitation (**Fig. 2B**), nor in a cell fractionation assay (**Fig. 2**) SLX4/FANCP was detected on Western blots. We conclude that the allele carrying the stop mutation gives rise to a truncated protein that is unstable and rapidly degraded. Similarly, the allele with the splice mutation does not express a stable protein, which could locate to the nucleus. Therefore, it is not surprising that interactions with the structure-specific nucleases XPF/ERCC1 and EME1/MUS81 are disrupted (**Fig. 2B**) and that ERCC1 is not able to form nuclear foci (**Fig. 2D**), as described for other FA-P patients[14].

In summary, our study adds a seventh patient to the most recently described FA subtype, FA-P. Neither of her compound heterozygous mutations has previously been reported. They extend the mutation spectrum of the latest member of the FA gene family, *FANCP*, and have been added to the Fanconi Anemia Mutation Database (http://www.rockefeller.edu/fanconi/). In contrast to the FA-P patients reported so far, cells derived from the present patient do not seem to be able to express any SLX4/FANCP protein[13,14]. The failure of coordination of structure-specific nucleases in ICL unhooking due to the absence of SLX4/FANCP does not result in a more severe phenotype as that of other FA-P patients previously reported, which is not comparable to the cancer-prone phenotype of subtypes FA-D1 or -N, but falls into the clinical spectrum of the other FA groups. These insights were facilitated by WES that proved a valuable tool for molecular diagnostics of FA, as of other heterogeneous diseases, by the identification of disease-causing genes so that it may increasingly replace classical genetic approaches.

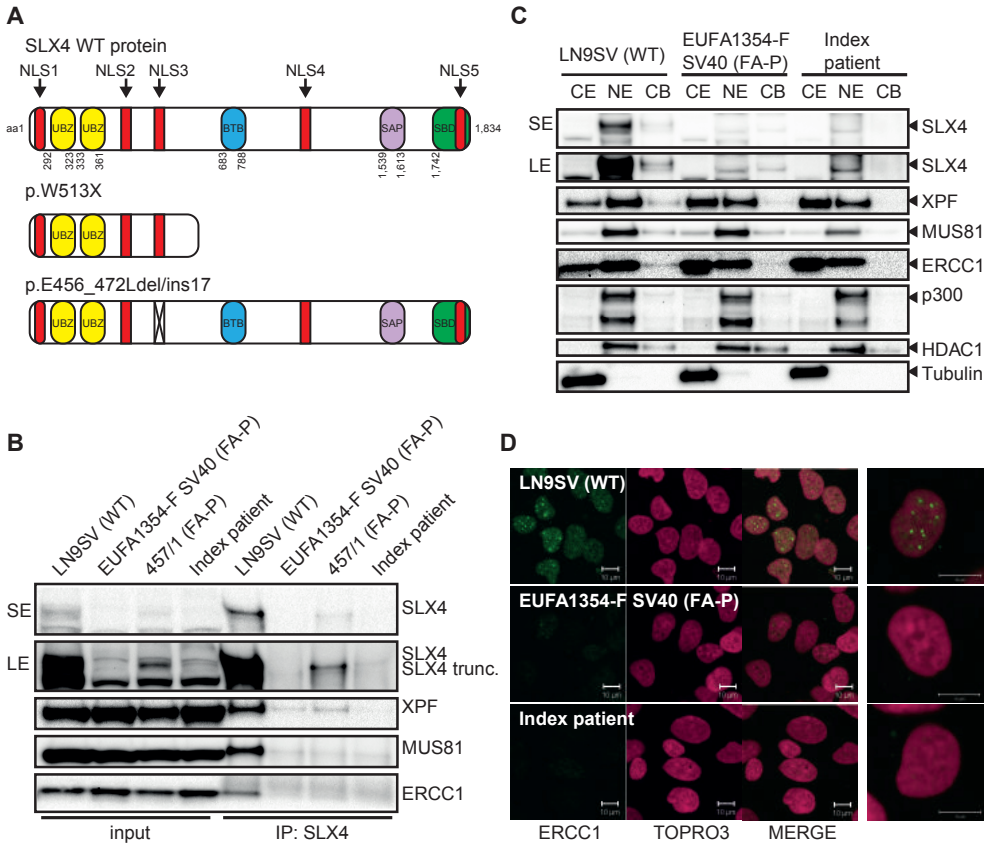

Figure 2. Mutant SLX4/FANCP expression and function.
(**A**) Ideograms of the SLX4/FANCP domain structure (modified after Svendsen *et al.*(ref 18)). Wild-type (WT) protein (top) contains in addition to reported domains (UBZ, yellow; BTB, blue; SAP, purple; and SBD, green) five potential nuclear localization signals (NLS, red) predicted by the Web tool *http://psort.hgc.jp/form2.html*, spanning amino acid (aa) positions 109_124 (NLS 1), 397_412 (NLS 2), 460_464 (NLS 3), 1079_1085 (NLS 4), and 1814_1830 (NLS 5). The ideograms below (middle and bottom) show the predicted protein effect of the SLX4/FANCP mutations in the present patient. c.1538G>A leads to protein truncation at p.W513X, whereas c.1367-2A>G leads to p.E456_472Ldelins17 and the loss of NLS 3. (**B**) Immunoprecipitation and Western blot analysis shows SLX4/FANCP deficiency in fibroblasts of the patient compared to WT and FA-P controls. There is no co-precipitation of XPF, MUS81 and ERCC1 with the mutant protein. SE and LE indicate short and long exposure of the blot, respectively. (**C**) Subcellular fractionation of patient's fibroblasts fails to demonstrate SLX4/FANCP protein in any fraction. Chromatin loading of XPF and MUS81 were not detected. Tubulin, p300 and HDAC1 served as loading controls for the cytoplasmic fraction (CE), nuclear extract (NE), and chromatin fraction (CB). The faint band observed in NE slightly below SLX4/FANCP is unspecific. (**D**) Formation of nuclear ERCC1 foci is abolished in patient's fibroblasts as in other FA-P cells (EUFA1354) in contrast to the wild-type control line (LN9SV). The ERCC1 antibody FL297 was used for immunofluoresence and TOPRO3 as a nuclear counterstain.

Acknowledgements
We are grateful to Helmut Hanenberg (Indianapolis) and Kornelia Neveling (Nijmegen) for earlier pre-classifications of patient's cells; Ralf Dietrich, executive director of the German FA support association "Deutsche Fanconi-Anamie-Hilfe e. V.," for facilitating contact to the family. The patient and her parents generously provided information on the disease course.

Author contributions
B.S. and K.K. designed and performed experiments, generated data, and wrote the manuscript; C.S. performed experiments (Immunoprecipitation and western blot analysis, Immunofluorescence ERCC1 foci) and contributed data; E.V. contributed vital materials; R.F. and B.M.-G. performed experiments; J.P.deW. and D.S. contributed data, directed experiments, and revised the manuscript.

Disclosure statement
The authors declare no financial conflict of interest.

Supplementary data

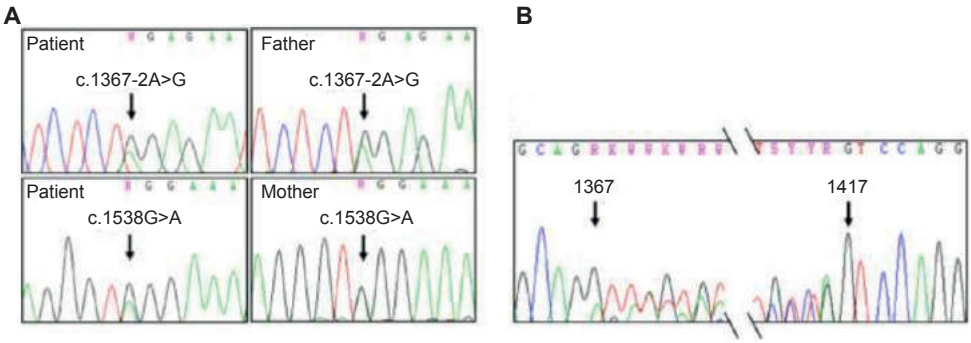

Supplementary Figure 1. Validation of Whole Exome Sequencing results by Sanger resequencing.
(**A**) Mendelian segregation of the *FANCP* mutations in the patient's family. The splice site change c.1367-2A>G was inherited from the father, while the nonsense mutation c.1538G>A is of maternal origin. (**B**) Consequence of c.1367-2A>G on transcript level. Sequencing the patient's cDNA revealed the replacement of exactly 51 exonic bases starting at cDNA position 1367 and ending at 1417 by the first 51 bases of the following intron.

Supplementary Table 1. Statistical summary of WES results including read counts and detected variants

Total read number	109,637,890
Reads passing QC	103,222,641
Reads on target	62,868,844 (61%)
Average exome coverage	87x
Total number of variants	32,013
Known SNPs/MNPs	17,194
Unknown variants in coding sequence	13,519
Unknown variants at canonical splice sites	377
Unknown homozygous variants	91
Unknown heterozygous variants	14,715
Unknown silent variants	2,983
Unknown missense variants	9,629
Unknown nonsense variants	510
Unknown insertions/deletions	468
Genes with heterozygous variants (≥2 altered bases)	131
Heterozygous variants in FA and FA associated genes	15

QC: quality control; SNP: single nucleotide polymorphism; MNP: multiple nucleotide polymorphism

References

1. Lobitz S, Velleuer E. 2006. Guido Fanconi (1892–1979): a jack of all trades. Nat Rev Cancer 6:893–898.
2. Rosenberg PS, Tamary H, Alter BP. 2011. How high are carrier frequencies of rare recessive syndromes? Contemporary estimates for Fanconi anemia in the United States and Israel. Am J Med Genet A 155A:1877–1883.
3. Callen E, Casado JA, Tischkowitz MD, Bueren JA, Creus A, Marcos R, Dasi A, Estella JM, Munoz A, Ortega JJ, deWinter J, Joenje H, *et al.* 2005. A common founder mutation in FANCA underlies the world's highest prevalence of Fanconi anemia in Gypsy families from Spain. Blood 105:1946–1949.
4. Alter BP, Kupfer G. 1993. Fanconi anemia. In: Pagon RA, Bird TD, Dolan CR, Stephens K, Adam MP, editors. GeneReviewsTM [Internet]. Seattle, WA: University of Washington, Seattle; 1993–2002 Feb 14 [updated 2012 Sep 06].
5. Rosenberg PS, Greene MH, Alter BP. 2003. Cancer incidence in persons with Fanconi anemia. Blood 101:822–826.
6. Seif AE. 2011. Pediatric leukemia predisposition syndromes: clues to understanding leukemogenesis. Cancer Genet 204:227–244.
7. Rosenberg PS, Alter BP, Ebell W. 2008. Cancer risks in Fanconi anemia: findings from the German Fanconi Anemia Registry. Haematologica 93:511–517.
8. Deans AJ, West SC. 2011. DNA interstrand crosslink repair and cancer. Nat Rev Cancer 11:467–480.
9. Auerbach AD. 1993. Fanconi anemia diagnosis and the diepoxybutane (DEB) test. Exp Hematol 21:731–733.
10. Schindler D, Kubbies M, Hoehn H, Schinzel A, Rabinovitch PS. 1987. Confirmation of Fanconi's anemia and detection of a chromosomal aberration (1Q12-32 triplication) via BrdU/Hoechst flow cytometry. Am J Pediatr Hematol Oncol 9:172– 177
11. Schroeder TM, Anschutz F, Knopp A. 1964. Spontaneous chromosome aberrations in familial panmyelopathy. Humangenetik 1:194–196.
12. Strathdee CA, Duncan AM, Buchwald M. 1992. Evidence for at least four Fanconi anaemia genes including FACC on chromosome 9. Nat Genet 1:196– 198.
13. Kim Y, Lach FP, Desetty R, Hanenberg H, Auerbach AD, Smogorzewska A. 2011. Mutations of the SLX4 gene in Fanconi anemia. Nat Genet 43:142– 146.
14. Stoepker C, Hain K, Schuster B, Hilhorst-Hofstee Y, Rooimans MA, Steltenpool J, Oostra AB, Eirich K, Korthof ET, Nieuwint AW, Jaspers NG, Bettecken T, *et al.* 2011. SLX4, a coordinator of structure-specific endonucleases, is mutated in a new Fanconi anemia subtype. Nat Genet 43:138–141.
15. Andersen SL, Bergstralh DT, Kohl KP, LaRocque JR, Moore CB, Sekelsky J. 2009. Drosophila MUS312 and the vertebrate ortholog BTBD12 interact with DNA structure-specific endonucleases in DNA repair and recombination. Mol Cell 35:128–135.
16. Crossan GP, van der Weyden L, Rosado IV, Langevin F, Gaillard PH, McIntyre RE, Gallagher F, Kettunen MI, Lewis DY, Brindle K, Arends MJ, Adams DJ, *et al.* 2011. Disruption of mouse Slx4, a regulator of structure-specific nucleases, phenocopies Fanconi anemia. Nat Genet 43:147–152.
17. Vaz F, Hanenberg H, Schuster B, Barker K, Wiek C, Erven V, Neveling K, Endt D, Kesterton I, Autore F, Fraternali F, Freund M, *et al.* 2012. Mutation of the RAD51C gene in a Fanconi anemia-like disorder. Nat Genet 42:406–409.
18. Svendsen JM, Smogorzewska A, Sowa ME, O'Connell BC, Gygi SP, Elledge SJ, Harper JW. 2009. Mammalian BTBD12/SLX4 assembles a Holliday junction resolvase and is required for DNA repair. Cell 138:63–77.

CHAPTER 4

Mutations in *ERCC4*, encoding the DNA-repair endonuclease XPF, cause Fanconi anemia

Massimo Bogliolo*, Beatrice Schuster*, **Chantal Stoepker**, Burak Derkunt, Yan Su, Anja Raams, Juan P. Trujillo, Jordi Minguillón, María J. Ramírez, Roser Pujol, José A. Casado, Rocío Baños, Paula Rio, Kerstin Knies, Sheila Zúñiga, Javier Benítez, Juan A. Bueren, Nicolaas G.J. Jaspers, Orlando D. Schärer, Johan P. de Winter, Detlev Schindler & Jordi Surrallés

*Both authors contributed equally to this work.

Published in The American Journal of Human Genetics, 2013. 92(5):800-806.

Fanconi anemia (FA) is a rare genomic instability disorder characterized by progressive bone marrow failure and predisposition to cancer. FA-associated gene products are involved in the repair of DNA interstrand crosslinks (ICLs). Fifteen FA-associated genes have been identified, but the genetic basis in some individuals still remains unresolved. Here, we used whole-exome and Sanger sequencing on DNA of unclassified FA individuals and discovered biallelic germline mutations in *ERCC4* (*XPF*), a structure-specific nuclease-encoding gene previously connected to xeroderma pigmentosum and segmental XFE progeroid syndrome. Genetic reversion and wild-type *ERCC4* cDNA complemented the phenotype of the FA cell lines, providing genetic evidence that mutations in *ERCC4* cause this FA subtype. Further biochemical and functional analysis demonstrated that the identified FA-causing *ERCC4* mutations strongly disrupt the function of XPF in DNA ICL repair without severely compromising nucleotide excision repair. Our data show that depending on the type of *ERCC4* mutation and the resulting balance between both DNA repair activities, individuals present with one of the three clinically distinct disorders, highlighting the multifunctional nature of the XPF endonuclease in genome stability and human disease.

Fanconi anemia (FA) is characterized by bone marrow failure (BMF), congenital malformations, hypersensitivity to DNA interstrand crosslink (ICL)-inducing agents, chromosome fragility, and a high susceptibility to cancer. Since the discovery of the first FA-associated gene 20 years ago, all together, 15 genes associated with FA have been identified; these include *FANCA*, *FANCB*, *FANCC*, *FANCD1* (*BRCA2*), *FANCD2*, *FANCE*, *FANCF*, *FANCG* (*XRCC9*), *FANCI*, *FANCJ* (*BRIP1*), *FANCL* (*PHF9*), *FANCM*, *FANCN* (*PALB2*), *FANCO* (*RAD51C*), and *FANCP* (*SLX4*)[1,2] (MIM 227650, 300514, 227645, 605724, 227646, 600901, 603467, 614082, 609053, 609054, 614083, 614087, 610832, 613390, and 613951, respectively). Studies to unravel the genetic basis of this rare disorder uncovered a genome-maintenance pathway that protects dividing cells against replication-blocking DNA lesions. To identify additional FA-associated genes, we used the SOLiD 4 platform for whole-exome sequencing on peripheral-blood DNA from a Spanish FA individual (FA104) who was previously excluded from all known FA complementation groups (this study was approved by the Institutional Committee on Ethical Research in Human Samples, and proper informed consent was obtained). FA104 was born to unrelated parents and was diagnosed neonatally with a malformative syndrome suggestive of FA, the symptoms of which included bilateral absent thumbs, microsomy, esophageal atresia, a ventrally translocated anus, and dysplastic and low-set ears. She did not show any dermatological abnormality such as skin hyperpigmentation, photosensitivity,

sunlight-induced scarring, or atrophy. FA104 developed BMF at the age of 2 years and died as a result of a hemorrhagic shock after bone marrow transplantation at the age of 4 years. A positive chromosome-breakage test unambiguously confirmed the FA diagnosis: 92% of the cells showed on average 4.4 diepoxybutane (DEB)-induced breaks. Lymphoblasts from this individual were hypersensitive to mitomycin-C (MMC) and melphalan but were insensitive to the topoisomerase I inhibitor camptothecin and the PARP inhibitor KU58948 (data not shown) and showed normal FANCD2 monoubiquitination and RAD51 focus formation[3]. This suggests a defect downstream within the FA pathway, which does not involve homologous recombination. On the basis of a recessive mode of inheritance, exome sequencing identified 17 candidate disease genes for FA104 (**Supplementary Table 1**); of these, *ERCC4* (MIM 133520; also known as *XPF*) immediately caught our attention given the involvement of the XPF-ERCC1-structure-specific nuclease in ICL repair[4]. Both *ERCC4* mutations were predicted to be pathogenic: a 5 bp deletion in exon 8 (c.1484_1488delCTCAA) was predicted to lead to a frameshift and a premature stop codon (p.Thr495Asnfs*6), and a missense mutation in exon 11 (c.2065C>A [p.Arg689Ser]; RefSeq accession numbers NG_011442.1, NM_005236.2, and NP_005227.1) was predicted to change a highly conserved arginine within the nuclease active site of XPF. Sanger sequencing on blood DNA confirmed these mutations (**Fig. 1A**) and their correct segregation (data not shown). In MMC-resistant FA104 lymphoblasts (FA104R) obtained after long-term exposure to a low dose of MMC, we detected a mutation that restored the *ERCC4* reading frame (**Supplementary Fig. 1A**), supporting the notion that MMC sensitivity is due to *ERCC4* mutations. Consistently, XPF levels were reduced in FA104 lymphoblasts but were normalized in the reverted FA104R lymphoblasts (**Supplementary Fig. 1B**). Immunoblotting did not detect a truncated XPF, indicating that only the p.Arg689Ser altered XPF was present in the FA104 cell line.

Sanger sequencing on 18 unclassified FA individuals from Germany revealed biallelic *ERCC4* mutations in another individual (1333). Individual 1333 was born in 2002 and was unambiguously diagnosed with FA at the age of 5 years as a result of multiple FA-related features, such as perinatal growth retardation, short stature, pronounced microcephaly, café-au-lait spots, an ostium-primum defect, biliary atresia with fibrosis of the liver, BMF, and a positive chromosome-fragility test (0.2, 6.7, and 9.4 breaks per cell at 0, 50, and 100 ng/ml MMC, respectively). Individual 1333 is redheaded and has pale skin color, but no spontaneous or UV-light-induced skin lesions were reported at the age of 10 years. Similar to those of FA104, lymphoblasts from individual 1333 were normal with regard to FANCD2 monoubiquitination and RAD51 focus formation and were sensitive to MMC and melphalan but insensitive to the topoisomerase I inhibitor camptothecin and to the PARP inhibitor KU58948 (data not shown). Individual 1333 carries a 28 bp duplication in exon 11 of the maternal

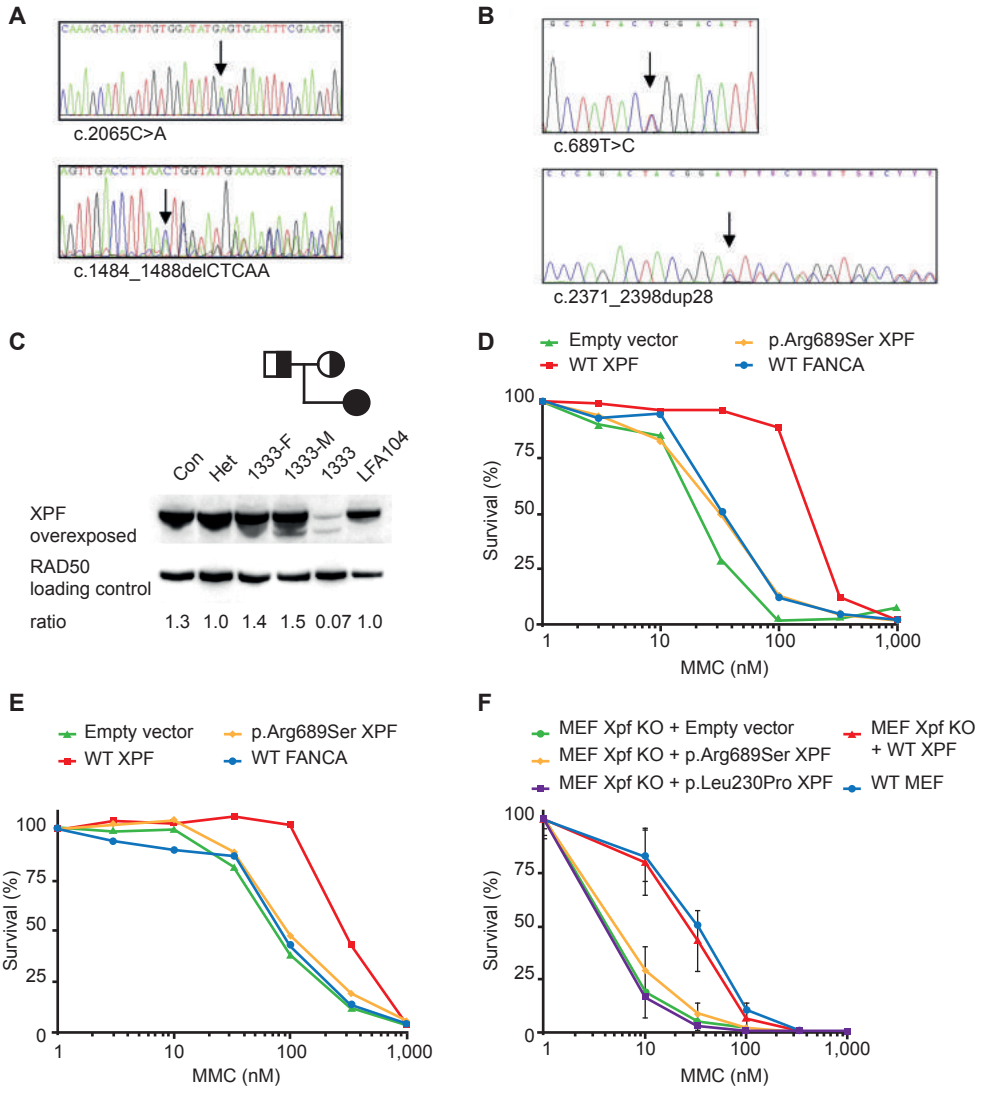

Figure 1. *ERCC4* Mutations and XPF Deficiency in FA Individuals.
(**A**) Sequence analysis of blood DNA from FA104 revealed a missense mutation in exon 11 (c.2065C>A [p. Arg689Ser]) (upper panel) and a 5 bp deletion in exon 8 leading to a frameshift and premature termination of translation (c.1484_ 1488delCTCAA [p. Thr495Asnfs*6]) (lower panel). (**B**) Sequence analysis of blood DNA from 1333 revealed a missense mutation in exon 4 (c.689T>C [p.Leu230Pro]) (upper panel) and a 28 bp duplication in exon 11 (lower panel) leading to a frameshift and a premature stop codon (c.2371_2398dup28 [p.Ile800Thrfs*24]). (**C**) Immunoblot analysis showing XPF expression in lymphoblasts from 1333 and FA104. Lymphoblasts from a healthy individual (Con), the parents of 1333 (1333-F and 1333-M), and an unrelated *ERCC4* mutation carrier (Het) were used as controls. XPF levels are expressed as a ratio relative to the loading control (RAD50). (**D**) Genetic complementation of MMC sensitivity in FA104 lymphoblasts by wild-type XPF, but not by p.Arg689Ser altered XPF. Site-directed mutagenesis was used for introducing point mutations into the pWPXL-XPF hemagglutinin (HA)-tagged plasmid with the QuickChange method (Stratagene) as described[5]. Lentiviral supernatant production and transduction were done as previously described[6], and cells were grown for 10 days in the presence of MMC.

Data represent a typical result of at least three independent experiments. (**E**) Genetic complementation of MMC sensitivity of 1333 lymphoblasts by wild-type XPF (experiments were performed as in D). (**F**) MMC-induced growth inhibition of *Ercc4*-knockout MEFs transduced with lentiviral particles coding for GFP (negative control vector), wild-type XPF, and p.Arg689Ser and p.Leu230Pro altered XPF. Data represent means and SD of at least three independent experiments.

allele (c.2371_2398dup28 [p.Ile800Thrfs*24]; **Fig. 1B**), and this duplication is predicted to result in a truncated XPF that lacks the double helix-hairpin-helix (HhH_2) domain involved in heterodimerization with ERCC1 and DNA binding[7]. The paternal allele contains a missense mutation that changes a highly conserved amino acid residue within the helicase-like domain (c.689T>C [p. Leu230Pro]; **Fig. 1B**). Immunoblot analysis showed that a missense altered XPF and a truncated 90–95 kDa XPF are present at very low levels (**Fig. 1C**). As expected, the truncated XPF was undetectable with an antibody against the C-terminal HhH_2 domain of XPF (amino acids 866–916, data not shown). Interestingly, the truncated XPF was absent in a MMC resistant lymphoblastoid cell line (1333R) generated by long-term exposure to MMC, and near-normal XPF levels were detected in this reverted cell line (**Supplementary Fig. 1C**). PCR amplification and sequence analysis revealed that the 28 bp duplication had disappeared in 1333R (**Supplementary Fig. 1D**) and had thus restored the wild-type sequence. Both the inherited duplication and the somatic reversion might have been triggered by an inverted 5 bp repeat flanking the region.

Genetic complementation of MMC sensitivity in lymphoblasts from both FA individuals was achieved by lentiviral transduction of wild-type *ERCC4* cDNA (**Fig. 1D and 1E**). In addition, we expressed wild-type and mutant human *ERCC4* cDNAs in embryonic fibroblasts (MEFs) from *Ercc4* (*Xpf*)-null mice. We found that ectopic expression of *ERCC4* mutants encoding p.Leu230Pro and p.Arg689Ser did not complement MMC sensitivity of these MEFs (**Fig. 1F**), providing additional evidence that the *ERCC4* missense mutations found in both FA individuals inactivate XPF. The genetic and functional data show that mutations in *ERCC4* cause FA in two unrelated nonconsanguineous individuals. Because mutations in *ERCC4* cause an additional FA subtype (FA-Q), we propose *FANCQ* as an alias for *ERCC4*.

ERCC4 mutations have been linked to the skin-photosensitive and nucleotide excision repair (NER)-deficient disorders xeroderma pigmentosum (XP [MIM 278700, 610651, 278720, 278730, 278740, 278760, 278780, and 278750])[8] and XFE progeroid syndrome (MIM 610965)[9], and we therefore tried to understand why the identified *ERCC4* variants specifically lead to FA. We hypothesized that these mutants cause an FA phenotype because of a strong deficiency in ICL repair but have sufficient NER activity to prevent clinically relevant skin photosensitivity and other NER-related features. Compared to an XP complementation group C (XP-C) lymphoblast line, FA104 lymphoblasts were indeed not sensitive to UVC light (**Fig. 2A**). Given that UV-light survival experiments are challenging in lymphoblastoid

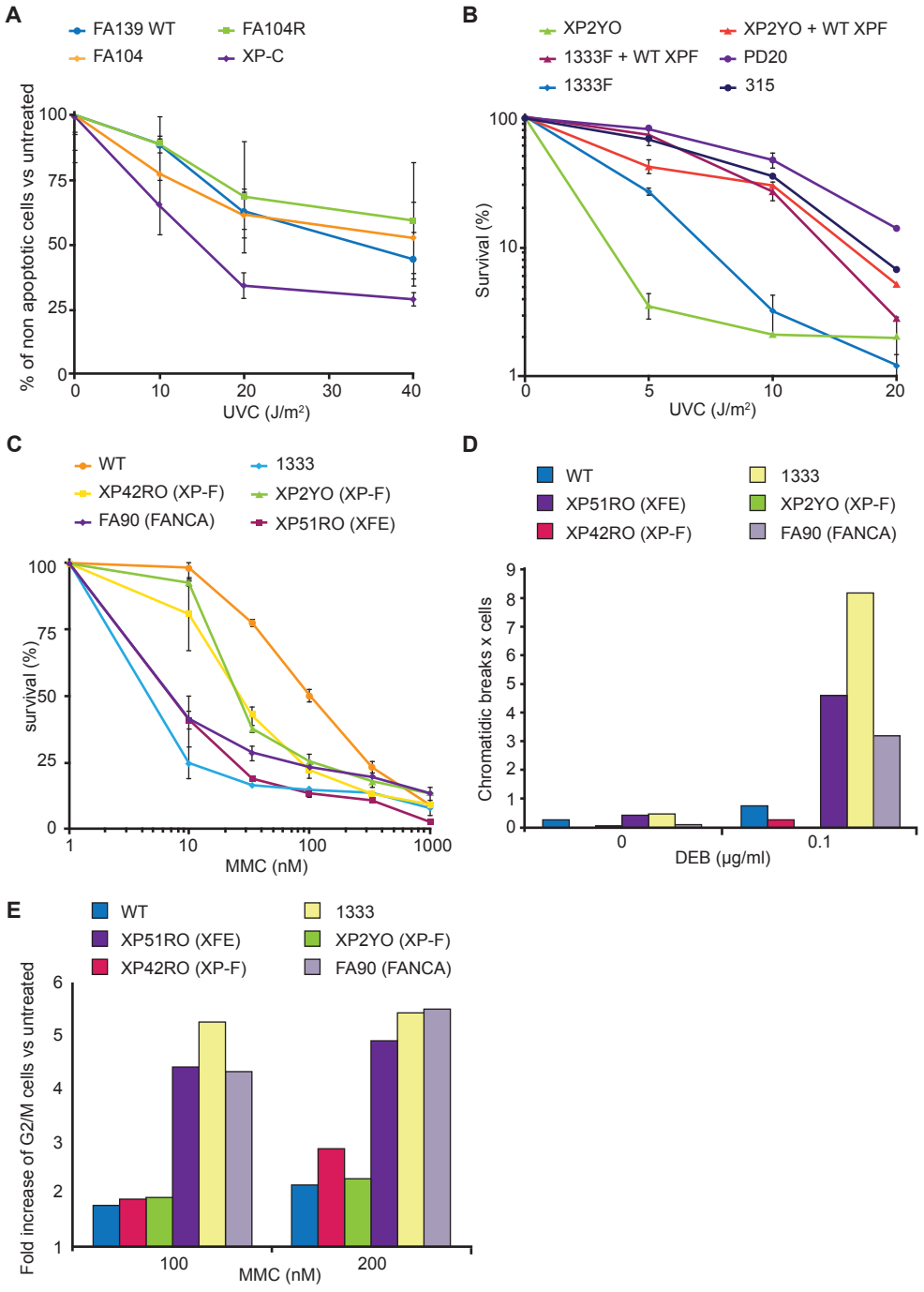

Figure 2. UV-Light and ICL Sensitivities of *ERCC4* Mutants Leading to FA.
(**A**) UVC-light-induced apoptosis in FA104 lymphoblasts. Cells were analyzed for UVC-light-induced apoptosis 24 hr after irradiation with the use of the AnnexinV-FLUOS Staining Kit (Roche). Data represent means and SD of at least three independent experiments. (**B**) UVC-light-induced growth inhibition of

human *ERCC4*-deficient immortal fibroblast cell lines (from XP individual XP2YO and FA individual 1333) transduced with lentiviral particles carrying cDNA coding for wild-type XPF. The results are expressed as a percentage of viable UVC-light-treated cells relative to untreated controls. Data represent means and SD of two independent experiments. (**C**) MMC sensitivity of human *ERCC4*- deficient primary fibroblasts from XP, FA, and XFE individuals (XP42RO, 1333, and XP51RO, respectively). Data represent means and SD of two independent experiments. (**D**) DEB-induced chromosome-fragility test in human *ERCC4*-deficient primary fibroblasts from XP, FA, and XFE individuals (XP42RO, 1333, and XP51RO, respectively). (**E**) MMC-induced G2/M cell-cycle arrest in the same cells as in (D). Experiments presented in (D) and (E) were performed as reported earlier[10].

cell lines, we studied skin fibroblasts from individual 1333 (FA104 fibroblasts were not available) and found that the UV-light sensitivity in FA individual 1333 was milder than that in XP complementation group F (XP-F) individual XP2YO (**Fig. 2B**). In addition, the FA-specific XPF alterations p.Leu230Pro and p.Arg689Ser rescued 100% of the UVC sensitivity of XP2YO fibroblasts (**Supplementary Fig. 2A**) and approximately 80% of the UVC-light sensitivity of *Ercc4*-null MEFs (**Supplementary Fig. 2B**) but were both unable to complement MMC sensitivity (**Fig. 1F**). Furthermore, XFE and 1333 fibroblasts responded typically like FA cells upon MMC-induced survival (**Fig. 2C**), DEB-induced chromosome breakage (**Fig. 2D**), and MMC-induced G2-phase arrest (**Fig. 2E**), whereas XP-F cells showed milder MMC sensitivity and lacked DEB-induced chromosome fragility and MMC-induced cell-cycle arrest (**Fig. 2C–2E**). Previous experiments in Chinese hamster ovary cells also demonstrated that the XFE-specific p.Arg153Pro altered XPF does not rescue MMC or UV-light sensitivity[11]. Therefore, we conclude that XP, XFE, and FA cells with *ERCC4* mutations clearly have a distinct response to UV light and MMC (**Supplementary Table 2**).

To further investigate the extent of NER deficiency in the FA-affected individuals, we measured UV-light-induced unscheduled DNA synthesis (UDS) in primary skin fibroblasts from individual 1333 and from an XP-F individual (XP42RO) with mild clinical UV-light sensitivity and found 24 ± 4% and 21 ± 3% residual UDS activity, respectively (**Fig. 3A**). We also determined UDS in *Ercc4*-null MEFs expressing the FA-specific XPF alterations p.Leu230Pro or p.Arg689Ser. The levels of UDS activity were 39.7% and 48.4% of the normal mean for p.Leu230Pro and p.Arg689Ser altered XPF, respectively (**Fig. 3B**), enough to complement 80% of UVC-light sensitivity of these MEFs (**Supplementary Fig. 2B**). In XPF-deficient human XP2YO fibroblasts, p.Leu230Pro and p.Arg689Ser altered XPF rather efficiently corrected the defective removal of 6-4 photoproducts (PPs) at sites of local UV damage (**Fig. 3C**). In contrast, XP2YO cells expressing the *ERCC4* mutant with the 28 bp duplication were completely deficient in NER activity, as predicted from the disruption of the ERCC1- and DNA-binding domain of this truncated protein. The studies presented in **Fig. 2 and 3** demonstrate that FA cells with *ERCC4* mutations are fully deficient in ICL repair but retain significant levels of NER activity.

Cell lines from XP-F individuals show a characteristic failure of the altered XPF

to properly translocate to the nucleus through aggregation of the protein in the cytoplasm[11]. This feature is evident for XP-causing mutations and accentuated in cells from the individual with XFE syndrome. However, FA-causing XPF missense altered proteins can actually translocate to the nucleus, where they are recruited to sites of active NER (**Supplementary Fig. 3A and 3B**) and can interact with SLX4 and ERCC1 (**Supplementary Fig. 3C and 3D**). These results might be functionally important, given that a recent article reports that SLX4 interaction with XPF is crucial for ICL repair and that SLX4-knockout mice phenocopy FA[13]. Using *Xenopus* extracts, J.C. Walter's group reported that the FA upstream pathway genes are required to regulate a nuclease that makes DNA incisions near the ICL[14]. Given that FA-specific altered XPF proteins can reach the site of damage, we then investigated their ability to cleave DNA. For this aim, the p.Arg689Ser altered XPF was purified as a heterodimer with ERCC1 as previously described[5]. Subsequently, NER reactions were performed with the purified altered protein, extracts from XPF-deficient XP2YO cells, and a plasmid containing an NER substrate (1,3-cisplatin intrastrand crosslink)[15]. Consistent with the functional data above, the purified heterodimer composed of ERCC1 and p.Arg689Ser XPF is proficient in the excision step of NER similarly to wild-type XPF, given that it restored the ability to cleave and remove the site-specific intrastrand crosslink from the plasmid in XP2YO cell extracts (**Fig. 4A**). Nevertheless, the excision reaction is not perfect given that the excised fragments are, on average, 1 nucleotide longer than expected from a normal reaction with wild-type-XPF-ERCC1 dimer (**Fig. 4A**, lane 4). We also performed in vitro nuclease activity assays with purified ERCC1-p.Arg689Ser-XPF and ERCC1-p.Arg689Ala-XPF on a stem-loop model DNA substrate. Unlike wild-type XPF and altered XPF proteins causing XP (p.Arg799Trp) or XFE progeroid syndrome (p.Arg153Pro)[11], p.Arg689Ser XPF is unable to cleave such a substrate (**Fig. 4B**), indicating that the nuclease-type activity of p.Arg689Ser XPF is grossly abnormal. Unfortunately, we could not perform these biochemical experiments with the p.Leu230Pro altered XPF because we were unable to express and purify ERCC1-p.Leu230Pro-XPF as a result of its low stability and tendency to aggregate. We finally checked whether the FA-specific altered XPF proteins ectopically expressed in *Ercc4*-null MEFs can perform the incision step of ICL repair. Both p.Leu230Pro and p.Arg689Ser altered XPF completely restored the incision defect of *Ercc4*-null MEFs, as measured by the COMET assay (data not shown), but the cells remained hypersensitive to ICLs (**Fig. 1F**). Although additional biochemical experiments are required, our results suggest that the ICL sensitivity of individuals FA104 and 1333 is not directly linked to the absence of XPF nuclease activity. It seems unlikely that the defect is a downstream step of homologous recombination because FA104 and 1333 cells are not sensitive to PARP inhibitors and are normal in Rad51 focus formation. Given that the nuclease activity of the FA-specific p.Arg689Ser altered XPF is grossly

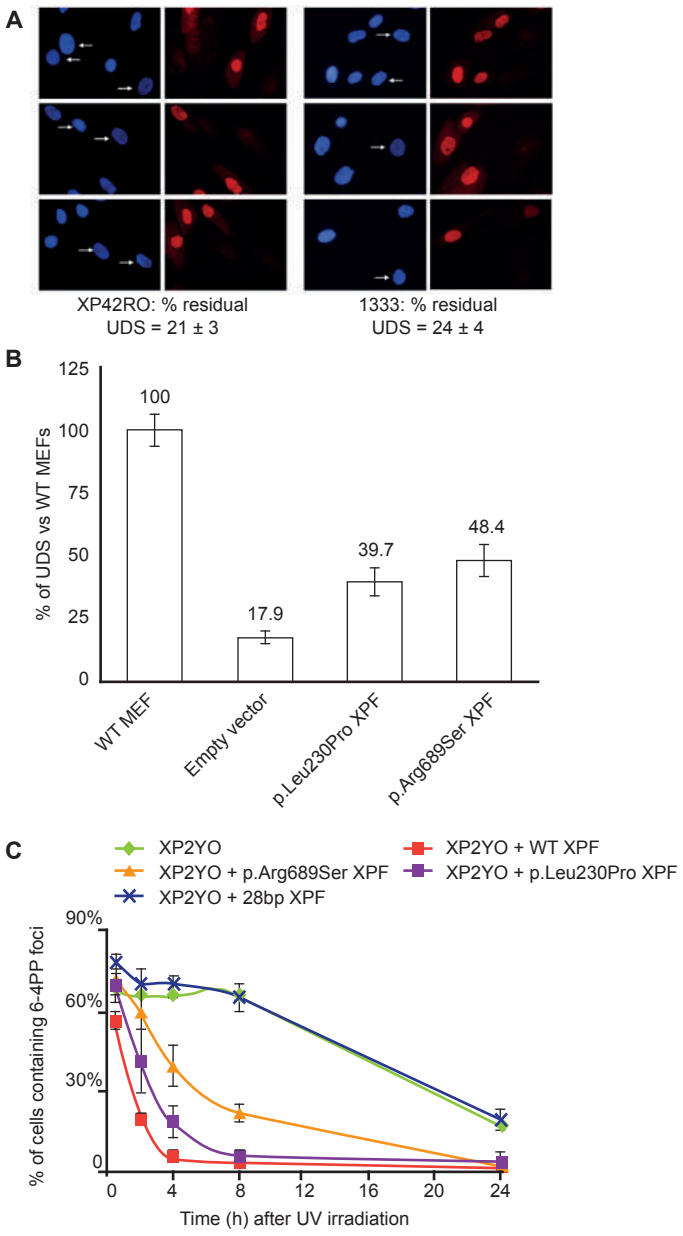

Figure 3. NER Analysis of *ERCC4* Mutants In Vivo.
(**A** and **B**) In primary fibroblasts, unscheduled DNA synthesis (UDS) representing global NER activity was measured with 5-ethynyl-deoxyuridine grossly as previously described[12]. (**A**) XP-F (XP42RO) and FA (1333) cells (arrows) were compared to mixed-in normal fibroblasts preloaded with polystyrene microbeads (no arrows), used as an internal control. UDS signal was quantified from 20–40 random XP-F or FA G1/G2 nuclei and expressed as a percentage of control wild-type cells. (**B**) UDS signals in *Ercc4*$^{-/-}$ MEFs measured as in (A) are expressed as a percentage of control wild-type MEFs. *Ercc4*$^{-/-}$ cells were stably expressing an empty vector or one of various *ERCC4* cDNAs (wild-type or encoding p.Leu230Pro or p.Arg689Ser). (**C**) Repair kinetics of UV-light-induced DNA damage by FA-specific *ERCC4* mutants in *ERCC4*- and NER-deficient human cells (XP2YO). Cells expressing wild-type XPF, p.Arg689Ser or p.Leu230Pro altered XPF, or XPF resulting from the 28 bp duplication were locally irradiated with UV light, cultured for the indicated times, fixed and stained for 6-4 PPs, and tagged with HA with the use of specific antibodies. Data represent the percentage of cells with 6-4 PP spots at various time points; means and SD of at least two independent experiments are shown. For each experiment, 100 cells were counted.

abnormal, it is tempting to speculate that the ICL-unhooking step in these FA cells leaves an intermediate aberrant substrate that is irreparable by subsequent ICL-repair factors.

Our genetic, biochemical, and functional studies, along with the characterization

of previous *ERCC4* mutations causing XP-F and XFE, provide a model for the mechanistic understanding of how mutations in *ERCC4* lead to three distinct diseases (**Supplementary Table 2**). Most of the presently known XP-F individuals suffer from a relatively mild form of XP[16]. Cells from these individuals have a reduced level of XPF in the nucleus because the altered XPF has a tendency to aggregate in the cytoplasm[11]. This reduced level of nuclear XPF is insufficient to mediate complete NER, but it still has enough ICL-repair-specific functions to prevent chromosome fragility, cell-cycle arrest, and subsequent FA clinical manifestations. A second set of *ERCC4* mutations, characterized in this study, allow localization of the protein to the nucleus, where they exert a certain level of NER activity but are fully deficient in ICL repair. p.Arg689Ser XPF is a stable and NER-proficient protein with an active site structure that prevents it from properly processing ICL-repair intermediates.

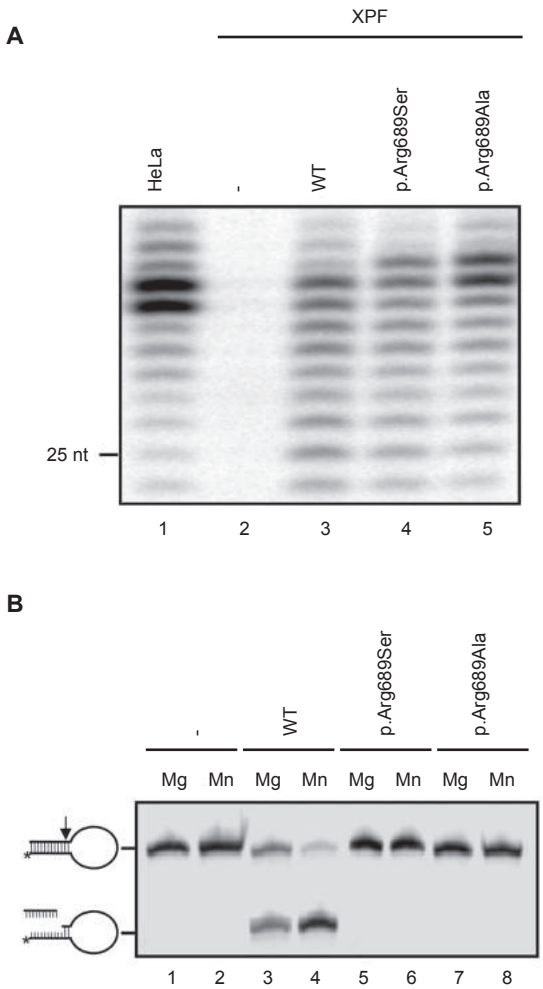

Figure 4. Nuclease Activity of Altered XPF.
(**A**) NER activity of wild-type and altered ERCC1-XPF dimer. A plasmid containing a site-specific 1,3-intrastrand cis-Pt DNA crosslink was incubated with whole-cell extracts from HeLa cells or XPF-deficient cells (XP2YO) complemented with recombinant ERCC1-XPF purified from Sf9 insect cells as reported[13]. The excised DNA fragments of 24–32 nucleotides are shown. The position of a 25-mer is indicated. (**B**) Incision of a stem-loop substrate with wild-type and altered XPF. The 30 Cy5-labeled substrate was incubated with recombinant ERCC1-XPF in the presence of 2 mM MgCl2 or 0.4 mM MnCl2, and the products were analyzed by denaturing PAGE. The incision reaction was performed essentially as described earlier[5,11].

p.Leu230Pro XPF is more similar to the products of previously described *ERCC4* mutations in that it is less stable and might have a tendency to aggregate in the cytoplasm. However, sufficient amounts of the protein are properly folded and reach chromatin, where it appears to have some activity in the removal of 6-4 PPs. Residual NER activity in the skin tissue of individual 1333 in vivo might explain why this individual has no clinically relevant skin photosensitivity, although we cannot exclude that dermatological problems will arise later in life. A final category of *ERCC4* mutations is associated with XFE progeroid syndrome, which is characterized by very low levels of nuclear XPF, apparently insufficient to support either NER or ICL repair. Importantly, the only XFE-affected individual described suffered from both skin photosensitivity and anemia[9,16] and shared some cellular features with XP (NER defect and UV-light sensitivity) and FA (extreme ICL sensitivity, DEB-induced chromosome fragility, and MMC-induced cell-cycle arrest), suggesting that XFE syndrome is characterized by a combination of XP and FA manifestations (**Supplementary Table 2**). Exhaustion of hematopoietic stem cells is also an attribute of ERCC1-XPF hypomorphic mice that mimic XFE (Laura Niedernhofer, personal communication). Microsomy, microcephaly, and liver fibrosis were likewise observed in FA individual 1333, in *Ercc1*- and *Ercc4*-deficient mice, and in the unique *ERCC1*-deficient individual, who all lack ICL-repair functions[17–21].

In a broader sense, this study demonstrates that depending on the type of *ERCC4* mutation and the balance between NER and ICL-repair activities, affected individuals present with one of three clinically distinct disorders. This resembles the case of *XPD*, which is involved in XP complementation group D, trichothiodystrophy (MIM 601675), or Cockayne syndrome (MIM 216400) depending on the type of mutation[22], and highlights the value of characterizing rare genetic disorders for gaining insight into the mechanisms of genome maintenance and human disease. XPF has a central role in preventing genome instability, cancer, BMF, developmental abnormalities, and premature aging. Like those of other breast and ovarian cancer susceptibility genes mutated in FA[23,24], the product of *ERCC4* also acts downstream of FANCD2 monoubiquitination. Therefore, it is important to study *FANCQ* as a candidate gene in hereditary breast and ovarian cancer.

Acknowledgements

The use of *FANCQ* as an alias for *ERCC4* was approved by the HUGO Gene Nomenclature Committee. We would like to thank the families affected by Fanconi anemia and their clinicians for providing samples and clinical data, as well as María A. Blasco (Centro Nacional de Investigaciones Oncológicas, Madrid) for providing *Ercc4*-deficient mouse embryonic fibroblasts. The J.A.B. laboratory is funded by grants from European Program "7FWP, Health" (PERSIST; agreement 222878), the Spanish Ministry of Science and Innovation (Refs110-90.1 and SAF 2009-07164), Programa RETICS-RD06/0010/0015 ISCIII, and Fundación Botín. O.D.S. acknowledges funding from the National Institutes of Health (GM080454 and CA092584). C.S. is funded by CCA/ V-ICI Amsterdam. D.S. and B.S. received grants from the Deutsche Fanconi-Anaemie-Hilfe, Aktionskreis Fanconi-Anaemie, and the Schroeder-Kurth Fund. J.S.'s laboratory is funded by the Generalitat de Catalunya (SGR0489-2009), the ICREA-Academia

award, the Spanish Ministry of Science and Innovation (Centre for Biomedical Network Research on Rare Diseases [CIBERER] CB06/07/0023, SAF2009-11936, and SAF2012-31881), and the European Regional Development FEDER Funds. CIBERER is an initiative of the Instituto de Salud Carlos III, Spain.

Author contribution
C.S. performed experiments shown in Supplementary fig. 1C, 1D and Supplementary Fig. 3C.

Supplementary data

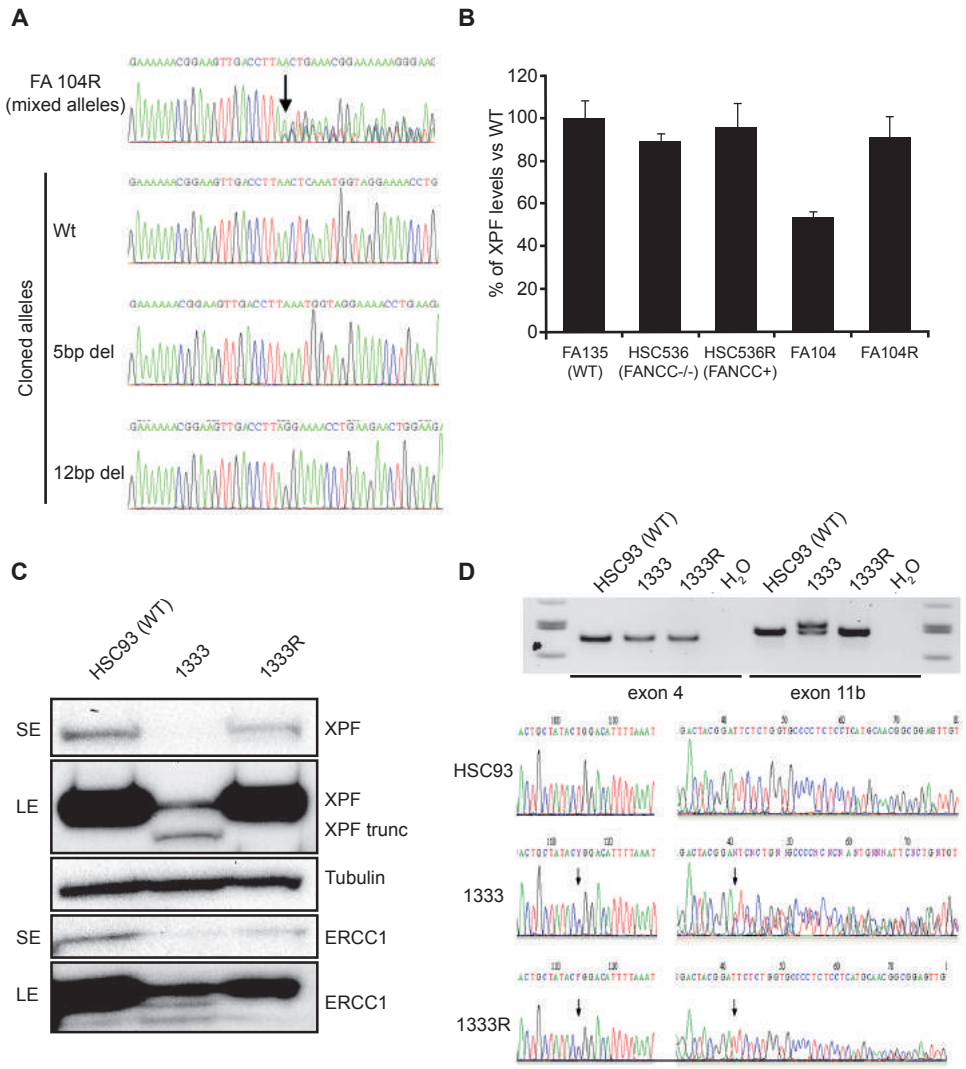

Supplementary Figure 1. Genetic Analysis of Back Mutations in *ERCC4* in Reverted MMC-Resistant FA Cell Lines.
(**A**) Sequence analysis of individual exon 8 alleles cloned from the FA104R cell line. Exons 8 was amplified from FA104R DNA and the PCR products were cloned with the Topo TA Cloning kit (Invitrogen) and

transfected into Library Efficiency DH5alpha Competent Cells (Invitrogen). The plasmids from single bacterial colonies were prepared with the NucleoSpin® Plasmid QuickPure Kit (Macherey-Nagel). Sequencing of single bacterial clones revealed the presence of a 12 bp deletion in exon 8 encompassing the pathogenic 5 bp deletion and restoring the reading frame of the *ERCC4* gene. (**B**) Quantification of XPF expression by immunoblot in lymphoblasts from FA104, FA104R, HSC536 (FA-C), HSC536R (HSC536 reverted to wt) and FA139 (wt). XPF levels are expressed as a ratio of the loading control (vinculin). Further details on antibodies used can be obtained upon request. The histogram represents XPF levels in the different cell lines normalized to the levels of the loading control. Means and SEM of at least three independent experiments are shown. (**C**) Immunoblot analysis showing low levels of two XPF proteins in 1333 and a normal size XPF protein in the reverted cell line 1333R. (**D**) Absence of the 28 bp duplication in *ERCC4* exon 11 in 1333R eliminating the longer *ERCC4* mutant allele with the 28 bp duplication (upper panel) and restoring the wt sequence in exon 11 (lower panel).

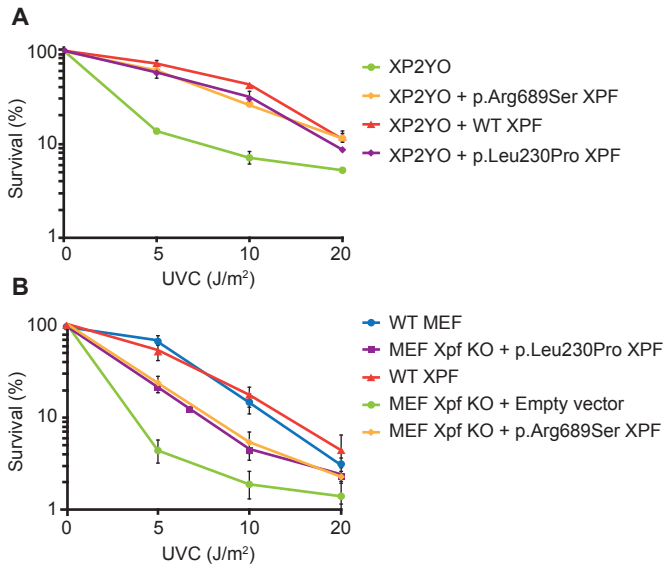

Supplementary Figure 2. XPF Mutants Leading to FA Restore UVC Resistance of NER-Deficient Human and Mouse Fibroblasts.
(**A**) UVC-induced growth inhibition of human XPF-deficient immortal cell lines from XP and FA individuals (XP2YO and 1333, respectively) transduced with lentiviral particles carrying cDNAs coding for XPF-WT, XPFp.Arg689Ser and XPF-p.Leu230Pro. Data represent means and SD of two independent experiments. (**B**) UV-induced growth inhibition of *Ercc4* KO MEFs transduced with lentiviral particles expressing GFP (negative control vector), wild type XPF, XPF-p.Arg689Ser and XPF-p.Leu230Pro. Data represent means and SD of at least four independent experiments. Lentivirus mediated cDNA transduction and survival analysis were performed as shown in **Fig. 1** and **2** (main text).

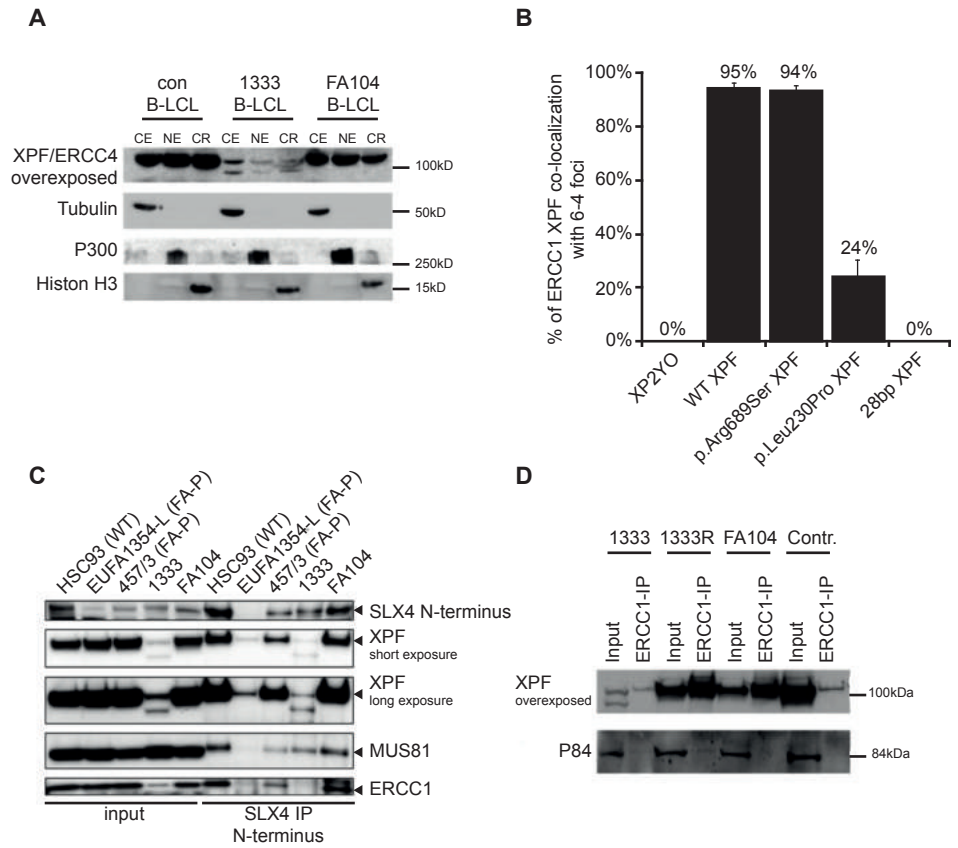

Supplementary Figure 3. XPF Relocation to DNA Damage and Protein-Protein Interactions.

(**A**) Immunoblot analysis of XPF protein in cytoplasmic (CE), nucleoplasmic (NE) and chromatin (CR) fractions from wild type, 1333 and FA104 lymphoblast cell lines. FA104 and FA104 show an abundance and a distribution of XPF between the cytoplasmic, nuclear and chromatin compartments comparable to a normal control, whereas 1333 reveals reduced abundance and two species of that protein with sizes predicted by its mutations but, of note, XPF is still detected in the nucleus and on chromatin with grossly unaffected ratios to the cytoplasmic fraction. Specificity of the separation of extracts from lymphoblasts is confirmed by the compartment-specific marker proteins tubulin, p300 and histone H3. Subcellular Protein Fractionation Kit from Pierce (Thermo Scientific) following the manufacturer's instructions. Further details on antibodies used and subfractioning conditions can be optained upon request. (**B**) Graphical representation of the percent co-localization of XPF with (6-4)PP in XP2YO cells expressing various forms of XPF. XP2YO cells were transduced with HA-tagged wild type XPF, XPF-p.Arg689Ser, XPFp.Leu230Pro, or XPF-28bp dup, irradiated with UVC (120 J m^{-2}) through a polycarbonate filter with 5 μm pores, incubated for 0.5 h, fixed and stained with antibodies to (6-4)PP and antibodies to HA. Data represent the average of at least 3 independent experiments ± the SD. For each experiment 100 cells were counted. (**C**) Normal SLX4 interactions in XPF-deficient FA individuals. SLX4 was immunoprecipitated with a polyclonal antibody raised against the first 300 amino acids of SLX4 (SLX4 N-terminus; gift from J. Rouse, Dundee). Precipitated proteins were visualized by immunoblotting with antibodies to SLX4 N-terminus, XPF, ERCC1 and MUS81. Reduced XPF and ERCC1 protein expression was found in lymphoblasts of individual 1333. In these cells, full-length and truncated XPF and MUS81 were coprecipitated with SLX4, whereas ERCC1 is barely detectable. In lymphoblasts of individual FA104, the interaction between SLX4 and its binding partners XPF-ERCC1 and MUS81 is normal. Wild type

lymphoblasts (HSC93) and lymphoblasts of FA-P individuals (EUFA1354-L and 457/3) were used as controls. (**D**) Normal ERCC1-XPF interactions in FA104 and 1333 lymphoblast cell lines. ERCC1 was immunoprecipitated with a polyclonal antibody against ERCC1 and the precipitated proteins were visualized by immunoblotting with antibodies against XPF and P84 as internal control. Further technical details on co-immunoprecipitation conditions and antibodies used can be obtained upon request.

Supplementary Table 1. List of Candidate Genes with Biallelic Mutations after Whole-Exome Sequencing

Chrom	Pos	Ref	Alt	Ensembl pred	AA change	GN	NRR	SNV Q	GT Q
1	169489751	A	W	SS	-	*F5*	42	171	171
1	169525877	T	Y	SS	-	*F5*	52	36	36
2	73675227	-	CTC	NFC	S/SP	*ALMS1*	16	N/A	N/A
2	73678183	G	R	NSC	G1509D	*ALMS1*	156	120	120
3	49094490	G	S	NSC	N381K	*QRICH1*	122	228	228
3	49095011	C	S	NSC	G208R	*QRICH1*	109	43	43
4	126238305	C	M	NSC	P247T	*FAT4*	52	178	178
4	126355484	C	M	NSC	A2368E	*FAT4*	56	190	190
5	156479444	TTG	-	NFC	TS/S	*HAVCR1*	61	N/A	N/A
5	156479568	-	GTT	NFC	T/TT	*HAVCR1*	106	N/A	N/A
6	31238942	G	W	NSC	A176V	*HLA-C*	23	61	39
6	31239577	A	C	NSC	S48A	*HLA-C*	21	90	90
6	32709309	A	R	SS	-	*HLA-DQA2*	29	84	84
6	32713044	C	Y	NSC	T64M	*HLA-DQA2*	192	228	228
6	32713188	C	Y	SS	-	*HLA-DQA2*	126	228	228
6	38840915	A	R	NSC	I2479V	*DNAH8*	72	216	216
6	38879340	A	T	NSC	E3267D	*DNAH8*	12	34	34
7	100686777	C	Y	NSC	T4027M	*MUC17*	323	228	228
7	100687107	G	R	SS	-	*MUC17*	66	79	79
8	30700598	T	Y	NSC	N1979S	*TEX15*	33	97	97
8	30701995	A	M	NSC	D1513E	*TEX15*	141	228	228
10	69682773	T	Y	NSC	D920G	*HERC4*	64	69	69
10	69785435	-	A	SS	-	*HERC4*	9	N/A	N/A
16	14029271	AACTC	-	FC	-	*ERCC4*	22	N/A	N/A
16	14041518	C	M	NSC	R689S	*ERCC4*	121	228	228
16	72137553	C	S	NSC	Q564E	*DHX38*	56	85	85
16	72142141	A	R	NSC	S994G	*DHX38*	52	106	106
17	74272839	C	Y	NSC	V1593M	*QRICH2*	54	33	33
17	74277009	T	Y	NSC	Q1264R	*QRICH2*	23	81	81
18	14105016	C	M	NSC	R508I	*ZNF519*	136	228	228
18	14105853	C	M	NSC	R229I	*ZNF519*	23	51	51
19	51918360	A	R	NSC	S445P	*SIGLEC12*	43	39	39
19	52004795	G	CT	FC	-	*SIGLEC12*	19	N/A	N/A
X	53561632	A	W	NSC	F4226I	*HUWE1*	42	53	53
X	53642759	C	M	NSC	E665D	*HUWE1*	16	33	33

Chrom: chromosome number; Pos: genomic position (GRCh37/hg19);Ref: reference allele; Alt: sample allele; Ensembl pred: consequence prediction of variants on transcript according to Ensembl v59. This

column contains one of the following values: SS=splice site, NSC=non-synonymous coding, FC=frameshift coding, NFC=non-frameshift coding; AA change: amino acid change in the affected protein; GN: Gene name; NRR: Number of non-redundant reads; SNV Q: the phred-scaled likelihood that the genotype is identical to the reference; GT Q: Phred-scaled likelihood that the genotype is wrong.

Supplementary Table 2. Comparative Summary of Clinical and Cellular/Molecular Features of XP, XFE, and FA Individuals with Mutations in *ERCC4*

Clinical/Cellular Features	XPF	XFE	FA
Skin photosensitivity	Mild	Severe	No
Atrophic epidermis	Variable	Yes	No
Neurologic features	Rare	Yes	No
Hematology	Normal	Anemia[a]	Anemia, BMF
Growth retardation[b]	No	Yes	Yes
Premature death	No	16yo	4yo (FA104), 1333 alive at age 10
UV sensitivity	Mild	Severe[c]	None (FA104)[d], mild (1333)
UDS defect	Mild	Severe[c]	Mild (1333), ND in (FA104)[d]
MMC sensitivity	Mild	Severe	Severe
DEB-test	Negative	Positive	Positive
MMC induced G2/M arrest	Negative	Positive	Positive
Nuclease activity on stem loop substrates	yes[e]	yes[e]	no

[a]It is not known whether anemia evolved to BMF in the XFE individual (Laura Niedernhofer, personal communication). [b]Include microsomy in 1333, FA104 and XFE and microcephaly in XFE and 1333. [c]Reported in Niedernhofer *et al.*, 2005. [d]UDS assay was not done in FA104 due to the lack of skin fibroblasts but FA104 lymphoblasts were resistant to UV. [e]Reported in Ahmad *et al.*, 2010 for XP mutation p.Arg799Trp and XFE mutation p.Arg153Pro. Typically XP and FA features are marked in yellow and green, respectively.

References

1. Stoepker, C., Hain, K., Schuster, B., Hilhorst-Hofstee, Y., Rooimans, M.A., Steltenpool, J., Oostra, A.B., Eirich, K., Korthof, E.T., Nieuwint, A.W., et al. (2011). SLX4, a coordinator of structure-specific endonucleases, is mutated in a new Fanconi anemia subtype. Nat. Genet. 43, 138–141.
2. Kim, Y., Lach, F.P., Desetty, R., Hanenberg, H., Auerbach, A.D., and Smogorzewska, A. (2011). Mutations of the SLX4 gene in Fanconi anemia. Nat. Genet. 43, 142–146.
3. Antonio Casado, J., Calle´n, E., Jacome, A., Río, P., Castella, M., Lobitz, S., Ferro, T., Muñoz, A., Sevilla, J., Cantalejo, A., et al. (2007). A comprehensive strategy for the subtyping of patients with Fanconi anaemia: conclusions from the Spanish Fanconi Anemia Research Network. J. Med. Genet. 44, 241–249.
4. Deans, A.J., and West, S.C. (2009). FANCM connects the genome instability disorders Bloom's Syndrome and Fanconi Anemia. Mol. Cell 36, 943–953.
5. Enzlin, J.H., and Schärer, O.D. (2002). The active site of the DNA repair endonuclease XPF-ERCC1 forms a highly conserved nuclease motif. EMBO J. 21, 2045–2053.
6. Almarza, E., R1´o, P., Meza, N.W., Aldea, M., Agirre, X., Guenechea, G., Segovia, J.C., and Bueren, J.A. (2007). Characteristics of lentiviral vectors harboring the proximal promoter of the vav proto-oncogene: a weak and efficient promoter for gene therapy. Mol. Ther. 15, 1487–1494.
7. de Laat, W.L., Sijbers, A.M., Odijk, H., Jaspers, N.G., and Hoeijmakers, J.H. (1998). Mapping of interaction domains between human repair proteins ERCC1 and XPF. Nucleic Acids Res. 26, 4146–4152.
8. Sijbers, A.M., de Laat, W.L., Ariza, R.R., Biggerstaff, M., Wei, Y.F., Moggs, J.G., Carter, K.C., Shell, B.K., Evans, E., de Jong, M.C., et al. (1996). Xeroderma pigmentosum group F caused by a defect in a structure-specific DNA repair endonuclease. Cell 86, 811–822.
9. Niedernhofer, L.J., Garinis, G.A., Raams, A., Lalai, A.S., Robinson, A.R., Appeldoorn, E., Odijk, H., Oostendorp, R., Ahmad, A., van Leeuwen, W., et al. (2006). A new progeroid syndrome reveals that genotoxic stress suppresses the somatotroph axis. Nature 444, 1038–1043.
10. Trujillo, J.P., Mina, L.B., Pujol, R., Bogliolo, M., Andrieux, J., Holder, M., Schuster, B., Schindler, D., and Surrallés, J. The American Journal of Human Genetics 92, 800–806, May 2, 2013 805 (2012). On the role of FAN1 in Fanconi anemia. Blood 120, 86–89.
11. Ahmad, A., Enzlin, J.H., Bhagwat, N.R., Wijgers, N., Raams, A., Appledoorn, E., Theil, A.F., J Hoeijmakers, J.H., Vermeulen, W., J Jaspers, N.G., et al. (2010). Mislocalization of XPFERCC1 nuclease contributes to reduced DNA repair in XP-F patients. PLoS Genet. 6, e1000871.
12. Limsirichaikul, S., Niimi, A., Fawcett, H., Lehmann, A., Yamashita, S., and Ogi, T. (2009). A rapid non-radioactive technique for measurement of repair synthesis in primary human fibroblasts by incorporation of ethynyl deoxyuridine (EdU). Nucleic Acids Res. 37, e31.
13. Crossan, G.P., van der Weyden, L., Rosado, I.V., Langevin, F., Gaillard, P.H., McIntyre, R.E., Gallagher, F., Kettunen, M.I., Lewis, D.Y., Brindle, K., et al.; Sanger Mouse Genetics Project. (2011). Disruption of mouse Slx4, a regulator of structurespecific nucleases, phenocopies Fanconi anemia. Nat. Genet. 43, 147–152.
14. Knipscheer, P., Ra¨schle, M., Smogorzewska, A., Enoiu, M., Ho, T.V., Scha¨rer, O.D., Elledge, S.J., and Walter, J.C. (2009). The Fanconi anemia pathway promotes replication-dependent DNA interstrand cross-link repair. Science 326, 1698–1701.
15. Moggs, J.G., Yarema, K.J., Essigmann, J.M., and Wood, R.D. (1996). Analysis of incision sites produced by human cell extracts and purified proteins during nucleotide excision repair of a 1,3-intrastrand d(GpTpG)-cisplatin adduct. J. Biol. Chem. 271, 7177–7186.
16. Gregg, S.Q., Robinson, A.R., and Niedernhofer, L.J. (2011). Physiological consequences of defects in ERCC1-XPF DNA repair endonuclease. DNA Repair (Amst.) 10, 781–791.
17. Weeda, G., Donker, I., de Wit, J., Morreau, H., Janssens, R., Vissers, C.J., Nigg, A., van Steeg, H., Bootsma, D., and Hoeijmakers, J.H. (1997). Disruption of mouse ERCC1 results in a novel repair syndrome with growth failure, nuclear abnormalities and senescence. Curr. Biol. 7, 427–439.
18. McWhir, J., Selfridge, J., Harrison, D.J., Squires, S., and Melton, D.W. (1993). Mice with DNA repair gene (ERCC-1) deficiency have elevated levels of p53, liver nuclear abnormalities and die before weaning. Nat. Genet. 5, 217–224.
19. Tian, M., Shinkura, R., Shinkura, N., and Alt, F.W. (2004). Growth retardation, early death, and DNA repair defects in mice deficient for the nucleotide excision repair enzyme XPF. Mol. Cell. Biol. 24, 1200–1205.
20. Jaspers, N.G., Raams, A., Silengo, M.C., Wijgers, N., Niedernhofer, L.J., Robinson, A.R., Giglia-Mari, G., Hoogstraten, D., Kleijer, W.J., Hoeijmakers, J.H., and Vermeulen, W. (2007). First reported patient with human ERCC1 deficiency has cerebro-oculo-facio-skeletal syndrome with a mild defect in nucleotide excision repair and severe developmental failure. Am. J. Hum. Genet. 80, 457–466.
21. Gregg, S.Q., Gutiérrez, V., Robinson, A.R., Woodell, T., Nakao, A., Ross, M.A., Michalopoulos, G.K., Rigatti, L., Rothermel, C.E., Kamileri, I., et al. (2012). A mouse model of accelerated liver

aging caused by a defect in DNA repair. Hepatology 55, 609–621.
22. Cleaver, J.E., Lam, E.T., and Revet, I. (2009). Disorders of nucleotide excision repair: the genetic and molecular basis of heterogeneity. Nat. Rev. Genet. 10, 756–768.
23. Meindl, A., Hellebrand, H., Wiek, C., Erven, V., Wappenschmidt, B., Niederacher, D., Freund, M., Lichtner, P., Hartmann, L., Schaal, H., et al. (2010). Germline mutations in breast and ovarian cancer pedigrees establish RAD51C as a human cancer susceptibility gene. Nat. Genet. 42, 410–414.
24. Levy-Lahad, E. (2010). Fanconi anemia and breast cancer susceptibility meet again. Nat. Genet. 42, 368–369.

CHAPTER

5

Defects in the Fanconi anemia pathway and chromatid cohesion in head and neck cancer

Chantal Stoepker, Najim Ameziane, Petra van der Lelij, Irsan E. Kooi, Anneke B. Oostra, Martin A. Rooimans, Saskia E. van Mil, Arjen Brink, Ralf Dietrich, Jesper A. Balk, Bauke Ylstra, Hans Joenje, Stephan M. Feller & Ruud H. Brakenhoff

Published in Cancer Research, 2015. 75(17):3543-3553.

Failure to repair DNA damage or defective sister chromatid cohesion, a process essential for correct chromosome segregation, can be causative of chromosomal instability (CIN), which is a hallmark of many types of cancers. We investigated how frequent this occurs in head and neck squamous cell carcinoma (HNSCC) and whether specific mechanisms or genes could be linked to these phenotypes. The genomic instability syndrome Fanconi anemia is caused by mutations in any of at least 16 genes regulating DNA interstrand crosslink (ICL) repair. Since patients with Fanconi anemia have a high risk to develop HNSCC, we investigated whether and to which extent Fanconi anemia pathway inactivation underlies CIN in HNSCC of non–Fanconi anemia individuals. We observed ICL-induced chromosomal breakage in 9 of 17 (53%) HNSCC cell lines derived from patients without Fanconi anemia. In addition, defective sister chromatid cohesion was observed in five HNSCC cell lines. Inactivation of FANCM was responsible for chromosomal breakage in one cell line, whereas in two other cell lines, somatic mutations in *PDS5A* or *STAG2* resulted in inadequate sister chromatid cohesion. In addition, *FANCF* methylation was found in one cell line by screening an additional panel of 39 HNSCC cell lines. Our data demonstrate that CIN in terms of ICL-induced chromosomal breakage and defective chromatid cohesion is frequently observed in HNSCC. Inactivation of known Fanconi anemia and chromatid cohesion genes does explain CIN in the minority of cases. These findings point to phenotypes that may be highly relevant in treatment response of HNSCC.

Introduction

Chromosomal instability (CIN) is a widespread phenomenon in many cancer types and can be caused by replication stress, inappropriate mitosis, aberrant telomere maintenance, or defective DNA double-strand break repair[1–3]. It can drive tumorigenesis by facilitating the loss of tumor suppressors and gain of oncogenes. The rare disorder Fanconi anemia is one of several genetic syndromes associated with CIN. This disorder is characterized by a broad variety of congenital malformations, bone marrow failure, and high risk of early-onset cancer, in particular acute myeloid leukemia and squamous cell carcinoma of the head and neck region (HNSCC)[4, 5]. Currently, biallelic mutations in any of at least 16 Fanconi anemia genes can cause Fanconi anemia[6, 7].

The observed CIN in Fanconi anemia cells is believed to emerge from impaired DNA interstrand crosslink (ICL) repair, leading to spontaneous and genotoxic-induced chromosomal breaks[8]. As a consequence, Fanconi anemia–deficient cells are hypersensitive to DNA crosslinkers and endogenously produced aldehydes[9–11].

Moreover, ICL sensitivity has been reported for a different class of syndromes: the cohesinopathies (*e.g.*, Robert syndrome and the Fanconi anemia–like Warsaw breakage syndrome[12–14]. These syndromes are caused by mutations in genes involved in sister chromatid cohesion, which is a tightly regulated process and is effectuated by the cohesin complex[15]. This complex consists of several subunits and holds newly replicated chromatids together from S-phase until they separate in mitosis. Thereby, sister chromatid cohesion is essential in regulating the proper distribution of chromosomes over the two dividing daughter cells and preventing CIN[3, 15].

The high frequency of HNSCC in individuals with Fanconi anemia shows the importance of the Fanconi anemia pathway in maintaining genomic stability and preventing cancer in squamous cells. Inactivation of the Fanconi anemia pathway is not exclusive to inherited cancer[16], but its significance in sporadic cancer, in particular HNSCC, remains unclear. Epigenetic silencing of *FANCF* has been reported in 15% of sporadic HNSCC[17], but this result may be an overestimation as the method used for methylation detection is prone to generate false-positive results[18]. Nevertheless, a comprehensive examination of Fanconi anemia pathway inactivation in sporadic HNSCC is desirable, as more Fanconi anemia genes have been discovered in recent years. Defects in this pathway may be exploited to improve anticancer therapies and yield opportunities to personalize treatment, as Fanconi anemia–deficient cells are hypersensitive to the commonly used chemotherapeutic drug cisplatin. Therefore, we examined CIN in terms of ICL-induced chromosomal breakage in head and neck tumors derived from individuals without Fanconi anemia and whether Fanconi anemia pathway inactivation may underlie this phenotype. Because of the diagnostic overlap in terms of ICL sensitivity between Fanconi anemia and cohesinopathies, we investigated the role of inadequate sister chromatid cohesion in HNSCC in parallel and analyzed candidate genes to explain the observed phenotypes.

Results

Chromosomal breakage and defective sister chromatid cohesion in the majority of sporadic HNSCC cell lines

Analysis of chromosomal breakage in prometaphase spreads is considered the gold standard for diagnosing Fanconi anemia[4, 8]. The same assay can, in addition, be used to score sister chromatid cohesion defects[14]. We performed this test to determine both spontaneous and ICL-induced chromosomal abnormalities in terms of chromosomal breakage or cohesion defects in 17 HNSCC cell lines derived from non–Fanconi anemia individuals (**Table 1**). Of note, cell lines UM-SCC-14ABC were derived from "recurrences" in the floor of mouth with 8 months between A and B and 18 months between B and C[28]. Despite that UM-SCC-14A was indicated as a recurrence, it was nonetheless staged as T1N0, which is somewhat peculiar, as

recurrences are not staged by convention. It is very likely based on stage, follow-up times, and clinical characteristics that UM-SCC-14ABC are independent multiple second primary tumors ("second field tumors") from a single precancerous field in the floor of the mouth. To reduce the risk of false-negative findings, we used two different ICL agents, mitomycin C and the commonly used chemotherapeutic agent cisplatin. Mitomycin C needs to be metabolically activated, of which the rate might differ between cell lines[29], whereas cisplatin response can be influenced by metabolic inactivation as well as by influx and efflux transporters[30]. Three HNSCC cell lines derived from tumors of patients with Fanconi anemia (FA-HNSCC) and their counterparts, in which the Fanconi anemia defect was genetically corrected, were used as controls. After treatment with either mitomycin C or cisplatin, almost all metaphase spreads (>90%) of FA-HNSCC cell lines exhibited ten or more break events per metaphase, whereas a large proportion of the corresponding genetically corrected cells had no breaks at all (**Fig. 1**). Of note, none of these cell lines displayed cohesion defects. Sporadic HNSCC cell lines were classified as ICL-sensitive when more than 50% of the cells had three or more break events per metaphase. On the basis of this phenotype, we found 9 sporadic HNSCC cell lines (VU-SCC-147, UM-SCC-14A and B, FaDu, UM-SCC-35, VU-SCC-OE, VU-SCC-41, VU-SCC-80, and VU-SCC-96a) to be sensitive to mitomycin C and/or cisplatin, whereas the remaining 8 cell lines showed a weak or no response at all. The number of chromosomal break events per metaphase was also scored in untreated cells (data not shown). Only metaphases of the most sensitive sporadic HNSCC cell lines VU-SCC-147, FaDu, and UM-SCC-14B exhibited a small increase of spontaneous breaks compared with other HNSCC cell lines (not shown).

While scoring chromosomal breakage in untreated sporadic HNSCC cell lines, we also screened for sister chromatid cohesion defects: loss of cohesion at the centromere, leading to a railroad phenotype (parallel/railroad chromosomes) or total loss of cohesion between sister chromatids, leading to premature chromatid separation (PCS). Quantification of railroad chromosomes and PCS revealed that 5 of 17 sporadic HNSCC cell lines (VU-SCC- 147, UM-SCC-14B, VU-SCC-OE, VU-SCC-78, and VU-SCC-120) displayed a substantial level (70%) of cohesion defects, almost as much as in the positive control cell line VU1199-F SV40 (Fig. 1). This cell line was derived from an individual suffering from Robert syndrome, a cohesinopathy caused by mutations in ESCO2 (ref 31). Together, these data demonstrate the presence of ICL-induced chromosomal breakage and/or defective chromatid cohesion in two thirds of the sporadic HNSCC cell lines examined.

ICL-induced accumulation of HNSCC cells in the G_2–M phase of the cell cycle

In addition to increased chromosomal breakage, normal cells from individuals with Fanconi anemia are characterized by an ICL-induced accumulation of cells

Table 1. Panel of 18 sporadic HNSCC and 3 FA-HNSCC cell lines

Cell line	Gender	Stage	Primary tumor site
Sporadic HNSCC cell lines			
VU-SCC-40	Female	T3N0	Tongue
VU-SCC-41	Male	T3N2	Floor of mouth
VU-SCC-78	Female	T3N2b	Tongue
VU-SCC-80	Male	Recurrence	Base of tongue
VU-SCC-94	Female	T3N1	Tongue
VU-SCC-96A	Male	T4N1	Retromolar trigone
VU-SCC-120	Female	T3N1	Tongue
VU-SCC-147[a]	Male	T4N2	Floor of mouth
VU-SCC-9917	Female	T2N2b	Oral cavity
VU-SCC-OE	Male	Lymph node metastasis	Floor of mouth
UM-SCC-11B	Male	T2N2a	Supraglottic larynx
UM-SCC-14A[b]	Female	T1N0	Floor of mouth
UM-SCC-14B[b]	Female	T1N0	Floor of mouth
UM-SCC-14C[b]	Female	T1N0	Floor of mouth
UM-SCC-22A	Female	T2N1	Hypopharynx
UM-SCC-35	Male	T4N1	Tonsillar fossa
FaDu	Male	NA	Hypopharynx
FA HNSCC cell lines			
VU-SCC-1131 (FA-C)	Female	T4N2b	Floor of mouth
VU-SCC-1365 (FA-A)	Male	NA	Mouth mucosa
VU-SCC-1604 (FA-L)	Female	NA	Tongue

Abbreviation: NA; not annotated. [a]Human papillomavirus (HPV)-positive, [b]local recurrences of a T1N0 carcinoma in floor of mouth.

in the G_2–M phase of the cell cycle. We performed cell-cycle analysis to determine whether FA HNSCC and sporadic HNSCC cell lines treated with either mitomycin C or cisplatin also arrested in the G_2–M phase of the cell cycle (**Fig. 1** and **Supplementary Fig. 1**). Indeed, despite the presence of tumor-promoting genetic changes, FA-HNSCC cells still accumulated in the G_2–M phase of the cell cycle after treatment with cross-linking agents, whereas this accumulation was not observed in the corrected cell lines. Of the 9 sporadic HNSCC cell lines that showed chromosomal breakage in response to mitomycin C and/or cisplatin, 5 cell lines arrested in the G_2–M phase of the cell cycle after treatment with mitomycin C and/or cisplatin (**Fig. 1** and **Supplementary Fig. 1**). One plausible explanation for the absence of G_2–M arrest in the other 4 sensitive cell lines is a defective G_2–M cell cycle checkpoint, enabling the cells to continue growing in the presence of DNA damage. Conversely, of the 8 cell lines that were classified as ICL-resistant in terms of chromosomal breakage, 4 still showed G_2–M arrest in response to mitomycin C and/or cisplatin

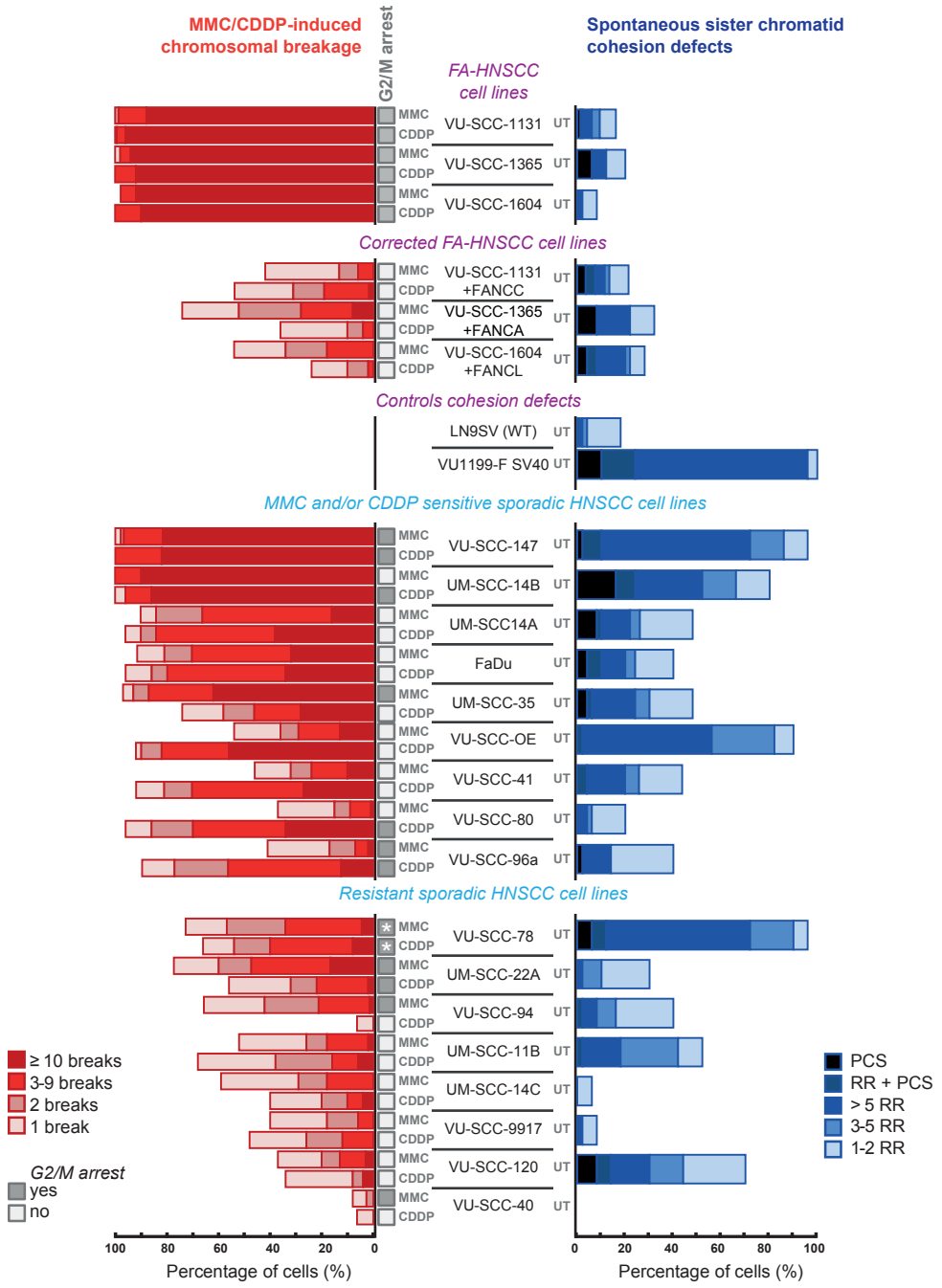

Figure 1. ICL-induced chromosomal breakage, G2–M arrest, and spontaneous sister chromatid cohesion defects in HNSCC cell lines.
Metaphase spreads of mitomycin-C (MMC)- and cisplatin (CDDP)-treated HNSCC cell lines were examined and scored for chromosomal breakage events. On the basis of this assay, two groups of sporadic HNSCC cell lines could be distinguished, mitomycin C- and/or cisplatin-sensitive and resistant cell lines.

FA-HNSCC cell lines and the corresponding corrected cells were used as controls. Metaphase spreads of untreated (UT) cells were scored for sister chromatid cohesion defects, railroad chromosomes (RR) and PCS. LN9SV [wild-type (WT)] and VU1199-F SV40 fibroblasts were used as negative and positive controls, respectively. Percentage of cells with the indicated number of chromosomal break events, railroad chromosomes, and PCS are shown. Mitomycin C- and cisplatin-induced accumulation in the G_2–M phase was also analyzed in Fanconi anemia as well as sporadic HNSCC cell lines (see also **Supplementary Fig. S1**). G_2–M arrest was classified positive (filled boxes) as the percentage of cells in G_2–M G1. Asterisks indicate that untreated VU-SCC-78 already had a high 4n peak.

(**Fig. 1** and **Supplementary Fig. 1**). Untreated VU-SCC-78 cells already showed a high 4n peak, which will be discussed below.

Somewhat remarkably, ICL-induced G_2–M arrest did not correlate with ICL-induced chromosomal breakage. This might be due to the variable genetic alterations that accumulated in these tumor cell lines. Because the chromosomal breakage assay is considered the gold standard in diagnosing Fanconi anemia, cell lines showing chromosomal breakage were classified as ICL-sensitive.

FANCM mutations in the sporadic head and neck tumor cell line FaDu

An ICL-induced increase in chromosomal breakage could be indicative for Fanconi anemia pathway inactivation. The Fanconi anemia pathway can be divided into two components: the upstream part, which is required for FANCD2 monoubiquitination, and a downstream part that is not essential for this posttranslational modification[6]. To test for a functional defect in the upstream part of the Fanconi anemia pathway, FANCD2 monoubiquitination and focus formation were analyzed. Mutations in any of the 8 upstream Fanconi anemia core complex genes (*FANCA*, *-B*, *-C*, *-E*, *-F*, *-G*, *-L*, and *-M*) abolish or reduce (in case of *FANCM* mutations) monoubiquitination and nuclear focus formation of FANCD2[6]. Five of the 9 ICL-sensitive sporadic HNSCC cell lines (UM-SCC-14B, FaDu, UM-SCC-35, VU-SCC- 41, and VU-SCC96a) and 1 ICL-resistant cell line (UM-SCC-14C) appeared only moderately able to monoubiquitinate FANCD2 (**Fig. 2A**). Notwithstanding, FANCD2 nucleus focus formation was observed in all cell lines tested, although slight differences in ICL-induced induction of FANCD2 foci cannot be excluded (**Fig. 2B**). A previous report[32] already showed that FaDu cells have abnormal FANCD2 monoubiquitination, which is consistent with our data. However, the underlying cause remained unknown. By using the Cancer Cell Line Encyclopedia, we found that FaDu harbors a homozygous nonsense mutation in *FANCM* (p.Ser1618*), which we confirmed by Sanger sequencing. As a result of this mutation, FaDu cells lack FANCM protein expression (**Supplementary Fig. 2**), which might explain the observed chromosomal breakage in this cell line.

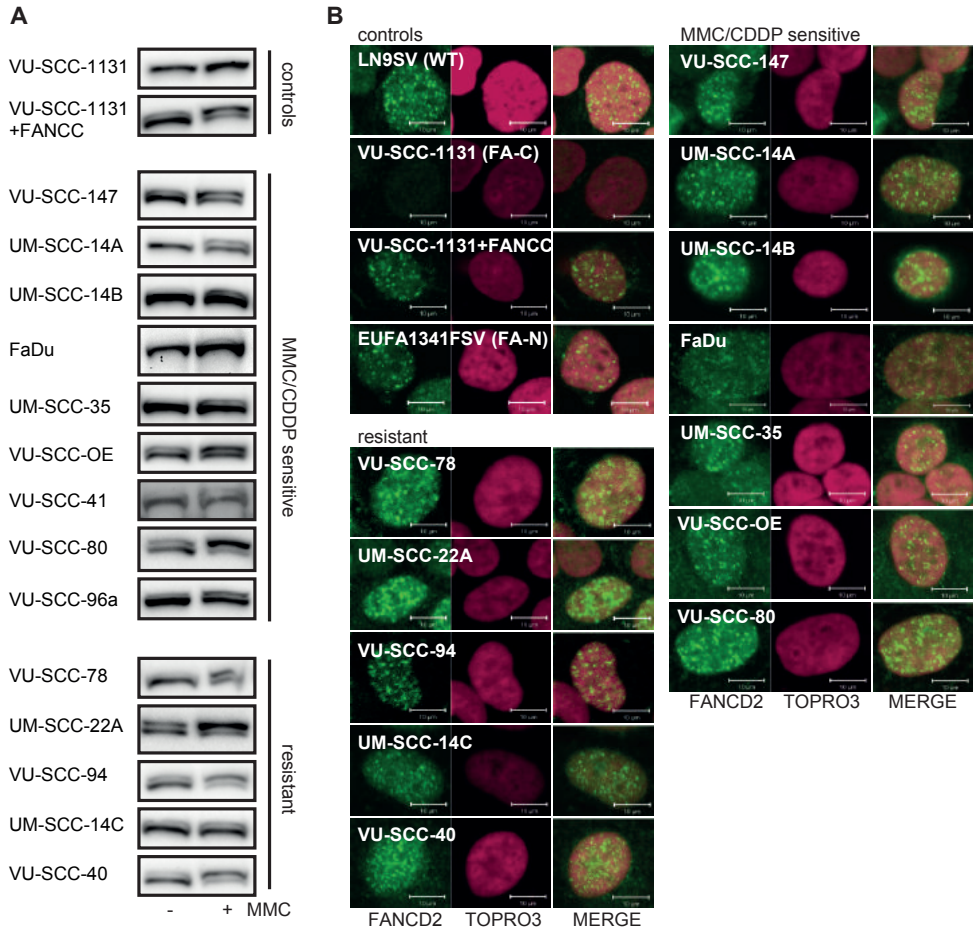

Figure 2. FANCD2 monoubiquitination and focus formation.
(**A**) Western blotting for FANCD2 monoubiquitination. Sporadic HNSCC cell lines were treated with or without 200 nmol/L mitomycin C (MMC) for 16 hours and whole-cell lysates were immunoblotted. The upper band represents the monoubiquitinated form of FANCD2. (**B**) Immunofluorescent analysis of FANCD2 focus formation (green). HNSCC cell lines were treated with 200 nmol/L mitomycin C for 16 hours. TO-PRO-3 (red) was used for nuclear counterstaining. Representative confocal images are shown. CDDP, cisplatin.

Whole-exome sequencing revealed several putative pathogenic mutations in Fanconi anemia genes

Nine cell lines in our panel of 17 sporadic HNSCC cell lines were sensitive to mitomycin C and/or cisplatin in terms of chromosomal breakage. To assess whether besides FaDu, other ICL-sensitive HNSCC cell lines contained mutations in any of the 16 known Fanconi anemia or 5 Fanconi anemia–associated genes, we sequenced the whole exomes of 6 ICL-sensitive cell lines (VU-SCC-80, VU-SCC-96a, VU-SCC-147, VU-SCC-OE, and UM-SCC-14B). This revealed possible pathogenic mutations in *TP53*, *HRAS*, *NOTCH1*, *PIK3CA*, *SMAD4*, and *FAT1*, which are frequently altered

in HNSCC (**Supplementary Fig. 3A**)[33–35]. Moreover, copy number alterations that often occur in HNSCC were found (*e.g.*, deletions encompassing *TP53* and *CDKN2A* and amplifications of *CCND1*, *MDM2*, and *EGFR*; **Supplementary Fig. 3B**). These results show that the cell lines are representative HNSCC cell lines.

Besides these oncogenic driver mutations, one hemizygous nonsense mutation and 8 missense variants in various Fanconi anemia genes were found (**Table 2**). The hemizygous nonsense mutation in *FANCD1/BRCA2* (p.Lys3326*), identified in cell line VU-SCC-147, is known as a polymorphic stop[36] and did not confer mitomycin C or cisplatin sensitivity in a mouse embryonic stem cell–based assay[37]. To further exclude this variant as possible pathogenic, we investigated PARP inhibitor response and nuclear RAD51 focus formation in VU-SCC-147 cells, as BRCA2-deficient cells are PARP inhibitor–sensitive and lack nuclear RAD51 focus formation[38–40]. VU-SCC-147 cells were resistant to PARP inhibitor (**Supplementary Fig. 4A**) and were able to form RAD51 foci (**Supplementary Fig. 4B**), suggesting that the resulting truncating *BRCA2* mutation did most likely not cause the observed ICL sensitivity in this cell line.

To assess the pathogenic potential of missense variants, we used three tools: (i) the *in silico* algorithms SIFT, MutationTaster, and PolyPhen for the prediction of deleterious mutations, (ii) minor allele frequencies (MAF; Exome Variant Server, http://evs.gs. washington.edu/EVS/), and (iii) the occurrence of these variants in patients with Fanconi anemia (Fanconi anemia gene variant database, www.rockefeller.edu/fanconi/). Variants with low MAFs (≤0.02) and predicted to be pathogenic by at least 2 of 3 *in silico* algorithms were classified as possibly damaging. Four of 8 identified variants with MAFs below 0.02 were predicted to be pathogenic by at least two prediction algorithms (**Table 2**). Although these variants in *FANCA*, *FANCJ*, *FANCP*, and *FANCQ* occurred heterozygously in the respective cell lines and Fanconi anemia is a recessive disease, haploinsufficiency or a dominant negative effect cannot be excluded, particularly not in cancer cells with their damaged genomes. Interestingly, the heterozygous variant in *FANCA* (p.Cys625Ser) in cell line UM-SCC-14B had been reported to occur in a patient with Fanconi anemia (**Table 2**)[41]. Therefore, this variant might be disease-causing, which is strengthened by the observation that the cell line containing this variant had poor FANCD2 monoubiquitination (**Fig. 2A**). The other variants were not identified in patients with Fanconi anemia.

Taken together, several sequence variants in Fanconi anemia genes were found, but their pathogenic nature remains elusive. In particular, the variants in *FANCA*, *FANCJ*, *FANCP*, and *FANCQ* predicted to be pathogenic might be disease causing, but their heterozygous nature indicates that they cannot explain the ICL induced chromosomal breakage phenotype.

Table 2. Sequence variants with MAF ≤ 0.02 in Fanconi anemia genes

Gene	Sequence variant	SIFT	MT	PP	MAF EA/AA	% reads	Remarks
Cell line VU-SCC-80							
FAAP16	c.370A>G; p.Asn124Asp	T	T	T	-	60/86 (70%)	Predicted tolerated
FANCD2	c.577A>G; p.thr193Ala	T	T	T	0.0007/ 0.0009	19/20 (95%)	Predicted tolerated
FANCQ/ XPF	c.241G>T; p.Val81Phe	P	P	P	-/ 0.0009	24/53 (45%)	Predicted pathogenic
Cell line VU-SCC-147							
FANCD1/ BRCA2	c.9976A>T; p.Lys3326*				0.0084/ 0.0027	39/41 (95%)	Hemizygous nonsense mutation, polymorphic stop[36]
FANCM	c.527C>T; p.Thr176Ile	T	T	T	0.0051/ 0.0005	27/71 (38%)	Predicted tolerated
Cell line VU-SCC-OE							
FANCI	c.480G>C; p.Leu160Phe	T	P	T	-	66/66 (100%)	Predicted tolerated
Cell line UM-SCC-14B							
FANCA	c.1874G>C; p.Cys625Ser	P	P	P	0.0031/ 0.0007	12/31 (39%)	Reported in Fanconi anemia patient[41]
FANCP/ SLX4	c.2854_2855delinsAT; p.Ala952Met				-	8/23% (35%)	Predicted pathogenic
Cell line UM-SCC-35							
FANCJ/ BRIP1	c.517C>T; p.Arg173Cys	P	P	P	0.0049/ 0.0011	39/125 (31%)	Predicted pathogenic

NOTE: Transcript refseq ID: *FAAP16* NM_199294.2; *FANCA* NM_000135.2; *FANCD1/BRCA2* NM_000059; *FANCD2* NM_033084.3; *FANCI* NM_001113378.1; *FANCJ/BRIP1* NM_032043; *FANCM* NM_020937.2; *FANCP/SLX4* NM_032444.2 and *FANCQ/XPF* NM_005236.2. MAF EA/AA represents minor allele frequency European/American and African/American populations, respectively.
Abbreviations: MT, MutationTaster; PP, polyphen; P, pathogenic; T, tolerated.

Absence of FANCD2 monoubiquitination in sporadic HNSCC cell line UPCI-SCC-154 due to FANCF methylation

On the basis of hydroxyurea (HU)-induced FANCD2 monoubiquitination analysis of a separate panel of 39 HNSCC cell lines (**Supplementary Table 1**), one cell line (UPCI-SCC-154) was selected for more detailed investigation. Upon mitomycin C treatment, FANCD2 monoubiquitination and nuclear FANCD2 focus formation were

absent in UPCI-SCC-154 cells (**Fig. 3A and B**). As with the 17 other sporadic HNSCC cell lines, chromosomal breakage and cell-cycle analysis were performed to examine ICL sensitivity. Upon treatment with either mitomycin C or cisplatin, UPCI-SCC-154 cells accumulated in the G_2–M phase of the cell cycle and exhibited in approximately 70% of scored metaphases more than three break events per metaphase (**Fig. 3C**). This was almost as sensitive as the FANCC-deficient control cell line VUSCC-1131. Furthermore, UPCI-SCC-154 cells were sensitive to cisplatin in a growth inhibition assay (**Supplementary Fig. S5**). We also found in 60% of metaphases of untreated UPCI-SCC-154 cells sister chromatid cohesion defects, mainly railroad chromosomes (**Fig. 3C**). Massive parallel sequencing of all known upstream Fanconi anemia genes in UPCI-SCC-154 cells did not reveal mutations that could explain the absence of FANCD2 monoubiquitination. Because promoter methylation of some Fanconi anemia genes has been observed in various tumors[16], we analyzed the methylation of Fanconi anemia genes using methylation-specific multiplex ligation-dependent probe amplification (MS-MLPA). Promoter methylation of the *FANCF* gene was detected in UPCI-SCC- 154 cells and transfection of this cell line with *FANCF* cDNA restored FANCD2 monoubiquitination (**Fig. 3D**) and reduced mitomycin C-induced chromosomal breakage (**Fig. 3C**). These results demonstrate that *FANCF* methylation is responsible for the observed Fanconi anemia phenotype in cell line UPCI-SCC-154.

Sister chromatid cohesion defects due to mutations in PDS5A and STAG2

As shown in **Fig. 1**, we also found sister chromatid cohesion defects in several sporadic HNSCC cell lines. To assess the molecular basis of cohesion defects, we followed a candidate gene approach by first investigating the levels of several known cohesion proteins (SMC1, SMC3, ESCO2, PDS5A, PDS5B, DDX11, STAG1, STAG2, and RAD21) by Western blotting, followed by DNA Sanger sequencing. Remarkably, PDS5A protein expression was absent in one cell line (VU-SCC-41) with only moderate cohesion defects (**Fig. 1** and **4A**). In contrast, no cohesion defects (data not shown) and normal PDS5A protein expression were observed in primary fibroblasts (VU-41-F) from the same patient (**Fig. 4A**), suggesting that a somatic mutation in *PDS5A* had occurred in the tumor. By using cDNA primers spanning exons 3 to 7, we detected a shorter PCR product in VU-SCC-41 cells compared with the wild-type fibroblasts from the same patient (**Supplementary Fig. 6A**). The shorter cDNA appeared to lack exon 6 sequence, resulting in a frameshift and premature stop (**Supplementary Fig. 6B**). Further examination of the *PDS5A* gene revealed an inversion combined with a duplication of part of the inverted sequence at the intron– exon boundary of exon 6, which removes the splice donor site (**Supplementary Fig. 6C**). This mutation was also found in paraffin-embedded tumor material (data not shown), indicating that the mutation was not induced by cell culture. In the tumor cell line,

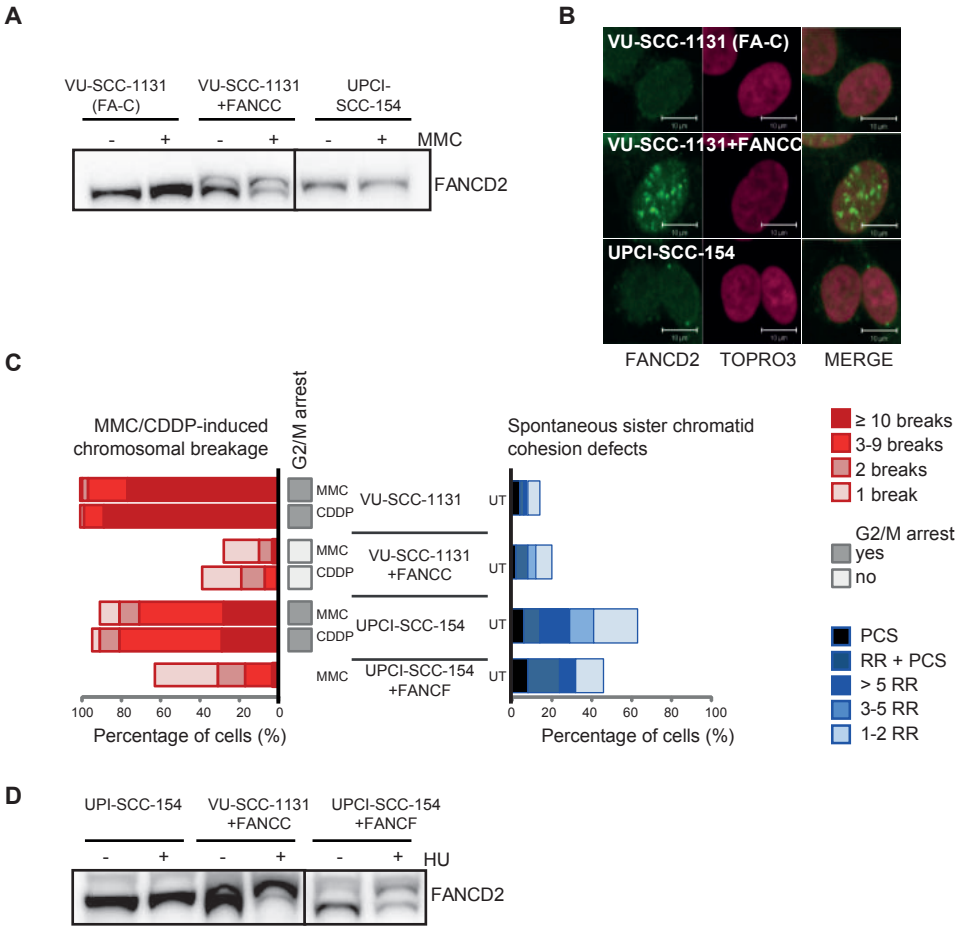

Figure 3. ICL sensitivity, FANCD2 monoubiquitination, and focus formation of sporadic HNSCC cell line, UPCI-SCC-154.
(**A**) and (**B**), untreated, or mitomycin C (MMC)-treated (200 nmol/L for 16 hours) UPCI-SCC-154 cells were immunoblotted for FANCD2 (**A**) or analyzed for FANCD2 focus formation (green; **B**). VU-SCC-1131 and VU-SCC-1131+FANCC were used as controls. Nuclei were counterstained by TO-PRO-3 (red). (**C**) ICL-induced chromosomal breakage events and spontaneous sister chromatid cohesion defects were observed in metaphase spreads of UPCI-SCC-154 and FANCF cDNA corrected UPCI-SCC-154 cells. CDDP, cisplatin. (**D**) Ectopic expression of FANCF in UPCI-SCC-154 cells restored FANCD2 monoubiquitination.

wild-type *PDS5A* sequence was absent, suggesting that the other *PDS5A* allele was deleted. Subsequent comparative genome hybridization (array CGH) indeed showed a heterozygous loss of the entire p-arm of chromosome 4, which is the region where the *PDS5A* gene is located (**Supplementary Fig. 6D**).

Absence of STAG2 protein expression was observed in sporadic HNSCC cell line VU-SCC-78 that showed severe cohesion defects (**Fig. 1** and **4B**). In this cell line, a heterozygous 1 base pair (bp) insertion in *STAG2* leading to a frameshift was identified by sequence analysis of gDNA (**Supplementary Fig. 7A**). Because

STAG2 maps to the X chromosome, a single mutational event could be enough for its complete inactivation. Sequencing of *STAG2* cDNA indeed revealed that *STAG2* mRNA expression was derived entirely of the mutant allele, indicating that the wild-type allele was not functional by X chromosome inactivation (**Supplementary Fig. 7B**). To exclude that the mutation was induced during cell culture, STAG2 protein expression was examined and indeed missing in paraffin-embedded tumor material derived from the same tumor of which cell line VU-SCC-78 was derived (**Fig. 4C**). In addition, it was previously shown that knockdown of STAG2 resulted in the generation of an octaploid population[42]. We detected a similar phenotype in VU-SCC-78 (**Supplementary Fig. 1B**).

Together, these results strongly suggest that the cohesion defects observed in VU-SCC-41 were due to an acquired mutation in the *PDS5A* gene, accompanied by a loss of the wild-type allele, whereas the cohesion defects in VU-SCC-78 were caused by a somatic mutation in *STAG2* in combination with X chromosome inactivation of the other allele.

Discussion

In the present study, we investigated the occurrence of Fanconi anemia pathway inactivation in sporadic HNSCC by analyzing a panel of Fanconi anemia and sporadic HNSCC cell lines. We found in 9 of 17 (53%) of the sporadic HNSCC cell lines ICL-induced chromosomal breakage, which can be indicative of a defective Fanconi anemia pathway, and in 29% (5 of 17) severe sister chromatid cohesion defects. However, this may be an overestimation as some of these cell lines are related. The UMSCC-14ABC cell lines are most likely derived from multiple primary tumors from a large preneoplastic field based on the clinical history and tumor characteristics[28]. Hence, these could be considered as separate tumors but nonetheless UM-SCC-14A and B share a similar phenotype, whereas UM-SCC-14C clearly behaves differently. Mutational inactivation of *FANCM* and methylation of *FANCF* were observed in two sporadic HNSCC cell lines from screened panels of 17 and 39 HNSCC cell lines, respectively. Although a few possible disease-causing variants in Fanconi anemia genes were found in the 6 ICL-sensitive HNSCC cell lines that were analyzed by whole-exome sequencing, their heterozygous nature suggests that they cannot explain the ICL-induced chromosomal breakage phenotype. This indicates that despite a frequent Fanconi anemia–like phenotype (ICL-induced chromosomal breakage), the Fanconi anemia pathway itself seems rarely involved. Silencing of *FANCF* by promoter hypermethylation has been demonstrated in a wide range of malignancies, including HNSCC[17]. However, the importance of *FANCF* promoter methylation in HNSCC is contradictory, as it was demonstrated that the methylation-specific PCR method that is routinely used to investigate *FANCF* methylation is liable to produce false-positive results[18]. By using the more specific method MS-MLPA, we showed that

FANCF methylation does occur in sporadic HNSCC, albeit infrequently. Screening of large sample series by more robust methods, such as quantitative methylation-specific PCR and sequencing, might substantiate our findings.

Interestingly, we found besides ICL-induced chromosomal breakage also spontaneous sister chromatid cohesion defects in a subset of sporadic HNSCC. Because of the role of sister chromatid cohesion in chromatid separation, DNA repair, and gene regulation, this pathway is important for chromosomal stability[15]. Mutations in cohesion genes could therefore lead to CIN by different mechanisms: mis-segregation of chromosomes followed by aneuploidy due to partial or total loss of cohesion or as a consequence of impaired DNA repair as well as altered gene expression. Recently, in several studies, alterations in sister chromatid cohesion genes were identified in a variety of cancers[27, 43–46]. In particular, inactivating alterations in *STAG2* have been frequently found. Likewise, we found mutational inactivation of *STAG2* in one HNSCC cell line, whereas in another cell line, *PDS5A* was mutated. The cohesion defects in VU-SCC-147 and UPCI-SCC-154 could be explained by the presence of the human papillomavirus (HPV) and subsequent inactivation of the retinoblastoma tumor suppressor proteins (pRb) in these cell lines. Loss of pRb has been demonstrated to alter H4K20 methylation and lead to sister chromatid cohesion defects[47–49]. The presence of HPV in these cell lines might well explain the inadequate sister chromatid cohesion.

Fanconi anemia and cohesinopathies have some overlapping features. ICL-induced chromosomal breakage is not an exclusive hallmark of Fanconi anemia cells and has been observed in T lymphocytes from individuals with Robert syndrome or Warsaw breakage syndrome as well[14]. Moreover, mitomycin C-induced, but not spontaneous cohesion, defects have been reported to occur in Fanconi anemia cells[14]. Whether these overlapping phenotypes also occur in cancer cells remains to be determined in functional studies. This is of relevance, as the screening for sequence variants in Fanconi anemia genes and cohesion genes might be exploited as biomarkers for cisplatin response. This is supported by previous work that demonstrated that FANCM-deficient cell line FaDu was approximately 6-fold more sensitive to cisplatin than the most resistant HNSCC cell line tested, although not as sensitive as FA-HNSCC cell lines[50]. In addition, in the present study, we showed sensitivity to cisplatin for the FANCF-deficient cell line UPCI-SCC-154 as well.

In summary, CIN in terms of ICL-induced chromosomal breakage or defective sister chromatid cohesion occurs frequently in HNSCC. In few cases, this is caused by defects in the Fanconi anemia pathway or mutational inactivation of chromatid cohesion genes. Further unraveling of the relevant mechanisms and/or genes causing these phenotypes may open new avenues for treatment and provide the biomarkers to predict treatment response.

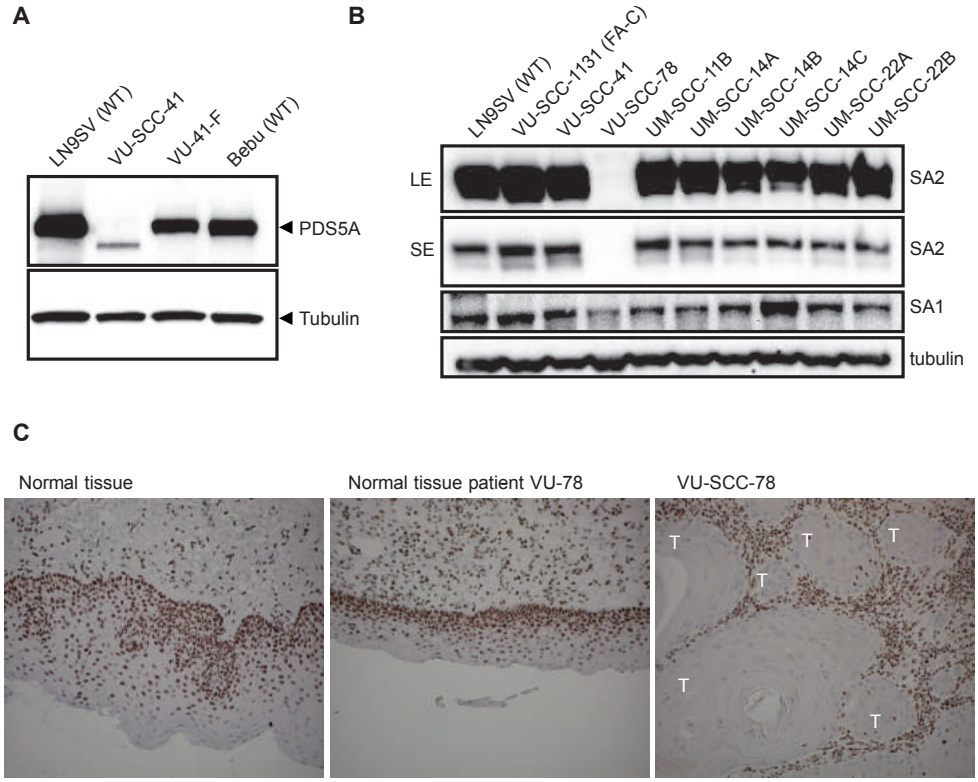

Figure 4. Mutational inactivation of *PDS5A* and *STAG2* in two HNSCC cell lines.
(**A**) Western blot analysis showing a truncated PDS5A protein in VU-SCC-41 and normal expression of PDS5A in fibroblasts (VU-41-F) of the same patient. (**B**) Western blot analysis showing absence of STAG2 protein expression in VU-SCC-78. Tubulin was used as a loading control. (**C**) Immunohistochemical analysis of STAG2 expression in paraffin-embedded tumor material of the same tumor of which cell line VU-SCC-78 was derived. STAG2 protein expression was absent in tumor (T) material but present in normal tissue surrounding the tumor.

Materials and Methods

Cell culture

All HNSCC cell lines (**Table 1**) and control fibroblast cell lines (wild-type controls LN9SV and VU-41-F, ESCO2-deficient VU1199-F SV40, and PALB2-deficient EUFA1341FSV) were cultured in DMEM supplemented with 10% FBS and 1 mmol/L sodium pyruvate (Gibco). Sporadic and Fanconi anemia HNSCC cell lines were established as described previously[19–21]. All three FA-HNSCC cell lines were genetically corrected. Cell lines UM-SCC-11B, UM-SCC-14A, UM-SCC-14B, UM-SCC-14C, UMSCC22A, and UM-SCC-35 were obtained from Dr. T. Carrey (University of Michigan, Ann Arbor, MI)[22, 23] and FaDu cells from the ATCC. HNSCC cell lines were authenticated by microsatellite profiling and TP53 mutation analysis. For information on cell line UPCI-SCC-154, see previously published data[24].

Chromosomal breakage assay

HNSCC cell lines were cultured for 48 hours in the absence or presence of 50 nmol/L mitomycin C (Kyowa Hakko Co.) or 1 mmol/L cisplatin (Pharmachemie BV Haarlem). After treatment with 200 ng/mL demecolcin (Sigma) for 30 minutes, cells were harvested, treated with 0.075 mol/L KCl for 20 minutes at room temperature, and fixed with 75% methanol, 25% acetic acid. Subsequently, cells were dropped onto glass slides and stained with 5% Giemsa (Merck). For each cell culture, 50 metaphases were analyzed for chromosomal breakage events and sister chromatid cohesion defects. All scoring was performed on coded slides to prevent counting bias.

Western blot and immunoprecipitation analysis

HNSCC cell lines were treated with or without 200 nmol/L mitomycin C overnight and harvested to examine FANCD2 monoubiquitination. Protein expression of FANCM, PDS5A, STAG1, and STAG2 was only examined in untreated cells. Whole-cell extracts were prepared in lysis buffer [50 mmol/L Tris (pH 7.5), 150 mmol/L NaCl, and 1% Triton X-100 supplemented with protease (cOmplete EDTA free tablets, Roche) and phosphatase (PhosSTOP, Roche) inhibitors. For immunoprecipitation reactions, cells were lysed and incubated with antiserum against FANCM (gift from Dr. W. Wang) for 2 hours at 4°C, followed by incubation with Protein A/G PLUS-Agarose (sc-2003, Santa Cruz Biotechnologies) for 30 minutes. Prior to immunoblot analysis, lysates were washed three times with lysis buffer. Proteins were separated on a 3% to 8% Tris-Acetate NUPAGE gradient gel (Invitrogen) and transferred to Immobilon-P membrane overnight. After blocking with 5% dry milk in TBST [10 mmol/L TRIS-HCl (pH 7.5), 150 mmol/L NaCl, 0.05% Tween-20], the membrane was incubated with the indicated primary antibodies overnight [1:500 mouse anti-FANCD2 (Fl17, sc-20022, Santa Cruz Biotechnologies), 1:1,000 rabbit anti-PDS5A (ab17960, Abcam), 1:5,000 goat anti-STAG1 (A300-156A, Bethyl), 1:1,000 goat antiSTAG2(A300-159A, Bethyl)], followed by washing with TBST and incubation with horseradish peroxidase–conjugated secondary antibodies to visualize with ECL (GE Healthcare). Mouse monoclonal anti-a-tubulin (1:5,000, B-5-1-2, SC23948, Santa Cruz Biotechnologies) was used as a control to ensure loading of equal amounts of protein in each Western blot lane.

FANCD2 and RAD51 immunofluorescence

Cells were cultured on sterile chamber slides (Nunc) and treated with 200 nmol/L mitomycin C for 16 hours. After prepermeabilization with 0.25% Triton X-100 in PBS for 1 minute on ice, cells were fixed with 4% formaldehyde [16% formaldehyde solution (w/v), methanol-free (Thermo Scientific Pierce, diluted in PBS)] for 15 minutes at room temperature prior to permeabilization with 0.5% Triton X-100 in PBS (20 minutes at room temperature). Unspecific binding sites were blocked by incubating with 10% FBS (1 hour at room temperature) followed by incubation with rabbit anti-FANCD2 (1:200 NB100-182 Novus Biologicals) or rabbit anti-RAD51 (1:1,000, gift from Dr. R. Kanaar) for 2 hours at room temperature. Slides were washed (0.2% Triton X-100 in PBS) and incubated with goat anti-rabbit ALEXA488 (1:1,000, A-11008, Invitrogen) for 1 hour, washed with 0.2% Triton X-100 in PBS, and counterstained with TO-PRO- 3 iodide (1:1,000, T3605, Invitrogen) for 30 minutes. Slides were washed with PBS, mounted by Vectashield (Vector Laboratories), and analyzed by a confocal microscope (Carl Zeiss).

Methylation-specific multiplex ligase–mediated probe amplification

FANCF promoter methylation was analyzed by using a MSMLPA test (MRC-Holland), as described previously[25].

Whole-exome sequencing
DNA samples were prepared for whole-exome sequencing with NimbleGen SeqCap EZ V3 enrichment kit as described previously[26] and sequenced on Illumina's HiSeq 2000. Three sample libraries were pooled per lane. Sequencing reads were mapped to UCSC genome version hg19 with BWA in paired-end mode. For variant calling, GATK was used to recalibrate base call scores, to realign reads around INDELs, and to call variants using the haplotype caller. Variants with low coverage (depth < 5 reads), low GATK variant quality (GATK variant QUAL < 50), and/or strand bias (FisherStrandBias > 60) were discarded and remaining variants were annotated with ANNOVAR. Annotated variants were further filtered by discarding synonymous variants, mappability > 0.9, mutant allele frequency in exome sequencing project (ESP) < 2%, and the number of samples carrying the variant < 3. For selection of sequence variants in Fanconi anemia and cohesion (-associated) genes, a cutoff of mutant allele frequency in ESP < 2% was used. For copy number analysis, log2 ratios between tumor samples and in-house generated sex-matched nontumor baselines were calculated for each target bait and were segmented using CGH call and CHG regions bioconductor packages into 5 copy number levels. LOH was determined by calculating mutant allele frequencies of polymorphic sites (snp138Common).

Immunohistochemistry (IHC)
IHC was performed on paraffin-embedded sections of an HNSCC tumor biopsy, of which cell line VU-SCC-78 was also derived. Sections were deparaffinized and subjected to Tris-EDTA (pH 9.0) antigen retrieval. A standard protocol was performed using STAG2 antibody (1:25, clone J-12, sc-81852, Santa Cruz Biotechnologies) and the BrightVision Poly-HRP-Anti Ms/Rb/Rt IgG kit (Immunologic BV). The staining was developed with diaminobenzidine as chromogen and counterstained with hematoxylin. The specificity of this antibody was previously verified by others[27].

Sanger sequencing
The presence of *FANCM*, *PDS5A*, or *STAG2* mutations was analyzed by Sanger sequencing. PCR products were purified using a SAP/EXO treatment (Amersham Biosciences) according to the manufacturer's instructions. Sequencing reactions were prepared using specific primers (available on request) and Big Dye Terminator Cycle Sequencing Kit (Applied Biosystems).

Acknowledgements
The authors thank Prof. Dr. Johan de Winter who initiated these studies, but died during the completion of the experimental work and the drafting of the final version of the manuscript. They also thank E. Polder, R. van der Willik, J. Steltenpool, M. Blijlevens, and P.P. Eijk for technical assistance, E. Velleuer for collecting tumor material, and H. te Riele for helpful discussions and comments.

Author Contributions
Conception and design: C. Stoepker, P. van der Lelij, R. Dietrich, S.M. Feller, R.H. Brakenhoff. Development of methodology: B. Ylstra. Acquisition of data (provided animals, acquired and managed patients, provided facilities, etc.): C. Stoepker, N. Ameziane, S.E. van Mil, A. Brink, R. Dietrich, B. Ylstra, H. Joenje, R.H. Brakenhoff. Analysis and interpretation of data (e.g., statistical analysis, biostatistics, computational analysis): C. Stoepker, N. Ameziane, I.E. Kooi, R.H. Brakenhoff. Writing, review, and/or revision of the manuscript: C. Stoepker, N. Ameziane, P. van der Lelij, A.B. Oostra, R. Dietrich, R.H. Brakenhoff. Administrative, technical, or material support (i.e., reporting or organizing data, constructing databases): A.B. Oostra, M.A. Rooimans, A. Brink, R. Dietrich, R.H. Brakenhoff. Study supervision: R.H. Brakenhoff. Other (practical support): J.A. Balk. Other (primarily involved in the initial stages of this project as a supervisor): H. Joenje. Other (generation of experimental data): S.M. Feller.

Grant Support
Financial support was provided from CCA/V-ICI Amsterdam, Dutch Cancer Society and Fanconi Anemia Research Fund (FARF), Portland, Oregon.

Disclosure of Potential Conflicts of Interest
No potential conflicts of interest were disclosed.

Supplementary materials and methods

Cell cycle analysis
Cell were untreated or exposed for 72 hours to either MMC (15 and 30 nM) or CDDP (250 and 750 nM) and permeabilized in buffer containing 100 mM TRIS-HCl (pH 7.5), 150 mM NaCl, 0.5 mM MgCl2, 1 mM CaCl2, 0.2% BSA and 0.1% IGEPAL (CA-630, Sigma). DNA was stained with PI/RNase staining buffer (BD Pharmingen) for 15 minutes and analyzed by flow cytometry.

siRNA knockdown of BRCA2 and PALB2 in VU-SCC-147
VU-SCC-147 cells plated in 96-well plates were reverse transfected with siRNAs (final concentration 25 nM) targeted against PALB2 and BRCA2 using Lipofectamine RNAiMAX (Invitrogen) according to the manufacturer's protocol. Non-targeting siCONTROL#2 (Dharmacon) and siRNA targeted against PLK1 were used as a negative and positive control, respectively. Twenty-four hours following transfection, increasing concentrations of PARP inhibitor (KU58948) were added. After 5 days, cell viability was determined by the CellTiter-Blue assay (Promega).

Array CGH
Labeling and hybridization was done as previously described[51]. In brief, genomic DNA (500 ng) of tumor and reference were labeled with Cyanine 3-UTP (Cy3) or Cyanine 5-UTP (Cy5) nucleotide mixture (CGH labeling Kit for Oligo Arrays, Enzo Life Sciences), respectively. Labeled DNA of tumor and reference were purified (QIAquick PCR Purification Kit (Qiagen) and mixed prior to hybridization onto Agilent 180 K oligonucleotide arrays (Agilent Technologies). After hybridization, slides were immediately scanned using microarray scanner G2505B (Agilent technologies) and image analysis was performed using feature extraction software (version 9.1, Agilent Technologies). The Agilent CGH-v4_91 protocol was applied using default settings. Oligonucleotides were mapped according to the human genome build NCBI 6 (May 2006). Of both Cy3 and Cy5 channels, local background was subtracted from the median intensities. The log2 tumor to normal intensity ratio was calculated for each spot and normalized against the median of the ratios of all autosomes.

Supplementary data

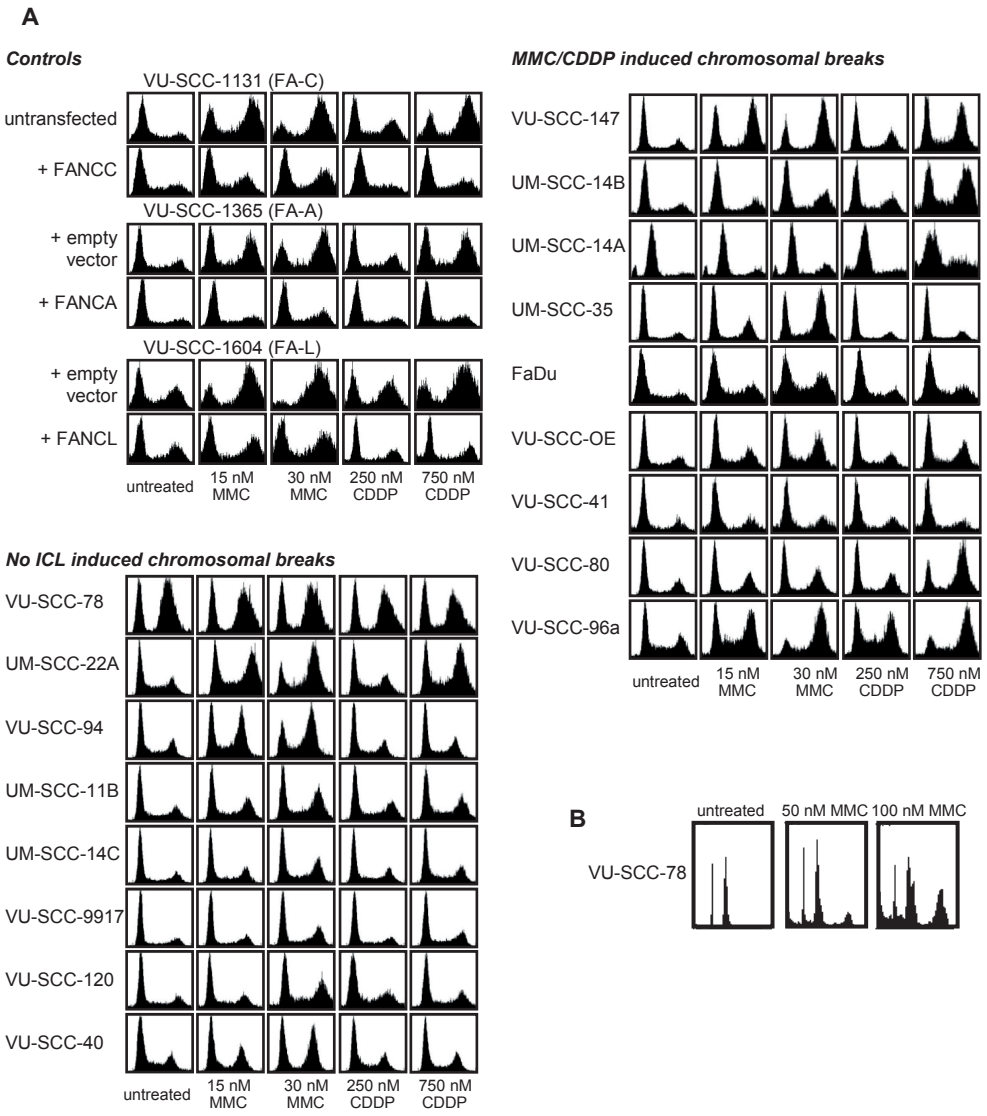

Supplementary Figure 1. Cell cycle analysis in FA and sporadic HNSCC cell lines upon ICL treatment.
(**A**) Cells were untreated or continuously exposed to 15 nM MMC, 30 nM MMC, 250 nM CDDP or 750 nM CDDP for 72 hours. G2/M arrest was analyzed by flow cytometry. (**B**) Untreated VU-SCC-78 cells showing a high 4n peak and additional 8n peak upon treatment with 50 or 100 nM MMC.

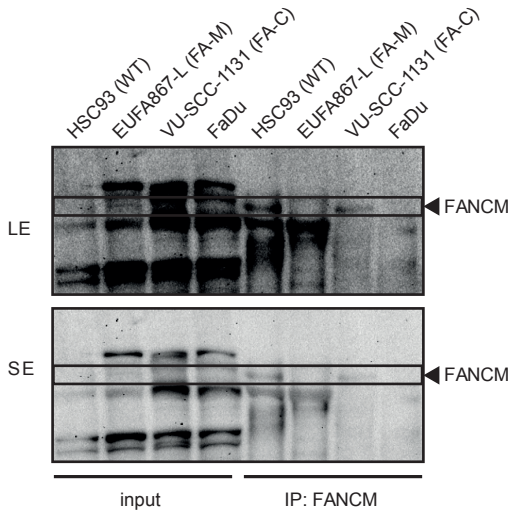

Supplementary Figure 2. FANCM protein expression is absent in FaDu cells. Immunoprecipitation and immunoblot analysis showing absence of FANCM expression in FaDu cells and the control cell line EUFA867-L (FA-M). LE and SE indicate short and long exposures of the blot.

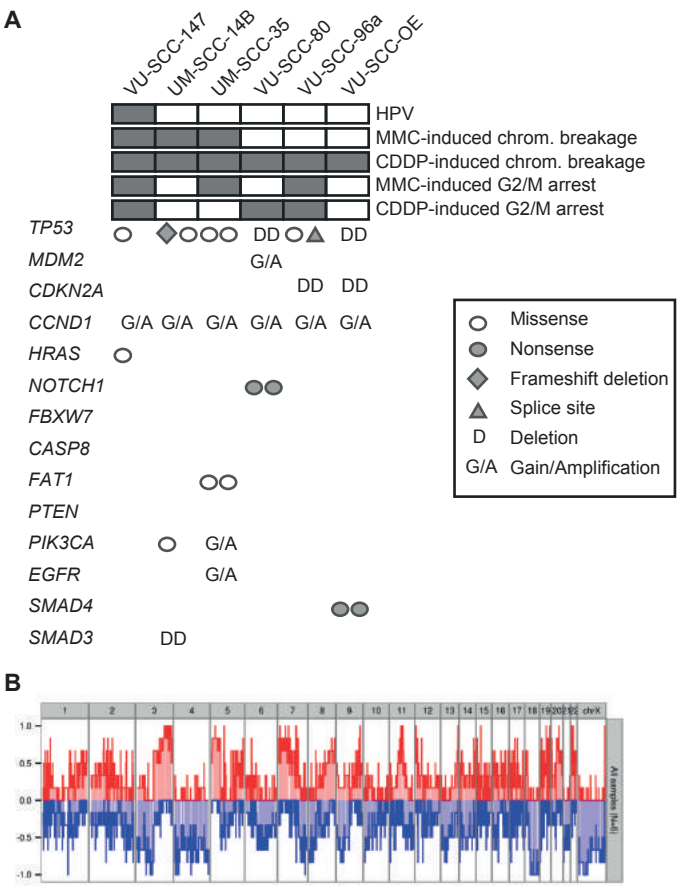

Supplementary Figure 3. Overview of possible pathogenic variants in genes that are frequently altered in HNSCC. (**A**) Six cell lines, which were sensitive to ICL agents manifesting as increased chromosomal breakage, were analyzed by whole exome sequencing. Potential pathogenic mutations in genes that are frequently altered in HNSCC are indicated. (**B**) Frequency plot of copy number alterations (gains in red, losses in blue) in the six HNSCC cell lines that were analyzed by whole exome sequencing.

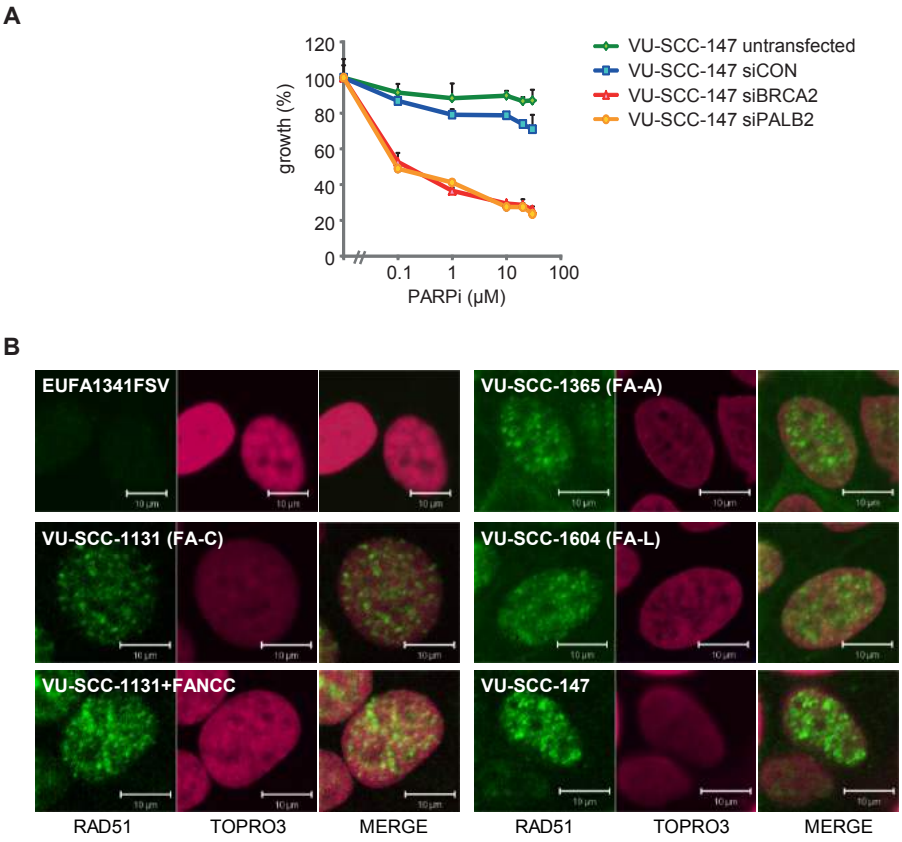

Supplementary Figure 4. PARP inhibitor resistance and normal RAD51 focus formation in VU-SCC-147.
(A) PARP inhibitor sensitivity after knockdown of BRCA2 or PALB2 in cell line VU-SCC-147. VU-SCC-147 cells, containing a hemizygous polymorphic nonsense variant in *BRCA2* (p.Lys3326*) and a heterozygous missense variant in *PALB2* (p.Gly998Glu), were transfected with siRNAs against BRCA2 (siBRCA2) or PALB2 (siPALB2) and treated with increasing concentrations PARP inhibitor (PARPi: Olaparib/KU0058948). Untransfected and VU-SCC-147 cells transfected with non-targeting siRNA (siCON) were used as controls. (**B**) RAD51 focus formation upon MMC treatment in VU-SCC-147 cells. Representative images of MMC-induced RAD51 foci (green) in FA (VU-SCC-1131, VU-SCC-1365 and VU-SCC-1604) and sporadic HNSCC (VU-SCC-147) cell lines. Cells were treated with 200 nM MMC for 16 hours. PALB2-deficient EUFA1341FSV cells and FA-HNSCC tumor cell lines were used as controls. Nuclei were counterstained with TO-PRO-3 (red).

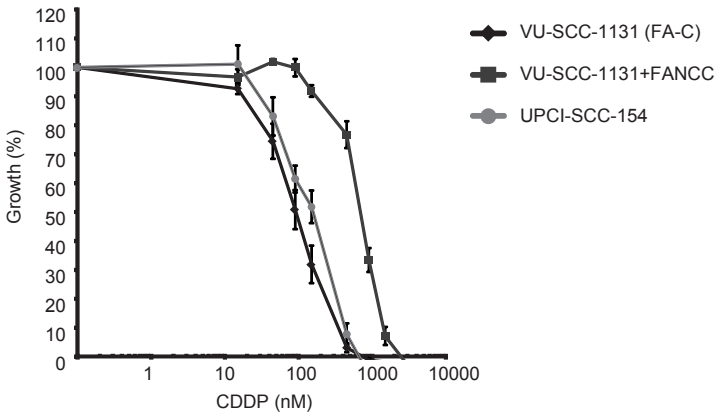

Supplementary Figure 5. Cell line UPCI-SCC-154 is sensitive to cisplatin.
FANCF-deficient cell line UPCI-SCC-154 and the control cell lines VU-SCC-1131 and VU-SCC-1131+FANCC were continuously exposed to increasing concentrations cisplatin (CDDP). After three population doublings of untreated cells, cell number for each CDDP concentration was determined using a Coulter counter. The data represent the percentage growth compared to untreated cells.

5

Right: Supplementary Figure 6. Cell line VU-SCC-41 is mutated in *PSC5A*.
(**A**) Analysis of PCR products from cDNA with primers spanning from exon 3 to 7 of the *PDS5A* gene, showing a shortened PCR product in VU-SCC-41, but not in normal fibroblasts of the same patient. (**B**) Analysis of the shorter cDNA with sanger sequencing revealed a deletion of exon 6 in VU-SCC-41 cells. (**C**) Sequencing of genomic DNA showed an inversion of a reverse compliment sequence including a duplication at the start of exon 6 in cell line VU-SCC-41. (**D**) Whole genome array comparative genomic hybridization (CGH) profiles of VU-SCC-41 compared to VU-41-F and VU-41-F compared to a pool of healthy controls. The X-axis represents the chromosomes and probes on the arrays ordered according to genomic locations, and the Y-axis the log2 ratios of the probes.

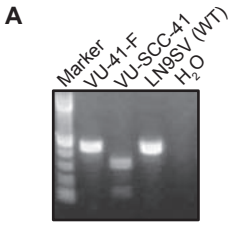
A
Marker
VU-41-F
VU-SCC-41
LN9SV (WT)
H2O

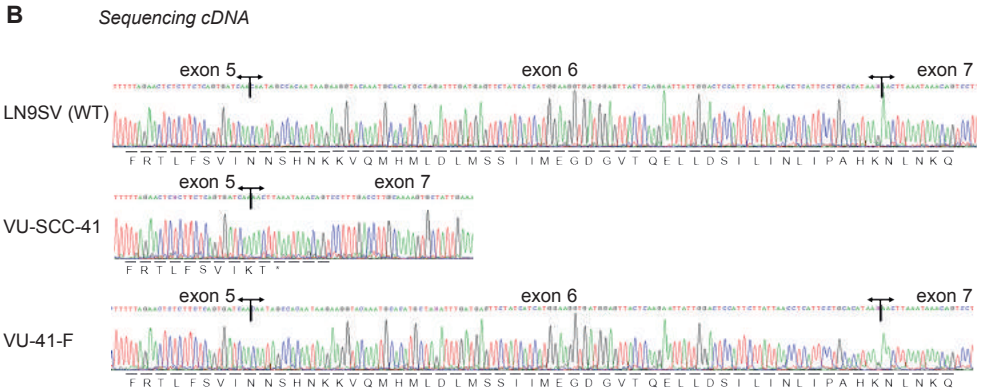
B
Sequencing cDNA
exon 5
exon 6
exon 7
LN9SV (WT)
F R T L F S V I N N S H N K K V Q M H M L D L M S S I I M E G D G V T Q E L L D S I L I N L I P A H K N L N K Q
exon 5
exon 7
VU-SCC-41
F R T L F S V I K T *
exon 5
exon 6
exon 7
VU-41-F
F R T L F S V I N N S H N K K V Q M H M L D L M S S I I M E G D G V T Q E L L D S I L I N L I P A H K N L N K Q


C
Sequencing genomic DNA
intron 5
exon 6
LN9SV (WT)
rev. complement rev. complement
VU-SCC-41
intron 5
exon 6
VU-41-F

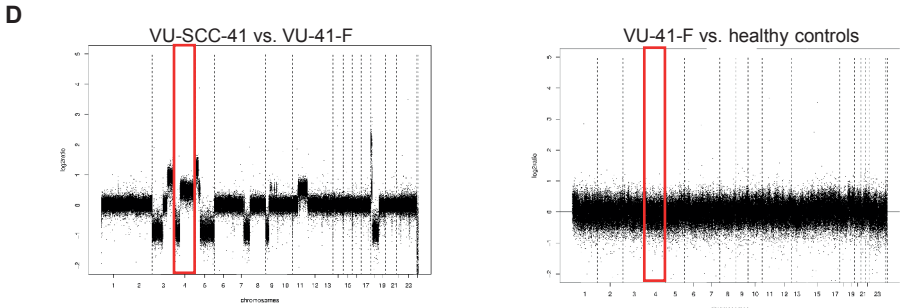
D
VU-SCC-41 vs. VU-41-F
VU-41-F vs. healthy controls

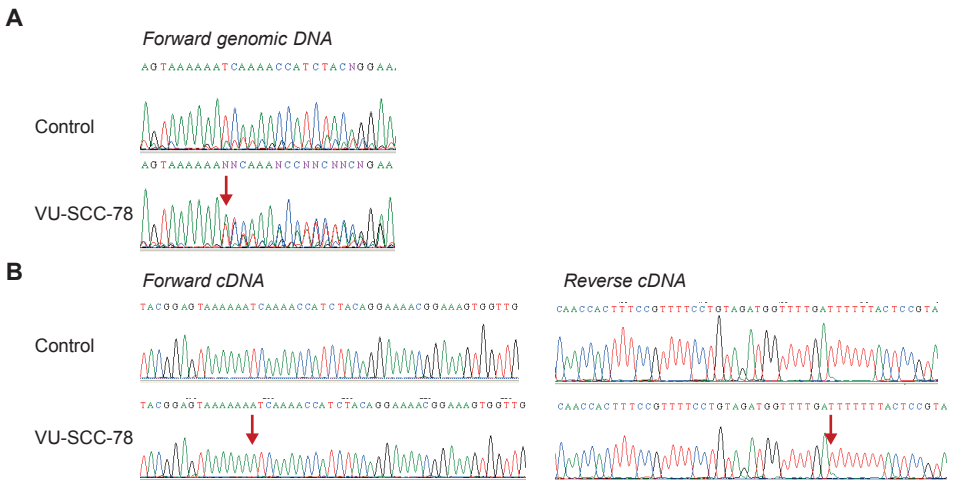

Supplementary Figure 7. Mutational inactivation of *STAG2* in cell line VU-SCC-78.
(**A**) Sequencing of genomic DNA of VU-SCC-78 cells revealed a heterozygous insertion of 1 base pair in *STAG2*. (**B**) Sequencing of cDNA demonstrated a homozygous 1 bp insertion, indication that *STAG2* mRNA expression was derived entirely from the mutant allele, whereas the wild type allele is probably inactivated by X chromosome inactivation.

Supplementary Table 1. Separate panel of 39 sporadic HNSCC cell lines

UT-SCC-10	UT-SCC-74A	UPCI-SCC-154	HN
UT-SCC-14	UT-SCC-76A	BICR16	BHY
UT-SCC-16A	UT-SCC-77	BICR56	HSC-3
UT-SCC-21	UT-SCC-87	SCC-4	HSC-4
UT-SCC-24A	UPCI-SCC-016	SCC-9	OSC-19
UT-SCC-30	UPCI-SCC-040	SCC-15	OSC-20
UT-SCC-37	UPCI-SCC-056	SCC-25	SAS
UT-SCC-40	UPCI-SCC-070	RPMI2650	SIHN-005A
UT-SCC-67	UPCI-SCC-103	CAL27	SIHN-006
UT-SCC-73	UPCI-SCC-122	CAL33	

For further information on these cell lines, see reference (52).

References

1. Lengauer C, Kinzler KW, Vogelstein B. Genetic instabilities in human cancers. Nature 1998;396:643–9.
2. Negrini S, Gorgoulis VG, Halazonetis TD. Genomic instability–an evolving hallmark of cancer. Nat Rev Mol Cell Biol 2010;11:220–8.
3. McGranahan N, Burrell RA, Endesfelder D, Novelli MR, Swanton C. Cancer chromosomal instability: therapeutic and diagnostic challenges. EMBO Rep 2012;13:528–38.
4. Auerbach AD. Fanconi anemia and its diagnosis. Mutat Res 2009;668: 4–10.
5. Kutler DI, Auerbach AD, Satagopan J, Giampietro PF, Batish SD, Huvos AG, *et al.* High incidence of head and neck squamous cell carcinoma in patients with Fanconi anemia. Arch Otolaryngol Head Neck Surg 2003;129: 106–12.
6. Kottemann MC, Smogorzewska A. Fanconi anaemia and the repair of Watson and Crick DNA crosslinks. Nature 2013;493:356–63.
7. Bogliolo M, Schuster B, Stoepker C, Derkunt B, Su Y, Raams A, *et al.* Mutations in ERCC4, encoding the DNA-repair endonuclease XPF, cause Fanconi anemia. Am J Hum Genet 2013;92:800–6.
8. Oostra AB, Nieuwint AWM, Joenje H, de Winter JP. Diagnosis of fanconi anemia: chromosomal breakage analysis. Anemia 2012;2012:238731.
9. Sasaki MS, Tonomura A. A high susceptibility of Fanconi's anemia to chromosome breakage by DNA cross-linking agents. Cancer Res 1973;33: 1829–36.
10. Auerbach AD, Wolman SR. Susceptibility of Fanconi's anaemia fibroblasts to chromosome damage by carcinogens. Nature 1976;261:494–6.
11. Langevin F, Crossan GP, Rosado IV, Arends MJ, Patel KJ. Fancd2 counteracts the toxic effects of naturally produced aldehydes in mice. Nature 2011; 475:53–8.
12. Van den Berg DJ, Francke U. Sensitivity of Roberts syndrome cells to gamma radiation, mitomycin C, and protein synthesis inhibitors. Somat Cell Mol Genet 1993;19:377–92.
13. Van der Lelij P, Chrzanowska KH, Godthelp BC, Rooimans MA, Oostra AB, Stumm M, *et al.* Warsaw breakage syndrome, a cohesinopathy associated with mutations in the XPD helicase family member DDX11/ChlR1. Am J Hum Genet 2010;86:262–6.
14. Van der Lelij P, Oostra AB, Rooimans MA, Joenje H, de Winter JP. Diagnostic overlap between fanconi anemia and the cohesinopathies: Roberts syndrome and warsaw breakage syndrome. Anemia 2010;2010: 565268.
15. Peters J-M, Nishiyama T. Sister chromatid cohesion. Cold Spring Harb Perspect Biol 2012;4: pii: a011130. doi.
16. Valeri A, Martínez S, Casado JA, Bueren JA. Fanconi anaemia: from a monogenic disease to sporadic cancer. Clin Transl Oncol 2011;13:215–21.
17. Marsit CJ, Liu M, Nelson HH, Posner M, Suzuki M, Kelsey KT. Inactivation of the Fanconi anemia/BRCA pathway in lung and oral cancers: implications for treatment and survival. Oncogene 2004;23:1000–4.
18. Ameziane N, Chen F, Leemans CR, Brakenhoff RH, Joenje H. No evidence for FANCF gene silencing in head-and-neck squamous cell carcinomas. Cell Oncol 2009;31:53–6.
19. Hermsen MA, Joenje H, Arwert F, Welters MJ, Braakhuis BJ, Bagnay M, *et al.* Centromeric breakage as a major cause of cytogenetic abnormalities in oral squamous cell carcinoma. Genes Chromosomes Cancer 1996;15:1–9.
20. Van Zeeburg HJT, Snijders PJF, Pals G, Hermsen MAJA, Rooimans MA, Bagby G, *et al.* Generation and molecular characterization of head and neck squamous cell lines of fanconi anemia patients. Cancer Res 2005; 65:1271–6.
21. Martens-de Kemp SR, Dalm SU, Wijnolts FMJ, Brink A, Honeywell RJ, Peters GJ, *et al.* DNA-bound platinum is the major determinant of cisplatin sensitivity in head and neck squamous carcinoma cells. PLoS One 2013;8: e61555.
22. Lin CJ, Grandis JR, Carey TE, Gollin SM, Whiteside TL, Koch WM, *et al.* Head and neck squamous cell carcinoma cell lines: established models and rationale for selection. Head Neck 2007;29:163–88.
23. Brenner JC, Graham MP, Kumar B, Saunders LM, Kupfer R, Lyons RH, *et al.* Genotyping of 73 UM-SCC head and neck squamous cell carcinoma cell lines. Head Neck 2010;32:417–26.
24. Wu Z, Doondeea JB, Gholami AM, Janning MC, Lemeer S, Kramer K, *et al.* Quantitative chemical proteomics reveals new potential drug targets in head and neck cancer. Mol Cell Proteomics 2011;10:M111.011635.
25. Hess CJ, Ameziane N, Schuurhuis GJ, Errami A, Denkers F, Kaspers GJL, *et al.* Hypermethylation of the FANCC and FANCL promoter regions in sporadic acute leukaemia. Cell Oncol 2008;30:299–306.
26. Knies K, Schuster B, Ameziane N, Rooimans M, Bettecken T, de Winter J, *et al.* Genotyping of fanconi anemia patients by whole exome sequencing: advantages and challenges. PLoS One 2012;7:e52648.

27. Solomon DA, Kim T, Diaz-Martinez LA, Fair J, Elkahloun AG, Harris BT, *et al.* Mutational inactivation of STAG2 causes aneuploidy in human cancer. Science 2011;333:1039–43.
28. Grenman R, Carey TE, McClatchey KD, Wagner JG, Pekkola-Heino K, Schwartz DR, *et al.* In vitro radiation resistance among cell lines established from patients with squamous cell carcinoma of the head and neck. Cancer 1991;67:2741–7.
29. Seow HA, Penketh PG, Baumann RP, Sartorelli AC. Bioactivation and resistance to mitomycin C. Methods Enzymol 2004;382:221–33.
30. Kelland L. The resurgence of platinum-based cancer chemotherapy. Nat Rev Cancer 2007;7:573–84.
31. Vega H, Waisfisz Q, Gordillo M, Sakai N, Yanagihara I, Yamada M, *et al.* Roberts syndrome is caused by mutations in ESCO2, a human homolog of yeast ECO1 that is essential for the establishment of sister chromatid cohesion. Nat Genet 2005;37:468–70.
32. Van Der Heijden MS, Brody JR, Kern SE. Functional screen of the fanconi anemia pathway in cancer cells by Fancd2 immunoblot. Cancer Biol Ther 2004;3:534–7.
33. Stransky N, Egloff AM, Tward AD, Kostic AD, Cibulskis K, Sivachenko A, *et al.* The mutational landscape of head and neck squamous cell carcinoma. Science 2011;333:1157–60.
34. Agrawal N, Frederick MJ, Pickering CR, Bettegowda C, Chang K, Li RJ, *et al.* Exome sequencing of head and neck squamous cell carcinoma reveals inactivating mutations in NOTCH1. Science 2011;333: 1154–7.
35. Leemans CR, Braakhuis BJM, Brakenhoff RH. The molecular biology of head and neck cancer. Nat Rev Cancer 2011;11:9–22.
36. Mazoyer S, Dunning AM, Serova O, Dearden J, Puget N, Healey CS, *et al.* A polymorphic stop codon in BRCA2. Nat Genet 1996;14:253–4.
37. Kuznetsov SG, Liu P, Sharan SK. Mouse embryonic stem cell-based functional assay to evaluate mutations in BRCA2. Nat Med 2008;14:875–81.
38. Bryant HE, Schultz N, Thomas HD, Parker KM, Flower D, Lopez E, *et al.* Specific killing of BRCA2-deficient tumours with inhibitors of poly(ADPribose) polymerase. Nature 2005;434:913–7.
39. Farmer H, McCabe N, Lord CJ, Tutt ANJ, Johnson DA, Richardson TB, *et al.* Targeting the DNA repair defect in BRCA mutant cells as a therapeutic strategy. Nature 2005;434:917–21.
40. Yuan SS, Lee SY, Chen G, Song M, Tomlinson GE, Lee EY. BRCA2 is required for ionizing radiation-induced assembly of Rad51 complex in vivo. Cancer Res 1999;59:3547–51.
41. Castella M, Pujol R, Callen E, Trujillo JP, Casado JA, Gille H, *et al.* Origin, functional role, and clinical impact of Fanconi anemia FANCA mutations. Blood 2011;117:3759–69.
42. Barber TD, McManus K, Yuen KWY, Reis M, Parmigiani G, Shen D, *et al.* Chromatid cohesion defects may underlie chromosome instability in human colorectal cancers. Proc Natl Acad Sci U S A 2008;105:3443–8.
43. Guo G, Sun X, Chen C, Wu S, Huang P, Li Z, *et al.* Whole-genome and whole-exome sequencing of bladder cancer identifies frequent alterations in genes involved in sister chromatid cohesion and segregation. Nat Genet 2013;45:1459–63.
44. Solomon DA, Kim J-S, Bondaruk J, Shariat SF, Wang Z-F, Elkahloun AG, *et al.* Frequent truncating mutations of STAG2 in bladder cancer. Nat Genet 2013;45:1428–30.
45. Kon A, Shih L-Y, Minamino M, Sanada M, Shiraishi Y, Nagata Y, *et al.* Recurrent mutations in multiple components of the cohesin complex in myeloid neoplasms. Nat Genet 2013;45:1232–7.
46. Thol F, Bollin R, Gehlhaar M, Walter C, Dugas M, Suchanek KJ, *et al.* Mutations in the cohesin complex in acute myeloid leukemia: clinical and prognostic implications. Blood 2014;123:914–20.
47. Van Harn T, Foijer F, van Vugt M, Banerjee R, Yang F, Oostra A, *et al.* Loss of Rb proteins causes genomic instability in the absence of mitogenic signaling. Genes Dev 2010;24:1377–88.
48. Manning AL, Longworth MS, Dyson NJ. Loss of pRB causes centromere dysfunction and chromosomal instability. Genes Dev 2010;24:1364–76.
49. Manning AL, Yazinski SA, Nicolay B, Bryll A, Zou L, Dyson NJ. Suppression of genome instability in pRB-deficient cells by enhancement of chromosome cohesion. Mol Cell 2014;53:993–1004.
50. Nagel R, Martens-de Kemp SR, Buijze M, Jacobs G, Braakhuis BJM, Brakenhoff RH. Treatment response of HPV-positive and HPV-negative head and neck squamous cell carcinoma cell lines. Oral Oncol 2013; 49:560–6.
51. Buffart,T.E., Israeli,D., Tijssen,M., Vosse,S.J., Mrsic,A., Meijer,G.A., and Ylstra,B. 2008. Across array comparative genomic hybridization: a strategy to reduce reference channel hybridizations. Genes Chromosomes. Cancer 47:994-1004.
52. Wu,Z., Doondeea,J.B., Gholami,A.M., Janning,M.C., Lemeer,S., Kramer,K., Eccles,S.A., Gollin,S.M., Grenman,R., Walch,A. *et al* 2011. Quantitative chemical proteomics reveals new potential drug targets in head and neck cancer. Mol. Cell Proteomics. 10:M111.

CHAPTER 6

DNA helicases FANCM and DDX11 are determinants of PARP inhibitor sensitivity

Chantal Stoepker, Atiq Faramarz, Martin A. Rooimans, Saskia E. van Mil, Jesper A. Balk, Eunike Velleuer, Najim Ameziane, Hein te Riele & Johan P. de Winter

Published in DNA Repair, 2015. 26:54-64.

The encouraging response rates of *BRCA1*- and *BRCA2*-mutated cancers toward PARP inhibitors make it worthwhile to identify other potential determinants of PARP inhibitor responsiveness. Since the Fanconi anemia (FA) pathway coordinates several DNA repair pathways, including homologous recombination in which BRCA1 and BRCA2 play important roles, we investigated whether this pathway harbors other predictors of PARP inhibitor sensitivity. Lymphoblastoid cell lines derived from individuals with FA or clinically related syndromes, such as Warsaw breakage syndrome, were tested for PARP inhibitor sensitivity. Remarkably, we found a strong variability in PARP inhibitor sensitivity among different FANCD1/BRCA2-deficient lymphoblasts, suggesting that PARP inhibitor response depends on the type of *FANCD1*/*BRCA2* mutation. We identified the DNA helicases FANCM and DDX11 as determinants of PARP inhibitor response. These results may extend the utility of PARP inhibition as effective anticancer treatment.

Introduction

Traditional cancer chemotherapy can cause severe side effects due to its aspecific action on normal cells[1]. One strategy to specifically kill cancer cells exploits the concept of synthetic lethality, in which simultaneous inactivation of two or more genes causes cell death, whereas inactivation of only one of these genes is tolerated[2–4]. Since tumor cells harbor genetic changes that are absent in normal cells, synthetic lethal targeting could be therapeutically advantageous. *E.g.*, inhibition of the abundant and extensively studied enzyme poly (ADP-ribose) polymerase 1 (PARP-1) that plays an important role in the repair of DNA single strand breaks (SSBs)[5,6], was found to be lethal in tumors with mutations in *BRCA1* or *BRCA2*[7,8]. These tumors are deficient in repairing DNA double strand breaks (DSBs) by homologous recombination (HR)[9,10]. Therefore, the initial model for the synthetic lethal interaction between BRCA deficiency and PARP inhibition hypothesized that continuous inhibition of PARP leads to unrepaired SSBs, which are converted to DSBs during S phase. These breaks are irreparable in BRCA-deficient cells, and consequently lead to apoptosis[7,8]. An alternative model proposed that PARP inhibitors trap PARP-1 onto DNA repair intermediates, causing replication fork blocking lesions, which require homologous recombination to be repaired[11–13]. PARP as well as HR proteins have an important role in reactivating stalled replication forks, which might also explain the observed PARP-BRCA synthetic lethality[12,14,15].

Given the promising response of BRCA-mutated breast and ovarian cancers to PARP inhibitors[4,16], it is of interest to identify additional determinants of PARP inhibitor sensitivity, thereby extending their utility in cancer therapy. Recently, PALB2-, RAD51C- and SLX4-deficiency have been coupled to PARP inhibitor

sensitivity[17–19]. Bi-allelic germ-line mutations in *BRCA2*, *PALB2* or *SLX4* cause Fanconi anemia (FA), a genomic instability syndrome characterized by congenital abnormalities, bone marrow failure and a high risk to develop cancer, whereas mutations in *RAD51C* lead to an FA-like syndrome[20–25]. To date, 16 FA proteins have been identified that act together in the FA pathway to repair DNA replication fork blocking lesions, such as DNA interstrand crosslinks[26,27]. FA proteins can be divided into two groups: the FA core complex consisting of FANCA, -B, -C, -E, -F, -G, -L and -M, which is required for the monoubiquitination of FANCD2-FANCI, and a group of proteins that function downstream or independently of this posttranslational modification (FANCD1/BRCA2, FANCJ/BRIP1, FANCN/PALB2, FANCO/RAD51C, FANCP/SLX4 and FANCQ/XPF). Although FANCM is part of the FA core complex, it may also function outside the FA pathway to stabilize or re-initiate stalled replication forks[28]. In the present study, we used lymphoblasts and head and neck tumor cell lines from FA patients to investigate whether and to which extent deficiency in FA proteins confers PARP inhibitor sensitivity. In addition, lymphoblasts of individuals with cohesinopathies (*e.g.*, Roberts syndrome and Warsaw breakage syndrome, which have some diagnostic overlap with FA) were tested for sensitivity to PARP inhibition.

Results

PARP inhibitor sensitivity depends on the type of BRCA2 mutation

Complementation group D1 of the genomic instability syndrome Fanconi anemia (FA) was found to be caused by bi-allelic mutations in the well-known breast cancer susceptibility gene *BRCA2*[20]. Since BRCA2-deficient breast cancer cells are hypersensitive to PARP inhibitors[7,8], we examined whether BRCA2-deficient EBV-immortalized lymphoblastoid cell lines derived from FA-D1 patients are also sensitive to PARP inhibition. None of the wild type lymphoblasts was sensitive to the PARP inhibitor Olaparib (KU0058948), as compared to BRCA2-deficient EUFA423 lymphoblasts (**Fig. 1A**). Remarkably, there was a large difference in IC50 values between different BRCA2-defective lymphoblastoid cell lines: EUFA943 lymphoblasts were the most sensitive with an IC50 value of 4.0 ± 0.8 nM, whereas HSC62 cells were only marginally sensitive (IC50 356.6 ± 30.0 nM) (**Fig. 1B**). These cell lines were also the most and least sensitive, respectively, to other DNA damaging agents, such as mitomycin C (MMC) (**Fig. 1C**) or camptothecin (**Fig. 1D**). Hence, in these cell lines, PARP inhibitor sensitivity was correlated with MMC and camptothecin sensitivity. To elucidate why some BRCA2-deficient lymphoblasts were more sensitive to PARP inhibitor than others, BRCA2 expression and RAD51 focus formation were investigated (for an overview of all data see **Fig. 1G**).

Table 1

Cell line	Gender	Mutated Gene	Mutation 1 *Predicted protein change*	Mutation 2 *Predicted protein change*	Ref.
HSC93	?	Wild type	na	na	-
MAN-EBV	M	Wild type	na	na	-
RUFA-EBV	M	Wild type	na	na	-
VU012-L	M	Wild type	na	na	-
EUFA689-L	F	*FANCA*	c.3788_3790del	c.3788_3790del	[29]
			p.Phe1263del	*p.Phe1263del*	
HSC72OT	?	*FANCA*	Deletion exon 18-28	Deletion exon 18-28	[30]
			p.?	*p.?*	
HSC230	M	*FANCB*[a]	c.1856_1857insT	-	[31]
			*p.Arg619Serfs*39*		
		FANCD1	c.2808_2811del	c.9976A>T	[20]
		(/BRCA2)	*p.Ala938Profs*21*	*p.Lys3326**	
EUFA178-L	M	*FANCB*[a]	Deletion promoter_exon 1	-	[31]
			No protein		
EUFA1386-L	M	*FANCB*[a]	c.829dup	-	[31]
			*p.Cys277Leufs*31*		
EUFA158-L	F	*FANCC*	c.67del (also known as 322delG)	c.67del (also known as 322delG)	[32]
			*p.Asp23Ilefs*23*	*p.Asp23Ilefs*23*	
EUFA1289-L	M	*FANCD2*	c.206-2A>T	c.1414-71_1545+256del459	[33]
			*p.Ala69Aspfs*7*	*p.Glu472_Lys515del*	
EUFA816-L	M	*FANCI*	c.3853C>T	c.3350-88A>G	[34]
			*p.Arg1285**	*p.Glu1117fs*	

Table 1 continued

EUFA868-L	F	*FANCL*	c.837-15_837-9delins177	c.837-15_837-9delins177	[35]
			p.?	*p.?*	
EUFA867-L	F	*FANCM*	c.2171C>A	c.4222+1978_4300del	[36]
			*p.Ser724**	*p.?*	
		FANCA	c.2557C>T	c.709+5G>A	[37]
			*p.Arg853**	*p.?*	
HSC62	M	*FANCD1*	c.8488-1G>A	c.8488-1G>A	[20]
		(/BRCA2)	*p.Trp2830_Lys2833del*	*p.Trp2830_Lys2833del*	
EUFA208-L	F	*FANCD1*	c.7878G>C	c.756_757del	Current study
		(/BRCA2)	*p.Trp2626Cys*	*p.Asp252Glufs*2*	
EUFA423-L	F	*FANCD1*	c.7463_7464insAT	c.9672dup	[20]
		(/BRCA2)	*p.Asp2489**	*p.Tyr3225Ilefs*30*	
EUFA579-L	F	*FANCD1*	c.7007G>A	5609_5610delinsAG	[20]
		(/BRCA2)	*p.?*	*p.Phe1870**	
EUFA932-L	M	*FANCD1*	c.2957dup	c.7684T>C	Current study
		(/BRCA2)	*p.Asn986Lysfs*2*	*p.Phe2562Leu*	
EUFA943-L	M	*FANCD1*	c.480_489del	c.480_489del	Current study
		(/BRCA2)	*p.Gly162Phefs*7*	*p.Gly162Phefs*7*	
EUFA1389-L	F	*FANCD1*	c.1597del	Deletion exon 15-16	Current study
		(BRCA2)	*p.Thr533Leufs*25*	*p.?*	
EUFA696-L	F	*FANCJ*	c.2392C>T	c.2492+2dup	[38]
		(/BRIP1)	*p.Arg798**	*p.?*	
EUFA1341-L	F	*FANCN*	c.1653T>A	Deletion exon 1-10	[21]
		(/PALB2)	*p.Tyr551**	*p.?*	

Table 1 continued

EUFA1354-L	M	*FANCP*	c.286del	c.286del	[24]
		(/SLX4)	*p.Thr96Leufs*30*	*p.Thr96Leufs*30*	
FA104	F	*FANCQ*	c.1484_1488del	c.2065C>A	[27]
		(/XPF)	*p.Thr495Asnfs*6*	*p.Arg689Ser*	
VU1177-L	F	*ESCO2*	c.1111dup	c.1111dup	[39]
			*p.Thr371Asnfs*32*	*p.Thr371Asnfs*32*	
VU1199-L	M	*ESCO2*	c.879_880del	c.879_880del	[39]
			*p.Arg293Serfs*7*	*p.Arg293Serfs*7*	
VU1202-L	M	*DDX11*	c.2689_2691del	c.2271+2T>C	[40]
			p. Lys897del	*p.?*	
CdLS11165	M	*NIPBL*[b]	c.3813_3815del	-	[41]
			p.Lys1271del		
CdLS11167	F	*NIPBL*[b]	c.3940dup	-	[41]
			*p.Thr1314Asnfs*9*		
EUFA1341F SV40	F	*FANCN*	c.1653T>A	Deletion exon 1-10	[21]
		(/PALB2)	*p.Tyr551**	*p.?*	
VU1199F SV40	M	*ESCO2*	c.879_880del	c.879_880del	[39]
			*p.Arg293Serfs*7*	*p.Arg293Serfs*7*	
VU-SCC-1131	F	*FANCC*	c.67del (also known as 322delG)	c.67del (also known as 322delG)	[42]
			*p.Asp23Ilefs*23*	*p.Asp23Ilefs*23*	
VU-SCC-1365	M	*FANCA*	c.3788-3790del	c.3788-3790del	[42]
			p. Phe1263del	*p.Phe1263del*	
VU-SCC-1604	F	*FANCL*	c.483_487del	c.906C>G	Current study
			*p.Glu161Aspfs*31*	*p.Ile302Met*	

Legend Table 1
[a] X-linked inheritance, [b] autosomal dominant inheritance. Na = not applicable, F = female, M = male. All lymphoblastoid cell lines and fibroblasts were EBV- or SV40-immortalized, respectively. The following transcript reference sequences were used: *FANCA* NM_000135.2; *FANCB* NM_001018113.1; *FANCC* NM_000136.2; *FANCD1/BRCA2* NM_000059.3; *FANCD2* NM_001018115.1; *FANCI* NM_001113378.1; *FANCL* NM_001114636.1; *FANCM* NM_020937.2; *BRIP1/FANCJ* NM_032043.2; *PALB2/FANCN* NM_024675.3; *SLX4/FANCP* NM_032444.2; *XPF/FANCQ* NM_005236.2; *ESCO2* NM_001017420.2; *DDX11* NM_030653.3 and *NIPBL* NM_015384.4.

Previously, Howlett *et al.*[20] demonstrated that EUFA423 and HSC62 cells express a truncated BRCA2 protein, which we clearly confirmed for EUFA423 cells (**Fig. 1E**). The distinction between normal size or truncated BRCA2 protein is difficult to visualize with Western blotting for HSC62 cells, because this cell line expresses BRCA2 protein with an in-frame deletion of only 4 amino acids. BRCA2 expression was not or hardly observed in three highly sensitive cell lines (EUFA943- L, EUFA579-L and EUFA1389-L), however, in another sensitive cell line, EUFA208-L, BRCA2 protein of approximately normal size was detected. The absence of BRCA2 protein expression can be explained by a frameshift mutation (c.1597del) and a large deletion of exon 15–16 in EUFA1389 cells, a homozygous frameshift mutation (c.480-489del) in EUFA943 cells and a splice site (c.7007G >A) and nonsense mutation (c.5609_5610delinsAG) in EUFA579 cells (see **Table 1** and **Fig. 1G** for an overview of mutations present in our panel of cell lines). In EUFA208 and in EUFA932 cells, one frameshift and one missense mutation in BRCA2 were found. The missense mutations were both present in the BRCA2 helical domain, which interacts with SHFM1/DSS1[43,44]. This interaction is important for homologous recombination and hence contributes to genomic stability[45,46]. Despite the fact that both cell lines expressed BRCA2, EUFA208 cells (IC50 7.2 ± 2.1 nM) were more sensitive to PARP inhibitor than EUFA932 cells (IC50 121.8 ± 71.8 nM). BRCA2 recruits RAD51 to double strand breaks to mediate homologous recombination[47,48]. To assess if HR repair activity was affected in FA-D1 lymphoblasts expressing mutant BRCA2 protein, MMC-induced RAD51 nuclear focus formation was analyzed by immunofluorescence as an indirect marker of HR. Upon treatment with MMC, RAD51 focus formation was only unambiguously observed in wild type HSC93 lymphoblasts and in the least sensitive HSC62 cells (**Fig. 1G**), suggesting that the mutant BRCA2 protein in HSC62 has partial activity. The mild phenotype of HSC62 cells was also reflected in the clinical characteristics of the FA patient of whom this cell line was derived. Although this patient scored positive in the chromosomal breakage assay and had the classical thumb abnormalities, he had not developed bone marrow failure or cancer at the age of 30, while the majority of FA patients with biallelic mutations in *BRCA2* has a severe phenotype with early onset bone marrow failure and high incidence of childhood solid cancers[20,49, 50]. These results indicate that although all *BRCA2* mutations conferred the FA phenotype, PARP inhibitor sensitivity depends on the type of *BRCA2* mutation and the level of BRCA2 inactivation.

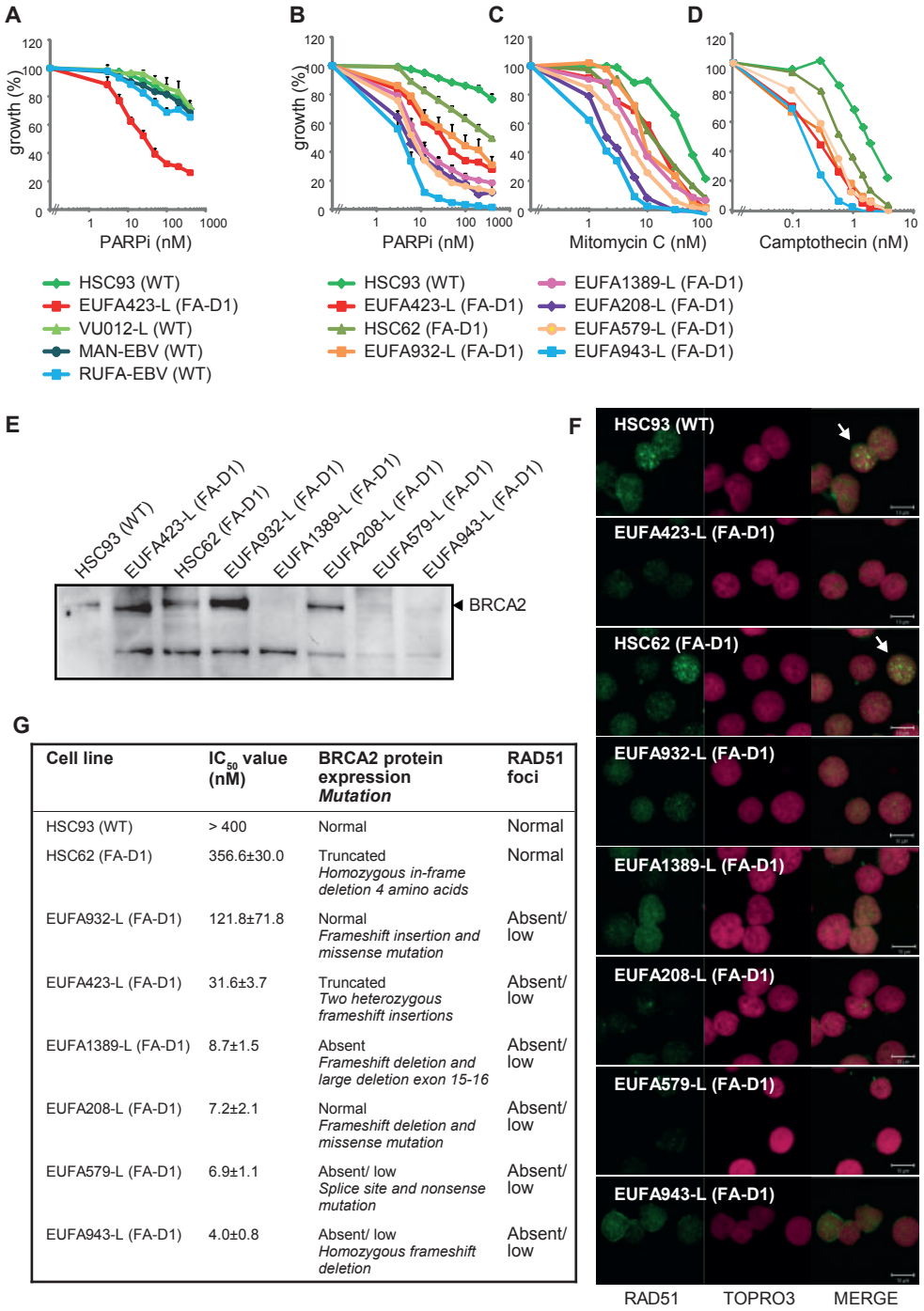

G

Cell line	IC_{50} value (nM)	BRCA2 protein expression *Mutation*	RAD51 foci
HSC93 (WT)	> 400	Normal	Normal
HSC62 (FA-D1)	356.6±30.0	Truncated *Homozygous in-frame deletion 4 amino acids*	Normal
EUFA932-L (FA-D1)	121.8±71.8	Normal *Frameshift insertion and missense mutation*	Absent/ low
EUFA423-L (FA-D1)	31.6±3.7	Truncated *Two heterozygous frameshift insertions*	Absent/ low
EUFA1389-L (FA-D1)	8.7±1.5	Absent *Frameshift deletion and large deletion exon 15-16*	Absent/ low
EUFA208-L (FA-D1)	7.2±2.1	Normal *Frameshift deletion and missense mutation*	Absent/ low
EUFA579-L (FA-D1)	6.9±1.1	Absent/ low *Splice site and nonsense mutation*	Absent/ low
EUFA943-L (FA-D1)	4.0±0.8	Absent/ low *Homozygous frameshift deletion*	Absent/ low

Figure 1. Variety in PARP inhibitor sensitivity due to different mutations in *BRCA2*.
(**A**) Different EBV-immortalized wild type lymphoblasts are resistant to PARP inhibitor (PARPi), whereas the indicated BRCA2-mutant lymphoblasts (FA-D1) derived from FA patients are sensitive (**B**). PARP

inhibitor sensitivity of BRCA2-mutant lymphoblasts is correlated with mitomycin C (**C**) and camptothecin (**D**) sensitivity. Lymphoblasts were continuously exposed to different concentrations PARP inhibitor (0–400 nM), mitomycin C (0–100 nM) or camptothecin (0–4 nM). After three population doublings of untreated cells, cell number for each drug concentration was determined using a Coulter counter. The data represent the percentage growth compared to untreated cells. The error bars show standard error ofthe mean of at least 3 independent experiments. (**E**) Western blot analysis showing BRCA2 protein expression in BRCA2-mutant lymphoblasts. (**F**) RAD51 foci (green and indicated by arrows) are evidently present in the control cell line HSC93 and the BRCA2-deficient cell line HSC62 upon mitomycin C treatment, but absent in the other BRCA2-defective lymphoblasts. Cell lines were treated with 100 nM MMC for 24 h. TOPRO3 was used as a nuclear counterstaining. (**G**) An overview of IC50 values (nM), BRCA2 protein expression and RAD51 focus formation of BRCA2-mutant lymphoblasts, showing a wide variety in PARP inhibitor sensitivity.

FA lymphoblasts with mutations in FANCM are hypersensitive to PARP inhibitor

A panel of FA lymphoblastoid cell lines with mutations in FA genes other than *BRCA2* (**Table 1**) was also tested for PARP inhibitor sensitivity. FA proteins can be divided into two groups: a subset that is essential for FANCD2-FANCI monoubiquitination and a group of proteins that function downstream of this posttranslational modification[26]. Lymphoblasts with mutations in the genes *FANCA*, *FANCB*, *FANCC* and *FANCL*, which encode proteins required for FANCD2-FANCI monoubiquitination, as well as those deficient in FANCD2 and FANCI, had IC50 values above 400 nM and were therefore classified as PARP inhibitor resistant (**Fig. 2A**). Among these resistant cell lines, there was one cell line (HSC230) derived from a FA patient who was classified to complementation group FA-B by cell fusion and the presence of a *FANCB* mutation[31]. However, HSC230 cells also contained two *BRCA2* variants: a deleterious frameshift mutation (c.2808_2811del) and a nonsense mutation (p.Lys3326*)[20]. This latter variant is known as a polymorphic stop and was found in >1% of normal individuals[51]. HSC230 cells were not sensitive to PARP inhibition, indicating that neither FANCB-deficiency nor the polymorphic stop in *BRCA2* conferred sensitivity to PARP inhibitor and that the resulting truncated BRCA2 protein was able to repair PARP inhibitor induced DNA damage.

Lymphoblasts with mutations in the genes *FANCJ*, *FANCQ*/*XPF* or *FANCP*/*SLX4*, which function downstream of FANCD2-FANCI monoubiquitination, were also not particularly sensitive. In contrast, lymphoblastoid cell lines with a defect in *FANCM* (EUFA867-L) or *FANCN*/*PALB2* (EUFA1341-L) were hypersensitive to PARP inhibition with IC50 values of 41.0 ± 1.9 and 2.5 ± 0.3 nM PARP inhibitor, respectively (**Fig. 2B**). In addition to bi-allelic *FANCM* mutations, EUFA867-L cells also have bi-allelic mutations in *FANCA*[37]. To investigate whether PARP inhibitor sensitivity was solely due to FANCM-deficiency, EUFA867 lymphoblasts stably expressing FANCA were tested for PARP inhibitor responsiveness. As shown in **Fig. 2C**, overexpression of FANCA in EUFA867 cells did not restore PARP inhibitor resistance, indicating that FANCA did not affect sensitivity to PARP inhibitor. This was further strengthened by the PARP inhibitor resistant phenotype in the FANCA-deficient lymphoblastoid cell lines EUFA689-L and HSC72OT (**Fig. 2A and C**).

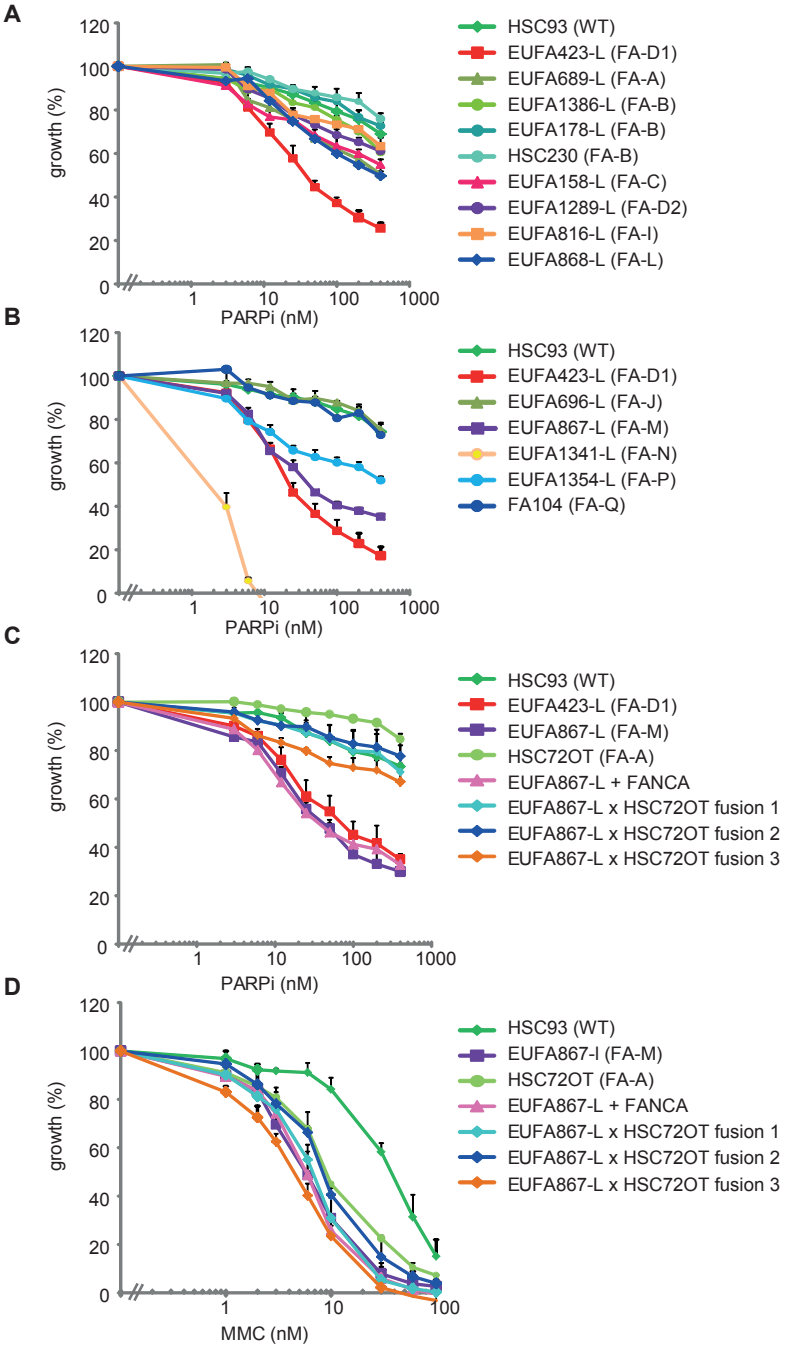

Figure 2. FANCN- and FANCM-deficient lymphoblasts are PARP inhibitor sensitive.
Lymphoblasts with mutations in genes encoding upstream FA proteins necessary for FANCD2 monoubiquitination are not sensitive to PARP inhibitor (PARPi) (**A**), whereas mutations in *FANCN* (EUFA1341-L) and *FANCM* (EUFA867-L) cause PARP inhibitor sensitivity (**B**). Lymphoblasts were continuously exposed to PARP inhibitor and cell growth was determined by counting after untreated cells

had reached at least three population doublings. The data represent mean ± S.E.M. (standard error of the mean) of 2 or 3 independent experiments. Different cell growth inhibition assays were combined into one graph. For each assay, HSC93 and BRCA2-deficient EUFA423 cells were used as controls. (**C**) EUFA867 lymphoblasts stably expressing wild type FANCA are still sensitive to PARP inhibitor, whereas correction of FANCM- but not FANCA-deficiency by cell fusion of EUFA867-L with HSC72OT cells (EUFA867-L × HSC72OT fusion 1–3) restores PARP inhibitor resistance. HSC93 and BRCA2-deficient EUFA423 cells were used as controls. (**D**) Overexpression of FANCA in EUFA867 or correction of FANCM by cell fusions did not rescue MMC sensitivity.

Moreover, cell fusion of FANCM- and FANCA-deficient EUFA867 lymphoblasts with FANCA-deficient HSC72OT lymphoblasts (EUFA867-L × HSC72OT fusion 1–3), in which FANCM- but not FANCA-deficiency was corrected, resulted in PARP inhibitor resistance, whereas MMC sensitivity remained (**Fig. 2D**). These results demonstrate that FANCM deficiency was responsible for the observed sensitivity to PARP inhibitor and that FANCM has a role in the cellular defense against PARP inhibitor.

DDX11 is a determinant of PARP inhibitor responsiveness

FA patients are diagnosed by performing the widely used chromosomal breakage test: upon treatment with MMC, FA deficient cells exhibit a significant increase in chromosomal breaks. However, MMC-induced chromosomal breakage has also been observed in other syndromes, such as Roberts syndrome and Warsaw breakage syndrome, and misdiagnosis may occur[52]. Since a subset of FA cells was sensitive to PARP inhibitors, we also tested lymphoblastoid cell lines derived from Roberts and Warsaw breakage syndrome patients for PARP inhibitor sensitivity. These syndromes together with Cornelia de Lange syndrome are characterized by defects in sister chromatid cohesion and therefore termed cohesinopathies[40,53]. As shown in **Fig. 3A**, lymphoblasts from individuals with Roberts (VU1177-L and VU1199-L) or Cornelia de Lange syndrome (CdLS11165 and CdLS11167) were resistant to PARP inhibitors. Interestingly, lymphoblasts from a Warsaw breakage syndrome patient (VU1202-L) with bi-allelic mutations in *DDX11* were almost as sensitive to PARP inhibitors as the BRCA2-deficient cell line EUFA423-L (**Fig. 3B**). This PARP inhibitor sensitivity phenotype was rescued by introducing *DDX11* cDNA intoVU1202 lymphoblasts, showing that DDX11 is important for cellular protection against PARP inhibitors.

Increased G2/M accumulation and chromosomal breakage in PARP inhibitor sensitive cells

We have used patient-derived lymphoblastoid cell lines to show that besides BRCA2 and PALB2, FANCM and DDX11 are determinants of PARP inhibitor responsiveness. Since FA-deficient cells treated with ICL-inducing agents arrest in the G2/M phase of the cell cycle and exhibit increased chromosomal breakage, we performed cell

cycle analysis and the chromosomal breakage test to investigate whether a similar cellular phenotype ensues from treatment with PARP inhibitor (**Fig. 4A and B**). BRCA2-, FANCM- and DDX11-deficient cells showed a PARP inhibitor induced increase in sub-G1 (<2N) and G2 (4N) content, indicating increased apoptosis and arrest in the G2/M phase of the cell cycle, respectively (**Fig. 4A**). This increase was lower in wild type cells (HSC93) and PARP inhibitor resistant FANCA-deficient cells (HSC72OT). However, a clearly increased number of chromosomal breaks was only observed in the BRCA2-deficient lymphoblastoid cell line EUFA423-L (**Fig. 4B**). After treatment with PARP inhibitor, 49% of EUFA423 cells contained one or more breaks, whereas this percentage was 6 and 20% in wild type and PARP inhibitor resistant FANCA-defective cells, respectively. In the PARP inhibitor sensitive cell lines EUFA867 and VU1202, breaks occurred in 28% and 26% of cells, respectively, which is more than in wild-type cells (6%) but similar to PARP inhibitor resistant FANCA-defective cells (20%). One model of the synthetic lethal interaction between PARP inhibition and HR deficiency hypothesized that PARP inhibition eventually leads to irreparable DNA double strand breaks[7,8]. Our data indicate that this model may explain PARP inhibitor sensitivity of BRCA2-deficient cells but not of FANCM- or DDX11-defective cells.

RAD51 focus formation and epistatic relationships in FANCM- and DDX11-deficient lymphoblasts

BRCA2 and PALB2 are directly involved in homologous recombination and cells that lack these proteins do not show RAD51 foci[21,48,54]. Therefore, RAD51 focus formation may be a biomarker for PARP inhibitor response. To investigate this possibility, RAD51 focus formation was analyzed in FANCM- and DDX11-deficient lymphoblasts. As shown in **Fig. 4C**, both lymphoblastoid cell lines as well as the control cell line HSC93 were able to form RAD51 foci upon treatment with mitomycin C. In contrast, the BRCA2-deficient cell line EUFA579 lacked RAD51 foci. These results indicate that RAD51 focus formation cannot be used as a general biomarker for PARP inhibitor response. This data might suggest that BRCA2, FANCM and DDX11 function in different pathways in the defense against PARP inhibitor induced damage. To investigate this further, we transfected SV40-immortalized wild type fibroblasts with siRNAs against BRCA2, FANCM and/or DDX11 (**Fig. 4D**). Knockdown of BRCA2, DDX11 or FANCM in wild type fibroblasts resulted in PARP inhibitor sensitization, thereby further confirming that these proteins are determinants of PARP inhibitor response. Knockdown of BRCA2 further increased PARP inhibitor sensitivity of FANCM knockdown cells and also, albeit to a lesser extent, of DDX11 knockdown cells. However, fibroblasts transfected with siRNAs targeting both *FANCM* and *DDX11* were as sensitive to PARP inhibition as siDDX11-transfected cells alone, indicating that DDX11-deficiency is epistatic with FANCM-

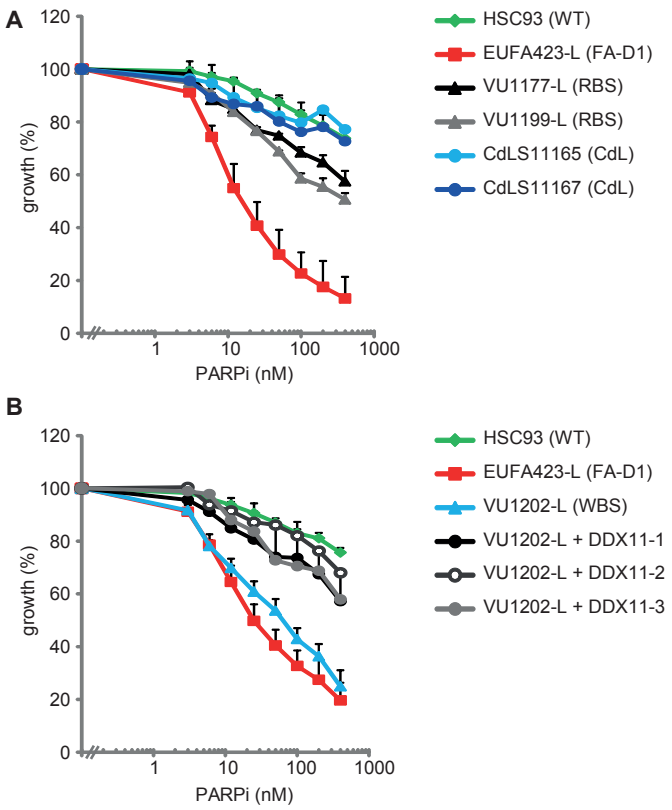

Figure 3. DDX11-deficient lymphoblasts are sensitive to PARP inhibitor.
(**A**) Lymphoblasts derived from individuals with Roberts syndrome (RBS) or Cornelia de Lange (CdL) syndrome with mutations in *ESCO2* or *NIPBL*, respectively, are resistant to PARP inhibitor (PARPi). (**B**) Warsaw Breakage syndrome (WBS) patient-derived lymphoblasts (VU1202-L) with bi-allelic mutations in *DDX11* are PARP inhibitor sensitive. The sensitive phenotype of VU1202 cells was restored by introducing *DDX11* cDNA. Wild type (HSC93) and BRCA2-deficient (EUFA423-L) lymphoblasts were used as controls. Multiple experiments were combined to one graph. The data represent the mean and standard error of the mean of at least 2 experiments, except for VU1202-L + DDX11-2 and 3.

deficiency. Taken together, these data suggest that FANCM and DDX11 function in the same pathway, whereas BRCA2 acts in another pathway to prevent PARP inhibitor induced DNA damage.

FA head and neck tumor cell lines are not particularly sensitive to PARP inhibitor

FA patients have an extremely high risk to develop tumors of the head and neck region. Treatment of these patients is complicated because of the hypersensitivity of FA cells to chemotherapeutic drugs and novel treatment options are urgently awaited. Since defects in upstream FA genes did not confer PARP inhibitor sensitivity in normal lymphoblastoid cell lines (see Section "*FA lymphoblasts with mutations in FANCM are hypersensitive to PARP inhibitor*"), we tested PARP inhibitor responsiveness in three FA head and neck cancer cell lines (VU-SCC-1131 (FA-C), VU-SCC-1365 (FA-A) and VU-SCC- 1604 (FA-L)). These tumor cell lines were sensitive to MMC (**Fig. 5A**) and cisplatin (CDDP) (**Fig. 5B**), a hallmark of FA cells. As expected, FANCD2 monoubiquitination (**Fig. 5C**) and focus formation (**Fig. 5D**) were absent, because these cell lines have mutations in upstream FA genes. Functional correction of these cell lines made them 10- fold more resistant to MMC and CDDP and restored the

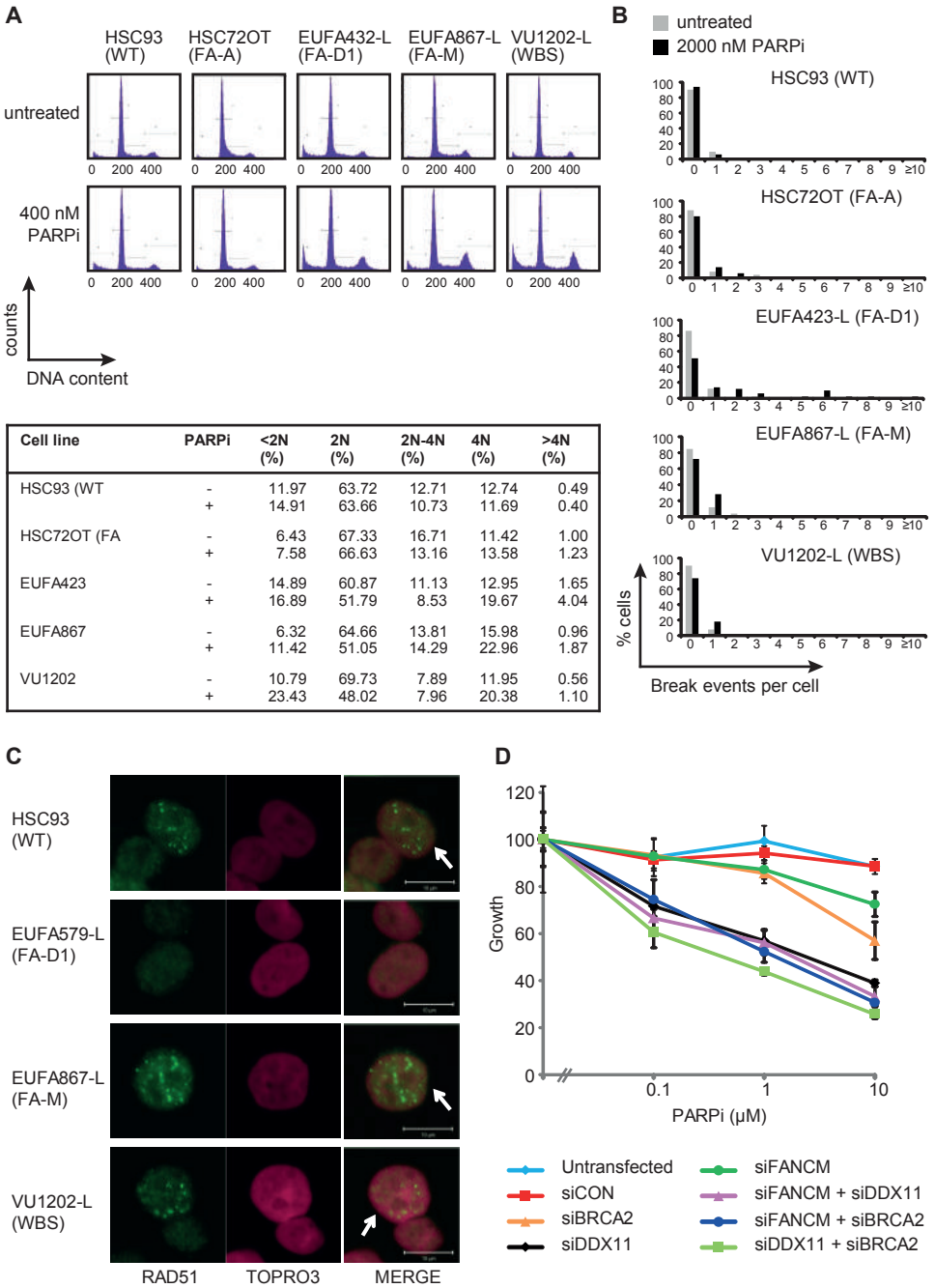

Cell line	PARPi	<2N (%)	2N (%)	2N-4N (%)	4N (%)	>4N (%)
HSC93 (WT	-	11.97	63.72	12.71	12.74	0.49
	+	14.91	63.66	10.73	11.69	0.40
HSC72OT (FA	-	6.43	67.33	16.71	11.42	1.00
	+	7.58	66.63	13.16	13.58	1.23
EUFA423	-	14.89	60.87	11.13	12.95	1.65
	+	16.89	51.79	8.53	19.67	4.04
EUFA867	-	6.32	64.66	13.81	15.98	0.96
	+	11.42	51.05	14.29	22.96	1.87
VU1202	-	10.79	69.73	7.89	11.95	0.56
	+	23.43	48.02	7.96	20.38	1.10

Figure 4. Cell cycle analysis, chromosomal breakage and RAD51 focus formation in PARP inhibitor sensitive cell lines.

(**A**) BRCA2-, FANCM- and DDX11-deficient lymphoblasts have increased sub-G1 (<2N) and (G2/M (4N) population of cells upon PARP inhibitor treatment. (**B**) Chromosomal breakage in untreated and PARP inhibited EUFA423 (FA-D1), EUFA867 (FA-M) and VU1202 (WBS) lymphoblasts. (**C**) RAD51 focus

formation upon mitomycin C treatment in FANCM- and DDX11-deficient lymphoblasts. Representative images of RAD51 foci (green and indicated by arrows) are shown in FANCM-(EUFA857-L) and DDX11-(VU1202-L) deficient cells. HSC93 (wild type) and BRCA2-deficient EUFA579 cells were used as controls. Cells were treated with 100 nM MMC, fixed after 24 h and stained with anti-RAD51. Nuclei were visualized with TOPRO3. (**D**) SV40- immortalized fibroblasts (Fen5280SV) were transfected with the indicated siRNAs and treated with increasing concentrations of PARP inhibitor. Untransfected and siCON (non-targeting)-transfected cells were used as negative controls.

ability to monoubiquitinate FANCD2 and to form FANCD2 foci (**Fig. 5A–D**). In contrast, FA-A and FA-C cell lines were not PARP inhibitor sensitive and functional correction did not affect PARP inhibitor responsiveness. Although, FANCL-deficient VU-SCC-1604 cells appeared slightly more sensitive to PARP inhibitor than the corrected VUSCC-1604 cells and the FA-A and FA-C cell lines, the sensitivity was not as profound as in PALB2-deficient fibroblasts (**Fig. 5E**). Our data demonstrate that defects in upstream FA genes in normal lymphoblasts as well as in HNSCC cells do not confer hypersensitivity to PARP inhibitor. Since most FA patients belong to upstream FA-complementation groups, PARP inhibition is likely to be unsuccessful in the treatment of FA head and neck cancer. However, this therapy might be successful in non-FA patients with tumors containing mutations in genes that determine PARP inhibitor sensitivity, such as *BRCA2*, *DDX11* or *FANCM*.

Discussion

In an effort to find determinants of PARP inhibitor sensitivity, we investigated whether defects in FA proteins other than BRCA2 are synthetic lethal with PARP inhibition. Using lymphoblastoid cell lines from individuals with FA or clinically related syndromes, we identified FANCM and DDX11 as determinants of PARP inhibitor responsiveness. Furthermore, we show that the response to PARP inhibitors of BRCA2-mutant cells depends on the type of mutation.

In our study we primarily used EBV-immortalized lymphoblastoid cell lines with different genetic defects. This allowed a detailed analysis of the role of different proteins in the response to PARP inhibitors within one specific cell type. In these lymphoblasts, the major determinants of PARP inhibitor sensitivity were the homologous recombination proteins BRCA2 and PALB2, but also the DNA helicases FANCM and DDX11. FA core complex proteins as well as FANCI and FANCD2 appeared to be dispensable for PARP inhibitor tolerance. Consistent with our results, HPV E6 and E7 immortalized fibroblasts established from FA patients with mutations in the FA genes FANCA, FANCD2, FANCI or FANCL were not sensitive to PARP inhibitor KU0058948 (ref 19). However, DT40 cells deficient in FANCC, FANCD2 or FANCG and mouse embryonic fibroblasts lacking *Fanca*, *Fancc* or *Fancd2* were sensitive to the same PARP inhibitor, suggesting a species- and/or cell-culture-specific requirement for the FA core complex in conferring PARP inhibitor resistance[13,55].

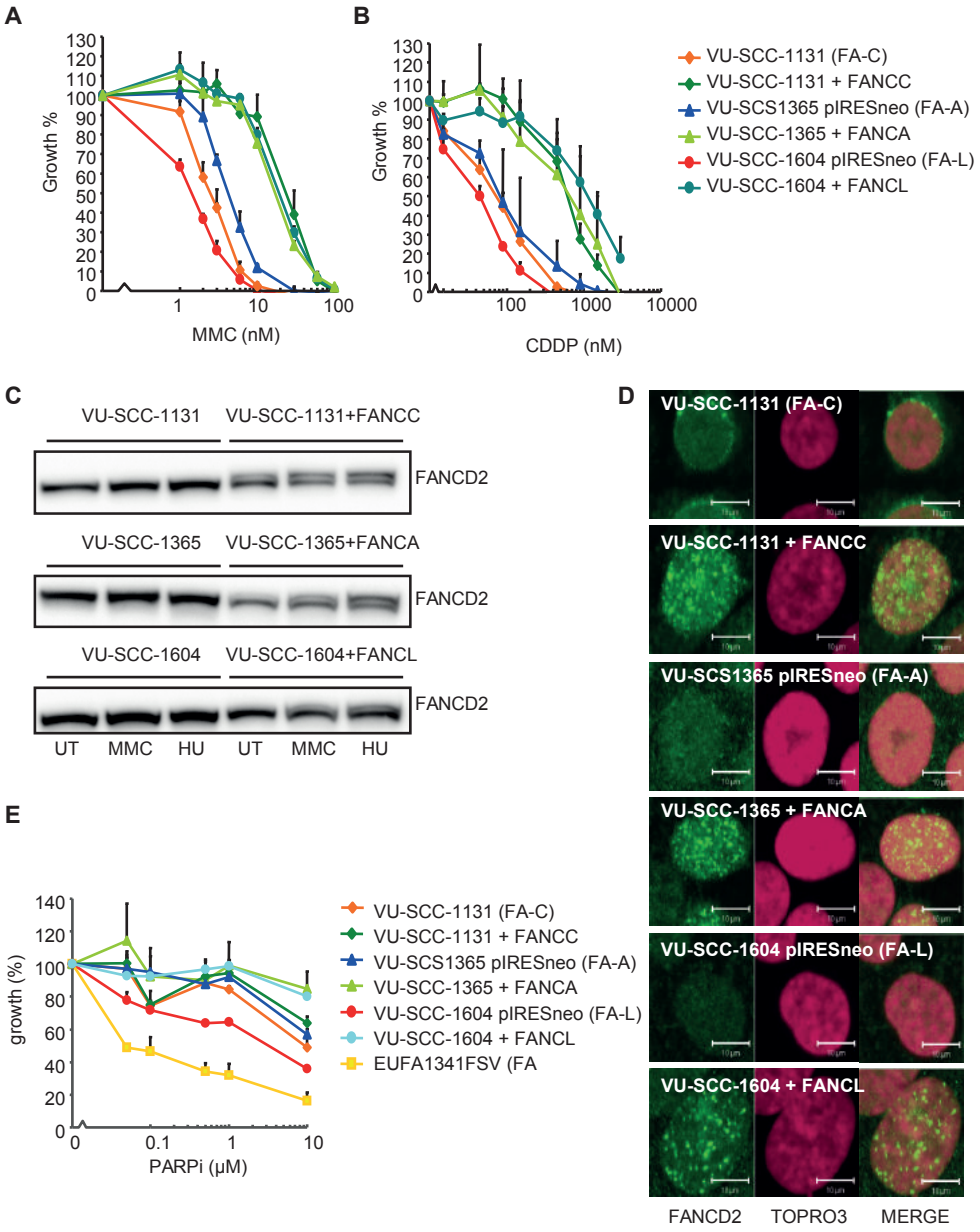

Figure 5. Upstream FA pathway defects do not affect sensitivity to PARP inhibitors in HNSCC cell lines.

Head and neck tumor cell lines (VU-SCC-1131 (FANCC-deficient), VUSCC-1365 (FANCA-deficient) and VU-SCC-1604 (FANCL-deficient)) derived from FA patients are hypersensitive to mitomycin C (MMC) (**A**) and cisplatin (CDDP) (**B**). Functional correction of these cell lines makes them 10-fold more resistant to these agents. VU-SCC-1365 and VU-SCC-1604 were transfected with an empty pIRESneo construct. The data represent mean ± S.E.M. (standard error of the mean) of three independent experiments. FA-deficient head and neck tumor cell lines lack FANCD2 monoubiquitination (**C**) and focus formation (**D**), which is restored after functional complementation. Western blot analysis was used to determine

FANCD2 monoubiquitination of untreated (UT), MMC-(200 nM) or hydroxyurea (HU) treated cells. Representative images of MMC-induced FANCD2 foci (green) are shown. Nuclei were visualized by TOPRO3. (**E**) PARP inhibitor (PARPi) response in FA tumor cell lines. The data represent mean ± S.E.M. of three independent experiments. For the cell growth inhibition assays, cells were continuously exposed to different concentrations PARP inhibitor, MMC or CDDP. Cell growth was compared to untreated cells and determined by counting cell number or colonies.

Several of our observations indicate that increased double strand break formation combined with defective homology directed break repair may explain PARP inhibitor sensitivity in BRCA2-defective cells but not in FANCM- or DDX11-defective cells. (1) Although RAD51 focus formation has been suggested as a biomarker to identify tumors that will respond to PARP inhibition, we have demonstrated here that PARP inhibitor sensitive FANCM and DDX11-deficient lymphoblasts were still able to form RAD51 foci. Therefore, RAD51 focus formation may be a relevant marker for BRCA2-deficient tumors, but not for PARP inhibitor sensitivity in general. (2) Double-strand break formation following PARP inhibition was strongly increased in BRCA2-deficient cells, but not in FANCM or DDX11-defective cells. Together with normal RAD51 focus formation, this suggests that double-strand breaks induced by PARP inhibition were effectively repaired in FANCM- or DDX11- defective cells. (3) Knockdown of BRCA2 reduced cell survival in FANCM or DDX11 knockdown cells whereas FANCM knockdown did not reduce survival of DDX11 knockdown cells. Taken together, these results indicate that different mechanisms exist for PARP inhibitor sensitivity in BRCA2-defective cells on the one side and FANCM- or DDX11-defective cells on the other.

The PARP inhibitor sensitivity of FANCM and DDX11-defective cells may be related to DNA replication, since recent studies demonstrated that PARP inhibitors not only caused DNA breaks but also formed replication fork blocking lesions[11–13]. In this respect, PARP inhibitors resemble topoisomerase inhibitors like camptothecin[56,57]. Interestingly, the cell lines that were PARP inhibitor sensitive were also sensitive to camptothecin, indicating that failure of repairing replication fork blocking lesions contributes to cytotoxicity. PARP and HR proteins as well as FANCM play important roles in restarting stalled replication forks[14,15,58]. FANCM is a multifunctional protein that not only recruits the FA core complex to stalled replication forks but also the Bloom's syndrome complex[59]. Besides an important role in ensuring replisome stability in S phase, FANCM is also involved in checkpoint activation upon damage[28,60,61]. Errors in DNA damage cell cycle checkpoints and in bypass of replication-blocking lesions might lead to PARP inhibitor sensitivity[62]. Therefore, it is possible that replisome instability and checkpoint defects due to FANCM deficiency both contribute to PARP inhibitor sensitivity.

Problems with replication fork maintenance may also underlie the observed PARP inhibitor sensitivity in DDX11-deficient cells. DDX11 is involved in the establishment of sister chromatid cohesion, which occurs in a replication dependent manner during

S phase[63]. The replication fork protection (RFP) complex, consisting of Timeless and Tipin, can interact and stabilize DDX11, leading to stable association of the cohesion complex with chromatin[64]. Moreover, DDX11 interacts with and enhances the activity of FEN1, a flap endonuclease involved in lagging-strand DNA synthesis[65]. Depletion of FEN1 also leads to cohesion defects and FEN1-deficient DT40 cells are sensitive to PARP inhibitor[13,65]. These results suggests that lagging-strand synthesis might be important for sister chromatid cohesion. Defective sister chromatid cohesion due to DDX11-deficiency might interfere with bypass of replication blocking lesions caused by PARP inhibitor.

By investigating PARP inhibitor sensitivity in the setting of patient derived lymphoblastoid cell lines, we could demonstrate the importance of examining PARP inhibitor sensitivity in the context of truncating mutations instead of reduced protein levels by using RNA interference. Depending on the mutation in *BRCA2*, mutant cells were more or less sensitive to PARP inhibition or to other DNA damaging agents, such as mitomycin C or camptothecin. Consistent with this observation, a previous report[19] showed variations in PARP inhibitor sensitivity depending on the type of *SLX4* mutation. SLX4 seems to play an important role in repairing PARP inhibitor induced damage via the interactions with MUS81 and to a lesser extent with SLX1[19]. EUFA1354 lymphoblasts with bi-allelic mutations in *SLX4* were not particularly sensitive to PARP inhibition. This cell line expresses a truncated SLX4 protein that is able to interact with MUS81 and SLX1[24] and therefore, might be less sensitive to PARP inhibitor. Thus, PARP inhibitor response may vary due to different underlying mutations in *BRCA2* or *SLX4*.

In summary, FANCM and DDX11 were newly identified as determinants of PARP inhibitor sensitivity. Since *FANCM* and *DDX11* mutations occur in tumors (COSMIC database), these results suggest that PARP inhibition might be a valuable anti-cancer approach not only for BRCA-associated cancers but also for other tumors. However, caution is necessary because PARP inhibitor sensitivity might dependent on the kind of mutation.

Materials and methods

Cell culture

For an overview of all cell lines used in this study see **Table 1**. Epstein–Barr virus (EBV)-transformed lymphoblasts were cultured in RPMI1640 medium supplemented with 10% fetal bovine serum (FBS) and sodium pyruvate (1 mM). Fibroblasts immortalized with SV40 large T antigen and head and neck squamous carcinoma cell lines were grown in DMEM supplemented with 10% FBS and 1 mM sodium pyruvate. Stable cell lines: EUFA867- L + FANCA, EUFA867 × HSC72OT fusion 1–3 and VU1202-L + DDX11 clones 1–3 were previously generated[37,40]. VU-SCC-1131 cells were functionally corrected by transduction with a phoenix retroviral construct containing FANCC-GFP and selected on puromycin dihydrochloride (P8833, 1 g/ml, Sigma). VU-SCC-1365 and VUSCC-1604 cell lines stably expressing FANCA or FANCL, respectively, were generated by transfection with a pIRESneo construct containing cDNAs encoding FANCA-flag or flag-FANCL and selected on 400 g/ml G418 sulfate (Calbiochem).

Cell growth inhibition assays
PARP inhibitor (KU0058948), cisplatin (CDDP), camptothecin and mitomycin C (MMC)-induced growth inhibition assays were performed as previously described[66]. In brief, cells were seeded in multiple flasks with increasing concentrations of the indicated drug. After untreated cells made 3 population doublings, the relative cell number compared to untreated cells for each drug concentration was determined using a Coulter counter.

Western blot analysis
For preparation of whole-cell extracts, cells were lysed for 10 min in lysis buffer (50 mM Tris–HCl (pH 7.4), 150 mM NaCl and 1% Triton X-100 supplemented with protease (cOmplete EDTA free tablets, Roche) and phosphatase inhibitors (PhosSTOP, Roche)). Proteins were separated on a 3–8% Tris–Acetate NuPAGE gradient gel (Invitrogen) and transferred to Immobilon-P membrane overnight. The membrane was blocked with 5% dry milk in TBST (10 mM Tris–HCl (pH 7.4), 150 mM NaCl, 0.05% Tween-20) and incubated with the indicated primary antibodies. After washing with TBST, the membrane was incubated with horseradish peroxidase-conjugated secondary antibody and proteins were visualized with ECL (GE Healthcare). The following primary antibodies were used: rabbit polyclonal anti-BRCA2 (1:1000, A303-434A, Bethyl Laboratories) and mouse monoclonal anti-FANCD2 (1:500, FI17, sc-20022, Santa Cruz Biotechnologies).

Immunofluorescence
Wild type, BRCA2-, DDX11- or FANCM-deficient lymphoblasts were treated with 100 nM MMC for 16 h and dropped onto Squarix Immunoselect® adhesion slides (Squarix biotechnology) in PBS. Immortalized fibroblasts and head and neck tumor cell lines were grown on sterile chamber slides (Nunc) and treated with 200 nM MMC for 16 h. Cells were pre-permeabilized with 0.25% Triton X- 100 inPBS (1 minonice)prior tofixation with4%paraformaldehyde for 15 min at room temperature. Cells were permeabilized with 0.5% Triton X-100 in PBS (20 min at room temperature). Unspecific binding sites were blocked by incubating with 10% FBS in PBS for 1 h at room temperature. Slides were then incubated with rabbit anti-RAD51 (1:1000, a gift from Dr. R. Kanaar) overnight at 4 ◦C or with rabbit polyclonal anti-FANCD2 (1:200, NB100-182, Novus Biologicals) for 2 h at room temperature and washed with 0.2% Triton X-100. Subsequently, slides were incubated with goat anti-rabbit ALEXA488 (1:500, A-11008, Invitrogen) for 2 h at room temperature. After excess antibody was removed by washing with 0.2% Triton X-100, cells were counterstained with TO-PRO®-3 iodide (1:500, T3605,Invitrogen,for 15 minat roomtemperature), washed with PBS and embedded. Slides were analyzed with a confocal microscope (Carl Zeiss).

BRCA2 sequencing
The presence of BRCA2 mutations was examined by direct Sanger sequencing of the entire coding region and intron–exon boundaries on genomic DNA isolated from EBV-immortalized lymphoblasts. Primer pairs that were used are available on request.

Cell cycle analysis
Lymphoblasts were untreated or exposed for 7 days to PARP inhibitor (400 nM) and permeabilized in buffer containing 100 mM Tris–HCl (pH 7.5), 150 mM NaCl, 0.5 mM MgCl2, 1 mM CaCl2, 0.2% BSA and 0.1% IGEPAL (CA-630, Sigma). DNA was stained with PI/RNase staining buffer (BD Pharmingen) for 15 min and analyzed by flow cytometry.

Chromosomal breakage assay
Lymphoblasts were cultured for 48 h in the absence or presence of 2000 nM PARP inhibitor. After treatment with 200 ng/ml demecolcin (Sigma) for 30 min, cells were harvested, treated with 0.075 M KCl for 20 min at room temperature and fixed with 75% methanol, 25% acetic acid. Subsequently, cells were dropped onto glass slides and stained with 5% Giemsa (Merck). For each cell culture, 50 metaphases were analyzed for chromosomal breakage events. All scoring was performed on coded slides to prevent counting bias.

siRNA knockdown of BRCA2, DDX11 and FANCM in wild type fibroblasts
SV40-immortalized fibroblasts (Fen5280 SV) plated in 96-well plates were reverse transfected with siRNAs (final concentration 25 nM) targeting BRCA2, DDX11 and/or FANCM using Lipofectamine

RNAiMAX (Invitrogen) according to the manufacturer's protocol. Non-targeting siCONTROL#2 (siCON) (Dharmacon) was used as a negative control. Twenty-four hours following transfection, increasing concentrations of PARP inhibitor were added. After 5 days, cell viability was determined by the CellTiter-Blue assay (Promega).

Acknowledgements
We thank Roland Kanaar for providing the RAD51 antibody; Roelie van der Willik for help in BRCA2 Western blotting and Rob M. Wolthuis and Ruud H. Brakenhoff for helpful discussions and comments. We acknowledge financial support from Cancer Center Amsterdam (CCA) and Fanconi Anemia Research Fund (FARF), Portland, OR, U.S.A.

Conflicts of interest statement
The authors declare that there are no conflicts of interest.

References

1. S. Hellman, E.E. Vokes, Advancing current treatments for cancer, Sci. Am. 275 (1996) 118–123.
2. L.H. Hartwell, P. Szankasi, C.J. Roberts, A.W. Murray, S.H. Friend, Integrating genetic approaches into the discovery of anticancer drugs, Science 278 (1997) 1064–1068.
3. W.G. Kaelin Jr., The concept of synthetic lethality in the context of anticancer therapy, Nat. Rev. Cancer 5 (2005) 689–698.
4. D.A. Chan, A.J. Giaccia, Harnessing synthetic lethal interactions in anticancer drug discovery, Nat. Rev. Drug Discov. 10 (2011) 351–364.
5. M.J. Menissier-de, M. Molinete, G. Gradwohl, F. Simonin, G. de Murcia, Zincbinding domain of poly(ADP-ribose)polymerase participates in the recognition of single strand breaks on DNA, J. Mol. Biol. 210 (1989) 229–233.
6. V. Schreiber, F. Dantzer, J.C. Ame, G. de Murcia, Poly(ADP-ribose): novel functions for an old molecule, Nat. Rev. Mol. Cell Biol. 7 (2006) 517–528.
7. H.E. Bryant, N. Schultz, H.D. Thomas, K.M. Parker, D. Flower, E. Lopez, S. Kyle, M. Meuth, N.J. Curtin, T. Helleday, Specific killing of BRCA2-deficient tumours with inhibitors of poly(ADP-ribose) polymerase, Nature 434 (2005) 913–917.
8. H. Farmer, N. McCabe, C.J. Lord, A.N. Tutt, D.A. Johnson, T.B. Richardson, M. Santarosa, K.J. Dillon, I. Hickson, C. Knights, N.M. Martin, S.P. Jackson, G.C. Smith, A. Ashworth, Targeting the DNA repair defect in BRCA mutant cells as a therapeutic strategy, Nature 434 (2005) 917–921.
9. M.E. Moynahan, J.W. Chiu, B.H. Koller, M. Jasin, Brca1 controls homologydirected DNA repair, Mol. Cell 4 (1999) 511–518.
10. M.E. Moynahan, A.J. Pierce, M. Jasin, BRCA2 is required for homology-directed repair of chromosomal breaks, Mol. Cell 7 (2001) 263–272.
11. C.E. Strom, F. Johansson, M. Uhlen, C.A. Szigyarto, K. Erixon, T. Helleday, Poly (ADP-ribose) polymerase (PARP) is not involved in base excision repair but PARP inhibition traps a single-strand intermediate, NucleicAcids Res. 39 (2011) 3166–3175.
12. T. Helleday, The underlying mechanism for the PARP and BRCA synthetic lethality: clearing up the misunderstandings, Mol. Oncol. 5 (2011) 387–393.
13. J. Murai, S.Y. Huang, B.B. Das, A. Renaud, Y. Zhang, J.H. Doroshow, J. Ji, S. Takeda, Y. Pommier, Trapping of PARP1 and PARP2 by clinical PARP inhibitors, Cancer Res. 72 (2012) 5588–5599.
14. H.E. Bryant, E. Petermann, N. Schultz, A.S. Jemth, O. Loseva, N. Issaeva, F. Johansson, S. Fernandez, P. McGlynn, T. Helleday, PARP is activated at stalled forks to mediate Mre11-dependent replication restart and recombination, EMBO J. 28 (2009) 2601–2615.
15. Y.G. Yang, U. Cortes, S. Patnaik, M. Jasin, Z.Q. Wang, Ablation of PARP-1 does not interfere with the repair of DNA double-strand breaks, but compromises the reactivation of stalled replication forks, Oncogene 23 (2004) 3872–3882.
16. P.C. Fong, D.S. Boss, T.A. Yap, A. Tutt, P. Wu, M. Mergui-Roelvink, P. Mortimer, H. Swaisland, A. Lau, M.J. O'Connor, A. Ashworth, J. Carmichael, S.B. Kaye, J.H. Schellens, J.S.de Bono, Inhibition of poly(ADP-ribose) polymerase in tumors from BRCA mutation carriers, N. Engl. J. Med. 361 (2009) 123–134.
17. R. Buisson, A.M. Dion-Cote, Y. Coulombe, H. Launay, H. Cai, A.Z. Stasiak, A. Stasiak, B. Xia, J.Y. Masson, Cooperation of breast cancer proteins PALB2 and piccolo BRCA2 in stimulating homologous recombination, Nat. Struct. Mol. Biol. 17 (2010) 1247–1254.
18. A. Min, S.A. Im, Y.K. Yoon, S.H. Song, H.J. Nam, H.S. Hur, H.P. Kim, K.H. Lee, S.W. Han, D.Y. Oh, T.Y. Kim, M.J. O'Connor, W.H. Kim, Y.J. Bang, RAD51C-deficient cancer cells are highly sensitive to the PARP inhibitor olaparib, Mol. Cancer Ther. 12 (2013) 865–877.
19. Y. Kim, G.S. Spitz, U. Veturi, F.P. Lach, A.D. Auerbach, A. Smogorzewska, Regulation of multiple DNA repair pathways by the Fanconi anemia protein SLX4, Blood 121 (2013) 54–63.
20. N.G. Howlett, T. Taniguchi, S. Olson, B. Cox, Q. Waisfisz, C. De Die-Smulders, N. Persky, M. Grompe, H. Joenje, G. Pals, H. Ikeda, E.A. Fox, A.D. D'Andrea, Biallelic inactivation of BRCA2 in Fanconi anemia, Science 297 (2002) 606–609.
21. B. Xia, J.C. Dorsman, N. Ameziane, V.Y. de, M.A. Rooimans, Q. Sheng, G. Pals, A. Errami, E. Gluckman, J. Llera,W.Wang, D.M. Livingston, H. Joenje, J.P. deWinter, Fanconi anemia is associated with a defect in the BRCA2 partner PALB2, Nat. Genet. 39 (2007) 159–161.
22. S. Reid, D. Schindler, H. Hanenberg, K. Barker, S. Hanks, R. Kalb, K. Neveling, P. Kelly, S. Seal, M. Freund, M. Wurm, S.D. Batish, F.P. Lach, S. Yetgin, H. Neitzel, H. Ariffin, M. Tischkowitz, C.G. Mathew, A.D. Auerbach, N. Rahman, Biallelic mutations in PALB2 cause Fanconi anemia subtype FA-N and predispose to childhood cancer, Nat. Genet. 39 (2007) 162–164.
23. Y. Kim, F.P. Lach, R. Desetty, H. Hanenberg, A.D. Auerbach, A. Smogorzewska, Mutations of the SLX4 gene in Fanconi anemia, Nat. Genet. 43 (2011) 142–146.
24. C. Stoepker, K. Hain, B. Schuster, Y. Hilhorst-Hofstee, M.A. Rooimans, J. Steltenpool, A.B. Oostra, K. Eirich, E.T. Korthof, A.W. Nieuwint, N.G. Jaspers, T. Bettecken, H. Joenje, D. Schindler, J. Rouse, J.P. de Winter, SLX4, a coordinator of structure-specific endonucleases, is mutated in a

new Fanconi anemia subtype, Nat. Genet. 43 (2011) 138–141.
25. F. Vaz, H. Hanenberg, B. Schuster, K. Barker, C. Wiek, V. Erven, K. Neveling, D. Endt, I. Kesterton, F. Autore, F. Fraternali, M. Freund, L. Hartmann, D. Grimwade, R.G. Roberts, H. Schaal, S. Mohammed, N. Rahman, D. Schindler, C.G. Mathew, Mutation of the RAD51C gene in a Fanconi anemia-like disorder, Nat. Genet. 42 (2010) 406–409.
26. M.C. Kottemann, A. Smogorzewska, Fanconi anaemia and the repair of Watson and Crick DNA crosslinks, Nature 493 (2013) 356–363.
27. M. Bogliolo, B. Schuster, C. Stoepker, B. Derkunt, Y. Su, A. Raams, J.P. Trujillo, J. Minguillon,M.J. Ramirez, R. Pujol,J.A. Casado, R. Banos, P. Rio,K.Knies, S. Zuniga, J. Benitez, J.A. Bueren, N.G. Jaspers, O.D. Scharer, J.P. de Winter, D. Schindler, J. Surralles, Mutations in ERCC4, encoding the DNA-repair endonuclease XPF, cause Fanconi anemia, Am. J. Hum. Genet. 92 (2013) 800–806.
28. R.A. Schwab, A.N. Blackford,W. Niedzwiedz, ATR activation and replication fork restart are defective in FANCM-deficient cells, EMBO J. 29 (2010) 806–818.
29. M. Wijker, N.V. Morgan, S. Herterich, C.G. van Berkel, A.J. Tipping, H.J. Gross, J.J. Gille, G. Pals, M. Savino, C. Altay, S. Mohan, I. Dokal, J. Cavenagh, J. Marsh, W.M. van, J.J. Ortega, D. Schuler, E. Samochatova, M. Karwacki, A.N. Bekassy, M. Abecasis, W. Ebell, M.L. Kwee, R.T. de, C.G. Mathew, Heterogeneous spectrum of mutations in the Fanconi anaemia group A gene, Eur. J. Hum. Genet. 7 (1999) 52–59.
30. H. Joenje, M. Levitus, Q. Waisfisz, A. D'Andrea, I. Garcia-Higuera, T. Pearson, C.G. van Berkel, M.A. Rooimans, N. Morgan, C.G. Mathew, F. Arwert, Complementation analysis in Fanconi anemia: assignment of the reference FA-H patient to group A, Am. J. Hum. Genet. 67 (2000) 759–762.
31. A.R. Meetei, M. Levitus, Y. Xue, A.L. Medhurst, M. Zwaan, C. Ling, M.A. Rooimans, P. Bier, M. Hoatlin, G. Pals, J.P. de Winter, W. Wang, H. Joenje, X-linked inheritance of Fanconi anemia complementation group B, Nat. Genet. 36 (2004) 1219–1224.
32. J.P. de Winter, L. van der Weel, G.J. de, S. Stone, Q. Waisfisz, F. Arwert, R.J. Scheper, F.A. Kruyt, M.E. Hoatlin, H. Joenje, The Fanconi anemia protein FANCF forms a nuclear complex with FANCA, FANCC and FANCG, Hum. Mol. Genet. 9 (2000) 2665–2674.
33. R. Kalb, K. Neveling, H. Hoehn, H. Schneider, Y. Linka, S.D. Batish, C. Hunt, M. Berwick, E. Callen, J. Surralles, J.A. Casado, J. Bueren, A. Dasi, J. Soulier, E. Gluckman, C.M. Zwaan, S.R. van, G. Pals, J.P. de Winter, H. Joenje, M. Grompe, A.D. Auerbach, H. Hanenberg, D. Schindler, Hypomorphic mutations in the gene encoding a key Fanconi anemia protein, FANCD2, sustain a significant group of FA-D2 patients with severe phenotype, Am. J. Hum. Genet. 80 (2007) 895–910.
34. J.C. Dorsman, M. Levitus, D. Rockx, M.A. Rooimans, A.B. Oostra, A. Haitjema, S.T. Bakker, J. Steltenpool, D. Schuler, S. Mohan, D. Schindler, F. Arwert, G. Pals, C.G. Mathew, Q. Waisfisz, J.P. de Winter, H. Joenje, Identification of the Fanconi anemia complementation group I gene, FANCI, Cell. Oncol. 29 (2007) 211–218.
35. A.R. Meetei, J.P. de Winter, A.L. Medhurst, M. Wallisch, Q. Waisfisz, H.J. van de Vrugt, A.B. Oostra, Z. Yan, C. Ling, C.E. Bishop, M.E. Hoatlin, H. Joenje, W. Wang, A novel ubiquitin ligase is deficient in Fanconi anemia, Nat. Genet. 35 (2003) 165–170.
36. A.R. Meetei, A.L. Medhurst, C. Ling, Y. Xue, T.R. Singh, P. Bier, J. Steltenpool, S. Stone, I. Dokal, C.G. Mathew, M. Hoatlin, H. Joenje, J.P. de Winter, W. Wang, A human ortholog of archaeal DNA repair protein Hef is defective in Fanconi anemia complementation group M, Nat. Genet. 37 (2005) 958–963. 64 C. Stoepker et al. / DNA Repair 26 (2015) 54–64
37. T.R. Singh, S.T. Bakker, S. Agarwal, M. Jansen, E. Grassman, B.C. Godthelp, A.M. Ali, C.H. Du, M.A. Rooimans, Q. Fan, K. Wahengbam, J. Steltenpool, P.R. Andreassen, D.A. Williams, H. Joenje, J.P. de Winter, A.R. Meetei, Impaired FANCD2 monoubiquitination and hypersensitivity to camptothecin uniquely characterize Fanconi anemia complementation group M, Blood 114 (2009) 174–180.
38. M. Levitus, Q. Waisfisz, B.C. Godthelp, V.Y. de, S. Hussain, W.W. Wiegant, E. Elghalbzouri-Maghrani, J. Steltenpool, M.A. Rooimans, G. Pals, F. Arwert, C.G. Mathew, M.Z. Zdzienicka, K. Hiom, J.P. de Winter, H. Joenje, The DNA helicase BRIP1 is defective in Fanconi anemia complementation group J, Nat. Genet. 37 (2005) 934–935.
39. H. Vega, Q. Waisfisz, M. Gordillo, N. Sakai, I. Yanagihara, M. Yamada, G.D. van, H. Kayserili, C. Xu, K. Ozono, E.W. Jabs, K. Inui, H. Joenje, Roberts syndrome is caused by mutations in ESCO2, a human homolog of yeast ECO1 that is essential for the establishment of sister chromatid cohesion, Nat. Genet. 37 (2005) 468–470.
40. P. van der Lelij, K.H. Chrzanowska, B.C. Godthelp, M.A. Rooimans, A.B. Oostra, M. Stumm, M.Z. Zdzienicka, H. Joenje, J.P. de Winter, Warsaw breakage syndrome, a cohesinopathy associated with mutations in the XPD helicase family member DDX11/ChlR1, Am. J. Hum. Genet. 86 (2010) 262–266.

41. M.G. Vrouwe, E. Elghalbzouri-Maghrani, M. Meijers, P. Schouten, B.C. Godthelp, Z.A. Bhuiyan, E.J. Redeker, M.M. Mannens, L.H. Mullenders, A. Pastink, F. Darroudi, Increased DNA damage sensitivity of Cornelia de Lange syndrome cells: evidence for impaired recombinational repair, Hum. Mol. Genet. 16 (2007) 1478–1487.
42. H.J. van Zeeburg, P.J. Snijders, G. Pals, M.A. Hermsen, M.A. Rooimans, G. Bagby, J. Soulier, E. Gluckman, J. Wennerberg, C.R. Leemans, H. Joenje, R.H. Brakenhoff, Generation and molecular characterization of head and neck squamous cell lines of fanconi anemia patients, Cancer Res. 65 (2005) 1271–1276.
43. N.J. Marston, W.J. Richards, D. Hughes, D. Bertwistle, C.J. Marshall, A. Ashworth, Interaction between the product ofthe breast cancer susceptibility gene BRCA2 and DSS1, a protein functionally conserved from yeast to mammals, Mol. Cell. Biol. 19 (1999) 4633–4642.
44. H. Yang, P.D. Jeffrey, J. Miller, E. Kinnucan, Y. Sun, N.H. Thoma, N. Zheng, P.L. Chen, W.H. Lee, N.P. Pavletich, BRCA2 function in DNA binding and recombination from a BRCA2-DSS1-ssDNA structure, Science 297 (2002) 1837–1848.
45. K. Gudmundsdottir, C.J. Lord, E. Witt, A.N. Tutt, A. Ashworth, DSS1 is required for RAD51 focus formation and genomic stability in mammalian cells, EMBO Rep. 5 (2004) 989–993.
46. N. Siaud, M.A. Barbera, A. Egashira, I. Lam, N. Christ, K. Schlacher, B. Xia, M. Jasin, Plasticity of BRCA2 function in homologous recombination: genetic interactions of the PALB2 and DNA binding domains, PLoS Genet. 7 (2011) e1002409.
47. A.K. Wong, R. Pero, P.A. Ormonde, S.V. Tavtigian, P.L. Bartel, RAD51 interacts with the evolutionarily conserved BRC motifs in the human breast cancer susceptibility gene brca2, J. Biol. Chem. 272 (1997) 31941–31944.
48. S.S. Yuan, S.Y. Lee, G. Chen, M. Song, G.E. Tomlinson, E.Y. Lee, BRCA2 is required for ionizing radiation-induced assembly of Rad51 complex in vivo, Cancer Res. 59 (1999) 3547–3551.
49. B. Hirsch, A. Shimamura, L. Moreau, S. Baldinger, M. Hag-alshiekh, B. Bostrom, S. Sencer, A.D. D'Andrea, Association of biallelic BRCA2/FANCD1 mutations with spontaneous chromosomal instability and solid tumors of childhood, Blood 103 (2004) 2554–2559.
50. J.E. Wagner, J. Tolar, O. Levran, T. Scholl, A. Deffenbaugh, J. Satagopan, L. Ben-Porat, K. Mah, S.D. Batish, D.I. Kutler, M.L. MacMillan, H. Hanenberg, A.D. Auerbach, Germline mutations in BRCA2: shared genetic susceptibility to breast cancer, early onset leukemia, and Fanconi anemia, Blood 103 (2004) 3226–3229.
51. S. Mazoyer, A.M. Dunning, O. Serova, J. Dearden, N. Puget, C.S. Healey, S.A. Gayther, J. Mangion, M.R. Stratton, H.T. Lynch, D.E. Goldgar, B.A. Ponder, G.M. Lenoir, A polymorphic stop codon in BRCA2, Nat. Genet. 14 (1996) 253–254.
52. P. van der Lelij, A.B. Oostra, M.A. Rooimans, H. Joenje, J.P. de Winter, Diagnostic overlap between Fanconi anemia and the cohesinopathies: Roberts syndrome and Warsaw breakage syndrome, Anemia 2010 (2010) 565268.
53. J. Liu,I.D.Krantz, Cohesinandhumandisease,Annu.Rev. Genomics Hum. Genet. 9 (2008) 303–320.
54. B. Xia, Q. Sheng, K. Nakanishi, A. Ohashi, J. Wu, N. Christ, X. Liu, M. Jasin, F.J. Couch, D.M. Livingston, Control of BRCA2 cellular and clinical functions by a nuclear partner, PALB2, Mol. Cell 22 (2006) 719–729.
55. N. McCabe, N.C. Turner, C.J. Lord, K. Kluzek, A. Bialkowska, S. Swift, S. Giavara, M.J. O'Connor, A.N. Tutt, M.Z. Zdzienicka, G.C. Smith, A. Ashworth, Defi- ciency in the repair of DNA damage by homologous recombination and sensitivity to poly(ADP-ribose) polymerase inhibition, Cancer Res. 66 (2006) 8109–8115.
56. Y.H. Hsiang, M.G. Lihou, L.F. Liu, Arrest of replication forks by drug-stabilized topoisomerase I-DNA cleavable complexes as a mechanism of cell killing by camptothecin, Cancer Res. 49 (1989) 5077–5082.
57. Y. Pommier, Topoisomerase I inhibitors: camptothecins and beyond, Nat. Rev. Cancer 6 (2006) 789–802.
58. A.N. Blackford, R.A. Schwab, J. Nieminuszczy, A.J. Deans, S.C. West, W. Niedzwiedz, The DNAtranslocase activity of FANCM protects stalled replication forks, Hum. Mol. Genet. 21 (2012) 2005–2016.
59. A.J. Deans, S.C.West, FANCM connects the genome instability disorders Bloom's syndrome and Fanconi anemia, Mol. Cell 36 (2009) 943–953.
60. S.J. Collis, A. Ciccia, A.J. Deans, Z. Horejsi, J.S. Martin, S.L. Maslen, J.M. Skehel, S.J. Elledge, S.C. West, S.J. Boulton, FANCM and FAAP24 function in ATR-mediated checkpoint signaling independently of the Fanconi anemia core complex, Mol. Cell 32 (2008) 313–324.
61. S. Luke-Glaser, B. Luke, S. Grossi, A. Constantinou, FANCM regulates DNA chain elongation and is stabilized by S-phase checkpoint signalling, EMBO J. 29 (2010) 795–805.
62. N.C. Turner, C.J. Lord, E. Iorns, R. Brough, S. Swift, R. Elliott, S. Rayter, A.N. Tutt, A. Ashworth, A synthetic lethal siRNA screen identifying genes mediating sensitivity to a PARP inhibitor,

EMBO J. 27 (2008) 1368–1377.
63. A. Lengronne, J. McIntyre, Y. Katou, Y. Kanoh, K.P. Hopfner, K. Shirahige, F. Uhlmann, Establishment of sister chromatid cohesion at the S. cerevisiae replication fork, Mol. Cell 23 (2006) 787–799.
64. A.R. Leman, C. Noguchi, C.Y. Lee, E. Noguchi, Human timeless and tipin stabilize replication forks and facilitate sister-chromatid cohesion, J. Cell Sci. 123 (2010) 660–670.
65. A. Farina, J.H. Shin, D.H. Kim, V.P. Bermudez, Z. Kelman, Y.S. Seo, J. Hurwitz, Studies with the human cohesin establishment factor, ChlR1. Association of ChlR1 with Ctf18-RFC and Fen1, J. Biol. Chem. 283 (2008) 20925–20936.
66. H. Joenje, J.R. Lo ten Foe, A.B. Oostra, C.G. van Berkel, M.A. Rooimans, T. Schroeder-Kurth, R.D. Wegner, J.J. Gille, M. Buchwald, F. Arwert, Classification of Fanconi anemia patients by complementation analysis: evidence for a fifth genetic subtype, Blood 86 (1995) 2156–2160.

CHAPTER 7

Synthetic lethal interactions with FA deficiency identified by genetic sreens in head and neck cancer cell lines

Chantal Stoepker, Ida H. van der Meulen, Renée X. de Menezes, Victor W. van Beusechem, Johan P. de Winter, Hein te Riele & Ruud H. Brakenhoff

Unpublished

The Fanconi anemia (FA) pathway is an important DNA repair pathway to resolve DNA damage, in particular DNA interstrand crosslinks, during DNA replication. Despite the role of this repair pathway in counteracting replication stress to help cells to survive, FA-deficient cells can transform into tumor cells as demonstrated by the highly increased cancer risk seen in FA patients. This suggests the existence of compensatory mechanisms that are essential for FA-deficient cells to survive, and which are particularly required when cells transform and replication stress increases. By performing genome-wide high-throughput siRNA screening, we have investigated whether these compensatory mechanisms can be identified and might be exploited to develop new anti-cancer therapies for tumors in FA patients as well as FA-deficient tumors in non-FA patients. More lethal siRNAs were found in the FA-deficient tumor cell line compared to the corresponding FA-corrected tumor cell line (312 versus 253), indicating that FA-deficient cells may indeed rely on specific survival mechanisms. Our screen identified the proteasome, the Vacuolar ATPase, the nuclear pore complex and mitosis as promising targets to further investigate for development of novel treatment strategies that are specific for FA-deficient tumors.

Introduction

Fanconi anemia (FA) is a rare chromosomal instability syndrome characterized by a variety of congenital abnormalities, bone marrow failure and a high incidence of malignancies, in particular squamous cell carcinomas of the anogenital and head and neck region[1]. Since physical abnormalities can be subtle or absent, hematological problems are often the first indication for FA and form a main cause of disease complications, often requiring bone marrow transplantation[2,3]. Because bone marrow transplantation outcomes have been improved tremendously in recent years, the high cancer susceptibility is the next life-threatening problem that FA patients are now facing[4]. The risk to develop head and neck squamous cell carcinomas (HNSCC) is 500- to 700-fold higher than in the general population[5–7]. These tumors are difficult to treat in FA patients. More advanced stages of HNSCC are treated by either surgery with postoperative radiotherapy or by chemoradiation, the concomitant application of systemic cisplatin with locoregional radiotherapy. However, FA patients frequently develop treatment associated toxicities due to the high sensitivity to the commonly used chemotherapeutic drug cisplatin and radiotherapy[4]. Therefore, it is important to find new, preferably targeted, therapies to treat cancer in individuals with FA.

FA cells have a defect in an essential genome maintenance pathway that resolves problems during DNA replication[8,9]. Currently, bi-allelic mutations in one

of 17 FA genes are known to be causative of FA[8–10]. Together the FA proteins function in the FA pathway to repair DNA interstrand crosslinks. This repair pathway can be divided into an upstream part, in which 8 FA proteins (FANCA, -B, -C, -E, -F, -G, -L and -M) together with several FA-associated proteins are responsible for mono-ubiquitination of FANCD2 and FANCI, and a downstream part (FANCD1/BRCA2, FANCJ, FANCN/PALB2, FANCO/RAD51C, FANCP/SLX4, FANCQ/XPF and FANCS/BRCA1), which is not required for this posttranslational modification[8,9]. Since tumor cells experience a lot of replication stress due to (epi)genetic alterations that deregulate cellular proliferation and apoptosis[11,12], it is surprising that cells with a deficient FA pathway can transform into a tumor. Moreover, FA pathway inactivation may even occur in sporadic tumors in non-FA patients[13,14]. We therefore hypothesize that tumors with a defect in the FA pathway require compensatory mechanisms to survive. As a consequence, these mechanisms may represent an Achilles' heel of the tumor and inactivation of such compensating mechanisms may result in reduced cellular fitness. These compensating processes will be synthetic lethal with the FA defect. By performing a high-throughput whole-genome RNA interference screen, we identified siRNAs targeting genes essential in FA-HNSCC but not the corrected cell line. Identification of these genes will aid in finding new treatment options for FA patients as well as for non-FA patients with FA-deficient tumors.

Results and discussion

High-throughput siRNA screening in FA-deficient and FA-corrected HNSCC cell lines

To identify genes that are essential for viability of FA head and neck tumor cells, we conducted high-throughput genome-wide siRNA screens in an FA-deficient HNSCC cell line with mutations in *FANCC* (VU-SCC-1131) and in the corresponding FANCC-corrected cell line (VU-SCC-1131+FANCC). The screening procedure was optimized for both cell lines to achieve uniform efficiency reflected by the sensitivity to transfection of a positive control siRNA SMARTpool (PLK1) and lack of sensitivity to transfection of a negative control siRNA SMARTpool (non-targeting siRNA (siCON)). Cells were reverse transfected in 384-wells format and after 5 days, cell viability was measured by adding CellTiter-Blue Reagent. Transfection of siRNAs targeting PLK1 (positive control) resulted in a reduction of at least 95% cell viability compared to cells transfected with the negative control siRNAs (data not shown). Toxicity of our transfection protocol was very modest since cell viability of negative control transfected cells was only slightly reduced (10-20%) compared to untransfected cells (data not shown). With these optimal transfection conditions, we conducted triplicate screens for each cell line. Raw viability values were normalized

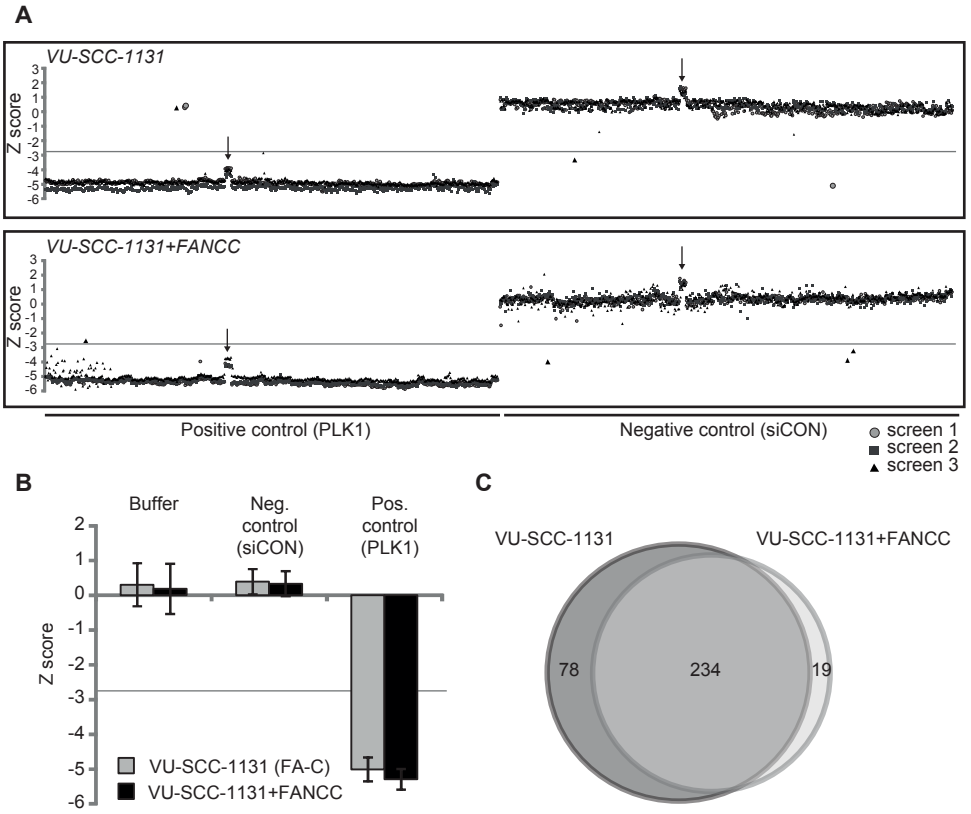

Figure 1 Genome wide siRNA screening in FA and FA-corrected HNSCC cell lines
(**A**) Z-scores of negative (non-targeting siRNA#2 (siCON)) and positive control (PLK1) used during high throughput siRNA screening in the FANCC-deficient FA-HNSCC cell line (VU-SCC-1131) and the corresponding genetically corrected cell line (VU-SCC-1131+FANCC). Symbols representing Z-scores above the cutoff of -2.75 for PLK1-transfected cells and below -2.75 for siCON-transfected cells are slightly enlarged. Note that there are some outliers (indicated with the arrow). These positive and negative controls were located on a plate with many lethal siRNAs and after normalization/re-scaling the data (see text), these Z-scores shifted upwards. (**B**) Average Z-score of untransfected (no siRNA (Buffer)), negative (siCON) and positive controls (PLK1). (**C**) Number of separate and overlapping lethal siRNAs (Z-score < -2.75) in VU-SCC-1131 and VU-SCC-1131+FANCC.

by first log2-transformation and subsequently corrected for an overall plate effect across the cell lines by using a linear regression model. Subsequently, Z-scores were calculated and a cutoff of Z=-2.75, which was previously used by others[15], was chosen as a threshold to identify lethal siRNAs. Only 5 out of 3,264 negative controls (siCON) reached this threshold, whereas 4 out of 3,264 positive controls had Z-scores above -2.75 (**Fig. 1A**). The average Z-scores of untransfected, negative or positive control transfected VU-SCC-1131 cells was 0.30, 0.39 and -5.01, respectively (**Fig. 1B**). For VU-SCC-1131+FANCC cells, similar Z-scores (untransfected 0.19, negative control 0.33 and positive control -5.29) were obtained (**Fig. 1B**). Finally, Z' factors for each screen were calculated to determine the quality of the screens and varied between

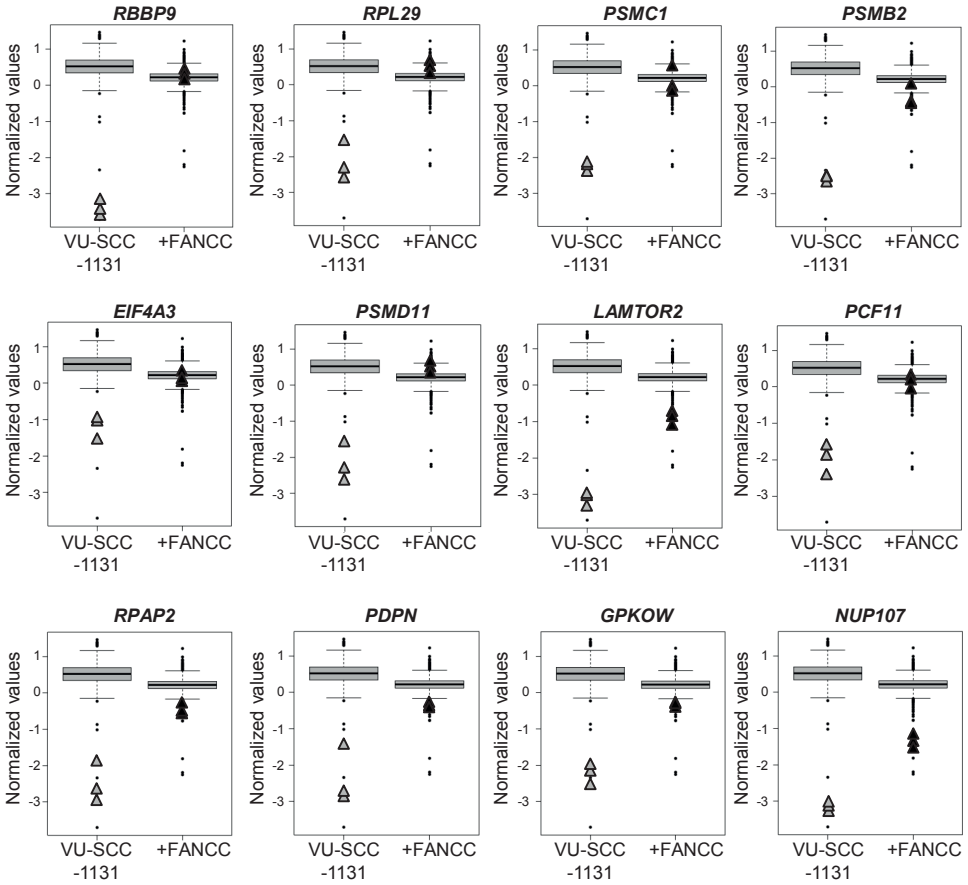

Figure 2 Top twelve genes that contribute to survival of FA-deficient tumor cells
Top twelve proteins of which knockdown decreased cell viability more in FA-deficient VU-SCC-1131 cells than in the FA-corrected tumor cell line. Boxplots and triangles correspond to negative controls (siCON) and the indicated siRNAs, respectively.

0.55 and 0.75 (**Table 1**). Taken together, the transfection efficiency, discriminating power and reproducibility of the screening procedure were high and the toxicity was limited.

Table 1 Z' factors of siRNA screens

	VU-SCC-1131	VU-SCC-1131+FANCC
Screen 1	0.55	0.74
Screen 2	0.75	0.73
Screen 3	0.63	0.55

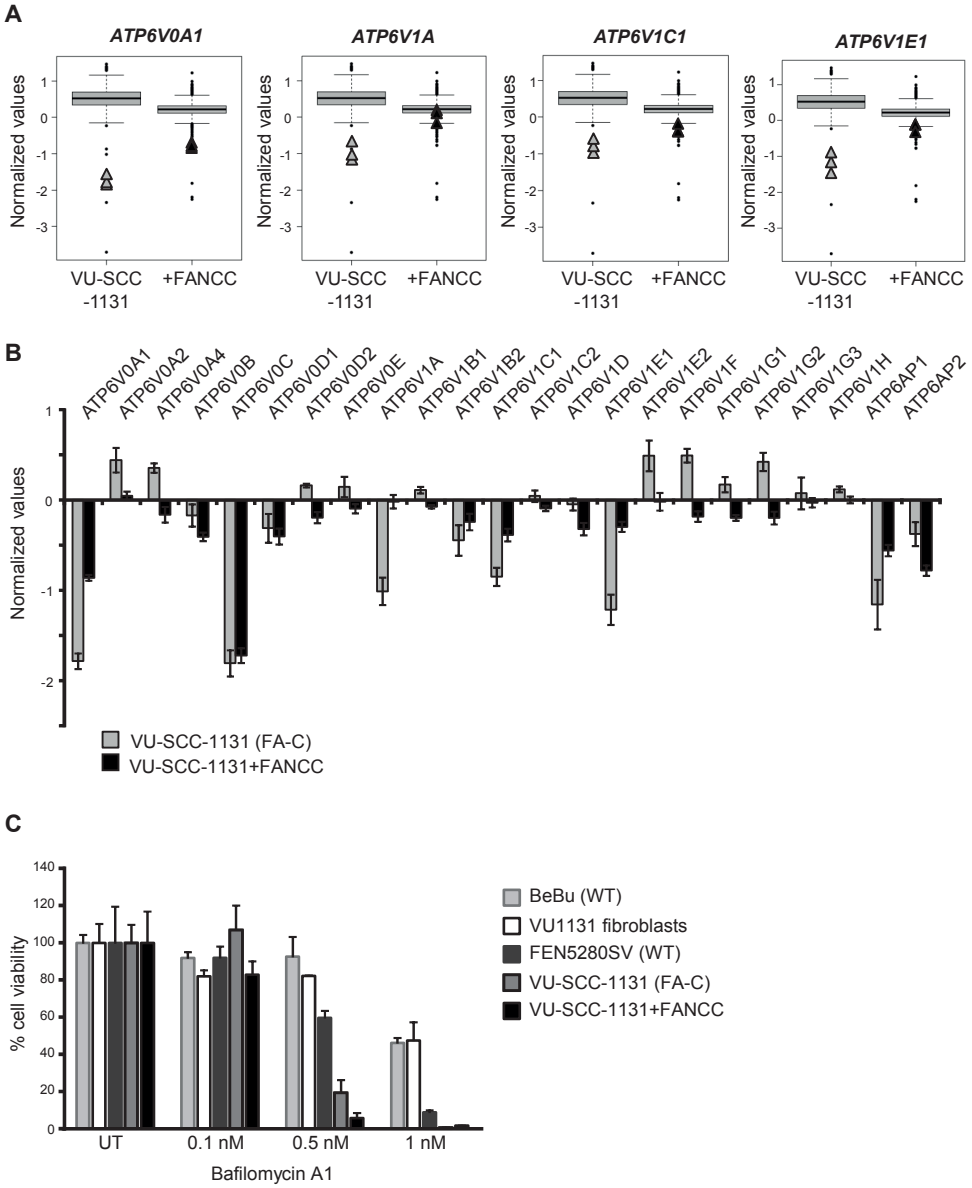

Figure 3 Inhibition of the Vacuolar ATPase decreases cell viability in FA-HNSCC
(**A**) Knockdown of four subunits of the Vacuolar ATPase reduced cell viability of VU-SCC-1131 more than that of VU-SCC-1131+FANCC. (**B**) Average of normalized values of all subunits of the Vacuolar ATPase after knockdown in VU-SCC-1131 and VU-SCC-1131+FANCC. (**C**) Inhibition of the Vacuolar ATPase with Bafilomycin A1 in wild-type primary (BeBu and VU1131 fibroblasts) and SV40-immortalized fibroblasts (FEN5280SV), VU-SCC-1131 and the corrected cell line VU-SCC-1131+FANCC.

Top twelve FA-specific lethal siRNAs

By using tumor cells with either a defective or corrected FA pathway, two sets of essential genes might be found: one set of genes, of which knockdown is specifically lethal in tumor cells regardless of a functional FA pathway (tumor-specific), and a second set of genes, of which knockdown is only lethal in combination with the FA defect (FA-specific). Knockdown of some genes might turn out to be lethal in FA-deficient tumor cells but not in FA-deficient normal cells, making these genes excellent targets for novel therapies to treat tumors in FA patients.

Firstly, we addressed whether FA-specific hits could be identified by comparing lethal siRNAs in VU-SCC-1131 and VU-SCC-1131+FANCC. The cutoff of Z-score set at <-2.75 yielded 312 and 253 siRNAs that substantially reduced cell viability in VU-SCC-1131 cells or VU-SCC-1131+FANCC cells, respectively (**Fig. 1C** and **Supplementary table 1**). Interestingly, more lethal hits were found in VU-SCC-1131 compared to the corrected cell line (**Fig. 1C**).

Secondly, we used 3 linear regression models (see material and methods) to find siRNAs that displayed different lethality in the FA-deficient and FA-corrected cell line. The top twelve genes that showed the largest difference between the two cell lines are shown in **Fig. 2**. Although not much is known of most of these genes, some (*RBBP9*, *RPL29* and *PSMD11*) have been implicated in carcinogenesis previously[16–21] and might be promising targets in the development of anticancer drugs for FA-deficient tumors. In addition, the proteins encoded by 3 of the 12 top genes are part of the proteasome (*PSMC1*, *PSMB2* and *PSMD11*), suggesting that proteasome inhibition by small molecule inhibitors such as bortezomib or carfilzomib might also be an effective strategy in the treatment of FA-deficient tumors.

Inhibition of the vacuolar-ATPase is a promising target in the treatment of FA-HNSCC

By comparing VU-SCC-1131 and VU-SCC-1131+FANCC we also noticed a difference in cell viability after knockdown of several subunits of the vacuolar-ATPase (V-ATPase). SiRNA-mediated depletion of ATP6V0A1, ATP6V1A, ATP6V1C1 and ATP6V1E1 resulted in decreased cell viability in VU-SCC-1131 compared to the corrected cell line (**Fig. 3A** and **B**). The multi-subunit V-ATPase functions as an ATP-dependent proton pump that is primarily involved in the acidification of intracellular compartments and extracellular environment, thereby regulating pH homeostasis[22]. Noteworthy, expression of the V-ATPase is upregulated in several cancers[23,24]. Since acidic pH alterations caused by high metabolic rates or altered metabolism of cancer cells favor cell proliferation, drug resistance and metastasis progression, interference with pH regulation has been suggested as an anti-cancer strategy[25–31]. Therefore, we tested whether FA-deficient tumor cells were more sensitive to the V-ATPase inhibitor Bafilomycin A1 than FA corrected cells. The difference in sensitivity in

terms of growth inhibition was small between the FA-deficient and FA-corrected cells. Whether this relates to drug specificity remains unclear, but the difference in sensitivity between tumor cells and normal fibroblasts derived from the same patient, was much larger (**Fig. 3C**). This suggests that inhibition of the V-ATPase might be beneficial in the treatment of HNSCC regardless of the FA defect.

The spindle assembly checkpoint is a potential therapeutic target for cancer therapy in FA patients

Based on Z-scores, many siRNAs (234) were lethal in both FA-deficient and corrected cells. Cluster analysis using the DAVID Functional annotation tool was performed on these hits (Z-score < -2.75) with the exception of the 15 genes that are now annotated as pseudogenes. This analysis revealed multiple clusters, of which the top ten with gene ontology enrichment scores above 2.67 are indicated in **Fig. 4** and **Supplementary table 2**. The largest five clusters contained genes involved in 1) (m)RNA processing and splicing, 2) regulation of ubiquitination and proteasome proteolysis, 3) ribonucleoprotein and ribosome biogenesis, 4) macromolecular complex assembly and 5) mitosis. In particular the fifth cluster of genes involved in mitosis attracted our attention as regulators of mitosis have been proposed as candidate drug targets for antitumor therapies before. Antimitotic agents, such as taxol, have indeed been in clinical use for many years, including in neoadjuvant protocols for head and neck cancer, and therefore these hits were analyzed in more detail.

The fifth cluster harbors genes encoding proteins involved in the G2/M phase transition (*e.g. WEE1* and *CDK1*) and (regulation of) mitotic spindle organization/ assembly (*e.g. NDC80*, *TPX2*, *KIF11* and *CKAP5*). In addition, the fifth cluster contained genes encoding spindle assembly checkpoint (SAC) proteins (*e.g. BUB1B*, *BUB3* and *MAD2*) and chromosomal passenger complex (CPC) proteins (*e.g. BIRC5*, *CDCA8* and *INCENP*), which are two complexes with an important role in the correct segregation of duplicated chromosomes during mitosis[32,33] (**Supplementary Fig. 1**). In an independent experiment, we transfected VU-SCC-1131 and VU-SCC-1131+FANCC cells with siRNA SMARTpools targeting the six key components of the SAC: BUB1, BUB1B, BUB3, MAD1, MAD2 and TTK (**Fig. 5A**). Knockdown of all components except MAD1 resulted in over 50% reduction in cell viability in both cell lines. Inhibition of BUB3 and MAD2, which also had the lowest Z-scores, resulted in more than 80% cell death (**Fig. 5B**). Although BUB1 and TTK were not scored as hits in the primary genome-wide siRNA screens, knockdown of BUB1 or TTK markedly reduced cell viability in the validation experiment (**Fig. 5B**). Since TTK already has been suggested to be a candidate drug target for anticancer therapies and several TTK inhibitors have been synthesized, we analyzed this hit in more detail. TTK (also known as MPS1) is a dual specificity protein kinase and besides a key component of

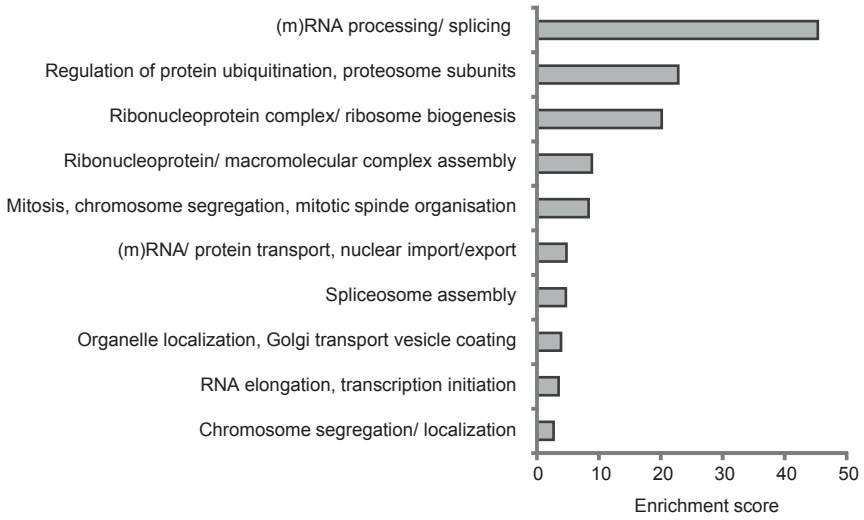

Figure 4 Cluster analysis of lethal hits in FA and FA-corrected HNSCC cell lines
Cluster analysis of lethal hits (Z-score below -2.75) in VU-SCC-1131 as well as VU-SCC-1131+FANCC. Using DAVID Functional annotation tool revealed multiple clusters, of which the top ten with gene ontology enrichment scores above 2.67 are shown.

the SAC, it is also involved in regulating the CPC by phosphorylating CDCA8 (ref 34). Overexpression of TTK has been reported in several tumor types[35–38] and knockdown of this protein can lead to accelerated mitosis through checkpoint abrogation, followed by apoptosis specifically in cancer cells[39]. Knockdown of TTK protein levels in TTK siRNA SMARTpool transfected cells was confirmed by western blotting (**Fig. 5C**). Deconvolution of the TTK siRNA smartpool, in which the four siRNAs that make up the pool were tested separately, resulted in > 40% cell death for all four siRNAs in both cell lines (**Fig. 5D**). This shows that TTK expression is essential in these tumor cell lines, regardless of FA status. To further explore TTK as a promising drug target, we tested two commercially available TTK inhibitors: Reversine and AZ3146. When treated with Reversine, primary fibroblasts (VU1131 fibroblasts) from the same FA patient from whom VU-SCC-1131 was derived, showed a very mild growth inhibition of approximately 10% compared to untreated cells (**Fig. 5E**). Similar results were obtained for other primary fibroblasts (BeBu) or for SV40-immortalized wild type fibroblasts (FEN5280SV). In contrast, tumor cell lines (VU-SCC-1131, VU-SCC-1365 and VU-SCC-1604) established from head and neck tumors from FA patients were more sensitive to Reversine treatment compared to wild type cells. Growth of these cell lines was reduced by approximately 60% to 90% (**Fig. 5E**). Previously, these three FA-HNSCC cell lines were functionally corrected for their FA defect[40]. These corrected cell lines were also tested for Reversine sensitivity and only VU-SCC-1604 FANCL-corrected cells were less sensitive to Reversine compared to uncorrected cells. Primary wild type fibroblasts (BeBu) and FA-HNSCC cell lines were also tested

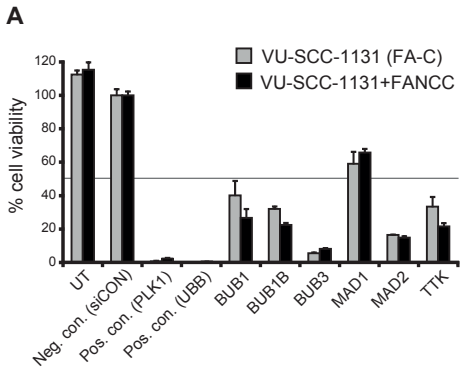

B

GENE	Z-score VU-SCC-1131	% cell viability VU-SCC-1131	Z-score +FANCC	% cell viability +FANCC
BUB1	-0.503	40.0±8.6	-0.803	26.5±5.4
BUB1B	-2.642	31.8±1.7	-3.591	22.5±1.1
BUB3	-4.149	5.5±0.5	-4.563	8.1±0.5
MAD1L1	-0.049	59.0±7.1	-0.407	65.6±2.3
MAD2L1	-3.089	16.3±0.3	-3.997	14.8±0.8
TTK	-2.448	33.3±5.8	-1.328	21.5±1.9

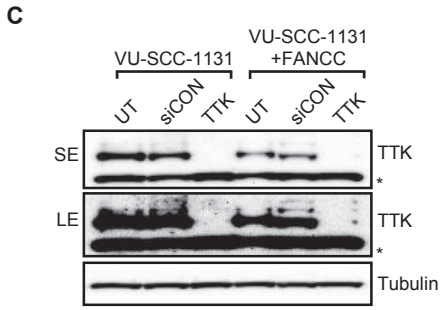

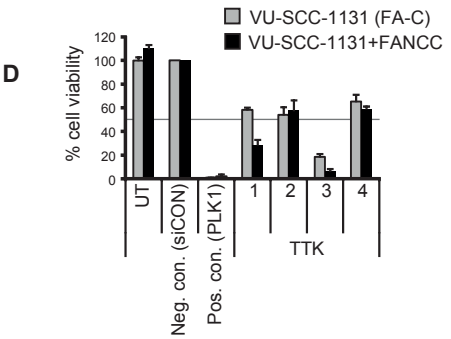

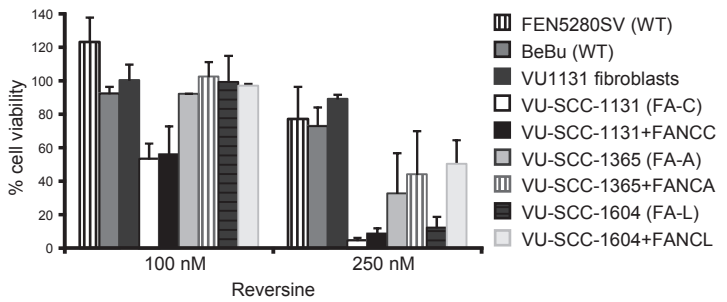

G

Cell line	# cell doublings
FEN5280SV	3.97±0.54
BeBu	2.68
VU1131 fibroblasts	2.03±0.08
VU-SCC-1131	5.95±1.20
VU-SCC-1131 +FANCC	4.85±0.34
VU-SCC-1365	5.09±0.31
VU-SCC-1365 +FANCA	4.55±0.27
VU-SCC-1604	4.24±0.31
VU-SCC-1604 +FANCL	3.77±0.51

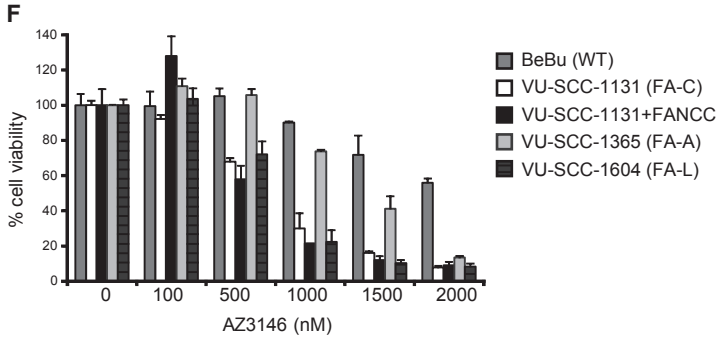

Figure 5 Inhibition of the spindle assembly checkpoint decreases cell viability in HNSCC
(**A**) SiRNA SMARTpools targeting subunits of the spindle assembly checkpoint decreased cell viability in VU-SCC-1131 and VU-SCC-1131+FANCC. Cell viability was measured in triplicate and calculated relative to non-targeting transfected cells. (**B**) Z-score values of SAC proteins from the genome-wide siRNA screen.

(**C**) Depletion of TTK/MPS1 protein after transfection with siRNAs (siGENOME SMARTpool) targeting TTK/MPS1 in VU-SCC-1131 and VU-SCC-1131+FANCC. Tubulin was used as a loading control. (**D**) Deconvolution of siGENOME SMARTpool targeting TTK/MPS1. Cell viability was measured in triplicate and calculated relative to siCON (negative control) transfected cells. Cell viability after inhibition of TTK/MPS1 by Reversine (**E**) or AZ3146 (**F**) in wild-type primary (BeBu) or SV40-immortalized fibroblasts (FEN5280SV), FA-HNSCC cell lines (VU-SCC-1131, VU-SCC-1365 and VU-SCC-1604) and corresponding FA-corrected cell lines (VU-SCC-1131+FANCC, VU-SCC-1365+FANCA and VU-SCC-1604+FANCL). (**G**) Number of cell doublings during growth inhibition assay with Reversine shown in (**E**).

for another TTK-inhibitor: AZ3146. Again, FA-HNSCC cell lines were more sensitive to AZ3146 than wild type fibroblasts (**Fig. 5F**). It should be noted though that the FA-HNSCC cell lines divided faster than the wild-type and FA fibroblasts. Rather than their tumor background per se, this might explain their higher sensitivity to Reversine and AZ3146 (**Fig. 5G**). More research, preferably by using mouse models, is required to establish the potency of TTK inhibition in treatment of sporadic and FA-HNSCC.

The nuclear pore complex as candidate drug target in FA-HNSCC

To identify more genes that are essential for the survival of HNSCC tumors regardless of an FA defect, we also analyzed the sixth cluster, which contained genes involved in (m)RNA and protein transport (**Fig. 4** and **Supplementary Fig. 2**). Many of these genes encode proteins that make up the nuclear pore complex (NPC). The NPC is the largest multiprotein complex in eukaryotic cells and its best-known and probably primary function is directing the transport of RNAs and proteins across the nuclear envelope. However, other functions, such as the regulation of genome organization, gene expression, mitosis and DNA repair, have been reported as well[41–43]. The NPC is built from a small number of proteins called nucleoporins (Nups), of which some (*e.g.* NUP88, NUP98, NUP214 and NUP358) have been implicated in cancer[44–46]. We selected 13 hits from the 6th cluster that are components of the NPC and 3 additional NPC genes with Z-scores above -2.75. For each gene, we tested the 4 separate siRNAs that composed the siRNA SMARTpools used in the screens, by transfecting VU-SCC-1131 and the corrected cells (**Fig. 6A** and **B**). Inhibition of 15 and 13 of the 16 selected genes in VU-SCC-1131 and VU-SCC-1131+FANCC, respectively, reduced cell viability by more than 50% with at least 2 of 4 siRNAs (**Fig. 6A-C**). Interestingly, knockdown of two genes (*AHCTF1*, also known as *ELYS*, and *NUP35*) with at least two separate siRNAs reduced cell viability in VU-SCC-1131 cells more than in the corrected cell line (VU-SCC-1131+FANCC). For 3 other genes (*SEH1L*, *NUP107* and *NUP155*) the difference in viability between the two cell lines was even larger (**Fig. 6D-F**). Whereas our initial analysis did not reveal differential effects of knockdown of NCP genes, deconvolution of the SMARTpools targeting these genes showed that for at least 2 of 4 siRNAs VU-SCC-1131 cells were approximately 2-fold more sensitive to knockdown than VU-SCC-1131+FANCC cells (**Fig. 6A-B**).

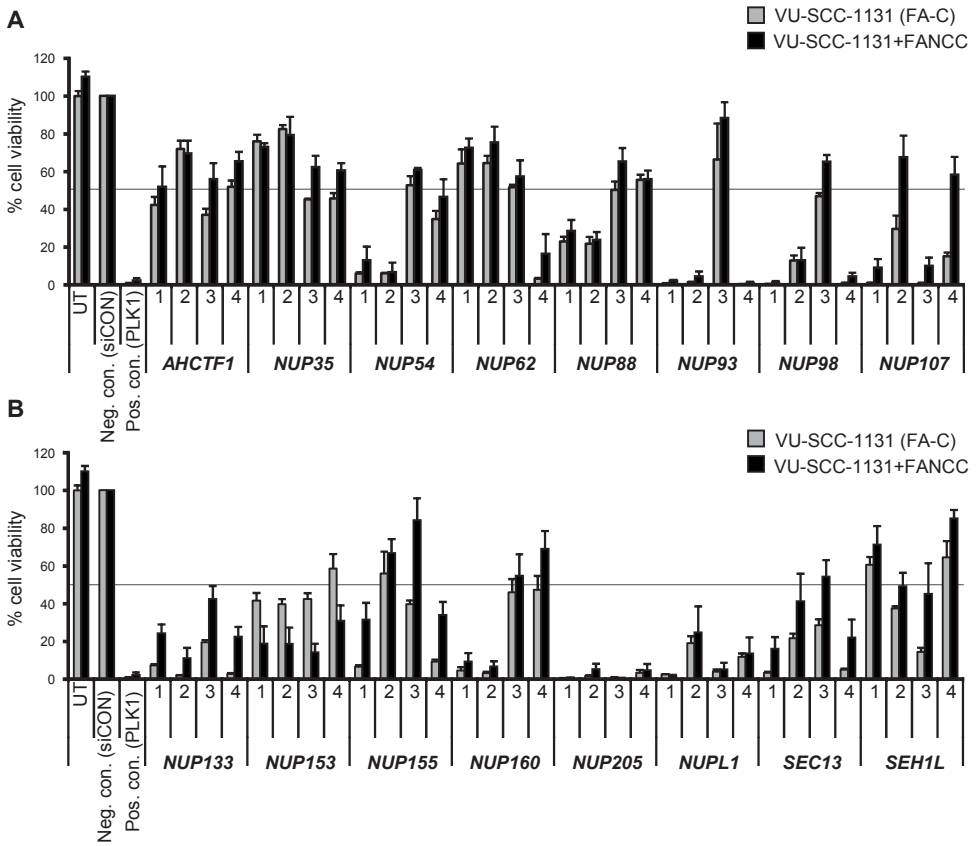

C

GENE	VU-SCC-1131 Z score	VU-SCC-1131 siRNAs scoring +	VU-SCC-1131+FANCC Z score	VU-SCC-1131+FANCC siRNAs scoring +
AHCTF1	-1.83	2	-0.73	0
NUP35	-1.82	2	-0.42	0
NUP54	-4.37	3	-4.08	3
NUP62	-4.98	1	-5.48	1
NUP88	-2.27	2	-2.17	2
NUP93	-4.98	3	-5.03	3
NUP98	-5.23	4	-4.98	3
NUP107	-4.64	4	-2.49	2
NUP133	-4.25	4	-3.55	4
NUP153	-1.55	3	-3.72	4
NUP155	-3.30	3	-1.31	2
NUP160	-3.05	4	-2.35	2
NUP205	-5.10	4	-5.05	4
NUPL1	-4.31	4	-4.95	4
SEC13	-3.52	4	-2.57	3
SEH1L	-3.00	2	-1.09	2

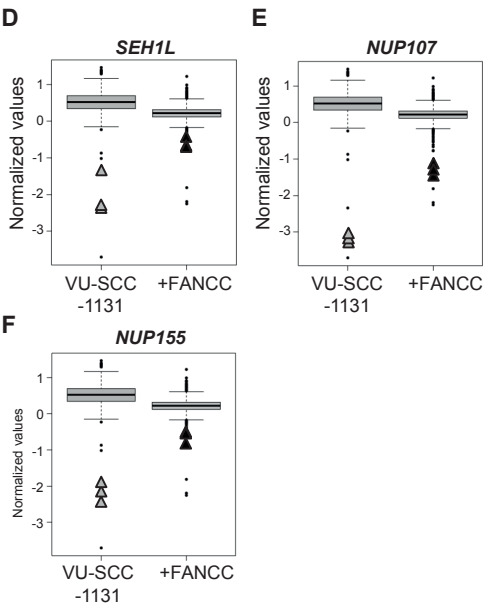

Figure 6 The nuclear pore complex is a potential drug target in FA-HNSCC
SiGENOME SMARTpools targeting the indicated genes (**A-B**) were deconvoluted in VU-SCC-1131 and VU-SCC-1131+FANCC. Cell viability was measured in triplicate and calculated relative to siCON (negative control) transfected cells. (**C**) Overview of Z-scores of the indicated genes from the genome-wide siRNA screen and the number of siRNAs that decreased cell viability by 50% (siRNAs scoring positive) after deconvolution as shown in (**A-B**). A difference in cell viability (indicated by normalized values) between VU-SCC-1131 and VU-SCC-1131+FANCC after knockdown of SEH1L (**D**), NUP107 (**E**) and NUP155 (**F**).

Although knockdown of these genes should be confirmed by RT-PCR and/or western blotting and more FA-HNSCC cell lines should be tested, it seems that the NPC is essential for the survival of FA-defective HNSCC tumor cells.

Conclusion

The larger number of lethal hits in the FA-deficient cell line VU-SSC-1131 compared to the corrected cell line suggests the existence of compensatory pathways that are essential for the survival of FA-defective tumor cells. Subsequent analyses revealed two classes of synthetic lethal interactions. The first class is tumor specific, but independent of FA status, and includes inhibition of the vacuolar ATPase and the spindle assembly checkpoint. This class may provide a cancer treatment strategy in both sporadic and FA patients. The second class is specific for the FA defect in HNSCC and includes inhibition of several nucleoporins and the proteasome. This class may be particularly interesting for the small subset of sporadic tumors with defects in the FA pathway.

Materials and methods

Cell culture
Primary (BeBu and VU1131 fibroblasts) and SV40-immortalized wild-type fibroblasts (FEN5280SV), VU-SCC-1131 (FANCC-deficient HNSCC cell line), VU-SCC-1365 (FANCA-deficient HNSCC cell line), VU-SCC-1604 (FANCL-deficient cell line) as well as the corresponding genetically corrected cell lines VU-SCC-1131+FANCC, VU-SCC-1365+FANCA and VU-SCC-1604+FANCL were cultured in Dulbecco's modified Eagle's medium (DMEM) supplemented with 10% fetal bovine serum and 1 mM sodium pyruvate (Gibco). FA-HNSCC cell lines were established as described previously[40,47].

High throughput siRNA screens
VU-SCC-1131 and VU-SCC-1131+FANCC cells were subjected to a genome-wide siRNA screen by reverse transfection in 384-well plates. Of in total 21,121 siRNA SMARTpools derived from the siARRAY Humane Genome library (Catalog items G-003500 (Sept05), G-003600 (Sept05), G-004600 (Sept05), and G-005000 (Oct05); Dharmacon, Thermo Fisher Scientific), 25 nmols were put in individual wells by using the Sciclone ALH 3000 workstation (Caliper LifeSciences) and a Twister II microplate handler (Caliper LifeSciences). The non-targeting siCONTROL #2 (siCON) and the PLK1 siGENOME SMARTpool were used as a negative and positive control, respectively, and manually added to 8 different wells on each plate. RNAiMAX (Invitrogen) at a final concentration of 0.01 µl/well was added to the siRNAs by a Multidrop Combi (Thermo Fisher Scientific). Subsequently, cells were seeded using a µFill microplate dispenser (BioTek). Plates were incubated for 5 days at 37°C and 5% CO2. After 5 days, cell viability was determined by adding CellTiter-Blue reagent (Promega) using a Multidrop Combi (Thermo Fisher Scientific). Two hours later fluorescence was analyzed at 540 nm excitation and 590 nm emission wavelength using an Infinite F200 microplate reader (Tecan Group Ltd). Deconvolution of siRNA SMARTpools targeting TTK

and NUP genes was performed by using the same automated procedure as described above.
The Z' factor[48] was used to assess screen quality and was calculated for each screen with the formula:

$$Z' = 1 - \frac{(3\sigma_{\text{positive control}} + 3\sigma_{\text{negative control}})}{|\mu_{\text{positive control}} - \mu_{\text{negative control}}|}$$

After measuring fluorescence using CellTiter Blue reagent (living cells convert resazurin (redox dye) into resorufin (fluorescent end product)), the obtained raw viability values (fluorescent signals) were re-scaled by first log2-transformation and subsequently corrected for an overall plate effect across the cell lines by using a linear regression model. These values were used to calculate Z-scores or were used together with 3 linear regression models to find siRNAs that caused a difference in cell viability between the FA-deficient and FA-corrected cells: We used a linear regression model to find siRNAs that differed significantly in their viability from the negative (siCON) controls, per cell line. Specifically, we explain normalized cell viability values by a factor indicating the siRNA or the siCON, using a linear regression that is fitted per siRNA and per cell line. P-values corresponding to the siRNA effect were corrected for multiple testing using Benjamini & Hochberg's step-up FDR procedure[49]. Subsequently, we used a linear regression model with both cell line and siRNA vs siCON effect, as well as the interaction of these, to find siRNAs that displayed different lethality in the two cell lines. Here we extracted p-values corresponding to the interaction effect, which were subsequently corrected for multiple testing as with the previous model.

Western blot analysis of TTK/MPS1 protein expression
Whole-cell extracts were prepared in lysis buffer (50 mM TRIS (pH 7.5), 150 mM NaCl and 1% Triton X-100 supplemented with protease (complete EDTA free tablets, Roche) and phosphatase (PhosSTOP, Roche) inhibitors). Proteins were separated on a 3-8% Tris-Acetate NUPAGE gradient gel (Invitrogen) and transferred to Immobilon-P membrane overnight. After blocking with 5% dry milk in TBST (10 mM TRIS-HCl (pH 7.5), 150 mM NaCl, 0.05% Tween-20), the membrane was incubated with TTK/MPS1 antibody (1:1,000, A300-296A, Bethyl Laboratories), followed by washing with TBST and incubation with horseradish peroxidase-conjugated secondary antibodies to visualize protein bands with ECL (GE Healthcare). Mouse monoclonal anti-α tubulin (1:5,000, B-5-1-2, SC23948, Santa Cruz Biotechnologies) was used as a control to ensure loading of equal amounts of protein in each western blot lane.

Drug treatments
Cells were seeded 6-well plates with increasing concentrations of drug (Reversine: R3904, Sigma-Aldrich, AZ3146: SC_361114, Santa Cruz, and Bafilomycin A1: B1793, Sigma-Aldrich). After two weeks of incubation with the indicated drugs or earlier after untreated cells had made 3 population doublings, the relative cell number compared to untreated cells for each drug concentration was determined using a Coulter counter.

Acknowledgements
We thank Irsan E. Kooi for help with the cluster analysis using the DAVID Functional annotation tool.

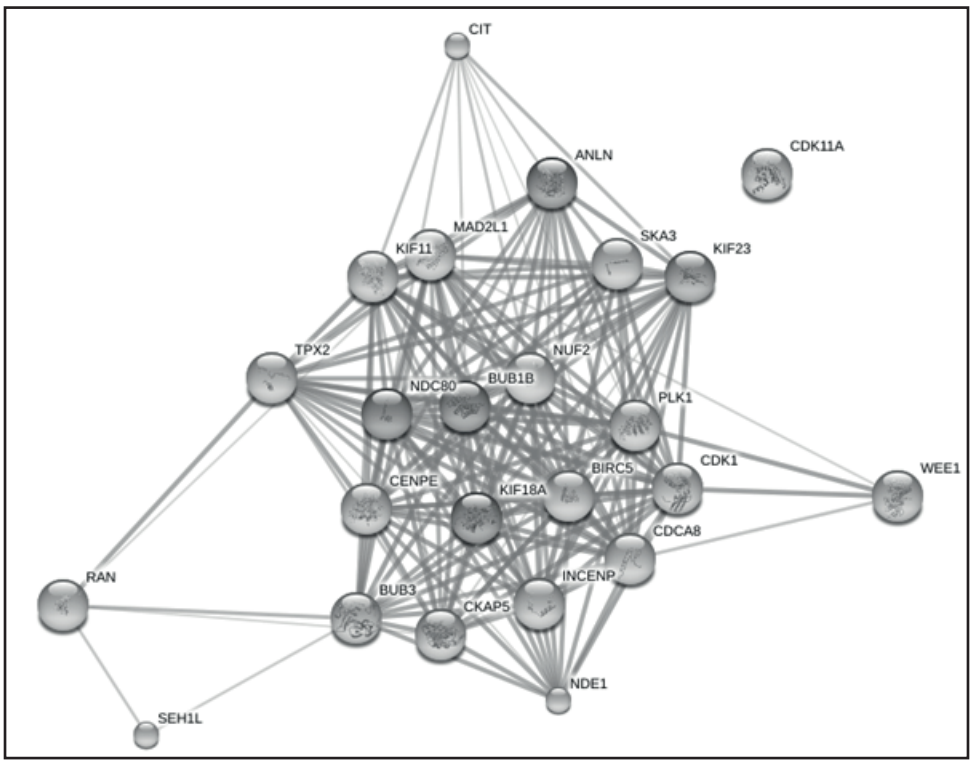

Supplementary figure 1 STRING protein analysis of the gene ontology term mitosis (GO:0007067) belonging to the fifth cluster.

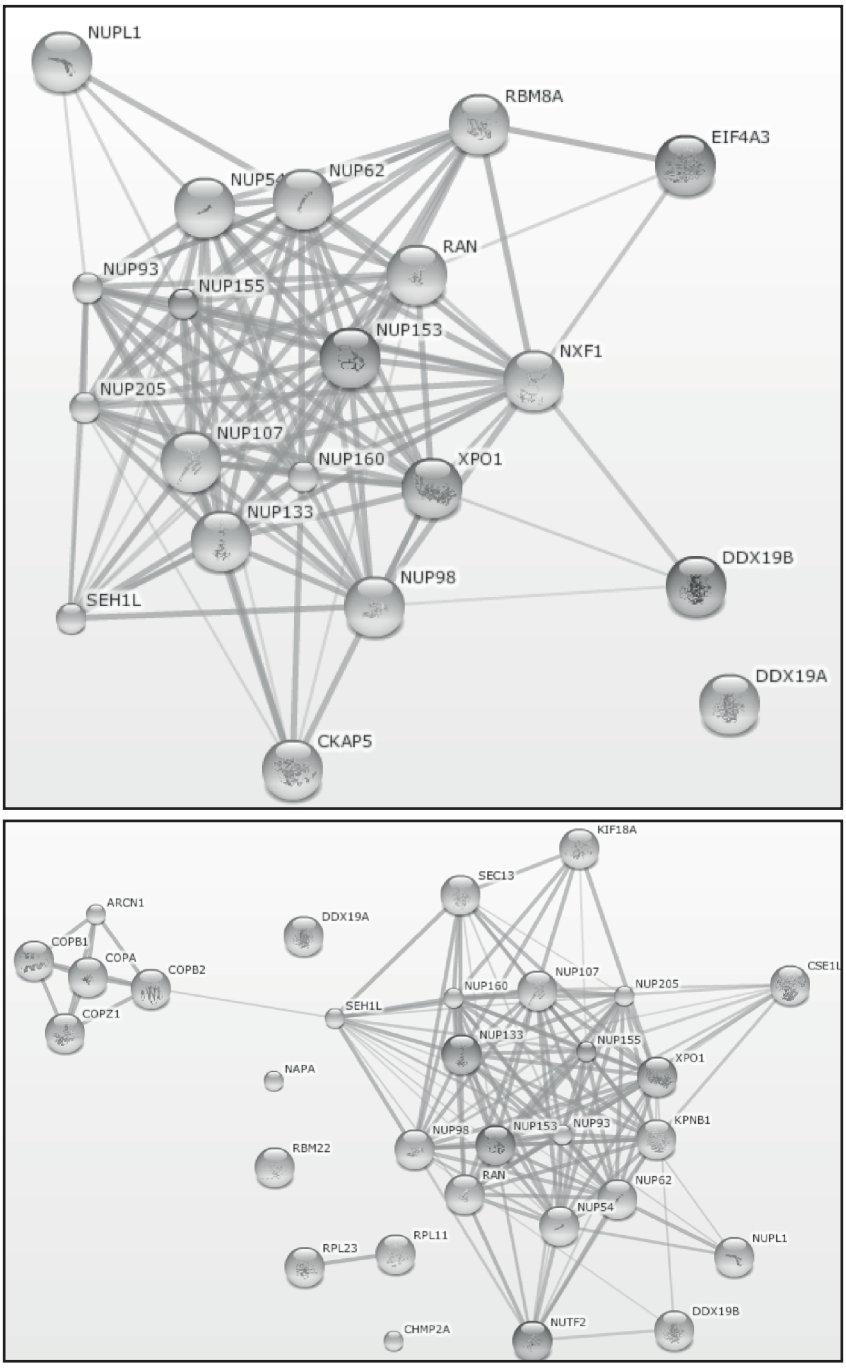

Supplementary figure 2 STRING protein analysis of gene ontology terms RNA and protein transport.

Supplementary table 1. SiRNAs identified by genome wide screening that caused decreased cell viability (Z-score < -2.75) in VU-SCC-1131 and/or VU-SCC-1131+FANCC

	VU-SCC-1131	+FANCC		VU-SCC-1131	+FANCC
Gene	**Z-score**	**Z-score**	**Gene**	**Z-score**	**Z-score**
UBC	-5.61134	-5.44161	*SNRNP200*	-5.09997	-5.28209
UBB	-5.55685	-5.40233	*PSMD7*	-5.08382	-5.02042
RRM2	-5.50381	-5.64482	*NUP62*	-4.98126	-5.48381
PSMD8	-5.50216	-5.58714	*NUP93*	-4.97748	-5.02728
RAN	-5.50108	-5.58607	*RBBP9*	-4.96028	0.424674
NXF1	-5.49255	-5.70452	*CKAP5*	-4.9072	-5.28382
SMU1	-5.4695	-5.63053	*SF3B5*	-4.90361	-4.79809
SON	-5.4546	-5.35276	*POLR2A*	-4.90211	-4.52265
RBM8A	-5.42686	-5.57497	*NUTF2*	-4.88388	-5.47033
EIF4A3	-5.40612	-2.68382	*RBM22*	-4.86103	-3.86354
POMP	-5.37867	-5.51214	*HNRNPK*	-4.8262	-4.78765
PSMD6	-5.36319	-5.52563	*PSMD2*	-4.82012	-4.63439
PSMA1	-5.35441	-5.39616	*AQR*	-4.81733	-5.38519
PSMA2	-5.35385	-5.55217	*CDK11A*	-4.80112	-3.6647
IK	-5.34288	-5.16901	~~*RPL10P9*~~	-4.7949	-4.35231
NHP2L1	-5.25718	-5.46258	*DDX19B*	-4.77101	-5.18705
NUP98	-5.23075	-4.98074	*EFTUD2*	-4.76826	-5.024
SFPQ	-5.22707	-4.73729	~~*RPL7AP66*~~	-4.74473	-3.7798
KPNB1	-5.22132	-5.62868	*RPS2*	-4.73204	-4.29219
PSMB4	-5.20831	-4.66094	*PPP1R12A*	-4.7105	-4.50192
RRM1	-5.20259	-5.54974	*PRPF31*	-4.69727	-5.04935
PSMD14	-5.18541	-5.52414	~~*RPL27AP6*~~	-4.66046	-4.03636
PLK1	-5.17226	-5.40492	*SF3A3*	-4.64675	-4.48556
NAPA	-5.17009	-5.59728	*NUP107*	-4.63844	-2.48775
PRPF8	-5.16702	-4.82449	*TUBA1B*	-4.6224	-3.4323
NDE1	-5.16352	-3.62667	*SF3B14*	-4.60961	-4.99473
CWC22	-5.15621	-5.31734	*SAP30BP*	-4.58968	-3.39838
CDC5L	-5.13775	-5.21408	~~*RPS3AP49*~~	-4.58551	-4.47959
TUBA1C	-5.11096	-5.06481	~~*RPL10P16*~~	-4.57257	-3.96157
CRNKL1	-5.10685	-4.83685	*LAMTOR2*	-4.5666	-1.77647
NUP205	-5.1004	-5.05423	*COPB2*	-4.53416	-5.245
SLU7	-4.5314	-4.418	*NUP54*	-4.36745	-4.08071
KIF11	-4.53001	-5.14719	*CCT6A*	-4.36478	-2.25553
COPA	-4.52909	-5.19966	*PSMD3*	-4.36146	-4.10593
RPL5	-4.51974	-4.51776	*PSMA5*	-4.3585	-4.25705
~~*RPL34P34*~~	-4.51521	-4.03996	*CCT7*	-4.3459	-3.53508

PSMD1	-4.50312	-3.96183	*SF3B4*	-4.34323	-4.77446
SALL1	-4.49941	-4.09468	*RPL32*	-4.34158	-4.12735
DDX19A	-4.49384	-4.49564	*ARL14*	-4.3279	-3.98336
SF3A1	-4.4823	-4.55114	*RPA1*	-4.32281	-3.83704
~~*RPL21P131*~~	-4.46961	-3.90377	*NUPL1*	-4.31378	-4.95382
USP39	-4.46911	-5.10536	*UBA52*	-4.30766	-4.02865
POLR2G	-4.46815	-4.5492	*U2AF2*	-4.30366	-5.17065
CACTIN	-4.46802	-2.55534	*RPL23*	-4.30002	-4.74026
FAU	-4.46451	-4.60391	*RPL10*	-4.29735	-3.96828
RPL14	-4.45781	-4.74982	*RPL37A*	-4.28498	-4.34787
NDC80	-4.45705	-3.77319	~~*RPL13P12*~~	-4.28334	-3.76244
EIF3G	-4.44909	-4.51661	*MC3R*	-4.26904	-4.4465
PSMC3	-4.44863	-4.20072	*PRPF19*	-4.26537	-3.6963
PSMA3	-4.44219	-3.4974	*PSMC5*	-4.26407	-3.88193
PSMA7	-4.43973	-4.28468	*EIF3B*	-4.25466	-4.53688
PSMB3	-4.43579	-4.27193	*NUP133*	-4.25221	-3.54633
XPO1	-4.42173	-4.44439	*EIF3A*	-4.24815	-4.38296
PSMC4	-4.42046	-4.16654	*SNW1*	-4.24653	-2.70467
PSMA6	-4.41855	-4.17843	*PSMB7*	-4.22816	-3.73567
POLR2C	-4.41505	-4.64191	*LSM2*	-4.21879	-3.38172
RPS5	-4.41094	-4.59819	*U2AF1*	-4.21601	-4.70368
DHX8	-4.40322	-4.84879	*NAA38*	-4.20897	-3.91765
XAB2	-4.38182	-3.19336	*EIF3C*	-4.20022	-4.34413
PSMB1	-4.37693	-4.18678	*RPS21*	-4.19926	-4.18601
PSMA4	-4.37554	-4.20789	*RPSA*	-4.1931	-4.62853
PRPF18	-4.37316	-4.03921	*CDC40*	-4.1912	-4.59492
LSM4	-4.18955	-4.63768	*POLR2F*	-3.97248	-4.63541
HNRNPC	-4.18137	-3.6349	*CWC15*	-3.97079	-4.20563
RPS19	-4.17772	-4.16768	*AHSP*	-3.94583	-2.73814
RPS29	-4.17771	-4.20697	*LSM7*	-3.94433	-4.75632
RPL37	-4.16028	-3.7196	*NUF2*	-3.94411	-4.43776
~~*RPS27AP5*~~	-4.15972	-2.42563	*SNRPB*	-3.94347	-4.01507
RPL13A	-4.15771	-3.90688	*COPZ1*	-3.93575	-5.26647
POLR2B	-4.15419	-4.63513	*SF3B1*	-3.93496	-3.78079
BUB3	-4.14868	-4.56291	*RPL35*	-3.9315	-2.36514
SRSF3	-4.1386	-3.68395	*ZNF226*	-3.90507	-2.10212
PSMB6	-4.10833	-2.34691	*SNRPD3*	-3.8864	-3.66706
PSMC6	-4.10599	-3.8238	*RPL10A*	-3.88157	-4.08143
~~*RPL18AP6*~~	-4.09827	-3.86608	*SYF2*	-3.86018	-4.57029

RPS16	-4.07727	-4.2704	*PSMB2*	-3.85783	-0.56549
CCT8	-4.07699	-4.15271	*VPRBP*	-3.85519	-4.08385
~~RPSAP47~~	-4.06176	-2.7617	*RPL18*	-3.83778	-3.79292
CCT4	-4.05637	-4.17708	*RPS3*	-3.82288	-3.38401
SNRPD1	-4.05544	-3.70442	*MFAP1*	-3.81372	-2.82928
SNRPD2	-4.05534	-3.7091	*ISY1*	-3.79463	-3.08057
RPS4X	-4.04588	-4.25448	*RPS9*	-3.78503	-4.13385
MBNL3	-4.04061	-1.84677	*RPL7A*	-3.78228	-3.39616
PSMD12	-4.0311	-3.67055	*DDX18*	-3.76789	-3.65996
EIF3I	-4.02673	-4.06242	*PPP1CB*	-3.76768	-3.12307
~~RPSAP55~~	-4.01905	-2.63344	*BIRC5*	-3.75777	-4.7303
AHSP	-4.00858	-2.76125	*PSMD11*	-3.74687	-0.6058
WEE1	-4.00265	-1.93392	*NKAP*	-3.7436	-3.04365
CHMP2A	-3.99967	-4.2446	*RPA2*	-3.74069	-3.40877
PHF5A	-3.99691	-3.64536	*RPAP2*	-3.73795	-0.96694
RPL36	-3.99312	-4.25147	*RPL7*	-3.71627	-3.32812
ARCN1	-3.98751	-4.66428	*POLR2E*	-3.71422	-3.71029
RPL11	-3.98013	-3.97839	*WBP11*	-3.7094	-4.362
RPL27A	-3.70416	-3.66061	*BCAS2*	-3.42788	-1.68012
RPS26	-3.69456	-3.3679	*RPL35A*	-3.42737	-3.35818
RPL15	-3.6499	-3.56077	*RPS13*	-3.42674	-3.11404
SF3B3	-3.63683	-3.18921	*RSL24D1*	-3.42289	-2.80722
CNKSR1	-3.63238	-1.93786	*RPL17*	-3.41929	-3.51489
RPS18	-3.61607	-3.50346	*RPS12*	-3.4098	-3.31502
POLR2L	-3.60844	-2.32363	*LSM6*	-3.40745	-3.87706
RPL4	-3.5919	-3.27891	*RPL9*	-3.40636	-3.14568
RPL21	-3.5908	-3.49151	*RPS15*	-3.40579	-3.31709
OSCP1	-3.56431	-1.86733	*PSMC1*	-3.40513	0.12177
SLC22A6	-3.5643	-1.364	*RPS28*	-3.40369	-3.19147
RPL38	-3.55179	-3.25076	*PSMC2*	-3.40056	-3.49359
FBL	-3.55154	-4.12298	*NSA2*	-3.39431	-3.06043
HLA-G	-3.55088	-1.74882	*SNRPA1*	-3.39006	-3.50471
RPS15A	-3.5411	-3.28907	*GPKOW*	-3.38527	-0.7254
CCDC12	-3.53676	-1.35877	*RPL34*	-3.38459	-3.69177
SEC13	-3.52486	-2.56989	*RRN3*	-3.38029	-2.6144
CSE1L	-3.51999	-1.21072	*UBL5*	-3.37968	-1.77381
RPL30	-3.50247	-3.50074	*RPS27*	-3.37699	-3.41004
RPL23A	-3.50183	-3.44842	*GSPT1*	-3.3722	-2.54729
RPL19	-3.49258	-3.46879	*RPL3*	-3.36216	-3.25888

RPS27A	-3.4866	-3.2748	*ODC1*	-3.35787	-3.18052
RPL27	-3.48419	-3.29306	*EIF2S2*	-3.34019	-2.54754
RPL8	-3.48127	-3.29859	*PKN3*	-3.34003	-1.69712
PDPN	-3.47426	-0.83012	*RPL22L1*	-3.33446	-2.41264
SNRPE	-3.46083	-2.8197	*MAK16*	-3.32075	-1.77161
RPL26	-3.45933	-3.37877	*RPL18A*	-3.3117	-3.27266
RPL6	-3.45565	-3.1967	*NUP155*	-3.29816	-1.31258
CCT2	-3.45376	-1.6505	*WDR43*	-3.29419	-3.05882
SF3A2	-3.43544	-1.99117	*RPLP0*	-3.28777	-2.86059
RPS23	-3.43473	-3.35288	*RPL29*	-3.28767	0.770134
RPS24	-3.287	-3.25421	*HES4*	-3.09865	-1.43476
SNRNP70	-3.28438	-3.38637	*RPS6*	-3.09136	-2.97638
TPX2	-3.28207	-3.7239	*TTC33*	-3.09075	-0.85596
KIF18A	-3.28058	-3.15388	*TNKS1BP1*	-3.0896	-1.07485
RPS20	-3.27639	-3.05256	*MAD2L1*	-3.0895	-3.99701
RPS7	-3.25055	-3.33207	*CIT*	-3.08478	-1.28655
ERH	-3.24954	-2.38287	*LSM3*	-3.08319	-3.70565
RPS8	-3.24875	-3.26226	*SUPT6H*	-3.05493	-3.7802
POLR2D	-3.2421	-2.84064	*NUP160*	-3.05324	-2.34943
RPS17	-3.23687	-2.86194	*KIF23*	-3.05278	-4.95022
RBM25	-3.23137	-0.83646	*HRK*	-3.0477	-1.10443
PLRG1	-3.22625	-1.34707	*FCF1*	-3.0451	-2.05344
RPL13	-3.20151	-2.92355	*UTP11L*	-3.04385	-2.13965
DNTTIP2	-3.20097	-2.85365	*GTPBP4*	-3.02134	-2.61845
RPS11	-3.19637	-3.25296	*MPHOSPH10*	-3.02092	-3.89715
HSPB1	-3.19009	-1.41258	*CDCA8*	-2.99987	-4.2881
RPS10	-3.18814	-3.17446	*SEH1L*	-2.99835	-1.08566
RPS14	-3.1837	-2.92964	*PCF11*	-2.98353	0.124074
RPL12	-3.17244	-2.91723	*DYNC1H1*	-2.97684	-2.40859
EIF3E	-3.15854	-4.64314	*DYNC1I2*	-2.9731	-2.32926
GBF1	-3.15757	-4.52469	~~*LOC402634*~~	-2.96686	-1.10273
~~*RPL32P36*~~	-3.15591	-0.42628	*RIOK1*	-2.96251	-1.07415
LCOR	-3.15493	-1.30516	*CDK18*	-2.95275	-0.45631
EIF2S1	-3.14387	-2.53745	*RPL24*	-2.94853	-2.91952
RPL31	-3.14163	-3.22043	*ETF1*	-2.93256	-2.76412
MT-ND3	-3.12292	-2.69748	*AMD1*	-2.92269	-1.55773
~~*LOC342293*~~	-3.12132	-1.71652	*NAT8B*	-2.91406	-0.58708
RPS3A	-3.11813	-2.98556	*PRPF40A*	-2.9055	-1.59367
POLR2I	-3.10721	-4.08045	*UTP6*	-2.89984	-2.91732

EIF2S3	-3.10544	-2.71673	*DDX10*	-2.6833	-2.75838
NCKAP5L	-3.09898	-0.6666	*BUB1B*	-2.64244	-3.59129
HIVEP3	-2.88088	-1.36203	*ARFGEF1*	-2.59446	-3.2245
RNPS1	-2.86538	-1.60425	*RPA3*	-2.57625	-2.83321
NOL7	-2.86389	-2.1014	*INCENP*	-2.54131	-3.68783
POLR1A	-2.84646	-2.31081	*Nop56*	-2.52621	-3.58817
WDR46	-2.84483	-3.13331	*MED14*	-2.42438	-4.11114
ANLN	-2.83465	-4.29108	*EIF3D*	-2.40932	-3.84617
UTP18	-2.82979	-2.75227	*WBSCR22*	-2.38471	-3.01754
ZNF490	-2.82332	-0.79394	*CENPE*	-2.33124	-3.23085
CEBPD	-2.81121	-2.30453	*LSM5*	-2.30286	-2.8874
MKI67IP	-2.80228	-2.39001	*TOP2A*	-2.19964	-3.44265
POLR1B	-2.79905	-2.22851	*POLR2J*	-2.07677	-2.95576
RACGAP1	-2.79308	-3.95117	*ISCU*	-2.89871	-2.96603
DDB1	-2.78793	-3.28431	*COPB1*	-2.89675	-2.45801
COL20A1	-2.77789	-1.17492	*EIF1AX*	-1.783	-2.88085
PRPF38A	-2.77126	-1.15455	*NUP153*	-1.54594	-3.71684
SSPN	-2.75469	-1.32844	*C8ORF59*	-1.13145	-3.18123
CDK1	-2.7541	-4.07291	*SKA3*	-0.73493	-3.1998
ATP6V0C	-2.74598	-3.18941	*GPX4*	-0.15914	-3.09123

Supplementary Table 2. Annotation cluster analysis of hits with Z-scores < 2.75 in FA and FA-corrected HNSCC cell lines

Term	Count	P value
Annotation cluster 1 (enrichment score: 45.358)		
GO:0006396; RNA processing	93	1.42E-39
GO:0008380; RNA splicing	70	2.41E-36
GO:0006397; mRNA processing	69	2.64E-31
GO:0016071; mRNA metabolic process	71	3.19E-29
GO:0000375; RNA splicing, via transesterification reactions	48	1.03E-26
GO:0000377; RNA splicing, via transesterification reactions with bulged adenosine as nucleophile	48	1.03E-26
GO:0000398; nuclear mRNA splicing, via spliceosome	48	1.03E-26
Annotation cluster 2 (enrichment score 22.828)		
GO:0031145; anaphase-promoting complex-dependent proteasomal ubiquitin-dependent protein catabolic process	36	5.78E-26
GO:0051439; regulation of ubiquitin-protein ligase activity during mitotic cell cycle	37	7.73E-26
GO:0051436; negative regulation of ubiquitin-protein ligase activity during mitotic cell cycle	35	3.16E-23
GO:0051438; regulation of ubiquitin-protein ligase activity	37	6.57E-24
GO:0051352; negative regulation of ligase activity	35	1.27E-22
GO:0051444; negative regulation of ubiquitin-protein ligase activity	35	1.27E-22
GO:0031397; negative regulation of protein ubiquitination	36	2.51E-23
GO:0051340; regulation of ligase activity	37	3.72E-23
GO:0051437; positive regulation of ubiquitin-protein ligase activity during mitotic cell cycle	34	1.17E-20
GO:0051443; positive regulation of ubiquitin-protein ligase activity	34	4.07E-21
GO:0031396; regulation of protein ubiquitination	38	1.36E-19
GO:0051351; positive regulation of ligase activity	34	2.41E-19
GO:0000278; mitotic cell cycle	60	1.26E-18
GO:0031398; positive regulation of protein ubiquitination	34	7.50E-18
GO:0043161; proteasomal ubiquitin-dependent protein catabolic process	36	2.31E-16
GO:0010498; proteasomal protein catabolic process	36	2.31E-16
GO:0031400; negative regulation of protein modification process	36	1.04E-13
GO:0032269; negative regulation of cellular protein metabolic process	38	2.97E-09
GO:0022402; cell cycle process	62	3.22E-09
GO:0051248; negative regulation of protein metabolic process	38	1.24E-08
GO:0006511; ubiquitin-dependent protein catabolic process	38	1.40E-04
GO:0031401; positive regulation of protein modification process	34	1.95E-04
GO:0007049; cell cycle	65	3.92E-04
GO:0032270; positive regulation of cellular protein metabolic process	35	2.46E-03

GO:0051247; positive regulation of protein metabolic process	35	9.31E-03
GO:0043086; negative regulation of catalytic activity	37	1.10E-01
GO:0031399; regulation of protein modification process	38	1.24E-01
GO:0032268; regulation of cellular protein metabolic process	47	3.01E-01
GO:0044092; negative regulation of molecular function	39	1.19E+00
GO:0044265; cellular macromolecule catabolic process	48	5.35E+05
GO:0043085; positive regulation of catalytic activity	39	1.55E+06
GO:0009057; macromolecule catabolic process	48	6.44E+05
GO:0019941; modification-dependent protein catabolic process	40	7.34E+05
GO:0043632; modification-dependent macromolecule catabolic process	40	7.34E+05
GO:0051603; proteolysis involved in cellular protein catabolic process	40	2.60E+06
GO:0010605; negative regulation of macromolecule metabolic process	45	2.73E+06
GO:0044257; cellular protein catabolic process	40	2.99E+07
GO:0044093; positive regulation of molecular function	39	4.52E+07
GO:0030163; protein catabolic process	40	7.06E+06
GO:0010604; positive regulation of macromolecule metabolic process	40	2.30E+10
GO:0006508; proteolysis	40	0.00154
Annotation cluster 3 (enrichment score 20.134)		
GO:0022613; ribonucleoprotein complex biogenesis	46	1.41E-19
GO:0042254; ribosome biogenesis	32	2.84E-08
GO:0016072; rRNA metabolic process	27	2.67E-05
GO:0006364; rRNA processing	26	1.46E-05
GO:0034470; ncRNA processing	26	7.65E+02
GO:0034660; ncRNA metabolic process	27	1.32E+05
Annotation cluster 4 (Enrichment score 8.869)		
GO:0022618; ribonucleoprotein complex assembly	17	2.06E+04
GO:0043933; macromolecular complex subunit organization	45	9.83E+05
GO:0034621; cellular macromolecular complex subunit organization	30	2.49E+07
GO:0065003; macromolecular complex assembly	41	1.43E+08
GO:0034622; cellular macromolecular complex assembly	26	6.28E+07
Annotation cluster 5 (enrichment score 8.327)		
GO:0000278; mitotic cell cycle	60	1.26E-18
GO:0022402; cell cycle process	62	3.22E-09
GO:0000087; M phase of mitotic cell cycle	25	2.56E+06
GO:0000280; nuclear division	24	9.96E+05
GO:0007067; mitosis	24	9.96E+05
GO:0048285; organelle fission	24	2.19E+07
GO:0000279; M phase	27	3.04E+06
GO:0022403; cell cycle phase	29	2.37E+09

GO:0051301; cell division	24	2.48E+09
GO:0007059; chromosome segregation	11	1.37E+10
GO:0007052; mitotic spindle organization	5	2.88E+12
GO:0000226; microtubule cytoskeleton organization	11	0.00188
GO:0007051; spindle organization	6	0.00334
GO:0007018; microtubule-based movement	9	0.00411
GO:0007017; microtubule-based process	14	0.00503
GO:0007010; cytoskeleton organization	13	0.28429
Annotation cluster 6 (enrichment score 4.756)		
GO:0051236; establishment of RNA localization	20	4.42E+02
GO:0050658; RNA transport	20	4.42E+02
GO:0050657; nucleic acid transport	20	4.42E+02
GO:0006403; RNA localization	20	7.89E+02
GO:0015931; nucleobase, nucleoside, nucleotide and nucleic acid transport	20	7.71E+03
GO:0051028; mRNA transport	18	8.09E+03
GO:0006913; nucleocytoplasmic transport	17	4.85E+08
GO:0051169; nuclear transport	17	5.77E+08
GO:0051168; nuclear export	8	3.91E+11
GO:0000059; protein import into nucleus, docking	5	4.84E+12
GO:0006606; protein import into nucleus	9	7.19E+11
GO:0051170; nuclear import	9	8.38E+11
GO:0034504; protein localization in nucleus	9	0.00129
GO:0045184; establishment of protein localization	32	0.00130
GO:0006405; RNA export from nucleus	6	0.00220
GO:0015031; protein transport	31	0.00221
GO:0046907; intracellular transport	27	0.00403
GO:0006886; intracellular protein transport	18	0.00517
GO:0008104; protein localization	33	0.00550
GO:0006406; mRNA export from nucleus	5	0.00626
GO:0017038; protein import	9	0.00982
GO:0034613; cellular protein localization	18	0.01239
GO:0070727; cellular macromolecule localization	18	0.01313
GO:0033365; protein localization in organelle	9	0.01795
GO:0006605; protein targeting	11	0.02451
GO:0043623; cellular protein complex assembly	9	0.03102
GO:0055085; transmembrane transport	17	0.21988
Annotation cluster 7 (enrichment score 4.676)		
GO:0000245; spliceosome assembly	10	2.45E+08
GO:0000389; nuclear mRNA 3'-splice site recognition	4	1.11E+12

GO:0006376; mRNA splice site selection	4	0.00347
Annotation cluster 8 (enrichment score 3.875)		
GO:0051656; establishment of organelle localization	13	4.03E+07
GO:0051640; organelle localization	13	1.04E+08
GO:0048200; Golgi transport vesicle coating	6	1.32E+10
GO:0048194; Golgi vesicle budding	6	1.32E+10
GO:0048205; COPI coating of Golgi vesicle	6	1.32E+10
GO:0048199; vesicle targeting, to, from or within Golgi	6	3.98E+09
GO:0006901; vesicle coating	6	1.43E+11
GO:0006900; membrane budding	6	2.04E+10
GO:0006890; retrograde vesicle-mediated transport, Golgi to ER	6	8.66E+10
GO:0006903; vesicle targeting	6	1.10E+12
GO:0051650; establishment of vesicle localization	6	8.09E+11
GO:0051648; vesicle localization	6	0.00137
GO:0016050; vesicle organization	6	0.00625
GO:0006891; intra-Golgi vesicle-mediated transport	4	0.00849
GO:0048193; Golgi vesicle transport	8	0.02932
GO:0016044; membrane organization	8	0.76311
GO:0016192; vesicle-mediated transport	9	0.95217
Annotation cluster 9 (enrichment score 3.478)		
GO:0006368; RNA elongation from RNA polymerase II promoter	10	1.06E+09
GO:0006354; RNA elongation	10	1.82E+10
GO:0006367; transcription initiation from RNA polymerase II promoter	11	2.76E+10
GO:0006352; transcription initiation	11	1.71E+11
GO:0006461; protein complex assembly	24	0.00116
GO:0070271; protein complex biogenesis	24	0.00116
GO:0006366; transcription from RNA polymerase II promoter	14	0.00262
GO:0006351; transcription, DNA-dependent	15	0.00677
GO:0032774; RNA biosynthetic process	15	0.00757
GO:0006350; transcription	31	0.99880
Annotation cluster 10 (enrichment score 2.672)		
GO:0007059; chromosome segregation	11	1.37E+10
GO:0050000; chromosome localization	5	2.88E+12
GO:0051303; establishment of chromosome localization	5	2.88E+12
GO:0000070; mitotic sister chromatid segregation	6	0.00122
GO:0000819; sister chromatid segregation	6	0.00138
GO:0007080; mitotic metaphase plate congression	3	0.01653
GO:0051310; metaphase plate congression	3	0.02451
GO:0051276; chromosome organization	12	0.54003

References

1. Auerbach, A. D. Fanconi anemia and its diagnosis. Mutat. Res. 668, 4–10 (2009).
2. Kutler, D. I. *et al.* A 20-year perspective on the International Fanconi Anemia Registry (IFAR). Blood 101, 1249–56 (2003).
3. Butturini, A. *et al.* Hematologic abnormalities in Fanconi anemia: an International Fanconi Anemia Registry study. Blood 84, 1650–5 (1994).
4. Scheckenbach, K., Wagenmann, M., Freund, M., Schipper, J. & Hanenberg, H. Squamous cell carcinomas of the head and neck in Fanconi anemia: risk, prevention, therapy, and the need for guidelines. Klin. Pädiatrie 224, 132–8 (2012).
5. Alter, B. P., Greene, M. H., Velazquez, I. & Rosenberg, P. S. Cancer in Fanconi anemia. Blood 101, 2072 (2003).
6. Kutler, D. I. *et al.* High incidence of head and neck squamous cell carcinoma in patients with Fanconi anemia. Arch. Otolaryngol. Head. Neck Surg. 129, 106–12 (2003).
7. Rosenberg, P. S., Greene, M. H. & Alter, B. P. Cancer incidence in persons with Fanconi anemia. Blood 101, 822–6 (2003).
8. Kottemann, M. C. & Smogorzewska, A. Fanconi anaemia and the repair of Watson and Crick DNA crosslinks. Nature 493, 356–63 (2013).
9. Walden, H. & Deans, A. J. The Fanconi anemia DNA repair pathway: structural and functional insights into a complex disorder. Annu. Rev. Biophys. 43, 257–78 (2014).
10. Domchek, S. M. *et al.* Biallelic deleterious BRCA1 mutations in a woman with early-onset ovarian cancer. Cancer Discov. 3, 399–405 (2013).
11. Hanahan, D. & Weinberg, R. A. Hallmarks of cancer: the next generation. Cell 144, 646–74 (2011).
12. Hanahan, D. & Weinberg, R. A. The hallmarks of cancer. Cell 100, 57–70 (2000).
13. Stecklein, S. R. & Jensen, R. A. Identifying and exploiting defects in the Fanconi anemia/BRCA pathway in oncology. Transl. Res. 160, 178–97 (2012).
14. Valeri, A., Martínez, S., Casado, J. A. & Bueren, J. A. Fanconi anaemia: from a monogenic disease to sporadic cancer. Clin. Transl. Oncol. 13, 215–21 (2011).
15. Martens-de Kemp, S. R. *et al.* Functional genetic screens identify genes essential for tumor cell survival in head and neck and lung cancer. Clin. Cancer Res. 19, 1994–2003 (2013).
16. Shields, D. J. *et al.* RBBP9: a tumor-associated serine hydrolase activity required for pancreatic neoplasia. Proc. Natl. Acad. Sci. U. S. A. 107, 2189–94 (2010).
17. Woitach, J. T., Zhang, M., Niu, C. H. & Thorgeirsson, S. S. A retinoblastoma-binding protein that affects cell-cycle control and confers transforming ability. Nat. Genet. 19, 371–4 (1998).
18. Jones, D. T. *et al.* Endogenous ribosomal protein L29 (RPL29): a newly identified regulator of angiogenesis in mice. Dis. Model. Mech. 6, 115–24 (2013).
19. Li, C., Ge, M., Yin, Y., Luo, M. & Chen, D. Silencing expression of ribosomal protein L26 and L29 by RNA interfering inhibits proliferation of human pancreatic cancer PANC-1 cells. Mol. Cell. Biochem. 370, 127–39 (2012).
20. Deng, S. *et al.* Over-expression of genes and proteins of ubiquitin specific peptidases (USPs) and proteasome subunits (PSs) in breast cancer tissue observed by the methods of RFDD-PCR and proteomics. Breast Cancer Res. Treat. 104, 21–30 (2007).
21. Qi, T. *et al.* Proteomic profiling identified multiple short-lived members of the central proteome as the direct targets of the addicted oncogenes in cancer cells. Mol. Cell. Proteomics 13, 49–62 (2014).
22. Marshansky, V., Rubinstein, J. L. & Grüber, G. Eukaryotic V-ATPase: novel structural findings and functional insights. Biochim. Biophys. Acta 1837, 857–79 (2014).
23. Sun-Wada, G.-H. & Wada, Y. Vacuolar-type proton pump ATPases: acidification and pathological relationships. Histol. Histopathol. 28, 805–15 (2013).
24. Fogarty, F. M. *et al.* HRG-1 enhances cancer cell invasive potential and couples glucose metabolism to cytosolic/extracellular pH gradient regulation by the vacuolar-H(+) ATPase. Oncogene 33, 4653–63 (2014).
25. Daniel, C. *et al.* The role of proton dynamics in the development and maintenance of multidrug resistance in cancer. Biochim. Biophys. Acta 1832, 606–17 (2013).
26. Estrella, V. *et al.* Acidity generated by the tumor microenvironment drives local invasion. Cancer Res. 73, 1524–35 (2013).
27. Fais, S., De Milito, A., You, H. & Qin, W. Targeting vacuolar H+-ATPases as a new strategy against cancer. Cancer Res. 67, 10627–30 (2007).
28. Neri, D. & Supuran, C. T. Interfering with pH regulation in tumours as a therapeutic strategy. Nat. Rev. Drug Discov. 10, 767–77 (2011).
29. Raghunand, N. & Gillies, R. J. pH and drug resistance in tumors. Drug Resist. Updat. 3, 39–47 (2000).
30. Rofstad, E. K., Mathiesen, B., Kindem, K. & Galappathi, K. Acidic extracellular pH promotes experimental metastasis of human melanoma cells in athymic nude mice. Cancer Res. 66, 6699–

707 (2006).
31. Simon, S., Roy, D. & Schindler, M. Intracellular pH and the control of multidrug resistance. Proc. Natl. Acad. Sci. U. S. A. 91, 1128–32 (1994).
32. Kitagawa, M. & Lee, S. H. The chromosomal passenger complex (CPC) as a key orchestrator of orderly mitotic exit and cytokinesis. Front. cell Dev. Biol. 3, 14 (2015).
33. Lara-Gonzalez, P., Westhorpe, F. G. & Taylor, S. S. The spindle assembly checkpoint. Curr. Biol. 22, R966–80 (2012).
34. Jelluma, N. *et al.* Mps1 phosphorylates Borealin to control Aurora B activity and chromosome alignment. Cell 132, 233–46 (2008).
35. Landi, M. T. *et al.* Gene expression signature of cigarette smoking and its role in lung adenocarcinoma development and survival. PLoS One 3, e1651 (2008).
36. Daniel, J., Coulter, J., Woo, J.-H., Wilsbach, K. & Gabrielson, E. High levels of the Mps1 checkpoint protein are protective of aneuploidy in breast cancer cells. Proc. Natl. Acad. Sci. U. S. A. 108, 5384–9 (2011).
37. Yuan, B. *et al.* Increased expression of mitotic checkpoint genes in breast cancer cells with chromosomal instability. Clin. Cancer Res. 12, 405–10 (2006).
38. Salvatore, G. *et al.* A cell proliferation and chromosomal instability signature in anaplastic thyroid carcinoma. Cancer Res. 67, 10148–58 (2007).
39. Colombo, R. *et al.* Targeting the mitotic checkpoint for cancer therapy with NMS-P715, an inhibitor of MPS1 kinase. Cancer Res. 70, 10255–64 (2010).
40. Stoepker, C. *et al.* DNA helicases FANCM and DDX11 are determinants of PARP inhibitor sensitivity. DNA Repair (Amst). 26, 54–64 (2015).
41. Hoelz, A., Debler, E. W. & Blobel, G. The structure of the nuclear pore complex. Annu. Rev. Biochem. 80, 613–43 (2011).
42. Ibarra, A. & Hetzer, M. W. Nuclear pore proteins and the control of genome functions. Genes Dev. 29, 337–349 (2015).
43. Strambio-De-Castillia, C., Niepel, M. & Rout, M. P. The nuclear pore complex: bridging nuclear transport and gene regulation. Nat. Rev. Mol. Cell Biol. 11, 490–501 (2010).
44. Köhler, A. & Hurt, E. Gene regulation by nucleoporins and links to cancer. Mol. Cell 38, 6–15 (2010).
45. Simon, D. N. & Rout, M. P. Cancer and the nuclear pore complex. Adv. Exp. Med. Biol. 773, 285–307 (2014).
46. Xu, S. & Powers, M. A. Nuclear pore proteins and cancer. Semin. Cell Dev. Biol. 20, 620–30 (2009).
47. Van Zeeburg, H. J. T. *et al.* Generation and molecular characterization of head and neck squamous cell lines of fanconi anemia patients. Cancer Res. 65, 1271–6 (2005).
48. Zhang, J., Chung, T. & Oldenburg, K. A Simple Statistical Parameter for Use in Evaluation and Validation of High Throughput Screening Assays. J. Biomol. Screen. 4, 67–73 (1999).
49. Y Benjamini, Y. H. Controlling the False Discovery Rate: A Practical and Powerful Approach to Multiple Testing. J. R. Stat. Soc. Ser. B 57, 289–300 (1995).

CHAPTER 8

Discussion

Fanconi anemia (FA) is a rare genomic instability syndrome characterized by a plethora of congenital malformations, bone marrow failure and a high risk to develop cancer, in particular acute myeloid leukemia and squamous cell carcinomas of the head and neck region[1]. Given the remarkable sensitivity of FA cells to a specific group of chemotherapeutic drugs (i.e. DNA interstrand crosslinking (ICL) agents)[2,3], many studies have been performed to unravel the molecular mechanism that explains this phenotype. This led to insights into chemotherapy response and the discovery of 17 currently known FA genes (see also **Chapter 1-4**), of which the encoding proteins function in the FA pathway to repair DNA crosslinks[4–8]. Although our knowledge of FA is increasing, it is still not clear why FA patients specifically develop head and neck tumors and whether the inactivation of the FA pathway is involved in the etiology of head and neck squamous cell carcinoma (HNSCC) in non-FA individuals. In this thesis, we addressed this last question by examining the occurrence of FA pathway inactivation in cell lines of head and neck tumors of individuals without FA. Moreover, we also investigated whether FA defects can be exploited as a target in cancer therapy.

The extremely high risk to develop head and neck cancer in FA patients[9], suggests that inactivation of the FA pathway drives carcinogenesis. The finding that HNSCC cell lines derived from FA patients were indistinguishable from those derived from non-FA patients in terms of whole-arm translocations and numerous gains and losses[10,11], may suggest that a deficient FA pathway also drives carcinogenesis in squamous cells of the head and neck region in non-FA patients. In agreement with this, we showed in **Chapter 5** that more than half (53%) of the sporadic HNSCC cell lines tested have a typical FA feature: sensitivity to crosslinking agents in terms of ICL-induced chromosomal breakage. However, we also found that inactivation of the FA pathway is rare in sporadic HNSCC (**Chapter 5**), and only a few sequence variants in some FA genes (i.e. *BRCA1*, *BRCA2*, *FANCM* and *SLX4*) were found by whole exome sequencing of large groups of head and neck tumors[12,13]. Based upon these results, we think it is unlikely that FA pathway inactivation is a frequent driver of carcinogenesis in non-FA patients, albeit FA-like features frequently occur.

Since the occurrence of FA defects is rare, other mechanisms may be involved in chromosomal instability in sporadic HNSCC. Of note, ICL-induced chromosomal breakage is not exclusively a hallmark of FA cells and has been observed in lymphoblasts or T lymphocytes from individuals with other diseases, such as Nijmegen breakage syndrome, Roberts syndrome or Warsaw breakage syndrome[14–18]. The last two syndromes (belonging to a group of diseases collectively known as cohesinopathies) are caused by mutations in *ESCO2* or *DDX11*, respectively[17,19]. Cells derived from Roberts or Warsaw breakage syndrome patients are in addition to ICL sensitivity, characterized by sister chromatid cohesion defects (premature separation of chromatids during mitosis)[17–20]. Severe sister chromatid cohesion

defects were also observed in 5 HNSCC cell lines (**Chapter 5**). In one of these cell lines, the severe sister chromatid cohesion defect could be explained by mutations in *STAG2*, whereas in another cell line with less severe cohesion defects mutations in *PDS5A* were found. Whether inactivation of these genes results in increased ICL-induced chromosomal breakage should be further tested by functional studies. Notably, inactivation of STAG2 has been observed in several tumor types[21]. One study showed that STAG2 knockdown in a pancreatic adenocarcinoma cell line increased sensitivity to the ICL-inducing chemotherapeutic agent cisplatin[22], while another study showed that STAG2-deficiency was associated with PARP inhibitor sensitivity in glioblastoma cells[23]. These results suggest that tumors with defective sister chromatid cohesion may respond well to treatment with cisplatin or PARP inhibitor. Considering the potential to exploit sister chromatid cohesion defects as a target in anti-cancer therapy in HNSCC, further research is required to 1) verify that tumors with defective sister chromatid cohesion have a favorable response to cisplatin treatment (or chemoradiation) and 2) if this is the case, it would be relevant to determine whether screening for sequence variants in genes involved in sister chromatid cohesion predict response.

The observed ICL-induced chromosomal breakage may also be caused by overexpression of oncogenes, such as cyclin E, viral oncogene E7 and CDC25A. Overexpression of these oncogenes accelerates progression from G1 to S phase of the cell cycle, resulting in oncogene-induced replication stress (recently defined as slowing or stalling of replication fork progression and/or DNA synthesis[24]) and has been found associated with the formation of DNA double strand breaks[25–28]. Oncogene-induced replication stress activates the DNA damage response, which is an important barrier against malignant transformation in precancerous lesions. Stalling or slowing down of replication forks is likely due to limiting nucleotide concentrations[29], increased DNA torsional stress[30], the interference between transcription and DNA replication[31] or exhausted RPA protein levels[32]. As a consequence, replication forks collapse and massive chromosomal breakage occurs upon a persistent G2/M arrest or premature mitotic entry[33]. Likewise, increased DNA damage due to defective ICL-repair results in enhanced replication stress and consequently FA-deficient cells are persistently arrested in G2/M with extensive chromosomal breakage. Interestingly, some of the ICL-sensitive HNSCC cell lines in terms of ICL-induced chromosomal breakage did not arrest in the G2/M phase of the cell cycle upon treatment with ICL agents, indicating that the cells continue growing in the presence of DNA damage. The absence of an ICL-induced G2/M arrest may lie in a defective G2/M phase checkpoint, resulting in premature mitosis. This in combination with elevated replication stress due to overexpression of oncogenes and increased DNA damage caused by ICL-inducing agents may explain the observed ICL-induced chromosomal breakage in these cell lines. Thus, other mechanisms

such as sister chromatid cohesion defects and oncogene-induced replication stress in combination with a G2/M checkpoint defect might be responsible for the observed ICL-induced chromosomal breakage in sporadic HNSCC cell lines.

Mutations in the tumor suppressor gene *TP53* and loss of *CDKN2A* ($p16^{Ink4a}$) are the earliest and most frequently detectable genetic alteration in HNSCC, which can already be detected in premalignant dysplastic lesions[34]. These changes are also found in HNSCCs of FA patients, suggesting that FA pathway inactivation accelerates the typical squamous cell carcinogenesis process, causing frequent HNSCCs at young age in FA patients. In response to DNA damage, p53 coordinates several signaling pathways to maintain genomic stability: it activates DNA repair, causes cell cycle arrest to allow enough time to repair the damage or, in certain instances, initiates apoptosis[35]. Inactivation of the FA pathway can result in unrepaired DNA damage, leading to the activation of p53. This elevated p53 response has indeed been demonstrated in hematopoietic stem and progenitor cells from FA patients and *Fancd2*$^{-/-}$ and *Fancg*$^{-/-}$ mice[36]. Consequently, the primary bone marrow cells are arrested in the G1 phase of the cell cycle, which might eventually lead to hematopoietic stem cell depletion, thereby explaining the progressive impairment of hematopoiesis in FA. Besides providing insights in the pathogenesis of bone marrow failure, a hyperactive p53 response might also explain the increased cancer proneness of FA patients. Due to an overactive p53 DNA damage response, FA deficient cells may have a growth disadvantage due to increased cell cycle arrest and/or apoptosis. This would be alleviated in rare cells that have gained a *TP53* pathway mutation. Although deletion of p53 enables cells to tolerate DNA damage and rescues the defects of FA human and mouse hematopoietic progenitors[36], it will also result in enhanced genomic instability and tumor formation. Indeed, loss of p53 accelerated tumor formation in *Fancd2*$^{-/-}$ and *Fancc*$^{-/-}$ mice[37,38]. Likewise, it might also explain why individuals with the telomere maintenance disease Dyskeratosis congenita have an increased risk to develop HNSCC as shortening of telomeres will also result in elevated p53 activation[39–41]. Taken together, an exacerbated p53 response due to unresolved DNA damage might trigger rapid selection for *TP53* mutations in FA patients, driving tumorigenesis. In contrast, inactivation of the FA pathway before loss of p53 in a cell in a non-FA individual will result in an adequate DNA damage response, p53 activation and cell cycle arrest, which will prevent malignant transformation. For this reason, the occurrence of FA pathway defects in sporadic HNSCC might be rare.

Notwithstanding, FA-deficient tumors do occur occasionally in non-FA individuals. These tumors may respond well to chemoradiation, making it of significant interest to find biomarkers of FA-deficiency to predict treatment response and thereby personalize treatment. Since chemoradiation can cause many side effects, FA-deficiency might be further exploited in the treatment of cancer, which we

have shown in **Chapter 6** by demonstrating that in addition to BRCA1/2- or PALB2-deficiency, FANCM-deficient cells were sensitive to PARP inhibitors. Moreover, in **Chapter 7**, we noticed that more siRNAs were lethal in FANCC-deficient tumor cells compared to the corresponding FA-corrected tumor cells, indicating that synthetic lethal interactions may exist between FA deficiency and other pathways. Confirming the synthetic lethal interactions and understanding the underlying mechanism, will open new avenues in the treatment of FA-deficient tumors.

References

1. Auerbach, A. D. Fanconi anemia and its diagnosis. Mutat. Res. 668, 4–10 (2009).
2. Sasaki, M. S. & Tonomura, A. A high susceptibility of Fanconi's anemia to chromosome breakage by DNA cross-linking agents. Cancer Res. 33, 1829–36 (1973).
3. Auerbach, A. D. & Wolman, S. R. Susceptibility of Fanconi's anaemia fibroblasts to chromosome damage by carcinogens. Nature 261, 494–6 (1976).
4. Kottemann, M. C. & Smogorzewska, A. Fanconi anaemia and the repair of Watson and Crick DNA crosslinks. Nature 493, 356–63 (2013).
5. Bogliolo, M. *et al.* Mutations in ERCC4, encoding the DNA-repair endonuclease XPF, cause Fanconi anemia. Am. J. Hum. Genet. 92, 800–6 (2013).
6. Kashiyama, K. *et al.* Malfunction of nuclease ERCC1-XPF results in diverse clinical manifestations and causes Cockayne syndrome, xeroderma pigmentosum, and Fanconi anemia. Am. J. Hum. Genet. 92, 807–19 (2013).
7. Domchek, S. M. *et al.* Biallelic deleterious BRCA1 mutations in a woman with early-onset ovarian cancer. Cancer Discov. 3, 399–405 (2013).
8. Sawyer, S. L. *et al.* Biallelic Mutations in BRCA1 Cause a New Fanconi Anemia Subtype. Cancer Discov. 5, 135–42 (2014).
9. Kutler, D. I. *et al.* High incidence of head and neck squamous cell carcinoma in patients with Fanconi anemia. Arch. Otolaryngol. Head. Neck Surg. 129, 106–12 (2003).
10. Hermsen, M. A. *et al.* Cytogenetic characteristics of oral squamous cell carcinomas in Fanconi anemia. Fam. Cancer 1, 39–43 (2001).
11. Van Zeeburg, H. J. T. *et al.* Generation and molecular characterization of head and neck squamous cell lines of fanconi anemia patients. Cancer Res. 65, 1271–6 (2005).
12. Stransky, N. *et al.* The mutational landscape of head and neck squamous cell carcinoma. Science 333, 1157–60 (2011).
13. Agrawal, N. *et al.* Exome sequencing of head and neck squamous cell carcinoma reveals inactivating mutations in NOTCH1. Science 333, 1154–7 (2011).
14. Nakanishi, K. *et al.* Interaction of FANCD2 and NBS1 in the DNA damage response. Nat. Cell Biol. 4, 913–20 (2002).
15. Gennery, A. R. *et al.* The clinical and biological overlap between Nijmegen Breakage Syndrome and Fanconi anemia. Clin. Immunol. 113, 214–9 (2004).
16. New, H. V *et al.* Nijmegen breakage syndrome diagnosed as Fanconi anaemia. Pediatr. Blood Cancer 44, 494–9 (2005).
17. Van der Lelij, P. *et al.* Warsaw breakage syndrome, a cohesinopathy associated with mutations in the XPD helicase family member DDX11/ChlR1. Am. J. Hum. Genet. 86, 262–6 (2010).
18. Van der Lelij, P., Oostra, A. B., Rooimans, M. A., Joenje, H. & de Winter, J. P. Diagnostic Overlap between Fanconi Anemia and the Cohesinopathies: Roberts Syndrome and Warsaw Breakage Syndrome. Anemia 2010, 565268 (2010).
19. Vega, H. *et al.* Roberts syndrome is caused by mutations in ESCO2, a human homolog of yeast ECO1 that is essential for the establishment of sister chromatid cohesion. Nat. Genet. 37, 468–70 (2005).
20. Van der Lelij, P. *et al.* The cellular phenotype of Roberts syndrome fibroblasts as revealed by ectopic expression of ESCO2. PLoS One 4, e6936 (2009).
21. Losada, A. Cohesin in cancer: chromosome segregation and beyond. Nat. Rev. Cancer 14, 389–93 (2014).
22. Evers, L. *et al.* STAG2 is a clinically relevant tumor suppressor in pancreatic ductal adenocarcinoma. Genome Med. 6, 9 (2014).
23. Bailey, M. L. *et al.* Glioblastoma cells containing mutations in the cohesin component STAG2 are sensitive to PARP inhibition. Mol. Cancer Ther. 13, 724–32 (2014).
24. Zeman, M. K. & Cimprich, K. A. Causes and consequences of replication stress. Nat. Cell Biol. 16, 2–9 (2014).
25. Mailand, N. *et al.* Rapid destruction of human Cdc25A in response to DNA damage. Science 288, 1425–9 (2000).
26. Bartkova, J. *et al.* DNA damage response as a candidate anti-cancer barrier in early human tumorigenesis. Nature 434, 864–70 (2005).
27. Bartkova, J. *et al.* Oncogene-induced senescence is part of the tumorigenesis barrier imposed by DNA damage checkpoints. Nature 444, 633–7 (2006).
28. Gorgoulis, V. G. *et al.* Activation of the DNA damage checkpoint and genomic instability in human precancerous lesions. Nature 434, 907–13 (2005).
29. Bester, A. C. *et al.* Nucleotide Deficiency Promotes Genomic Instability in Early Stages of Cancer Development. Cell 145, 435–446 (2011).
30. Bermejo, R., Lai, M. S. & Foiani, M. Preventing replication stress to maintain genome stability: resolving conflicts between replication and transcription. Mol. Cell 45, 710–8 (2012).

31. Jones, R. M. *et al.* Increased replication initiation and conflicts with transcription underlie Cyclin E-induced replication stress. Oncogene 32, 3744–53 (2013).
32. Toledo, L. I. *et al.* ATR prohibits replication catastrophe by preventing global exhaustion of RPA. Cell 155, 1088–103 (2013).
33. Neelsen, K. J., Zanini, I. M. Y., Herrador, R. & Lopes, M. Oncogenes induce genotoxic stress by mitotic processing of unusual replication intermediates. J. Cell Biol. 200, 699–708 (2013).
34. Leemans, C. R., Braakhuis, B. J. M. & Brakenhoff, R. H. The molecular biology of head and neck cancer. Nat. Rev. Cancer 11, 9–22 (2011).
35. Vogelstein, B., Lane, D. & Levine, A. J. Surfing the p53 network. Nature 408, 307–10 (2000).
36. Ceccaldi, R. *et al.* Bone marrow failure in Fanconi anemia is triggered by an exacerbated p53/p21 DNA damage response that impairs hematopoietic stem and progenitor cells. Cell Stem Cell 11, 36–49 (2012).
37. Freie, B. *et al.* Fanconi anemia type C and p53 cooperate in apoptosis and tumorigenesis. Blood 102, 4146–52 (2003).
38. Houghtaling, S. *et al.* Heterozygosity for p53 (Trp53+/-) accelerates epithelial tumor formation in fanconi anemia complementation group D2 (Fancd2) knockout mice. Cancer Res. 65, 85–91 (2005).
39. Cosme-Blanco, W. *et al.* Telomere dysfunction suppresses spontaneous tumorigenesis in vivo by initiating p53-dependent cellular senescence. EMBO Rep. 8, 497–503 (2007).
40. d'Adda di Fagagna, F. *et al.* A DNA damage checkpoint response in telomere-initiated senescence. Nature 426, 194–8 (2003).
41. Feldser, D. M. & Greider, C. W. Short telomeres limit tumor progression in vivo by inducing senescence. Cancer Cell 11, 461–9 (2007).

SUMMARY

Fanconi anemia (FA) is a rare genomic instability syndrome characterized by a variety of congenital malformations, bone marrow failure and cancer predisposition. The majority of FA patients develops bone marrow failure during the first decade of life, which has been a major cause of death. Since bone marrow transplantation outcomes have improved considerably in recent years, the next life-threatening problem FA patients are facing is the high chance of developing solid tumors, most particularly of the head and neck region. At the cellular level, FA cells are defective in repairing DNA damage induced by DNA interstrand crosslinking (ICL) agents, such as the widely used chemotherapeutic agent cisplatin. As a consequence of deficient DNA repair, FA cells exhibit increased genomic instability, which can lead to cancer. A better understanding of the FA proteins involved in this DNA repair pathway will provide insights into the mechanisms of ICL repair and malignant transformation as well as in chemotherapy response as FA cells are hypersensitive to the chemotherapeutic agent cisplatin. Therefore, part of the research described in this thesis focused on the identification of additional FA genes and the encoded proteins. Given the high susceptibility of FA patients to develop head and neck cancer, we also examined if errors in FA proteins occur in head and neck tumors of non-FA patients. Finally, we investigated if defects in the FA repair mechanism can be exploited in anti-cancer therapies.

In the first chapters of this thesis (**Chapter 2-4**), we describe the identification of two genes (*FANCP/SLX4* and *FANCQ/ERCC4/XPF*) that cause FA when mutated. Bi-allelic mutations in *FANCP/SLX4* were found in one Dutch and four German FA patients, whereas bi-allelic mutations in *FANCQ/ERCC4/XPF* were causative for FA in one German and one Spanish individual. Currently, 17 FA genes have been identified and the corresponding proteins function in the FA pathway to repair ICLs. The SLX4 protein plays a role in the coordination of several structure-specific endonucleases, including XPF, which are able to cut the DNA thereby initiating the removal of the ICL. XPF also functions in another DNA repair pathway, which is involved in repairing UV-induced DNA damage. Mutations in *FANCQ/ERCC4/XPF* have previously been identified in two other syndromes: Xeroderma pigmentosum (XP) and XPF-ERCC1 (XFE) progeroid syndrome. XP is characterized by increased sensitivity to UV light (sun light) and an associated enhanced risk to develop skin cancer, while the only reported XFE progeroid syndrome patient had a very severe phenotype with characteristics of both FA and XP. Thus, mutations in one gene (*XPF)* are now associated with three clinically different diseases: XP, XFE progeroid syndrome and FA. Depending on the type of mutation in *FANCQ/ERCC4/XPF*, one or both of the two DNA repair mechanisms in which XPF is involved are affected and this dictates the distinct clinical outcomes. In FA patients, the repair of ICLs is mainly affected, while the repair of UV-induced DNA damage is primarily defective in XP patients. When both repair mechanisms are deficient by mutations in *FANCQ/*

ERCC4/*XPF*, individuals will present with XFE progeroid syndrome.

In **Chapter 5**, we describe the occurrence of pathogenic mutations in FA genes in head and neck squamous cell carcinoma (HNSCC) cell lines derived from individuals without FA. Although we showed that a large number (53%) of these HNSCC cell lines had a typical FA feature (ICL-induced chromosomal breakage), the occurrence of FA gene defects in these cell lines was rare. Within panels of 17 and 39 HNSCC cell lines, we found one cell line with bi-allelic mutations in *FANCM* and one with promotor hypermethylation and loss of expression of *FANCF*. Inactivation of FA genes by mutations or promotor methylation leads to defective DNA repair and can result in ICL-induced chromosomal breakage and chromosomal instability (CIN), which is a hallmark of many types of cancer. Another possibility that can be causative of CIN is the unequal distribution of chromosomes to daughter cells when a cell divides. Chromosome segregation is regulated by several processes including sister chromatid cohesion and inherited defects in this process are associated with diseases collectively called cohesinopathies (*e.g.* Roberts syndrome and Warsaw Breakage syndrome). Since cells derived from Roberts syndrome or Warsaw breakage syndrome patients resemble cells from FA patients in terms of ICL-induced chromosomal breakage, we also studied the occurrence of sister chromatid cohesion defects in HNSCC cell lines. Severe sister chromatid cohesion defects were observed in 29% of HNSCC cell lines, which could be explained by mutations in *PDS5A* in one cell line and in *STAG2* in another cell line. Thus, inactivation of FA genes or defective sister chromatid cohesion occasionally occur in HNSCC cell lines, providing possible explanations for the observed CIN in a subset of head and neck tumors. Screening of tumor samples for these mutations might be of relevance to predict response to the chemotherapeutic agent cisplatin as FA deficient cells are hypersensitive to this drug. In many cases, however, we could not identify the responsible mutated gene that might explain the described cellular phenotypes.

In **Chapter 6**, we provide evidence that FA and sister chromatid cohesion defects might be exploited in anti-cancer therapies. Previous studies showed that FANCD1/BRCA2, FANCN/PALB2, FANCO/RAD51C or FANCP/SLX4 deficiency results in sensitivity to inhibitors of the protein PARP, and that this might be used in the treatment of cancer. We confirmed these results by demonstrating that lymphoblasts derived from FA patients with mutations in *FANCD1*/*BRCA2* and *FANCN*/*PALB2* were sensitive to PARP inhibitors as expected. However, FANCP/SLX4-deficient lymphoblasts were not particularly sensitive to inhibition of PARP, which could be explained by the presence of truncated SLX4 protein with a residual function in these cells. We newly identified FANCM deficiency as a determinant of PARP inhibitor response as lymphoblasts with *FANCM* mutations were sensitive to inhibition of PARP. We also showed that the level of sensitivity of *FANCD1*/*BRCA2* mutant cells to PARP inhibition depended on the type of mutation. To test whether

cells derived from individuals with syndromes clinically related to FA also exhibited PARP inhibitor sensitivity, lymphoblasts of individuals with a cohesinopathy were also tested. Cells with mutations in *DDX11*, which is causative for Warsaw breakage syndrome, were also sensitive to PARP inhibition. Hence, we newly identified FANCM and DDX11 as determinants of PARP inhibitor response, which possibly extends the utility of these agents in the treatment of cancer.

To find additional targets that might be exploited to develop new anti-cancer therapies for tumors in FA patients as well as FA-deficient tumors in individuals without FA, we have performed a genome-wide high-throughput siRNA screen (see **Chapter 7**). Although more research is required, we found two classes of synthetic lethal interactions. The first class is tumor specific and independent of FA status, which thereby may provide a cancer treatment strategy in patients with or without FA. This class includes inhibition of the vacuolar ATPase, a proton pump involved in pH homeostasis, and the spindle assembly checkpoint, which is required for the correct distribution of chromosomes during cell division. The second class is FA-specific and is particularly promising to further exploit to develop anti-cancer treatments for the small group of patients that have a tumor with a defect in the FA pathway. This class includes inhibition of several nucleoporins (proteins that are part of a large multi-subunit complex involved in among others protein transport, gene expression and DNA repair) and the proteasome, which has an important role in protein degradation.

Overall the work presented in this thesis has led to the identification of two FA genes (*FANCP/SLX4* and *FANCQ/ERCC4/XPF*), the demonstration of rare known FA defects in head and neck tumor cell lines of non-FA individuals and the first steps in investigating whether these defects in tumors can be exploited to develop new anti-cancer treatment strategies.

NEDERLANDSE SAMENVATTING

Fanconi anemie (FA) is een zeldzaam genomisch instabiliteitssyndroom gekenmerkt door een verscheidenheid aan aangeboren afwijkingen, beenmergfalen en verhoogd risico op het krijgen van kanker. De meerderheid van de FA patiënten ontwikkelt al op jonge leeftijd beenmergfalen, wat een belangrijke doodsoorzaak is. Aangezien de uitkomsten van beenmergtransplantaties bij FA patiënten de laatste jaren enorm verbeterd zijn, is de grote kans op het krijgen van een solide tumor, en met name hoofd-en-hals kanker, het volgende levensbedreigende probleem. Cellen van FA patiënten laten een defect zien in het repareren van DNA schade geïnduceerd door chemische middelen die DNA interstrand crosslinks (ICL) veroorzaken. Een voorbeeld van zo'n middel is het veelgebruikte chemotherapeuticum cisplatine. Als gevolg van een kapot DNA reparatie mechanisme vertonen FA cellen meer genomische instabiliteit en dit kan leiden tot kanker. Het identificeren van alle FA eiwitten betrokken bij dit DNA reparatie mechanisme zal inzicht geven in hoe ICLs worden gerepareerd, en wellicht ook in het ontstaan van kanker. Daarnaast leidt het tot een beter begrip van de respons op chemotherapie aangezien FA cellen overgevoelig zijn voor sommige chemotherapeutische middelen, zoals cisplatine. Om deze redenen is een deel van het onderzoek beschreven in dit proefschrift gericht geweest op het identificeren van FA eiwitten. Gezien FA patiënten specifiek een hoge kans hebben op het krijgen van een plaveiselcarcinoom in het hoofd-hals gebied (HHPCC), hebben we ook onderzocht of mutaties in FA genen voorkomen in HHPCC van niet-FA patiënten. Ten slotte hebben we bekeken of defecten in het FA reparatie mechanisme benut kunnen worden bij de behandeling van kanker.

In de eerste hoofdstukken van dit proefschrift (**Hoofdstuk 2-4**) beschrijven we de identificatie van twee genen (*FANCP*/*SLX4* en *FANCQ*/*ERCC4*/*XPF*). Mutaties in deze genen kunnen FA veroorzaken. Mutaties in *FANCP*/SLX4 werden gevonden in één Nederlandse en vier Duitse FA patiënten, terwijl mutaties in *FANCQ*/*ERCC4*/*XPF* verantwoordelijk waren voor het krijgen van FA in een Duits en een Spaans individu. Momenteel zijn er 17 FA genen bekend en de eiwitten die worden gecodeerd door deze genen functioneren in het FA reparatie mechanisme om ICLs te verwijderen. Het SLX4 eiwit speelt een belangrijke rol bij de coördinatie van verschillende structuur-specifieke endonucleases, zoals XPF, die in staat zijn het DNA te knippen als onderdeel van het reparatie process. Behalve in DNA interstrand crosslink reparatie, functioneert XPF ook in een ander DNA reparatie mechanisme, dat betrokken is bij het herstellen van UV-geïnduceerde DNA schade. Mutaties in *FANCQ*/*ERCC4*/*XPF* waren eerder al geassocieerd met twee andere syndromen: Xeroderma pigmentosum (XP) en XPF-ERCC1 (XFE) progeroid syndroom. XP wordt gekenmerkt door gevoeligheid voor UV-licht (zonlicht) en daarmee gepaard een verhoogd risico op het krijgen van huidkanker, terwijl de enige patiënt beschreven met XFE progeroid syndroom zowel kenmerken van FA als XP heeft. Dus mutaties in één enkel gen worden nu geassocieerd met drie verschillende klinische

aandoeningen:XP, XFE progeroid syndroom en FA. Het type mutatie in *FANCQ*/*ERCC4*/*XPF*, en daaruit volgend welk DNA reparatie mechanisme niet meer werkt, bepaalt welk syndroom de patiënt krijgt. Bij FA patiënten wordt hoofdzakelijk de reparatie van ICLs belemmerd, terwijl het herstel van UV-geïnduceerde DNA schade met name defect is bij XP patiënten. Wanneer de werking van beide mechanismen is aangedaan, zal dit resulteren in XFE progeroid syndroom.

In **Hoofdstuk 5** beschrijven we het voorkomen van pathogene mutaties in FA genen in hoofd-hals tumor cellijnen afkomstig van individuen zonder FA. Hoewel we aangetoond hebben dat een groot aantal (53%) van deze HHPCC cellijnen een typisch FA kenmerk heeft (ICL-geïnduceerde chromosomale breuken), zijn defecten in de bekende FA genen in deze cellijnen zeldzaam. In groepen van 17 en 39 onderzochte HHPCC cellijnen, vonden we één cellijn met mutaties in *FANCM* en in één met promotor hypermethylering van *FANCF*. Het inactiveren van FA genen door mutaties of promotor methylering zorgt ervoor dat DNA schade niet kan worden hersteld met als gevolg een verhoogde gevoeligheid voor chemische stoffen die ICLs veroorzaken en chromosomale instabiliteit (CIN). Dit laatste is een kenmerk van vele soorten kanker. CIN kan ook ontstaan door de ongelijke verdeling van chromosomen over de twee dochtercellen wanneer een cel deelt. Chromosoom segregatie wordt geregeld door verschillende processen, inclusief een proces dat bekend staat als "zuster-chromatidecohesie". Een defect in dit proces wordt geassocieerd met verschillende ziektebeelden, gezamenlijk bekend als cohesinopathieën (bijvoorbeeld Roberts syndroom en Warsaw breakage syndroom). Aangezien cellen afkomstig van patiënten met Roberts syndroom of Warsaw breakage syndroom net als FA cellen ICL-geïnduceerde chromosomale breuken laten zien, hebben we ook bekeken of defecten in zuster-chromatidecohesie voorkomen in HHPCC cellijnen. Ernstige zuster-chromatidecohesie defecten werden waargenomen bij 29% van de onderzochte HHPCC cellijnen. Deze defecten konden in twee cellijnen verklaard worden door mutaties in *PDS5A* of *STAG2*. Dus inactivatie van FA genen of genen betrokken bij zuster-chromatidecohesie komt af en toe voor in HHPCC cellijnen, en daarmee geven we mogelijke verklaringen voor de waargenomen CIN in een deel van de hoofd-hals tumoren. Het screenen van tumoren met deze mutaties kan relevant zijn voor het voorspellen van de respons op het chemotherapeutische middel cisplatine, omdat FA deficiënte cellen overgevoelig zijn voor dit geneesmiddel. Echter in veel gevallen konden we geen bekend FA gen vinden dat de cellulaire fenotypes kon verklaren.

In **Hoofdstuk 6**, leveren we bewijs dat FA en zuster-chromatidecohesie defecten in anti-kanker therapieën kunnen worden benut. Eerdere studies toonden al aan dat FANCD1/BRCA2, FANCN/PALB2, FANCO/RAD51C of FANCP/SLX4 deficiëntie resulteert in gevoeligheid voor remmers van het eiwit PARP. Dit zou kunnen worden gebruikt bij de behandeling van tumoren met mutaties in de corresponderende FA genen. We hebben bevestigd dat lymfoblasten afkomstig van FA-patiënten met

mutaties in *FANCD1/BRCA2* of *FANCN/PALB2* gevoelig zijn voor de remming van PARP. Daarnaast toonden we aan dat lymfoblasten afkomstig van FA-patiënten met mutaties in *FANCM* gevoelig zijn voor PARP-remmers. Echter, SLX4-deficiënte lymfoblasten waren niet bijzonder gevoelig voor remming van PARP, wat kan worden verklaard door de aanwezigheid van een verkorte versie van het SLX4 eiwit in deze cellen. Verder lieten we zien dat afhankelijk van de mutatie in *FANCD1/BRCA2*, cellen meer of minder gevoelig zijn voor PARP-remming. Om te testen of cellen afkomstig van personen met een syndroom klinisch gerelateerd aan FA ook gevoelig zijn voor PARP-remmers, werden lymfoblasten van personen met een cohesinopathie getest. Cellen met mutaties in *DDX11*, de oorzaak voor Warsaw breakage syndroom, bleken ook gevoelig voor PARP-remming. Samenvattend, hebben we FANCM en DDX11 als determinanten van PARP-remmer respons geïdentificeerd en dit kan de bruikbaarheid van deze middelen bij het behandelen van kanker verder uitbreiden.

PARP remmers zijn een voorbeeld van een mogelijk doelgerichte kanker therapie (een therapie die erop gericht is tumoren met bepaalde eigenschappen (zoals FA defecten) te behandelen). Om extra aanknopingspunten te vinden voor doelgerichte therapie bij zowel FA patiënten als patiënten met FA-deficiënte tumoren, hebben we een genoom-brede siRNA screen (zie **Hoofdstuk 7**) uitgevoerd. Hoewel er meer onderzoek nodig is, vonden we twee klassen van synthetische dodelijke interacties. De eerste klasse is tumor-specifiek (celviabiliteit wordt alleen of sterker verminderd in kankercellen vergeleken met gewone cellen) en onafhankelijk van FA status waardoor deze klasse een behandelingsstrategie kan verschaffen voor patiënten met of zonder FA. Deze tumor-specifieke klasse omvat remming van de vacuolaire ATPase, een proton pomp betrokken bij pH homeostase en de spindle assembly checkpoint, welke nodig is voor de juiste verdeling van chromosomen tijdens de celdeling. De tweede klasse is FA-specifiek (celviabiliteit wordt alleen of sterker verminderd in cellen met een FA defect) en is veelbelovend om verder te onderzoeken voor de kleine groep patiënten die een tumor met een defect in het FA reparatie mechanisme hebben. Deze klasse omvat de remming van verscheidene nucleoporins (eiwitten die deel uitmaken van een groot multi-subunit complex betrokken bij onder andere eiwittransport, genexpressie en DNA reparatie) en het proteasoom, dat een belangrijke rol speelt bij eiwitafbraak.

Samenvattend heeft het werk in dit proefschrift geleid tot de identificatie van twee FA genen (*FANCP/SLX4* en *FANCQ/ERCC4/XPF*), het aantonen van het zelden voorkomen van FA defecten in HHPCC cellijnen van niet-FA individuen en de eerste stappen in het onderzoek of deze FA defecten in tumoren kunnen worden benut om nieuwe behandelingen tegen kanker te ontwikkelen.

ADDENDUM

Curriculum Vitae

Chantal Stoepker
January 29th 1985, Den Helder, The Netherlands

Education

2008-2012	PhD student at VU University Medical Center, Department Clinical Genetics (Oncogenetics), Amsterdam, The Netherlands
2006-2008	MSc in Oncology, Vrije Universiteit, Amsterdam, The Netherlands *Graduated cum laude*
2003-2005	BSc Biomedical Sciences, Vrije Universiteit, Amsterdam, The Netherlands
1997-2003	Pre-academic education, Atheneum/VWO, Nieuwediep, Den Helder, The Netherlands

Awards & prizes

2013	German award (Ehrenauszeichnung), Deutsche Fanconi-anämie-hilfe e.V.
2013	Best poster on clinical translational research, Fanconi Anemia Research Fund
2013	Discovery award FANCQ, Fanconi Anemia Research Fund
2011	Discovery award FANCP, Fanconi Anemia Research Fund

Publications

2015 **Defects in the Fanconi anemia pathway and chromatid cohesion in head and neck cancer**
Chantal Stoepker, Najim Ameziane, Petra van der Lelij, Irsan E. Kooi, Anneke B. Oostra, Martin A. Rooimans, Saskia E. van Mil, Arjen Brink, Ralf Dietrich, Jesper A. Balk, Bauke Ylstra, Hans Joenje, Stephan M. Feller & Ruud H. Brakenhoff

Published in Cancer Research, 2015. 75(17):3543-3553.

2015 **DNA helicases FANCM and DDX11 are determinants of PARP inhibitor sensitivity**
Chantal Stoepker, Atiq Faramarz, Martin A. Rooimans, Saskia

E. van Mil, Jesper A. Balk, Eunike Velleuer, Najim Ameziane, Hein te Riele & Johan P. de Winter

Published in DNA Repair, 2015. 26:54-64.

2013 **Mutations in *ERCC4*, encoding the DNA-repair endonuclease XPF, cause Fanconi anemia**
Massimo Bogliolo*, Beatrice Schuster*, **Chantal Stoepker**, Burak Derkunt, Yan Su, Anja Raams, Juan P. Trujillo, Jordi Minguillón, María J. Ramírez, Roser Pujol, José A. Casado, Rocío Baños, Paula Rio, Kerstin Knies, Sheila Zúñiga, Javier Benítez, Juan A. Bueren, Nicolaas G.J. Jaspers, Orlando D. Schärer, Johan P. de Winter, Detlev Schindler & Jordi Surrallés

*Both authors contributed equally to this work.

Published in The American Journal of Human Genetics, 2013. 92(5):800-806.

2013 **Whole exome sequencing reveals uncommon mutations in the recently identified Fanconi anemia gene *SLX4/FANCP***
Beatrice Schuster*, Kerstin Knies*,**Chantal Stoepker**, Eunike Velleuer, Richard Friedl,Birgit Gottwald-Mühlhauser, Johan P. de Winter & Detlev Schindler

* These authors contributed equally to this work.

Published in Human Mutation, 2013. 34(1):93-96.

2011 **SLX4, a coordinator of structure-specific endonucleases, is mutated in a new Fanconi anemia subtype**
Chantal Stoepker, Karolina Hain, Beatrice Schuster, Yvonne Hilhorst-Hofstee, Martin A. Rooimans, Jûrgen Steltenpool, Anneke B. Oostra, Katharina Eirich, Elisabeth T. Korthof, Aggie W.M. Nieuwint, Nicolaas G.J. Jaspers, Thomas Bettecken, Hans Joenje, Detlev Schindler, John Rouse & Johan P. de Winter

Published in Nature Genetics, 2011. 43(2): 138-141.

2009 **Regulation of growth differentiation factor 15 expression by intracellular iron**

Samira Lakhal, Nick P. Talbot, Alexi Crosby, **Chantal Stoepker**, Alain R.M. Townsend, Peter A. Robbins, Christopher W. Pugh, Peter J. Ratcliffe & David R. Mole

Published in Blood, 2009. 113(7): 1555-1563.

Dankwoord/ Acknowledgements

Yes! Eindelijk is het zover: mijn boekje is klaar/af/fini! :)
En natuurlijk hoort daar het veelgelezen dankwoord bij. Als eerste wil ik degene bedanken aan wie ik dit boekje heb opgedragen: prof. dr. Johan de Winter. Eerst was je mijn copromotor en na een welverdiende benoeming tot hoogleraar, zou je mijn promotor worden. Helaas liep het anders en kan je het eindresultaat nu niet meer aanschouwen (al weet ik dat je ontzettend trots zou zijn geweest!). Ik heb weleens iemand horen zeggen: "één keer in Nature (Genetics) publiceren is geluk, een tweede keer is al een heel stuk moeilijker". Met maar liefst 9 artikelen in Nature Genetics, kan ik alleen maar beamen dat je een ongelooflijk goede wetenschapper was met veel aanstekelijk enthousiasme. Ik heb veel van je geleerd, waar ik ontzettend dankbaar voor ben en met plezier denk ik terug aan de kleine dingetjes: van de goedemorgen met een glimlach tot gezellig kletsen over wetenschap bij de koffie en altijd je kantoor kunnen binnen rennen met de nieuwste resultaten.

Ook wil ik mijn promotoren prof. dr. Hein P.J. te Riele en prof. dr. Ruud H. Brakenhoff bedanken voor alle hulp. Hein, ik ben ontzettend blij dat jij de vervanger van Johan bent geworden. Samen met Ruud vormen jullie een perfect team: de enorme kennis van Ruud op het gebied van hoofd-hals kanker en Hein die helemaal thuis is in het veld van DNA reparatie, zorgden voor veel bruikbare input. Het is inspirerend om te zien hoe kalm en down to earth jullie je vak uitvoeren. Ontzettend bedankt voor alle nuttige suggesties, de hulp bij het submitten van artikelen (wat een hel! Maar gelukkig is alles wat we wilden publiceren inmiddels gepubliceerd!) en het helpen afronden van mijn promotie.

De leden van de leescommissie, prof. dr. Peter J.F. Snijders, prof. dr. Michiel van den Brekel, dr. Rob M. Wolthuis en dr. Puck Knipscheer, wil ik bedanken voor het zorgvuldig lezen van mijn proefschrift.

Prof. dr. Hanne Meijers-Heijboer, afdelingshoofd van de Klinische genetica, wil ik bedanken voor de mooie toespraken en het herstellen van de rust na het overlijden van Johan.

Vanzelfsprekend en zeer terecht wil ik natuurlijk ook al mijn (oud-) collega's van de sectie Oncogenetica bedanken voor alle hulp

bij experimenten, nuttige discussies en tips (en niet te vergeten: gezelligheid!): de stafleden Quinten, Rob, Josephine en Hans; de analisten Saskia, Davy, Jesper, Martin, Anneke O. en Yne; mede aio's Janine, Maarten, Irsan, Atiq, Petra, Kash, Monique, Stephanie, Berber en Anneke H. (super dat jullie, Berber en Anneke H., ook mijn paranimfen willen zijn!); de post-docs Najim, Job en Sheba en voor al het bureaucratische geregel en luisterende oor Dominique. Wat hadden we een geweldige tijd! Naast al het harde werken deden we een hoop leuke dingen. Van alle uitjes en borrels, mis ik de koffiemomentjes nog het meest, met name die om half 9 's ochtends, waarvoor ik rustig een half uur eerder op stond. Memorabel waren de tripjes naar Amerika (oa roadtrip to Chicago), Barcelona, de Ardennen en de weekendjes naar Wenen. Mede door jullie en wat spannende wetenschappelijke ontdekkingen heb ik een onvergetelijke tijd gehad bij de afdeling Klinische genetica.

Trots ben ik op mijn stagiaires Roelie, Anne (hadden we maar mooi even groep Stoepker!) en Maxime. Dankjewel voor al jullie hulp en gezelligheid! Ik had me geen betere studenten kunnen wensen.

Ook (oud-) collega's van andere afdelingen binnen het VUmc of het NKI ben ik dankbaar voor alle hulp bij experimenten of nuttige tips: Muriel, Sanne, Ida, Sietske en Henri. Ida, super fijn dat je me gerust stelde tijdens het screenen (1 fout en er gaan zo duizenden euro's de prullenbak in…probeer dan maar rustig te blijven!).

I would also like to thank all co-authors for their contribution and nice collaboration.

I admire Lynn and Dave Frohnmayer (in Memoriam), who started the Fanconi Anemia Research Fund, and Ralf Dietrich of the Deutche Fanconi-Anämie-Hilfe for their dedication to Fanconi anemia research. The anneal meetings were great, informative and inspiring. Fanconi anemia is an awful disease! I wish the best to all FA patients and their families and loved ones.

Mijn nieuwe collega's van de afdeling Humane genetica van het LUMC wil ik bedanken voor alle steun en begrip (mbt afwezigheid bij borrels) in de laatste fase van mijn promotietraject.

Verder wil ik mijn lieve vrienden (San en Jo, Marloes en Bruce, Chantal en Johan, Ebelien en Pieter, Gosia en Olle, Brenda en Martijn, Cassandra, Yordi, Joyce, Jessyca, Linda, Suus en Pascal) bedanken voor alle steun, interesse en leuke afleiding! San, Jo en Cas, super dat jullie zo ontzettend trots waren na het publiceren van mijn SLX4 artikel! Bruce, ook ontzettend bedankt voor het prikken en kraken, waardoor ik weer verder kon met typen!

Ook wil ik mijn ouders bedanken voor al hun steun en liefde! Mam, het is grappig dat jij nog veel enthousiaster dan ik kan zijn na een publicatie, en pap, jouw kalmte en je niet snel druk maken houdt alles mooi in evenwicht. Mijn broer Dennis en schoonzus Desiree (Geweldig dat er nu een kleine Stoepker (Hanna) bij is. Wat een schatje!), zusje Yvonne en vriendlief Ricky, Oma Stoepker, Opa Stegeman, ooms en tantes wil ik ook bedanken voor alle interesse in mijn proefschrift! En niet te vergeten: hopelijk ooit officieel mijn schoonfamilie (Barry dit is een hint): At (handig dat je altijd wat bewaart en dat ik mooi je gereedschapskist mocht gebruiken voor de foto op de voorkant) en Patricia (helaas kan jij ook het eindresultaat niet aanschouwen, maar ik weet zeker dat ook jij ontzettend trots zou zijn geweest!). Sander en Lieselotte, bedankt voor jullie interesse, steun en afleiding. Jullie hebben 2 geweldige kinderen (Merle en Tobias) en ik denk zowaar dat Tobias de voorkant van mijn boekje ook prachtig zal vinden.

Als laatste maar zeker niet als minste: mijn lieve vriend Barry. Je bent geweldig en ik ben stapelgek op je! Je werd misschien (of misschien kan ik beter het "misschien" weglaten) af en toe ook gek van mij, maar dat heeft je niet tegen gehouden om me onvoorwaardelijk te blijven steunen, heerlijk te koken en veel meer huishoudelijke taakjes tot je te nemen (die je overigens zo goed doet, dat we dat misschien maar na mijn promotie zo moeten laten).

Chantal